Design and synthesis of site-selective and supramolecular mechanophores

by

Aliya Sembayeva

A thesis submitted to

the University of Liverpool

for the degree of

Doctor of Philosophy

Department of Chemistry

School of Engineering and Physical Sciences

University of Liverpool

February 2021

ACKNOWLEDGMENTS

First and foremost, I would like to express my sincere gratitude to my supervisor Professor Roman Boulatov for his mentorship, help, and generous support during my PhD period. I am very thankful for accepting me and opportunities to investigate a new chemistry field under his guidance. I want to thank Luke and Chen for helping me with SEC and sonochemical experiments of my PhD project, and all members of our group Davide, Suonan, Watsuwach, Qihan, Alex, Caili, and Rob, for your help and friendly atmosphere throughout three years in Liverpool. I would also like to thank all the analytical facility members of the University of Liverpool and Swansea National Mass Spectrometry Facility for characterizing my compounds.

I would also like to express my special thanks to Embassy of Kazakhstan in the UK, specifically Ambassador HE Erlan Idrissov for support and future development opportunities.

My gratitude is endless in front of my parents, for investing in my education, support and love! I want to thank my relatives and friends who always showed their enduring support and love. I especially want to thank Dr Jason Carr for reading the final draft of my introduction, Ivan, Alfiya, Madina, and Adil, for our discussions and your readiness to always help during my PhD studies. All this support has been invaluable, especially when you are far from home.

Design and synthesis of site-selective and supramolecular mechanophores

Abstract

Polymer mechanochemistry is defined as the destructive or constructive coupling between mechanical load and chemical reactivity. An example of a destructive case is a conventional material's irreversible failure due to stretching or shearing. In contrast, mechanoresponsive materials can convert stress into useful chemical reactions such as stress-triggered ring-opening reactions. Early constructive examples include gem-dichlorocyclopropane (gDCC)- and spiropyran-based polymers towards olefin and merocyanine formation via a ring-opening mechanism under force conditions. This work aims to introduce nature's concepts like allostery and supramolecular chemistry using complex mechanophores into the service of polymer science, which led to the study of new chemistry at the interface of the two fields.

This dissertation focuses on three distinct areas of study, the first part devoted to synthetic methods of novel mechanophore formation with allosteric properties. Synthesis of an allosteric stiff-stilbene containing macrocycle was achieved via McMurry coupling of two indanone units, followed by successful ring-closure metathesis using a combination of second-generation Grubbs catalyst and cesium chloride (CsCl).

The second part of this work describes the preparation of foldamers as potent supramolecular mechanophores. As a result, a series of aromatic oligomers with 3, 7, and 15 aromatic units were prepared using a doubling segment strategy, which involved chelidamic acid and 2,6-diaminopyridine. An essential double-helical 15-mer moiety exhibited desirable robust properties at extreme conditions such as elevated temperatures, dilute conditions, and polar organic solvents.

The final part describes the attempts to polymerize the allosteric mechanophore via ring-opening metathesis polymerization under typical conditions (Grubbs II 1 mol%, 1 M, DCM, RT) and prepare supramolecular polymers via end-derivatization of model foldamer with carboxylic acid terminated polystyrene.

Abbreviations

AFM	atomic force microscopy
AOA	aromatic oligoamide
ATP	adenosine triphosphate
aq	aqueous
Ar	aryl
Boc	tert-butyloxycarbonyl
bp	boiling point
br	broad (spectral)
Bu	butyl
°C	degrees Celsius
calcd	calculated
cat	catalytic, catalyst
Cbz	carboxybenzyl
cm	centimeter(s)
cm^{-1}	wavenumber(s)
co-ROMP	co-ring-opening metathesis polymerization
d	doublet
DCC	N,N'-dicyclohexylcarbodiimide
DCM	dichloromethane
DMF	dimethylformamide
DMSO	dimethyl sulfoxide
DNA	deoxyribonucleic acid

eq	equivalent
ESI	electrospray ionization
EDC	1-ethyl-3-(3-dimethylaminopropyl)-carbodiimide
EOR	end-of-run
ERO	electrocyclic ring opening
gDCC	gem-dichlorocyclopropane
gDXC	gem-dihalocyclopropane
h	hour
HRMS	high resolution mass spectrometry
Hz	hertz
IR	infrared
J	coupling constant (in NMR spectrometry)
LAH	lithium aluminium hydride
m	multiplet (spectral)
M	molar (moles per liter)
Me	methyl
MeCN	acetonitrile
MHz	megahertz
min	minute(s)
mol	mole(s)
mmol	millimole(s)
mp	melting point
MS	mass spectrometry, molecular sieves
m/z	mass-to-charge ratio

Napy	2,7-diamido-1,8-naphthyridine
s	singlet (spectral)
S_N2	bimolecular nucleophilic substitution
t	triplet (spectral)
tBu	tert-butyl
NMR	nuclear magnetic resonance
Ph	phenyl
ppm	part(s) per million
iPr	isopropyl
py	pyridine
q	quartet (spectral)
PEG	Polyethylene glycol
PDA	photodiode array
PS	polystyrene
PyBOP	benzotriazol-1-yl-oxytripyrrolidinophosphonium hexafluorophosphate
RCM	ring-closure metathesis
ROMP	ring-opening metathesis polymerization
RI	refractive index
RT	room temperature
SS	stiff-stilbene
THF	tetrahydrofuran
TLC	thin layer chromatography
TFA	trifluoroacetic acid
quant	quantitative

SEC	size-exclusion chromatography
SMFM	single molecule force microscopy
UPy	2-ureido-4[1H]-pyrimidinone
UV	ultraviolet

Table of Contents

Chapter 1. INTRODUCTION

The development of polymer mechanochemistry from destructive bond scissions to constructive mechanochemical activation[1] has been with multidisciplinary approaches involving organic chemistry, computational chemistry, polymer physics, and different areas of engineering.[2] Polymer mechanochemistry is defined as the coupling of the applied mechanical force and chemical reactivity,[3] i.e., it studies the transformation of mechanical energy into chemical products. The mechanical degradation of the material is a destructive, harmful, and unwanted process, which cannot be predicted within a material and leads to the catastrophic failure of the material. A need to understand and control these processes has attracted scientists to design and synthesize polymers with mechanically active moieties, mechanophores.[2, 3]

Polymers become stretched in many circumstances, and therefore polymer mechanochemistry and corresponding phenomena are found almost anywhere where polymers are found.[4] Dough kneading is a daily and straightforward example of polymer mechanochemistry,[4] where repeated compression and stretching of dough accelerate the fragmentation of wheat flour protein and leads to breakage of sulfur-sulfur bond within glutenin to make it more digestible. Another destructive mechanochemical example is associated with melt processing of polymers due to polymer chain fragmentation, which is one of the first processes that initiate the catastrophic failure of polymeric materials. An underlying concept of car tire chemistry is a mechanochemical phenomenon of bond homolysis within a rubber,[5] carbon-carbon, carbon-sulfur, or sulfur-sulfur bond scissions. Polymer mechanochemistry is important in chemically enhanced oil recovery, where a dilute solution of guar polymer is injected at high pressure into the ground to push natural gas out.

Alternatively, whenever polymer solutions are used to control rheological properties of liquids such as ink-jet printing and in the fire-fighting equipment. Another actively exploited application area of polymer mechanochemistry is the design of bulletproof polymers and composites, which involve the breakage of a covalent bond to absorb energy deposited by the bullet.[2, 6, 7]

Polymer mechanochemistry has progressed over recent years, changing its focus from destructive fragmentations to productive outputs by developing stress-sensing molecules with mechanically labile bonds, mechanophores. The most studied examples of mechanophores are gem-dihalocyclopropane (gDXC),[8] spiropyran,[9-11] azobenzene[12] and stiff-stilbene,[13, 14] which our group desgined. The most critical element of a mechanophore is its design, which is based on the structural components that will respond to force in a predicted way. Attachment of polymer chains to mechanophore, followed by shearing, performs a wide range of chemical transformations effectively unachievable by applying elevated temperatures, light, or electricity.

Mechanochemical responses range from isomerization reactions to selective bond scission.[4, 15, 16] For example, sonication of diazolinked-PEG polymer facilitates extrusion of dinitrogen from the diazo linkage due to the homolytic C-N bond breakage (Figure 1). Mechanical cycloreversion of the maleimide-anthracene cycloadduct can break in the midpoint of the chain and find applications as new sensing material (Figure 1). Sijbesma demonstrated that sonication activates polymer-functionalized silver bis(N-heterocyclic carbene) complex into N-heterocyclic carbene organocatalyst that facilitated transesterification reactions (Figure 1),[17] while heating the reaction mixture with the same silver complex provides less than 3%

conversion. The mechanochemical response includes also configurational and constitutional isomerizations.

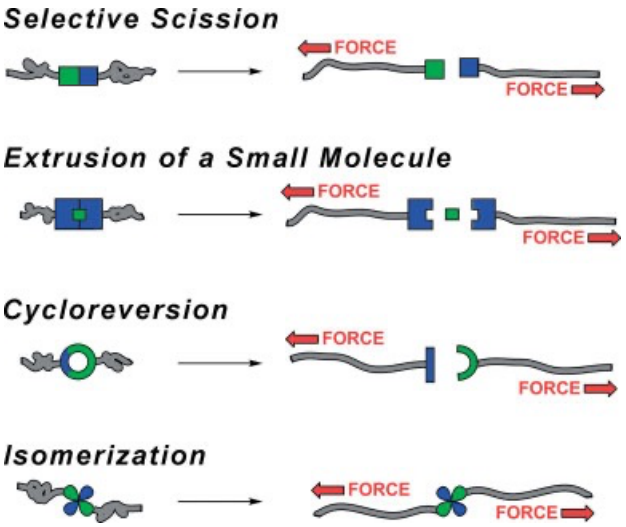

Figure 1. Generalized mechanisms of mechanophore-containing polymers as the response to force.[15] Application of force facilitates the change of functional moiety by configurational or constitutional isomerization, selective bond scission, extrusion of a small molecule, and cycloreversion.

Introduction of more complex functionalized mechanophores to polymer science offers attractive opportunities to study the unexplored interface between several fields and the design of new smart materials with unique properties such as self-healing,[18 19] catalysis,[19] stress-sensing,[9] and cooperativity.[2] The incorporation of supramolecular forces into the commercial polymer will lead to the formation of new material containing a series of supramolecular interactions with a covalent backbone. When force is applied, the sample material becomes distorted and experiences energy flowing somewhere. Flow scenarios can be the following: introduced energy (1) breaks supramolecular bonds so that object remains intact due to dynamic properties of non-covalent interactions or (2) increases the potential energy of covalent bond and breaks the material into two. This concept found industrial applications such as producing protective clothing using impact-hardening polymers, exhibiting softness-stiffness switch properties, used in bulletproof vests, knee pads, and

helmets. D3O,[20] PORON XRD,[21] and DEFLEXION[21] are examples of commercial smart polymers, solids at standard conditions, but when the material is subjected to force, it becomes liquid due to the breakage of supramolecular interactions. Stopping the shearing of the polymer heals non-covalent interactions and turns it back to the original solid matter. The petroleum industry also utilizes the concept of shear-thinning behavior using a ubiquitous guar biopolymer for hydraulic fracturing to extract natural gas. 2-ureido-4[1H]-pyrimidinone (UPy) and 2,7-diamido-1,8-naphthyridine (NaPy) are also standard synthetic building blocks of supramolecular telechelic polymers. Due to their high association constants of hydrogen bonds, a high degree of polymerization is obtained, but commercial applications of UPy and NaPy are awaiting. [22,23]

Nature can offer biological alternatives of polymers and inspire to translate its concepts towards engineering more advanced polymers. For example, many biochemical reactions utilize mechanical stress as a critical factor to control the physiological processes[24] based on a protein's conformation to trigger a cascade of chemical reactions in the organism such as ATP hydrolysis and cellular respiration[2, 24] that refer to allosteric regulation. Allostery is a process by which biological macromolecules transmit, amplify or inhibit a specific effect at one site to another functional site, allowing for regulation of the macromolecule's activity.[25] Allostery can be explained using structural changes. A well-known allosteric protein is the oxygen carrier hemoglobin.[26, 27] The binding of the first oxygen molecule to one of the four heme subunits activates the protein by changing its shape, facilitating cooperative binding of additional oxygen molecules to other oxygene molecules in heme residues (Figure 2). Inspired by this concept, new polymeric material with cooperative behavior driven by molecular-level deformation can be developed.[28, 2, 27]

Figure 2. Cooperative binding of oxygen to hemoglobin. When the first oxygen binds to haemoglobin, it changes the structures of adjacent heme sites and makes it easier for the subsequent binding events.[28]

1.1 Thesis objectives and project outlook

The work described herein focuses on the designing and synthesizing advanced mechanophores with either allosteric or dynamic properties.

The first part of the project is devoted to the design and synthesis of a polymerizable model, utilizing the underlying principle of allostery, i.e., the monomer's ability to regulate the interconversion process between two conformational states (tense and relaxed forms).[29] The primary design criterion of allosteric biomolecules is to have two or more equivalent binding sites, where the first site's activation by external stimuli causes a conformational change that allows activating the remaining units much more accessible. From the synthetic perspective, we envision this monomer as a symmetrical polymerizable macrocycle with two molecular force probes, Z-stiff-stilbenes, located at different sites far from each other due to the electronic coupling linked by an inert spacer (Scheme 1).

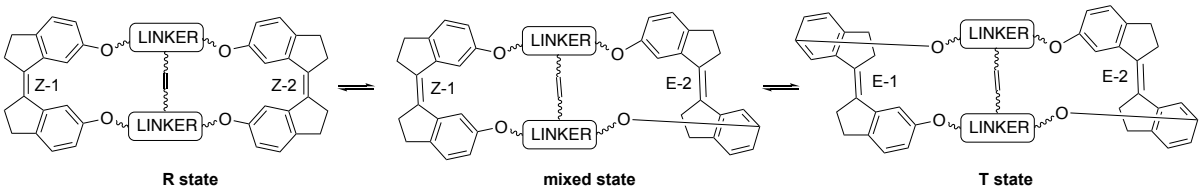

Scheme 1. The cooperativity model of stiff-stilbene macrocycle **1**. The wavy line represents an inert aliphatic chain. When the first isomerization happens (Z-2 to E-2), the second occurs immediately due to the formed strain.

Inspired by hemoglobin's example, the proposed mechanophore model can act as a switch by isomerizing from (Z,Z) – strain-free stiff stilbenes (R state) to (E,E) - strained analog (T state). To isomerize the first Z-stiff stilbene requires more force than the second isomerization due to the strain effect (mixed state). The double bond is the essential prerequisite for polymerization reaction via ring-opening metathesis polymerization (ROMP).

The second part of this project focuses on integrating supramolecular chemistry into a polymer using foldamer mechanophore towards studying energy flow, specifically if shearing breaks the covalent bond in the presence of weak interactions (Figure 3).

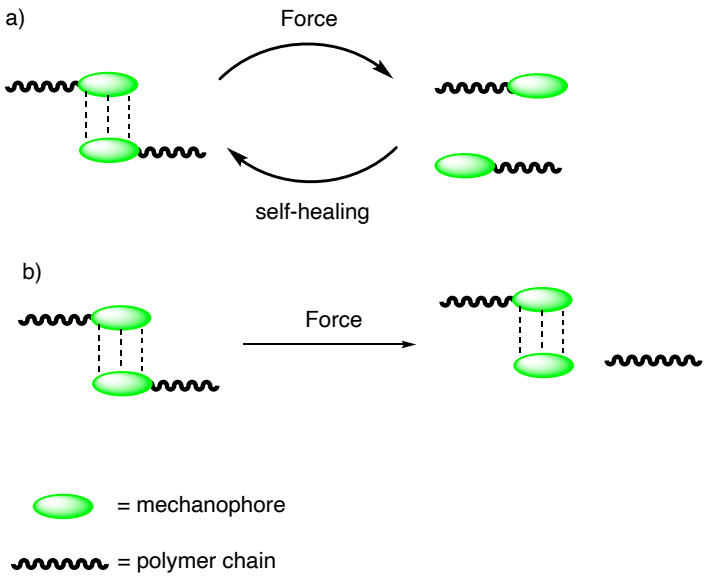

Figure 3.Potential mechanisms of shearing supramolecular systems with supramolecular bonds orthogonal to the backbone: a) breakage of weak supramolecular force under force and self-healing; b) breakage of covalent bond in the presence of weak supramolecular forces. Green is mechanophore; a wavy line is a polymer chain, a hash line represents non-covalent bonding.

In contrast to supramolecular telechelic polymers with common UPy, Napy mechanophores,[30] which disrupt weak supramolecular forces upon stretching, double-helical foldamer is a three-dimensional chain-centered mechanophore which can answer to question if the binding affinity between non-covalent strands is more robust compared to a strain-polymer covalent bond. Stretching the system with non-covalent interactions can lead to the disruption of weak forces (Figure 3a), but the breakage of mechanically labile covalent bonds in the presence of weak supramolecular interactions is a possible scenario (Figure 3b). [31, 32]

1.2. Strain and cyclic mechanophores

Our group's approach towards developing a polymer mechanochemistry conceptual framework has started with a qualitative empirical understanding of mechanical phenomena using the idea of a molecular strain of mechanophores. The molecular strain is the underlying

concept of all mechanochemical activation processes due to the accelerated intrinsic reactivity of polymers.[2, 16, 33] To demonstrate this phenomenon, we can use the example of gem-dihalocyclopropane-based polymer. gDXC is a stable molecule at room temperature and needs billions of years to transform into a thermodynamically stable form.[16, 33] Shearing solid dihalocyclopropane at low temperatures forms the olefin in several hours, while shearing the dilute solution containing this material affords the product within minutes, and stretching the moiety using single-molecule force spectroscopy (SMFS) accelerates the formation of alkenes up to seconds.[8, 34, 35] Instead of using polymer chains attached at both ends of the mechanophore, we can attach inert hydrocarbon Z-stiff-stilbene to the macrocycle and irradiate at 400 nm, which switches Z-stiff-stilbene into strained E form, facilitating the opening of gDXC on the order of milliseconds (Figure 4).[7, 13, 35]

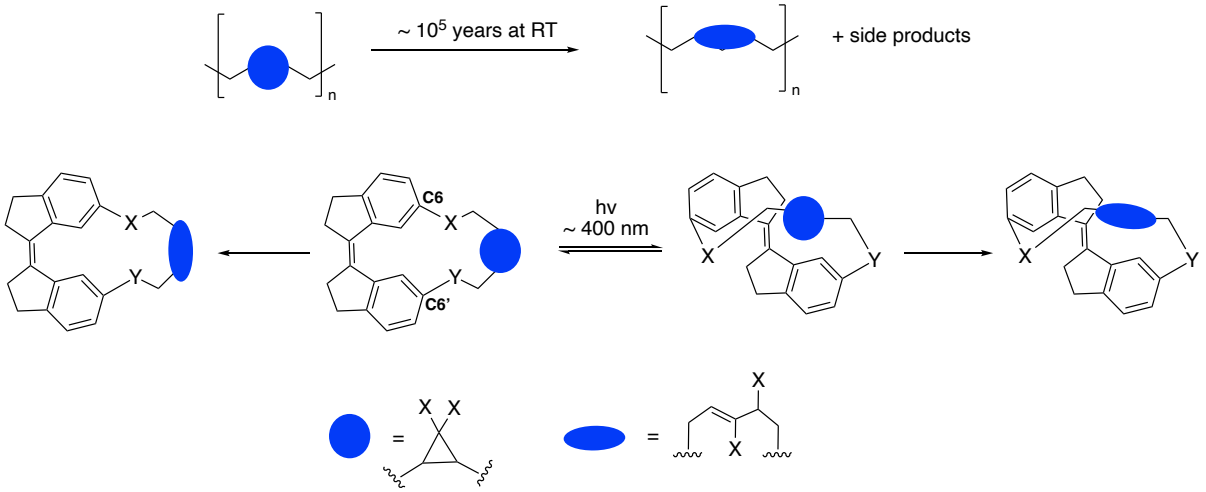

Figure 4. General scheme of mechanochemical transformation of gDXC incorporated polymer vs gDXC-functionalized stiff stilbene. [13, 35]

Despite considerable progress in the polymer mechanochemistry field today due to the qualitative description of the mechanochemical phenomena, establishing a quantitative model is still a non-trivial process. A way of approaching the problem of developing the

conceptual framework of mechanochemistry is solving the problem of quantifying molecular strain using the restoring force, which is a force required to transform strained object, for example, E-cycle, into its unstrained Z-form. Gaub and co-workers in 2002 showcased that a single chain of E-oligoazobenzene stretched between AFM tip and a glass slide can induce E to Z transition, which generates quantifiable restoring force.[12]

1.2.1. Stiff-stilbene

In 2009, our group discovered a new molecular force probe, stiff-stilbene, which has two stable E and Z isomers, like azobenzene, but with much higher activation energy (~60 kJ/mol) of thermal Z to E isomerization, in addition to greater conformational stiffness and clean isomerization by ~400 nm light.[2] From the synthetic perspective, strained derivatives of stiff-stilbene can be obtained by attaching a linker of 14 or fewer atoms at C6 and C6' atoms.[2]

The previous study's synthesis towards gDXC-functionalized stiff-stilbene macrocycle used indanone 2 as the precursor and McMurry coupling to afford Z-stiff-stilbene as a single isomer, followed by nucleophilic substitution to generate the desired macrocycles 3-6 (Scheme 2). [33]

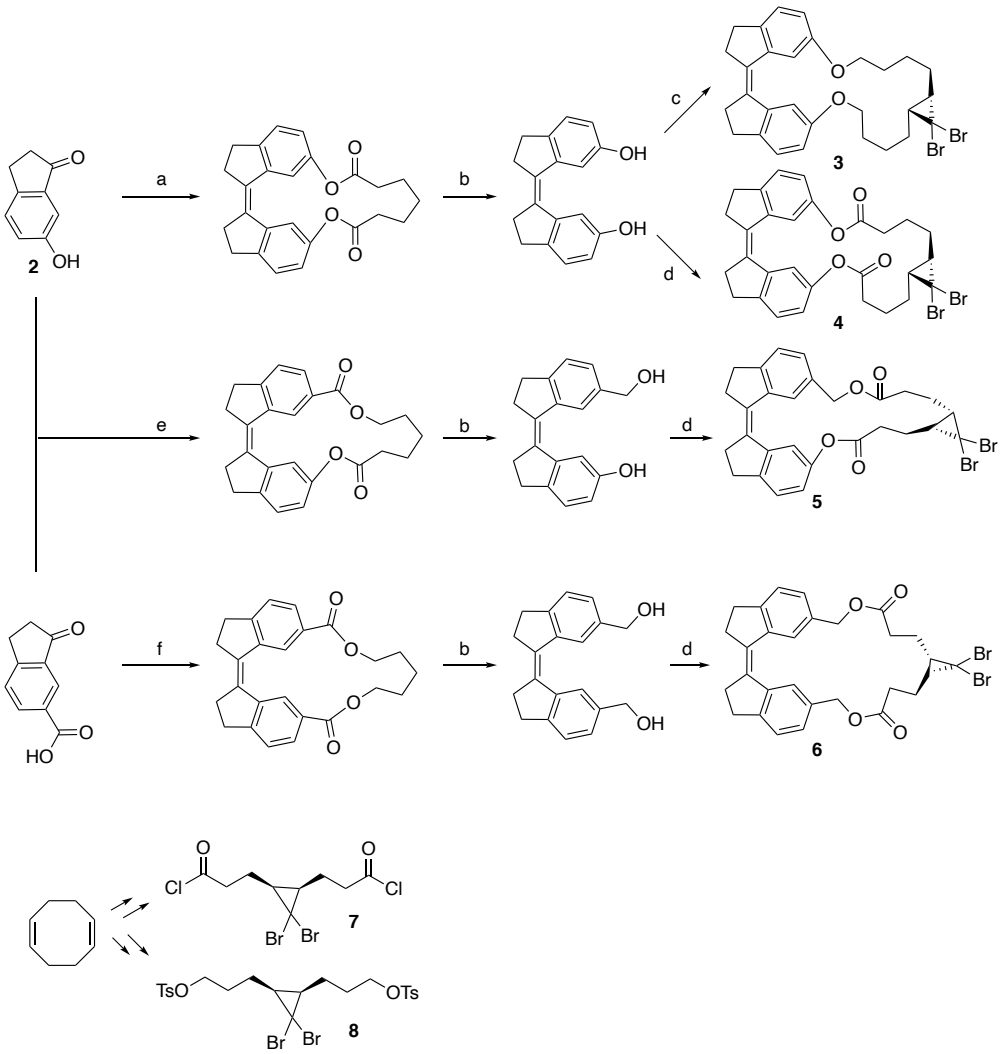

Scheme 2. Synthesis of stiff-stilbene macrocycles **3**-**6**. [33] Conditions: a) i) $ClC(O)(CH_2)_5C(O)Cl$, K_2CO_3, Bu_4NBr, DMF; ii) $TiCl_4$/Zn, THF; b) $LiAlH_4$, THF; c) **8,** Et_3N, $CHCl_3$; d) **7,** K_2CO_3, Bu_4NBr, DMF; e) $Br(CH_2)_5C(O)Cl$, K_2CO_3, Bu_4NBr, DMF; f) $Br(CH_2)_5Br$, K_2CO_3, Bu_4NBr, DMF.

To the best of our knowledge, stiff-stilbene is the only molecular force probe available,[13] which allows quantifying mechanochemical reactivity by measuring a restoring force directly upon stretching that makes stiff-stilbene highly attractive compared to other mechanophores. However, stiff stilbene has two major disadvantages[36] that do not allow it to be used in SMFS: (i) a much smaller applied maximum force for isomerization and (ii) the small size of the reactive sites that can be stretched. Our group's findings show that the UV application provides a strained E structure, which can be used as a measuring tool of strain

energy which is relevant to the almost linearly decreasing quantum yield (Figure 4). However, the proposed allosteric multimechanophore approach using ED-ROMP will allow measuring activation of stiff stilbene directly using SMFS of independent monomers and poorly understood activation effect of one mechanophore towards adjacent ones.

1.3. Supramolecular mechanophores

Non-covalent interactions such as π stacking and H-bonding are based on weaker and reversible intermolecular forces than covalent bonds. Biochemical processes such as molecular recognition, secondary, tertiary, and quaternary structure protein formation, DNA helices coiling, and many other vital processes affecting the structure and activity/function of the moiety are controlled by weak dynamic forces.[2, 37] Ideas of supramolecular chemistry such as host-guest interactions and molecular recognition have found applications in drug discovery, biological systems, engineering, materials chemistry, and molecular machines.[37] Exploiting supramolecular chemistry in the service of polymer science to create self-healing materials has gained much attention over recent years for the design of non-covalent polymers due to their abilities to recover their original mechanical properties after damage.[38]

The advantages of supramolecular forces over covalent mechanochemical bonds include the fast binding/unbinding dynamics, which allows the load-sensitive processes to be under thermodynamic or kinetic control, as dictated by potential applications.[39] The supramolecular 3D forces embedded into conventional materials like plastics or rubber lead to the formation of new smart materials with the ability to mimic the behaviour of biomolecules. These forces can be incorporated in various ways by forming supramolecular polymers, linear polymers with non-covalent cross-links, and arm polymers (dendrimers) with the non-covalent core.[1]

One approach to introduce supramolecular forces relies on dynamic load-bearing bonds that can dissociate reversibly, thus dissipating mechanical load into heat without undergoing irreversible failure of the network of the load-bearing bonds.[40] Reported examples of dynamic polymers include alkoxyamine bonds and Diels-Alder adducts, which can be regenerated upon heating the damaged material.[40] Non-covalent dynamic bonds offer the potential of autonomic self-repair, i.e., repair that does not require special treatment of the damaged material and can occur spontaneously during regular use. However, the existing solutions for autonomic self-repair come at the expense of reduced toughness, i.e., the amount of stress (energy per unit volume) that the material can sustain without failing.

Another fundamentally new approach focuses on the idea of a load-induced covalent bond scission in the presence of rigid three-dimensional supramolecular motifs' assembly as a chain-centered mechanophore. Previous efforts to understand the mechanochemical properties of supramolecular structures was limited to end-capped single helical foldamer with aromatic-aromatic and H-bonding intermolecular interactions or telechelic polymers, where supramolecular forces are parallel to the backbone, but, to our best knowledge, no examples of efficient design and synthesis of double- or higher stranded moieties, able to be employed as mechanophores (high dimerization constant, solubility, UV-Vis), currently exists.

1.3.1. Aromatic foldamers

Nature creates a fantastic variety of polymers' structures and functions using only 21 proteogenic amino acid building blocks, but synthetic chemistry has more tools and available abiotic monomers[41] to create a much broader library of non-natural materials, mimicking biopolymers. To exploit this field, foldamers or synthetic oligomers that adopt a well-defined

3D structure using non-covalent interactions have attracted many researchers over the last two decades. The chemistry of foldamers is promising but a poorly understood area of supramolecular chemistry, mimicking natural self-assembly behavior. [41-45] The incorporation of foldamers into polymers may lead to the discovery of new advanced materials with desired stress-sensing behavior dictated by potential applications.[2, 37] The design of such mechanophores would be comprised of units with easy synthetic accessibility, high 3D structural stability, rigid folding predictability, large dimerization constant, and solubility in non-polar solvents.[41]

Aromatic oligoamide foldamers[46-49] showcase most of these attractive properties with the tuning ability to afford α-helix-like structures.[48, 50] Para- and meta-substituted monomeric units form helical structures with a large hollow. Units size affects the diameter of the foldamer but does not affect the number of units per turn.[51] For transport, catalysis, or recognition purposes quinoline-based oligoamides with a larger diameter compared to pyridine-based strands will be a suitable choice. Alternatively, pyridine-based foldamers can increase their units per turn from 4.5 to 6 by introducing H-bonding at meta-positions relative to the backbone.[51, 52]

1.3.2. Synthesis and characterization of aromatic oligoamides

Despite considerable progress in developing efficient syntheses of abiotic foldamers, none can yield foldamers that even approach the size of biopolymers. To date, the longest protein-like foldamers have been pyridine/quinoline derivatives[42, 43] obtained by converged synthesis (Scheme 3, Scheme 4).[44]

The synthetic protocol uses a double segment strategy based on the coupling between acid chlorides and amines.[42, 43] First, carboxylic acid groups undergo activation using chlorinating agents or can be protected as esters, which can be saponified without affecting aromatic amide linkages. Amines can be prepared from nitro compounds by reduction or from carbamates by selective deprotection. Adopted segment-doubling protocol generally relies on the monomers' coupling to form dimers, which undergo another coupling to afford tetramers, etc., or two monomeric blocks, for example, amines, can be coupled to dichloride to generate the corresponding trimer, heptamer, etc. (Scheme 3, Scheme 4).[43]

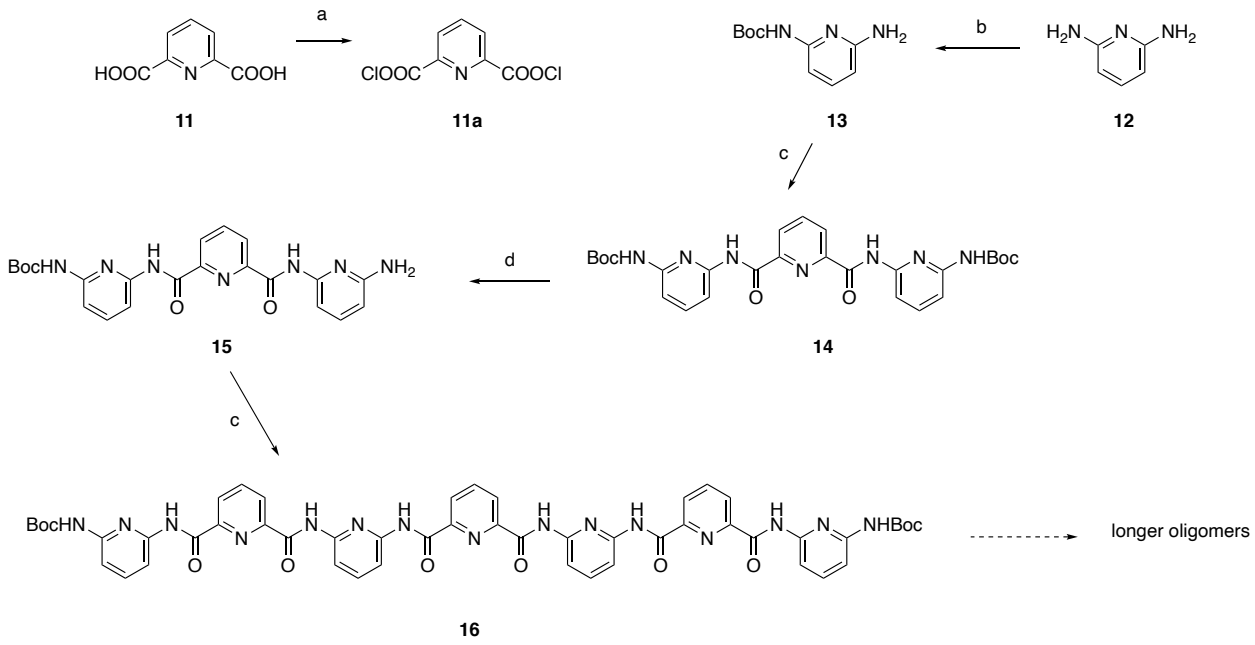

Scheme 3. Synthesis of heptamer **16**.[42] Conditions: a) $SOCl_2$, MeOH; b) $(Boc)_2O$, THF; c) i) DIPEA, THF, ii) **11a**, THF; d) TMSI, MeOH.

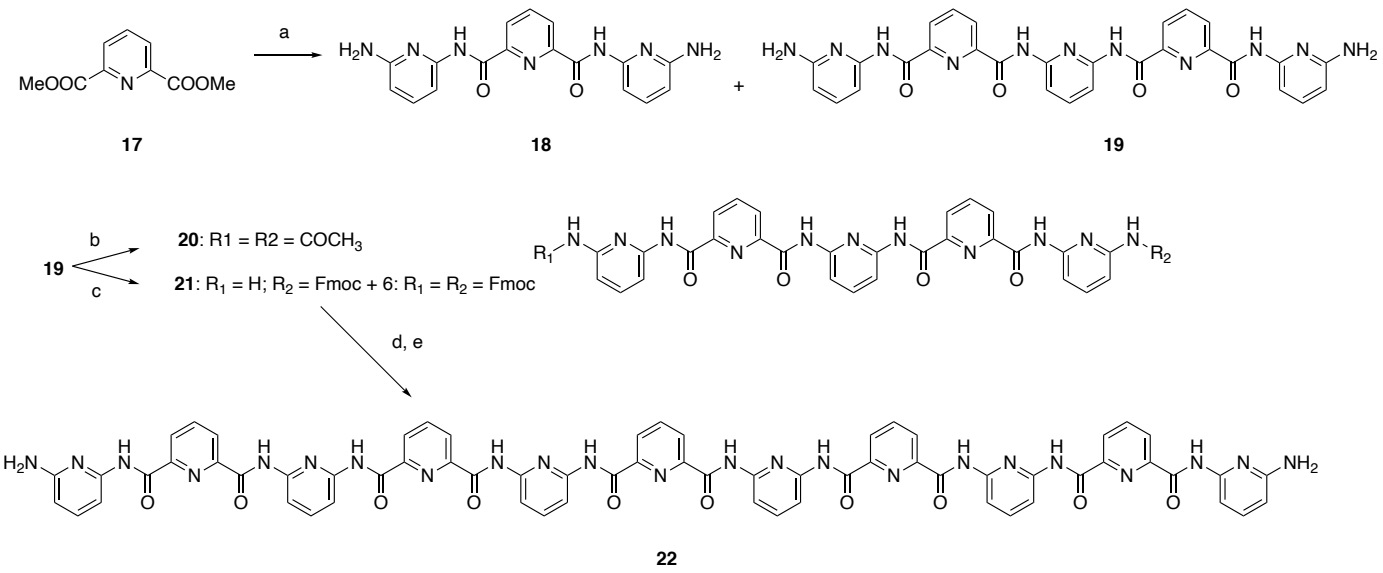

Scheme 4. Synthesis of 11mer **22**.[42] Conditions: a) 2,6-diaminopyridine, nBuLi, THF, - 78 °C ; b) CH_3COCl, NEt_3 , THF, RT ; c) FmocCl, NEt_3 , THF, RT ; d) 2,6-pyridinedicarbonyl dichloride, NEt_3 , THF, RT; e) piperidine, DMF.

The main techniques used to characterize the secondary structures of long aromatic foldamers are X-Ray and ^{1}H NMR spectroscopy.[42, 46-48, 50, 51] Despite the high accuracy of single-crystal X-Ray techniques, it is not always appropriate due to the solubility issues of oligomers.[47, 53] Deshielding of H-bonded amides and/or shielding of aromatic protons in π-π stacking can be easily observed and assigned on NMR spectra. Previous observations on NMR analysis concluded that proton amides, regardless of their location, in the middle or end of the structure, are the most shielded (Figure 5). If the explanation of the core protons shielding is apparent due to their location between aromatic rings, higher conformational mobility of strands at the periphery is the potential explanation for the chemical shift of the end amide groups' protons.[43]

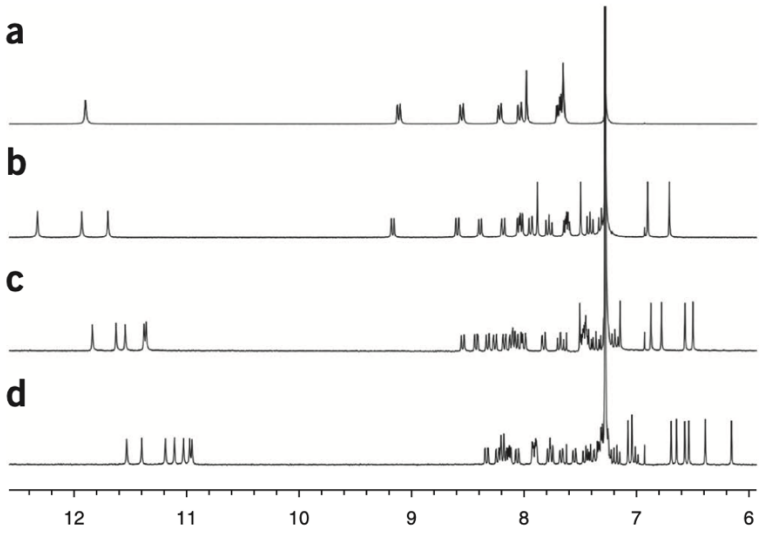

Figure 5. NMR of aromatic foldamers ($CDCl_3$, 25 °C, 300 MHz): a) dimer, b) tetramer, c) hexamer, d) octamer.[43]

Depending on the solvent, the concentration of the oligomer and its length, and the temperature, these oligomers either fold in a single helix or dimerize into a double helix.[46] Non-polar solvents (eg. chlorohydrocarbons), high concentrations and low temperatures favour dimerization (Figure 6). Even small amounts of H_2O destroy the double helix, presumably by interfering with the formation of H-bonds within the foldamer. The kinetics and thermodynamics of folding depend somewhat on the foldamer length and the nature of the side chains, with dimerization constant increasing and dissociation rates decreasing with as the number of aromatic moieties in the backbone and the overall length.[46, 54]

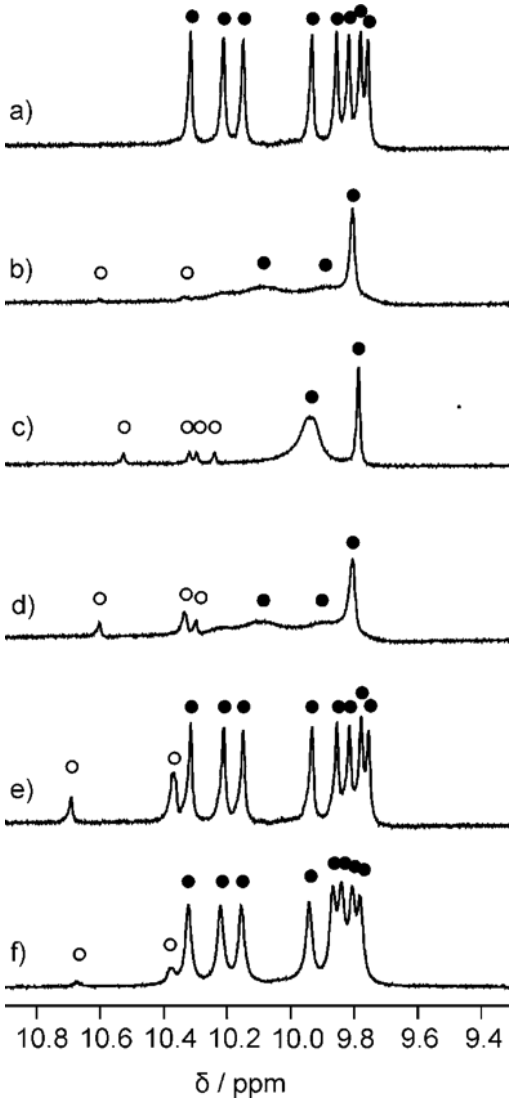

Figure 6. The evolution of foldamer's spectra with temperature and concentration. [50]

CHAPTER 2. BIS-STIFF-STILBENE MACROCYCLE

2.1. Overview

Essential to our synthetic route for obtaining a macrocyclic monomer **1**, the preparation of stiff-stilbene was necessary as an initial compound and was synthesized using an established procedure.[33] Before running the complex synthesis of the macrocycle **1**, the proposed conditions of ring-closure metathesis were tested on the model system, shown below (Scheme 5).

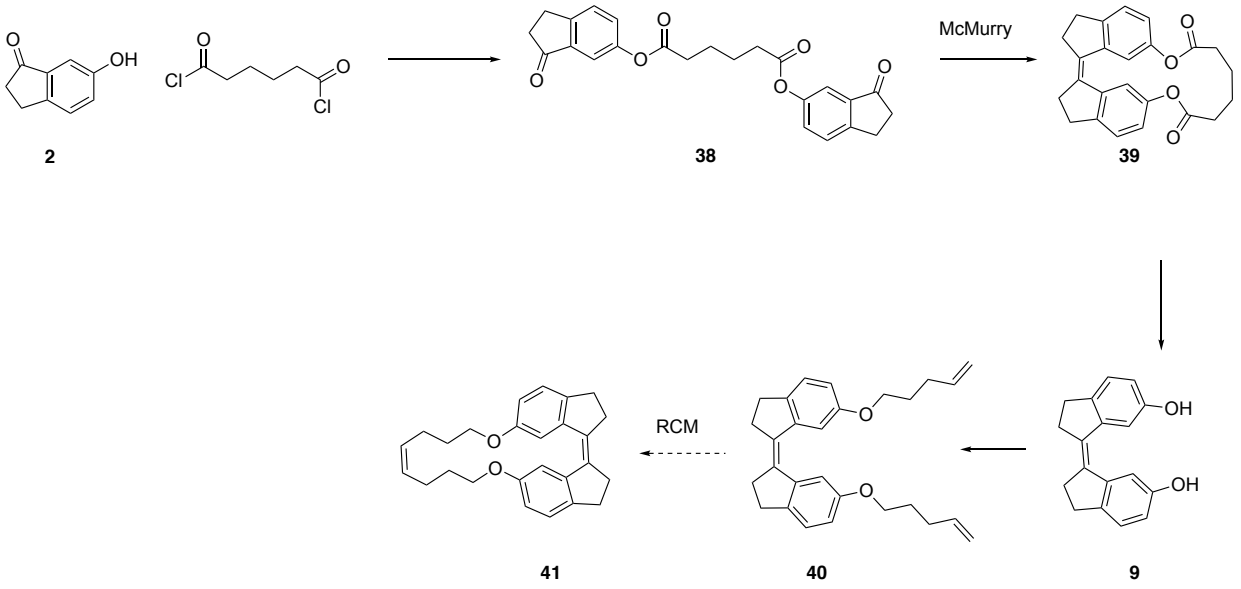

Scheme 5. Proposed synthesis of a model compound **41**

The next step was to find an efficient method towards second stiff stilbene formation, which is proposed by McMurry reaction, followed by RCM to afford a macrocycle **1** as the precursor for ROMP. The synthetic strategy of the general macrocyclic monomer **1** is based on the following retrosynthetic analysis (Scheme 6), using 6-hydroxyindanone **2** as the starting material, McMurry coupling, and ring-closure metathesis to close the ring and deliver the final monomeric product **1**.

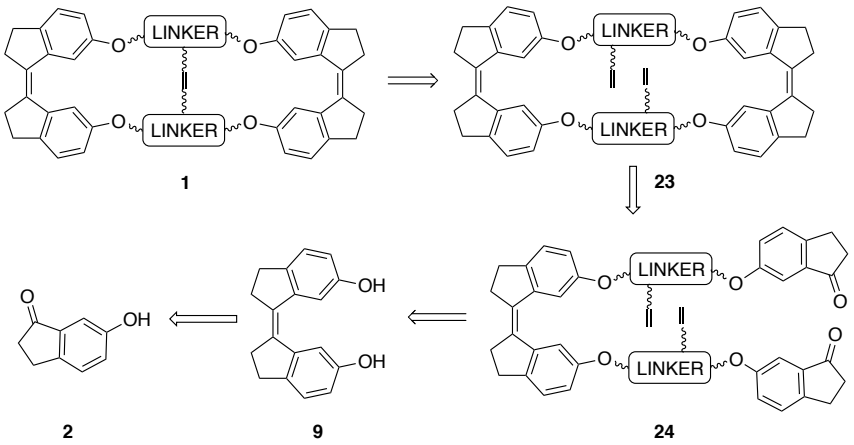

Scheme 6. Retrosynthesis of macrocycle **1.** A linker is a trisubstituted inert compound with two aliphatic sp^3 chains (wavy lines) and one aliphatic chain with a terminal alkene.

The main question to consider is if the proposed macrocycle **1** has enough strain relief to afford high molecular weight polymer suitable for quantifying response at a single molecular chain level. If not, what design modifications need to be made to afford a strained allosteric monomer. Therefore, the synthetic protocol is generalized that can be applied for a similar model with different linkers.

2.1.1. McMurry coupling

The McMurry reaction is one of the most powerful methods for synthesizinnng olefins from carbonyl reagents using the reductive coupling mechanism via a metallopinacol intermediate (Scheme 7). Mukaiyama,[55] Tyrlik,[56] and McMurry[57] discovered this coupling reaction independently in 1973 and 1974, but only McMurry's Ti(III)-$LiAlH_4$ system was found to be synthetically achievable. Nowadays, the McMurry coupling reaction is widely used to accomplish successful transformations of both aliphatic and aromatic aldehydes and ketones into the corresponding alkenes via intra- and intermolecular rearrangements.[58-60]

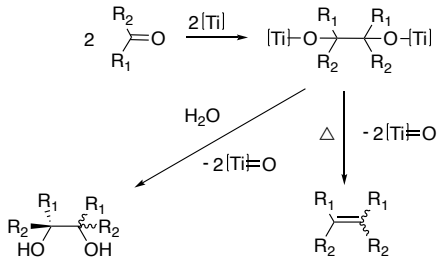

Scheme 7. Reductive coupling of ketones via a metallopinacol intermediate

The McMurry synthetic protocol is a critical step in our synthesis to form stiff-stilbene. McMurry reaction was previously used to create one stiff-stilbene-containing macrocycle, but the challenge of this work is to confirm the effectiveness of McMurry conditions to deliver coupling of the second stiff-stilbene in desired Z configuration the second Z-stiff-stilbene (Scheme 6, compound **23**). Up to our knowledge, no previous synthesis was established to form a macrocompound with two stiff-stilbene, and it is crucial to understand the structure-reactivity correlation of the macrocompound.

2.1.2. Ring-Closure Metathesis

Ring-Closure Metathesis [61-64] is a powerful and easy reaction to make a wide variety of organic rings, including medium & large-sized, hindered, strained, heterocyclic and polycyclic, using well-known Schrock[63] and Grubbs[64] catalysts as well as advanced fine-tuning catalysts (Figure 7).[65]

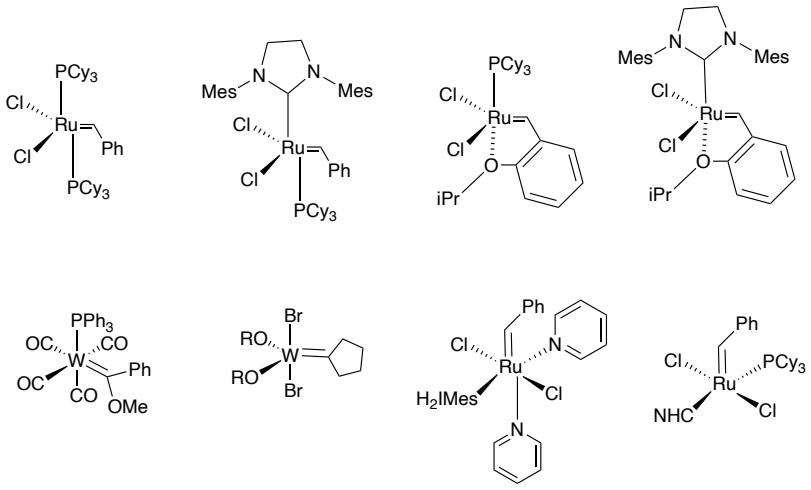

Figure 7. RCM catalysts[65]

However, as with any other cyclization method, the synthetic efficiency of RCM is limited by the competition between intramolecular ring-closing and intermolecular oligomerization reactions (Scheme 8).[66, 67] In most of the cases, RCM products are irreversible, but the reversibility of products still depends on the substrate, catalyst's choice and the experimental conditions (temperature, concentration, solvent).

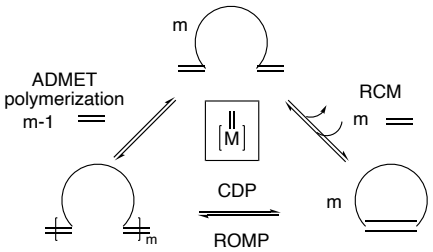

Scheme 8**.** Equilibrium between intramolecular ring-closing and intermolecular oligomerization reactions

For example, a change of Hoveyda catalyst to more reactive Schrock's Mo catalyst led to the successful transformation to ring **27**, but not dimer formation (Scheme 9).

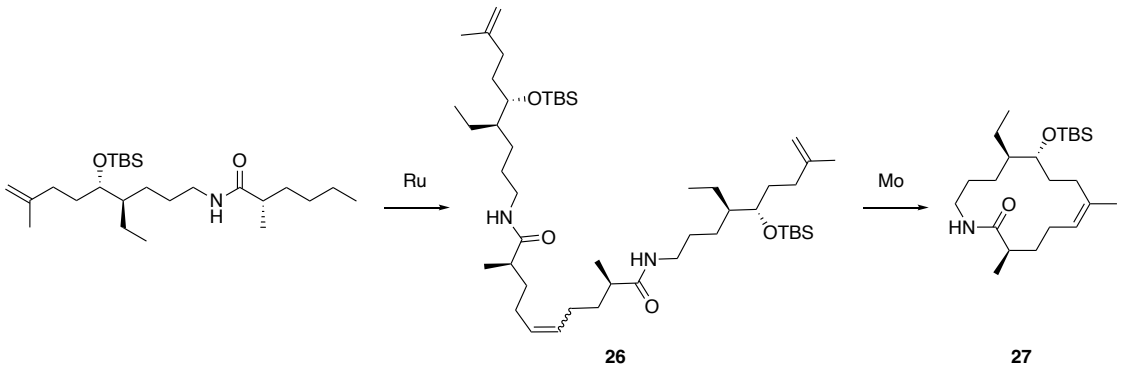

Scheme 9. RCM via dimer intermediate[68]

The standard conditions of RCM (Ru-based catalyst, DCM, RT) are widely employed to synthesize medium rings (5-7 members), but macrocycles remain a challenge and need a specific approach. Examples of RCM of macrocycles formation by coupling terminal olefins were accomplished using Ru catalysts and summarized below (Figure 8, Table 1).[65]

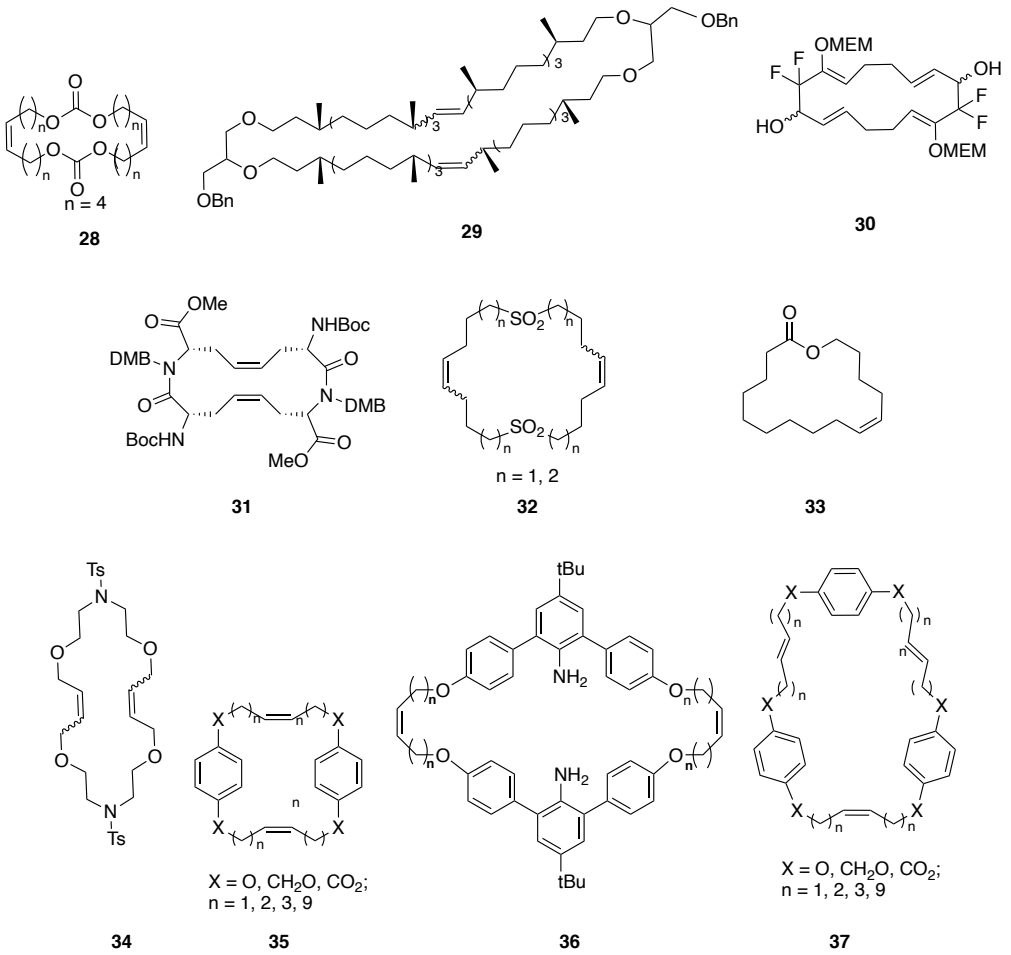

Figure 8. RCM products

Table 1. Reaction condition of RCM macrocycles[65]

Product	Catalyst	Experimental conditions	ref
28	Grubbs I	20 mM, DCM, reflux, 2-24 h	[69]
29	Grubbs I	3.8-29 mM, DCM, reflux, 12-42 h	[70]
30	Grubbs II	10 mM, DCM, reflux, 48h	[71]
31	Grubbs I, Grubbs II	3-100 mM, DCM, RT, 23h	[72]
32	Grubbs I, Grubbs II	25 mM, DCM, reflux, 4h	[73, 74]
33	Grubbs III	5 mM, $CDCl_3$, reflux, 1 h	[75]
34	Grubbs I	2 mM, DCM, RT, 15 h	[76]
35	Grubbs I, Grubbs II	5 mM, DCM, reflux, 14-32 h	[77]
36	Grubbs I, Grubbs II	0.3 mM, DCM, reflux, 48 h	[78]
37	Grubbs I, Grubbs II	5 mM, DCM, reflux, 14-32 h	[77]

According to the table above, the concentration is the main factor that controls ring-chain equilibria, and RCM product prefers highly concentrated solution, but examples below show that concentration can be as low as 3 mM at RT using first- or second-generation Grubb's catalyst in DCM. To maximize the yields of RCM products, sufficient time should be allowed at RT, but the reaction time can be much shortened at elevated temperatures.

Examples include the synthesis under Grubbs III catalysis that provides the desired RCM product in 1 hour at RT with 5 mM concentration and 5 mol% catalyst loading. Time was essential to afford the desired product as the reaction mixture after 15 min was dominated by oligomers, but after 1 hour the major product was compound **33**. A ring-chain equilibrium

under Grubbs III catalysts is highly dependent on the concentration and sufficient time to suppress the oligomerization of the RCM product **33**.

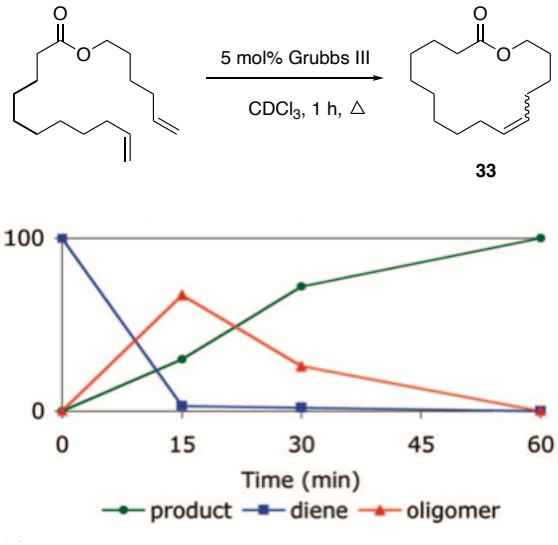

Figure 9. Monitoring the RCM reaction under Grubbs III catalysis as a function of time [65]

2.2. Synthesis of the Model compound

A stiff stilbene intermediate **9** was prepared based on our group's optimized route starting from 6-hydroxyindanone,[33] followed by the addition of terminal alkene chain and RCM based on several methods available in the literature (Table 1).

Diester **38**, prepared by the reaction of 6-hydroxyndanone and adipoyl dichloride in 75% yield, which further underwent McMurry coupling and gave the desired product **39**. The first trial of the McMurry reaction using metallic Zn resulted in a low-yielding product (45%), while the other two trials with powder Zn allowed increasing the yield up to 85%. A color change of the reaction mixture from dark-green to black is essential as, first, a solution of Zn in THF and $TiCl_4$

react to form reduced low valent Ti species, and then diester is slowly added to the solution (Scheme 10).

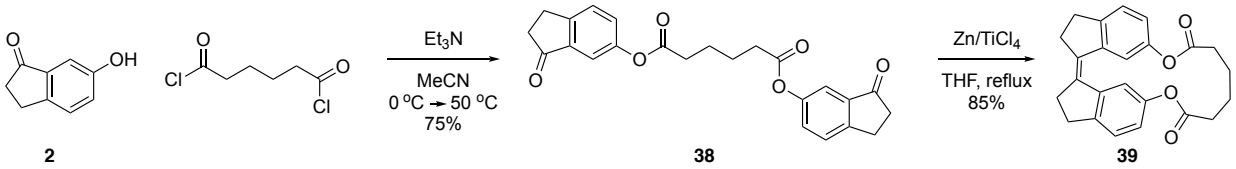

Scheme 10. Synthesis of compound **39**

Macrocycle **39** was further reduced to diol **9** using $LiAlH_4$, followed by the addition of bromopentene under basic conditions in DMF to form the corresponding **40** in 32% yield over two steps. The addition reaction of 5-bromopentene to stiff stilbene **9** at RT did not lead to any conversion, overnight heating at 45 °C provided a product in 35% yield, while heating at higher temperatures led to decomposition of starting materials (Scheme 11).

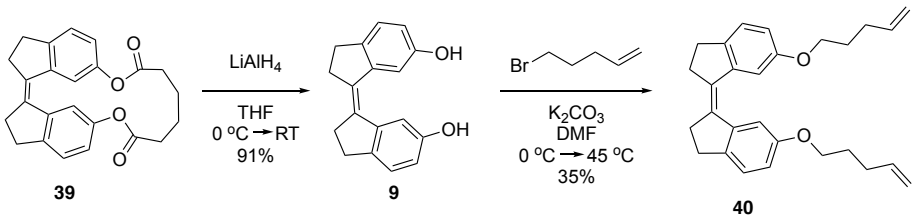

Scheme 11. Synthesis of compound **40**

To synthesize compound **41**, compound **40** underwent RCM in the presence of Grubbs II (10 mol%) at RT conditions and provided **41** as *Z* stiff-stilbene in a quantitative amount (Scheme 12). Compound **41** was characterized by NMR and HRMS (Figure 10).

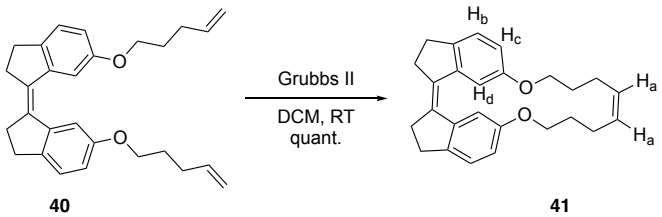

Scheme 12**.** RCM of compound **40**

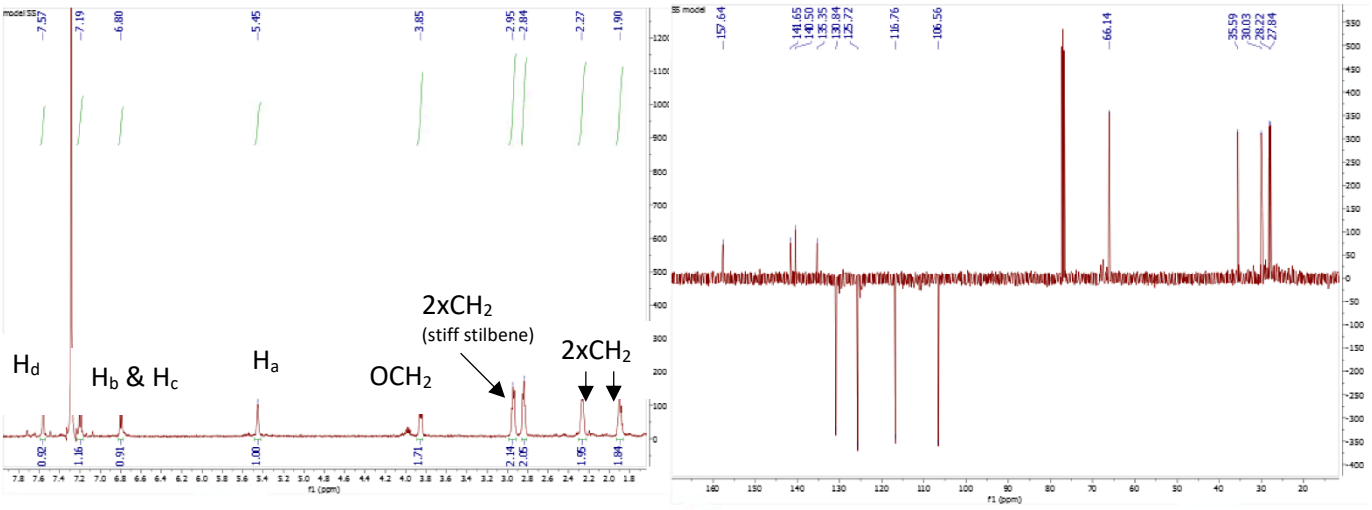

Figure 10. ^{1}H and ^{13}C NMR of a model stiff stilbene compound **41**

2.3. Synthesis of the stiff-stilbene macrocycle

A synthesis of bis-stiff-stilbene containing macrocycle was started by adopting previously reported literature procedures towards stiff-stilbene derivative **47**, using diol **42** as the initial material to connect indanones towards *Z*-stiff-stilbene formation (Scheme 13).[23, 79]

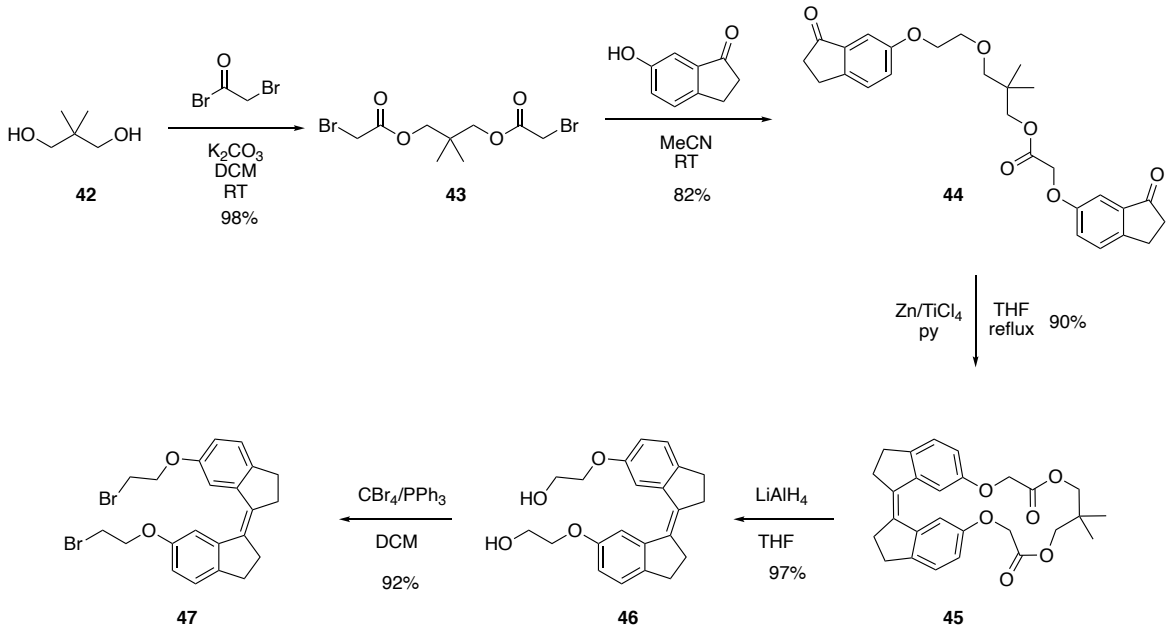

Scheme 13. Synthesis of stiff-stilbene unit

First, diol **42** was transformed into bromoester **43** using bromoacetyl bromide in basic conditions (Scheme 14). **43** proceeded to the next step without purification and yield matched previously reported ^{1}H NMR data.

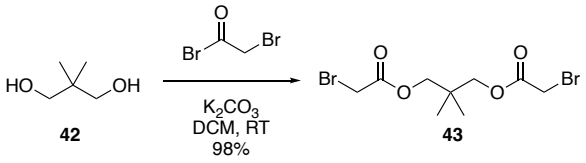

Scheme 14. Synthesis of compound **43**

Coupling of bromoester and 6-hydroxyindanone under basic conditions in acetonitrile afforded compound **44** as the precursor to McMurry reaction (Scheme 15). The literature reports the formation of **44** in 95% yield, which was sufficiently pure and did not require purification. During the synthesis, compound **44** underwent flash chromatography due to the presence of impurities on TLC place, which afforded a product in 82% yield.

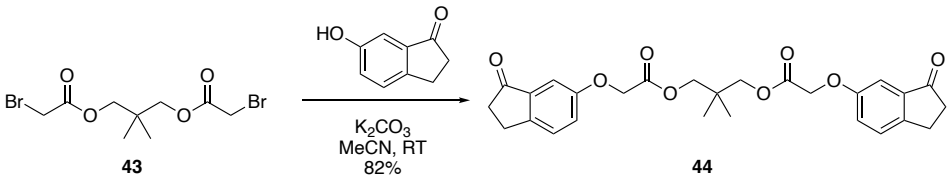

Scheme 15. Preparation of compound **44.**

Next step, the McMurry reaction was applied to the resulting diketone **44** to form Z-stiff-stilbene **45** in 90% yield (Scheme 16). The procedure of McMurry reaction was based on our group's protocol [79] without the addition of pyridine as described in the literature. [23] In this step, as described in the model study, a color change was essential before the slow addition of **44**. The moisture of solvent and glassware also affected the yield, flame-drying of glassware, and drying THF overnight over flame-dried molecular sieves allowed to obtain a yield of 90%.

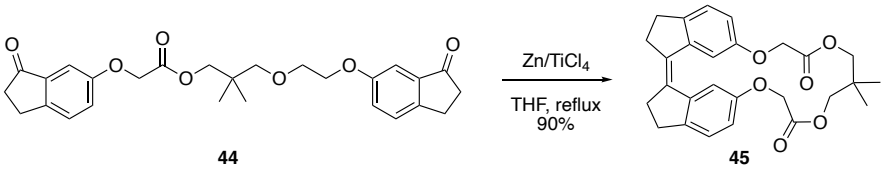

Scheme 16. McMurry reaction

The addition of reducing agent $LiAlH_4$ to the mixture of diester **45** in THF afforded diol **46** in h 97% yield (Scheme 17). Compound **46** was sufficiently pure to be used in the next step.

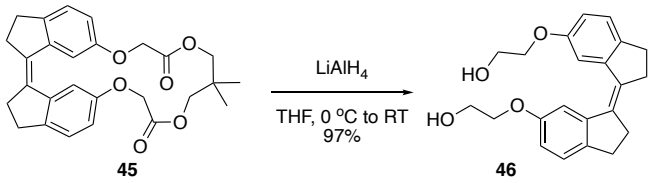

Scheme 17. Reduction of compound **45**

The next step was a bromination reaction using CBr_4 and freshly recrystallized PPh_3 and acetone/DCM mixture (1 drop of acetone per 5 mL of DCM) as a solvent, which provided **46** in 20 min at RT in 92% yield (Scheme 18).

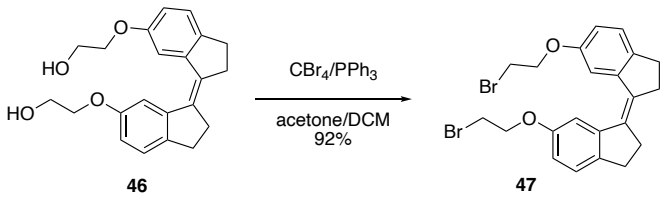

Scheme 18. Synthesis of compound **47**

The overall yield (64%) has been improved compared to the previous literature data (50%) on 14%, possibly due to recrystallized PPh_3 and fresh $LiAlH_4$.

The linker between stiff-stilbene units was synthesized using a simple commercially available trisubstituted aromatic ring. The essential components of the linker are hydroxyindanone derivative and terminal alkene, which react under McMurry and RCM conditions, respectively.

First, bromoalkene was attached to 3,5-dihydroxybenzoic acid to obtain ester **49** at RT in 85% yield (Scheme 19).

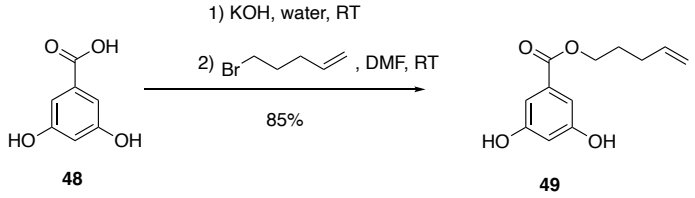

Scheme 19. Synthesis of compound **49**

The addition of dibromoethane to 6-hydroxyindanone in the presence of K_2CO_3 using acetone as solvent provided a new compound **50** in 75% yield (Scheme 20). Next, to a solution of **49** and K_2CO_3 in acetone, bromoindanone **50** was added in small portions to afford the linker **51** at 60 ^oC in 84% yield (Scheme 20).

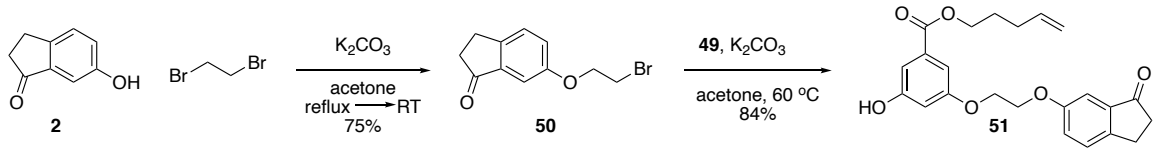

Scheme 20**.** Formation of **51**

The next step was a coupling reaction between stiff-stilbene unit **47** and a linker **51** to form a new compound **52** in the presence of base K_2CO_3 in DMF at RT in 82% yield (Scheme 21).

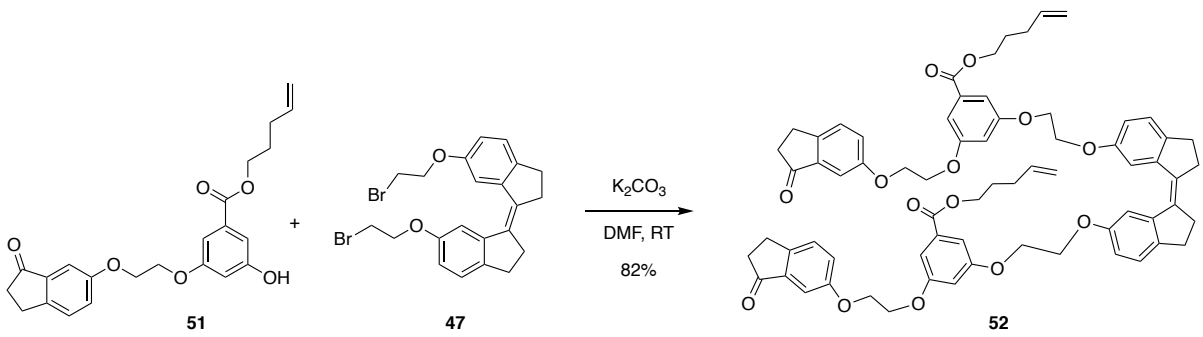

Scheme 21. Synthesis of compound **52**

The second McMurry coupling of to give a mixture of isomers **53** in 1:4 *E:Z* ratio by corresponding peak integration area of ^{1}H NMR peaks (Scheme 22, Figure 11, Figure 12). A new compound was fully characterized by ^{1}H NMR and HRMS.

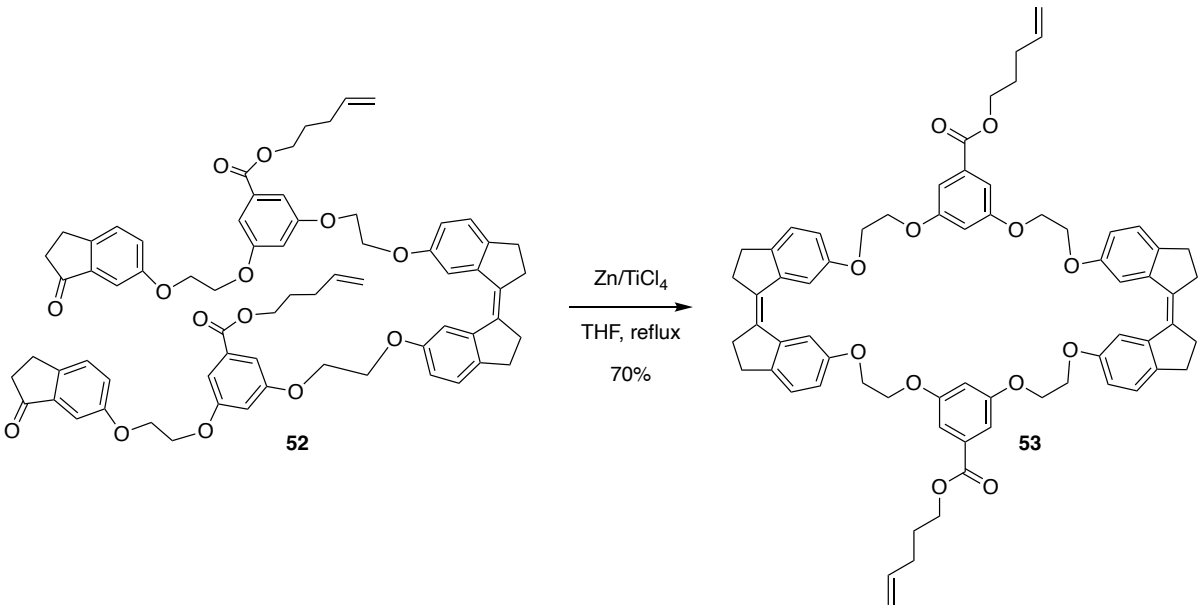

Scheme 22. Synthesis of macrocycle **53**

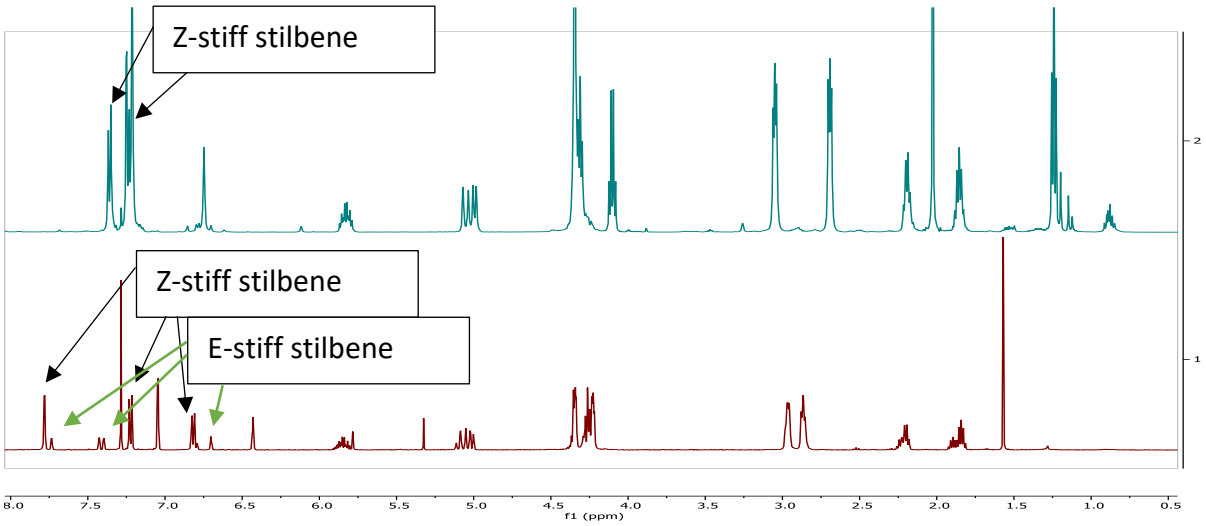

Figure 11. Stacked ^{1}H NMR spectra of compound **52** (top, green) and compound **53** (bottom, red). Aromatic hydrogens of stiff stilbene are indicated by arrows (the black arrow is for Z configuration; the green arrow is for E isomer).

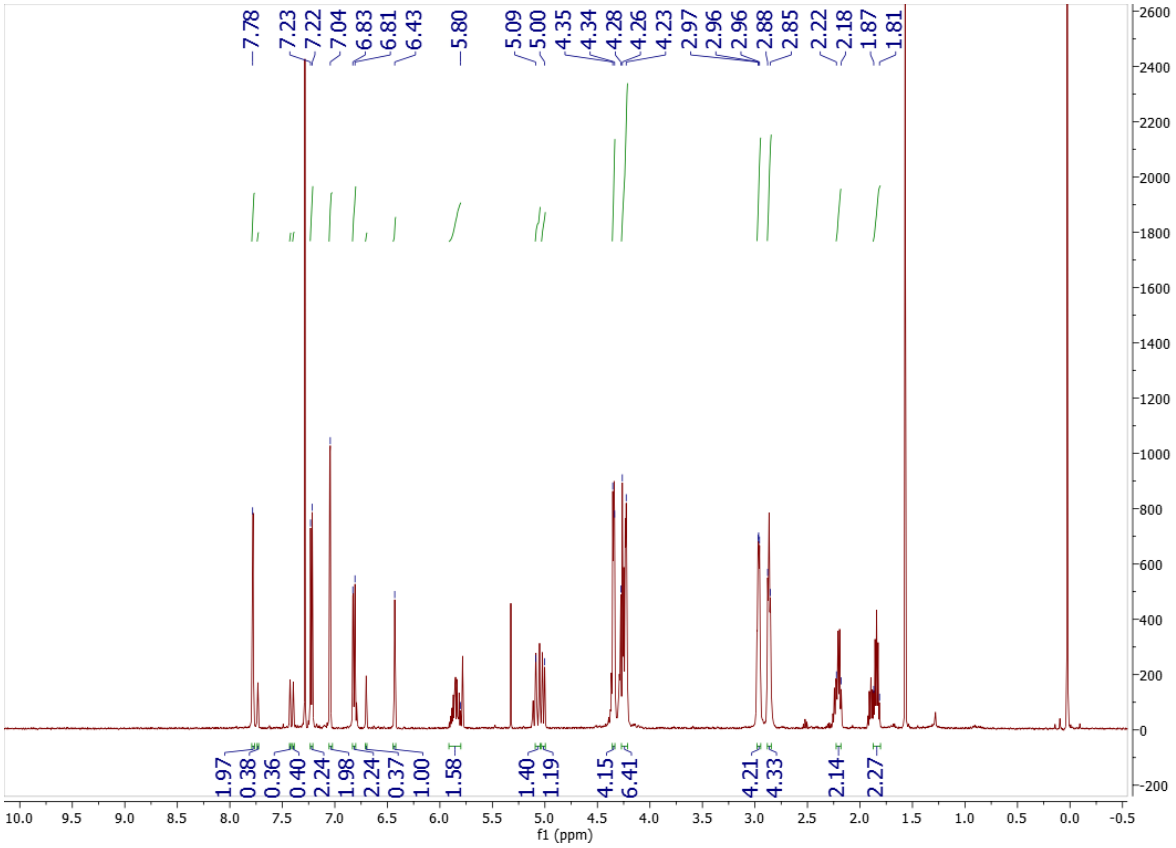

Figure 12. integrated ^{1}H NMR spectra of compound **53**. Integration values (E:Z) = 0.38:1.97; 0.36:1.98; 0.4:2.24.

To synthesize the desired macrocyclic stiff-stilbene monomer **54**, compound **53** underwent RCM in the presence of Grubbs II catalyst (5 mol%) and CsCl[80] (2 eq.) under reflux for 1 h (Scheme 23). The progress of the reaction was monitored by ^{1}H NMR until the alkene peaks at ~5.05 and ~5.85 ppm disappeared (Figure 13).

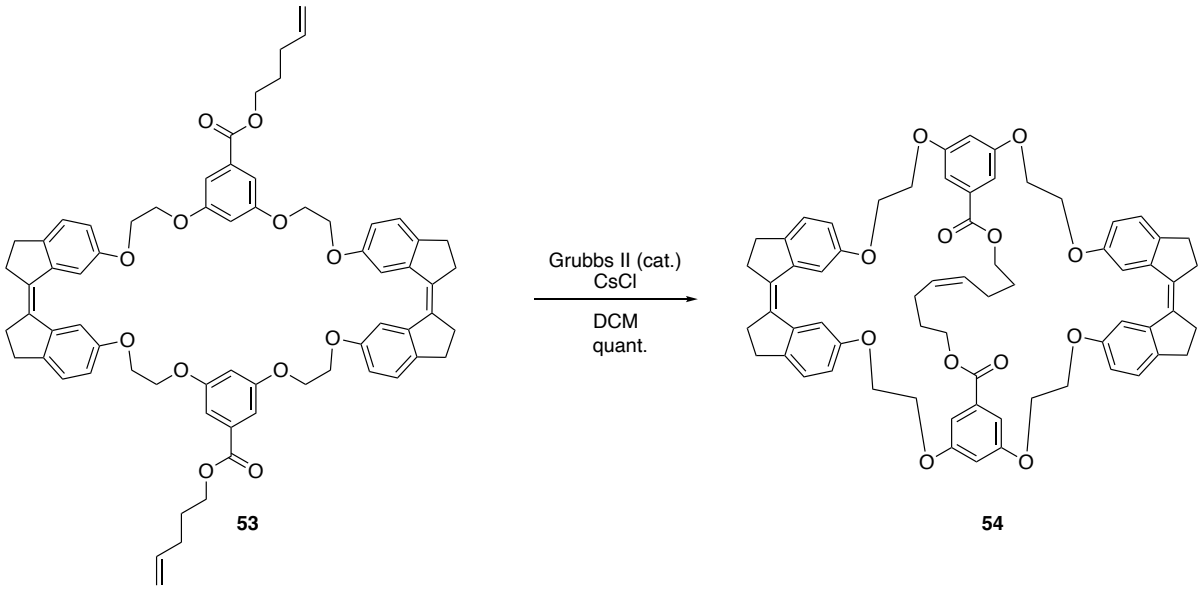

Scheme 23. RCM of compound **54**

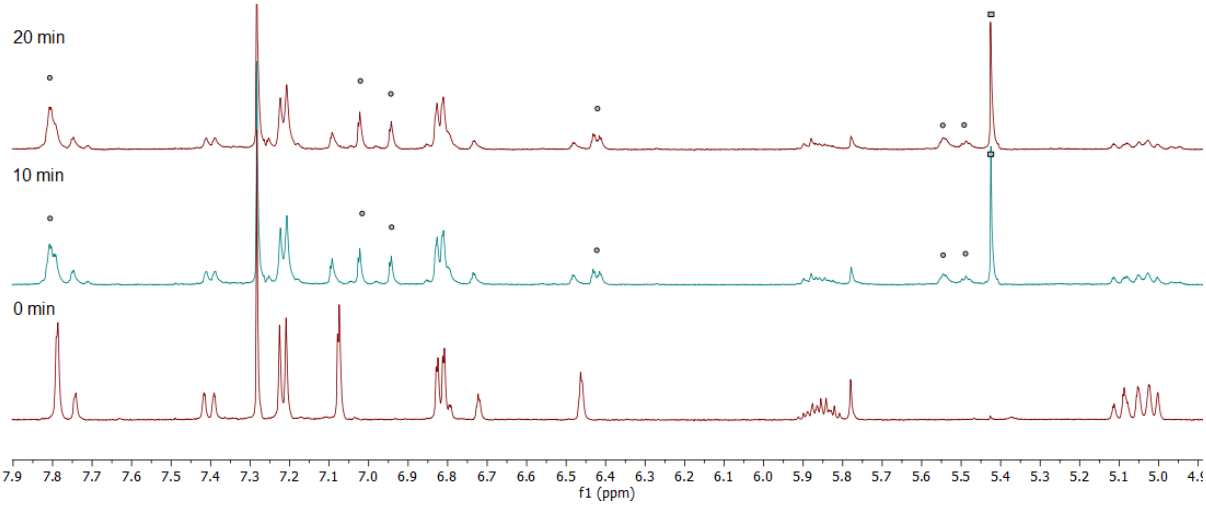

Figure 13. Excerpt of ^{1}H NMR spectra of the kinetic experiment of RCM reaction in the NMR tube at RT (t = 0 min; 10 min; 20 min). Dots-labeled peaks are assigned for compound **54**; ethylene peak is labeled by square.

No product of RCM reaction was observed in the presence of only Grubbs II catalyst at RT; by heating the reaction mixture, slight conversion was recorded. The presence of CsCl is essential due to the chelating properties of Cs^{+}.[80] The ethylene formation was observed (singlet at ~

5.40 ppm) using $CDCl_3$ as a solvent. The equilibrium was further driven to completion by removing the ethylene by-product by N_2 purging. With pyridine-based indenylidene Grubbs III, despite superior properties[81] such as excellent stability, faster initiation,[81, 82] and propagation[83] compared to phosphine ligands containing Ru catalysts, no reaction was observed during 1 h under the same conditions.

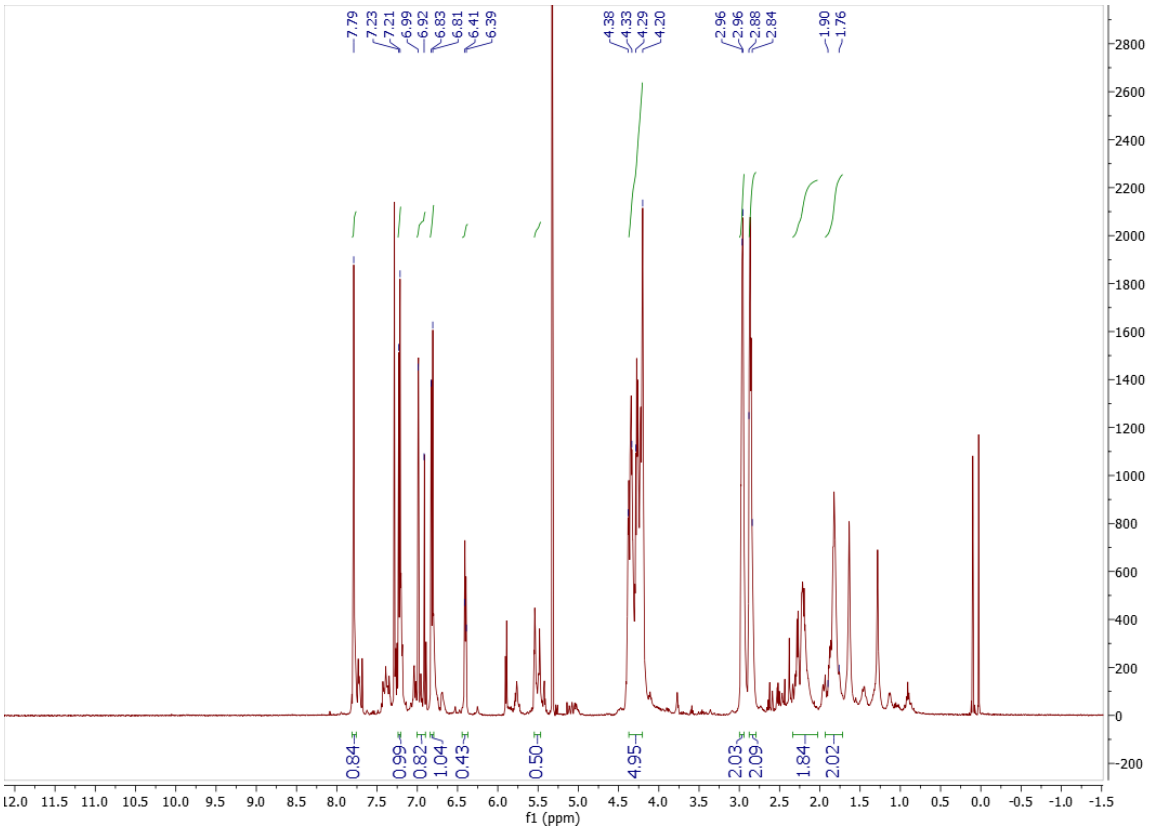

Figure 14. ^{1}H NMR of compound **54**.

Purification of separate isomers was not achievable using column chromatography, and characterization of **54** was done based on ^{1}H NMR and HRMS data. Due to broad alkene isomers peaks, appearing at 5.40 – 5.53 ppm, exact integration values cannot be calculated between cis and trans isomers.

2.4. Experimental

All reactions were performed under a nitrogen atmosphere using oven-dried glasswares unless otherwise stated. Solvents were purified by passing through activated alumina columns or used directly from a MBraun MB-SPS solvent purification system and were transferred under nitrogen. All reactions which required heating were conducted using oil bath on stirrer hotplates and the temperature controlled externally. Reactions requiring lower temperatures used the following cooling baths: -15 °C (NaCl/ice/water) and 0 °C (ice/water).

All reagents which were available commercially were purchased from Acros, Alfa Aesar, Fisher Scientific, Fluorochem, Sigma Aldrich or TCl.

PPh_3 was purified, firstly, by dissolving 20 g of PPh_3 in 150 mL of conc. HCl, followed by the addition of 150 mL of H_2O to form a precipitate that was filtered and recrystallized from EtOH/Et_2O (1:1) mixture.

Analytical TLC to monitor reactions and measure Rf values was carried out on Merck 60F254, aluminium support silica gel plates using short wave UV radiation (245 nm), potassium permanganate/Δ and vanillin/Δ as visualizing agents. Purification was done by column chromatography using CombiFlash Rf by Teledyne ISCO.

IR was recorded neat on a Perkin Elmer Spectrum 100-series FT-IR Spectrometer with Universal ATR Sampling Accessory in the total internal reflection mode between 600 cm-1 and 4000 cm-1 with the scan number of 4. Melting points were recorded using open glass capillaries on a Gallenkamp melting points apparatus and are uncorrected. UV-vis spectra were measured with a Cary 50 UV-vis spectrometer equipped with a multi-sample thermostatic holder from Quantum Technologies with the temperature set at 25 °C.

Analytical SEC was carried out on Waters Acquity UPLC system with an isocratic solvent manager, sample manager, column heater, photodiode array (PDA) detector and RI detector using three Waters Acquity APC columns in series (APC XT 900, 150 × 4.6 mm, APC XT 450, 150 × 4.6 mm, APC XT 200, 150 × 4.6 mm). The flow rate of THF is 0.6 mL/min. Column heater temperature is 35 ^{o}C. The PDA detector monitors absorbance of light of wavelength from 240 to 400 nm. The temperature of RI flow cell is 35 ^{o}C. All polymers solutions were filtered through PTFE syringe filters (pore size: 0.45 μm) prior to analysis. The SEC columns were calibrated using narrow polystyrene standards obtained from Sigma-Aldrich and Scientific Polymers Inc.

Mass spectra were recorded on a LCT, QTOF or LTQ Orbitrap XL spectrometer utilizing electrospray ionization (recorded in the positive mode) with a methanol, acetonitrile or acetonitile/NH_4OAc mobile phase, or electron impact ionization, and are reported as m/z (%). ^{1}H and ^{13}C NMR spectra were recorded on a Bruker AVIII500MHz spectrometer (^{1}H, 500 MHz; ^{13}C, 125 MHz, T = 295 K) in the solvents indicated. The solvent signals were used as references and the chemical shifts converted to the TMS scale, residual $CHCl_3$ (^{1}H, 7.26 ppm; ^{13}C, 77.16 ppm), MeOD (^{1}H, 3.31 ppm; ^{13}C, 49.00 ppm), DMSO (^{1}H, 2.50 ppm; ^{13}C, 39.52 ppm), C_6D_6 (^{1}H, 7.16 ppm; ^{13}C, 128.0 ppm). Coupling constants (J) are reported in Hz. The following abbreviations are used to describe multiplicity in ^{1}H-NMR: m (multiplet), s (singlet), d (doublet), t (triplet), q (quartet), br-broad. 1D ^{13}C-NMR spectra were recorded using CPD or APT pulse program from the Bruker standard pulse program library. 2D ^{1}H-^{13}C-NMR HSQC, ^{1}H-^{1}H-NMR COSY, and ^{1}H- ^{13}C-NMR HMBC spectra were recorded using the Bruker standard pulse program library. Spectra were processed using MestRenova and TopSpin.

Synthesis of bis(3-oxo-2,3-dihydro-1H-inden-5-yl) adipate 38

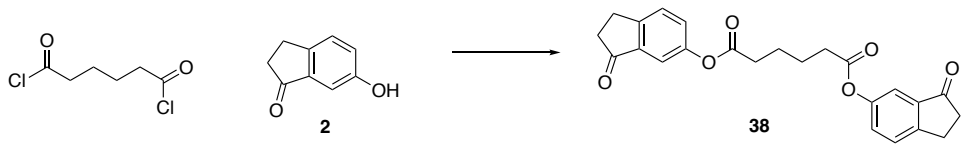

A new compound **38** was prepared using the literature procedure.[33]

Adipoyl dichloride (0.6 mL, 4.05 mmol) was added to a homogeneous solution of 6-hydroxy-2,3-dihydro-1H-inden-1-one (1 g, 6.75 mmol) and triethylamine (1.4 mL, 10.12 mmol) in 10 mL MeCN at 0 °C. The mixture was allowed to stir for 18 h at 50 °C overnight.

Upon completion, the solvent was evaporated, and the residue was extracted with EtOAc from water and dried over with Na_2SO_4. Purification by column chromatography (3:97 MeOH:DCM) afforded yellow solid in 83% yield (1.03 g).

^{1}H NMR (500 MHz, $CDCl_3$): 1.90 (quint, J = 3.6 Hz, 3.1 Hz; 4H, 2xCH_2CH$_2$C(O)O), 2.64-2.67 (m, 4H, 2xCCH_2CH$_2$C(O)), 2.71-2.75 (m, 4H, 2xCCH$_2$CH_2C(O)), 3.11-3.15 (m, 4H, 2xCH_2C(O)O), 7.31 (dd, J = 8.25 Hz, 2.25 Hz; 2H, 2xCCH$_{Ar}$CH_{Ar}CO), 7.45 (d, J = 2.25 Hz, 2H, 2xCCH_{Ar}CH$_{Ar}$CO), 7.48 (br s, J = 8.25 Hz, 2H, 2xCCH_{Ar}CO); ^{13}C NMR (125 MHz, $CDCl_3$): 23.9 (*C*H$_2$CH$_2$C(O)O), 29.4 (C*C*H$_2$CH$_2$C(O)), 33.7 ((CCH$_2$*C*H$_2$C(O))), 33.8 (CH$_2$*C*H$_2$C(O)O), 116.4 (*C*H$_{Ar}$CO), 127.5 (*C*H$_{Ar}$ *C*H$_{Ar}$CO), 128.3 (C*C*H$_{Ar}$CO), 138.3 (*C*C(O)), 150.0 (*C*CH$_2$), 152.3 (*C*OC(=O)), 162.3 (O*C*=O), 205.9 (*C*=O); HRMS (ESI, [M+Na]): obs. 429.1299, calcd. 429.1309.

Synthesis of ester 39

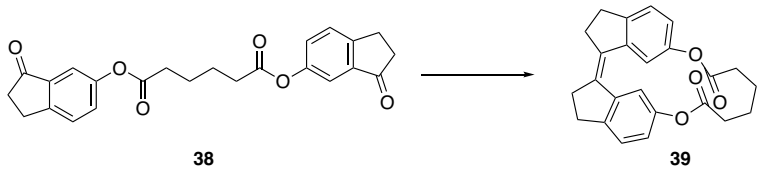

A new compound **39** was prepared using the literature procedure.[33]

A solution of zinc (4.83 g, 73.8 mmol) in THF (150 mL) was cooled to 0 °C, followed by the addition of titanium tetrachloride (4.1 mL, 36.9 mmol) under N_2. The mixture was refluxed for 1 hour (color was changed to black), followed by the addition of ester **38** (3 g, 7.38 mmol) in THF (10 mL) dropwise over 2 h. The reaction was completed in 1 h after full addition of ester and the mixture was filtered through Celite. As a work-up, water was added to the filtered mixture, and the product was extracted with EtOAc. Organic layer was dried over $MgSO_4$, concentrated, and purified using flash chromatography (100% DCM). Product **39** was formed as a yellow liquid (2.4 g) in 85%.

^{1}H NMR (500 MHz, $CDCl_3$): 1.86-1.91 (m, 4H, 2xCH_2CH$_2$C(O)O), 2.75-2.79 (m, 4H, 2xCCH_2CH$_2$C=), 2.81-2.84 (m, 4H, 2xCCH$_2$CH_2C=), 2.94-2.98 (m, 4H, 2xCH_2C(O)O), 6.80 (dd, J = 8.1 Hz, 2.0 Hz, 2H, 2xCCH$_{Ar}$CH_{Ar}CO), 7.22 (br d, J = 8.0 Hz, 2H, 2xCCH_{Ar}CH$_{Ar}$CO), 7.70 (d, J = 1.9 Hz, 2H, 2xCCH_{Ar}CO); ^{13}C NMR (125 MHz, $CDCl_3$): 24.1 (*C*H$_2$CH$_2$C(O)O) , 30.1 (*C*H$_2$CH$_2$C=), 34.4 (CH$_2$*C*H$_2$C=), 34.6 (*C*H$_2$C(O)O), 118.1 (*C*H$_{Ar}$CO), 120.0 (*C*H$_{Ar}$ *C*H$_{Ar}$CO), 135.1 (C*C*H$_{Ar}$CO), 141.3 (*C*C=), 145.4 (*C*CH$_2$), 148.6 (*C*O), 174.4(C=O).

Synthesis of (*Z*)-2,2',3,3'-tetrahydro-[1,1'-biindenylidene]-6,6'-diol

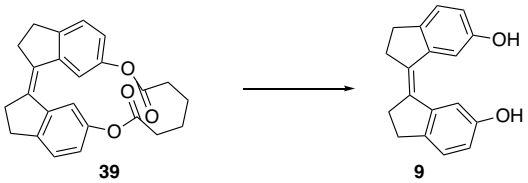

39 **9**

A known compound **9** was prepared using the literature procedure.[33]

To a solution of ester **39** (350 mg, 0.94 mmol) in THF (5 mL), lithium aluminum hydride (106 mg, 2.8 mmol) was added in several portions at 0 °C. The reaction was monitored by TLC. Upon completion, the mixture was cooled down to 0 °C and was quenched by water, followed by extraction with EtOAc. The organic layer was dried over $MgSO_4$, concentrated and purified

using flash chromatography (50:50 EtOAc: PE) to afford diol as a colorless oil (225 mg) in 91% yield.

^{1}H NMR (500 MHz, $CDCl_3$): 2.78-2.81 (m, 4H), 2.88-2.91 (m, 4H), 6.72 (dd, J = 8.1 Hz, 2.2 Hz, 2H), 7.12 (d, J = 8.1 Hz, 2H), 7.69 (d, J = 2.1 Hz, 2H); ^{13}C NMR (125 MHz, $CDCl_3$): 29.7, 35.1, 110.6, 114.8, 125.8, 135.4, 140.8, 141.6, 153.3. MS (ESI, [M+H]): 265.2, calcd. 265.1.

Synthesis of (*Z*)-6,6'-bis(pent-4-en-1-yloxy)-2,2',3,3'-tetrahydro-1,1'-biindenylidene

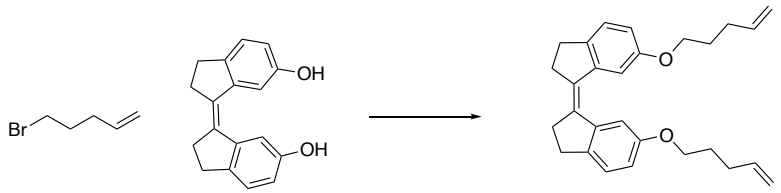

9 **40**

A new compound **40** was prepared using the procedure below.

To a solution of diol **9** (225 mg, 0.85 mmol) in DMF (3 mL), K_2CO_3 (353 mg, 2.55 mmol) was added, followed by the addition of bromopentene (254 mg, 1.7 mmol) at 0 °C. The mixture was heated at 45-50 °C overnight, followed by the extraction with EtOAc. Purification by flash chromatography (5:95 MeOH:DCM) afforded an ether **40** in 35% yield as a yellow oil (0.12 g). ^{1}H NMR (500 MHz, $CDCl_3$): 1.84 (quint, J = 7.0 Hz, 6.5 Hz, 4H, 2xOCH_2CH_2), 2.21 (q, J = 7.6 Hz, 7.1 Hz, 4H, 2x$OCH_2CH_2CH_2$), 2.80-2.83 (m, 4H, 2xCCH_2CH_2C=), 2.91-2.93 (m, 4H, 2xCCH_2CH_2C=), 3.93 (t, J = 6.3 Hz, 4H, 2xOCH_2), 5.01 (dd, J = 35.6 Hz, 10.7 Hz, 4H, 2xCH=CH_2), 5.79-5.88 (m, 2H, 2xC*H*=CH_2), 6.75 (dd, J = 8.2 Hz, 2.2 Hz, 2H, 2x$CCH_{Ar}CH_{Ar}CO$), 7.17 (d, J = 8.2 Hz, 2H, 2x$CCH_{Ar}CH_{Ar}CO$), 7.64 (d, J = 2.1 Hz, 2H, 2x$CCH_{Ar}CO$); ^{13}C NMR (125 MHz, $CDCl_3$): 28.6 (OCH_2CH_2), 29.9 ($OCH_2CH_2CH_2$), 30.2 (=CCH_2), 35.4(=CCH_2CH_2), 67.4 (OCH_2), 109.2 ($CCH_{Ar}CO$), 114.6 ($CH_{Ar}CH_{Ar}CO$), 115.1 (CH_2=CH), 125.5 ($CCH_{Ar}CH_{Ar}CO$), 135.4 (*C*=*C*), 137.8 (*C*H=CH_2), 140.6 ($CCH_{Ar}CH_{Ar}CO$), 141.6 ($CCH_{Ar}CO$), 157.4 (*C*O); HRMS (ESI, [M+H]): 401.2464, calcd. 401. 2475.

Synthesis of model compound 41

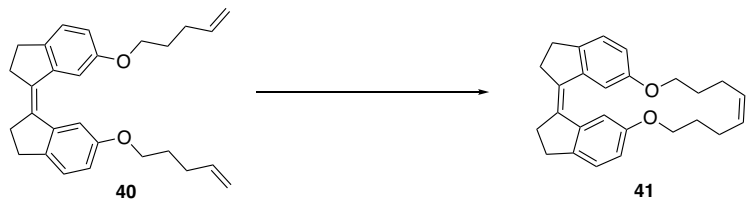

40 41

A new compound **41** was prepared using the procedure below.

To a solution of ether **40** (100 mg, 0.25 mmol) in DCM (3 mL), Grubbs II catalyst (10 mg, 0.012 mmol) were added under N_2 atmosphere at RT. The reaction mixture was monitored by NMR and was finished in 3 h, followed by filtration using Celite and extraction with DCM to afford a model compound **41** as brown solid (90 mg) in quantitative yield.

^{1}H NMR (500 MHz, $CDCl_3$): 1.85-1.88 (m, 4H, 2xOCH$_2$C*H$_2$*), 2.21-2.26 (m, 4H, 2xOCH$_2$CH$_2$C*H$_2$*), 2.80-2.83 (m, 4H, 2xCC*H$_2$*CH$_2$C=), 2.91-2.93 (m, 4H, 2xCCH$_2$C*H$_2$*C=), 3.83 (t, 4H, J = 6.2 Hz, 2xOC*H$_2$*), 5.43 (app t, J = 3.2 Hz, 2H, C*H*=C*H*), 6.77 (dd, J = 7.9 Hz, 2.0 Hz, 2H, 2xCCH$_{Ar}$C*H$_{Ar}$*CO), 7.17 (d, 2H, J = 8.4 Hz, 2xCC*H$_{Ar}$*CH$_{Ar}$CO), 7.54 (d, 2H, J = 2.2 Hz, 2xCC*H$_{Ar}$*CO); ^{13}C NMR (125 MHz, $CDCl_3$): 27.8 (OCH$_2$*C*H$_2$) , 28.2 (OCH$_2$CH$_2$*C*H$_2$) , 30.0 (=C*C*H$_2$) , 35.6 (=CCH$_2$*C*H$_2$), 66.1 (O*C*H$_2$), 106.5 (C*C*H$_{Ar}$CO), 116.7 (CH$_{Ar}$*C*H$_{Ar}$CO), 125.7 (*C*H=*C*H), 130.8 (C*C*H$_{Ar}$CH$_{Ar}$CO), 135.3 (*C*=*C*), 140.5 (*C*CH$_{Ar}$CH$_{Ar}$CO), 141.6 (*C*CH$_{Ar}$CO), 157.6 (*C*O); HRMS (ESI, [M+H]): 373.2151, calcd. 373.2162.

Synthesis of 2,2-dimethylpropane-1,3-diyl bis(2-bromoacetate)[23]

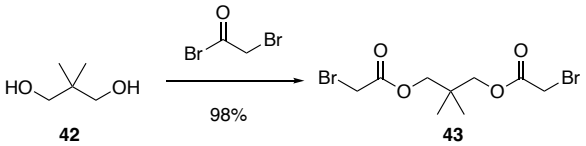

42 43

A known compound **43** was prepared using the literature procedure. [23]

To a solution 2,2-dimethylpropane-1,3-diol (1.04 g, 9.99 mmol) and K_2CO_3 (5.52 g, 39.9 mmol) in 60 mL dry CH_2Cl_2 was added 2-bromoacetyl bromide (1.827 ml, 20.97 mmol) then the

mixture was stirred at room temperature for 5 h. The mixture was washed with water (100 ml) three times. The collected organic phase was concentrated to afford a colorless oil (3.40 g, 98%).

^{1}H NMR ($CDCl_3$, 500 MHz): 0.98 (s, 6H, 2C*H*$_3$), 3.81 (s, 4H, 2xOC*H*$_2$), 3.96 (s, 4H, 2xC*H*$_2$Br); ^{13}C NMR ($CDCl_3$, 125 MHz): 21.4, 25.5, 35.0, 70.3, 166.9; MS (ESI, [M+NH_4]): 364.0

Synthesis of 2,2-dimethylpropane-1,3-diyl bis(2-((3-oxo-2,3-dihydro-1H-inden-5-yl)oxy)acetate)

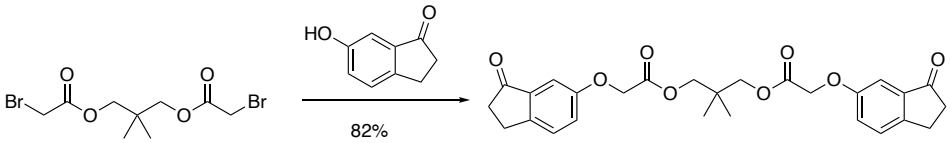

43 **44**

A known compound **44** was prepared using the literature procedure. [23]

To a solution of 2,2-dimethylpropane-1,3-diyl bis(2-bromoacetate) (1.7 g, 4.91 mmol) in MeCN (20 mL) was added 6-hydroxy-2,3-dihydro-1H-inden-1-one (1.52 g, 10.26 mmol), followed by the addition of K_2CO_3 (2.76 g, 19.97 mmol). The reaction mixture was allowed to stir at RT over 12 h. Upon completion, the reaction mixture was washed with brine, and dried over Na_2SO_4. Purification by flash chromatography (30:70 EtOAc:PE) afforded the product **44** as a white solid (1.93 g) in 82% yield.

IR: 1735, 1690; ^{1}H NMR ($CDCl_3$, 500 MHz): 0.89 (s, 3H, 2xC*H*$_3$), 2.69 (t, 4H, 2xCH_2C*H*$_2$C=O), 3.05 (t, 4H, 2xC*H*$_2$$CH_2$C=O), 3.85 (s, 4H, 2xCC*H*$_2$O), 4.67 (s, 4H, 2xC*H*$_2$O), 7.11 (d, 2H, 2xC*H*$_{Ar}$), 7.24 (dd, 2H, 2xC*H*$_{Ar}$), 7.38 (d, 2H, 2xC*H*$_{Ar}$); ^{13}C NMR ($CDCl_3$, 125 MHz): 21.5, 25.1, 34.6, 36.9, 65.1, 69.5, 105.7, 124.4, 127.7, 138.1, 147.1, 157.4, 168.3, 206.7.

Synthesis of 6-(2-bromoethoxy)-2,3-dihydro-1H-inden-1-one

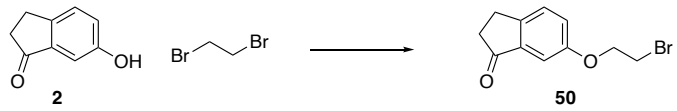

2 50

A known compound **50** was prepared using the literature procedure.[79]

To a solution of 6-hydroxy-2,3-dihydro-1H-inden-1-one (1 g, 6.75 mmol) in 70 mL acetone was added 1,2-dibromoethane (3.51 ml, 40.5 mmol) and K_2CO_3 (1.399 g, 10.12 mmol), then the mixture was stirred under reflux overnight.

The reaction mixture was cooled down to RT, poured into water, and extracted with DCM three times. The combined organic layer was dried over $MgSO_4$, filtered, and evaporated under reduced pressure. The purification using flash chromatography (25:75 EtOAc:PE) afforded a product as a white solid (1.3 g) in 75% yield.

^{1}H NMR ($CDCl_3$, 500 MHz): 2.72 (t, J = 5.80 Hz, 5.65 Hz, 2H, CH_2CH_2C=O), 3.08 (t, J = 5.85 Hz, 5.55 Hz, 2H, CH_2CH_2C=O), 3.65 (t, J = 6.0 Hz, 2H, OCH_2), 4.32 (t, J = 6.0 Hz, 2H, CH_2Br), 7.17 (d, J =2.5 Hz, 1H, CH_{Ar}), 7.23 (dd, J = 8.3 Hz, 2.5 Hz, 1H, CH_{Ar}), 7.39 (d, J = 8.3 Hz, 1H, CH_{Ar}); ^{13}C NMR ($CDCl_3$, 125 MHz): 25.1, 28.9, 37.0, 68.1, 105.9, 124.5, 127.6, 138.3, 148.6, 157.8, 206.7; MS (CI, [M+H]): 255.

Synthesis of compound 45

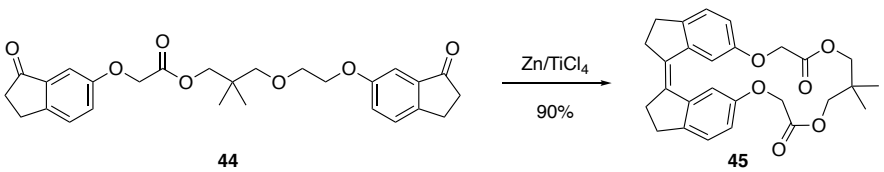

44 45

A known compound **45** was prepared using the literature procedure. [23]

To a rapidly stirred solution of zinc (1.701 g, 26.0 mmol) in anhydrous THF (25 mL), titanium (IV) chloride (1.974 g, 10.41 mmol) was added dropwise at 0 °C, followed by reflux for 1 h.

Then, 2,2-dimethylpropane-1,3-diyl bis(2-((3-oxo-2,3-dihydro-1H-inden-5-yl)oxy)acetate) (0.5 g, 1.041 mmol) was slowly added over a 5 h period. When the addition was finished, the reaction was allowed to reflux for additional 30 min. The reaction mixture was cooled down to RT, washed with saturated solution of K_2CO_3, filtered through Celite and extracted with DCM. Purification by flash chromatography (100% DCM) afforded a product as a white solid (0.42 g, 90%).

IR: 1760, 1621, 1188; ^{1}H NMR ($CDCl_3$, 500 MHz): 0.85 (s, 6H, 2xC*H*$_3$), 2.80-2.83 (m, 4H, 2xCH$_2$C*H*$_2$C=O), 2.91-2.93 (m, 4H, 2xC*H*$_2$CH$_2$C=O), 4.04 (s, 4H, 2xCC*H*$_2$O), 4.69 (s, 4H, 2xOC*H*$_2$), 6.77 (dd, 2H, J = 8.6 Hz, 1.8 Hz, 2x C*H*$_{Ar}$), 7.18 (d, J = 8.2 Hz, 2H, 2xC*H*$_{Ar}$), 7.67 (d, J = 1.4 Hz, 2H, 2xC*H*$_{Ar}$); ^{13}C NMR ($CDCl_3$, 125 MHz): 21.5, 29.7, 34.8, 35.1, 66.0, 72.6, 109.6, 114.1, 125.7, 135.4, 141.5, 141.7, 156.3, 169.1.

Synthesis of pent-4-en-1-yl 3,5-dihydroxybenzoate

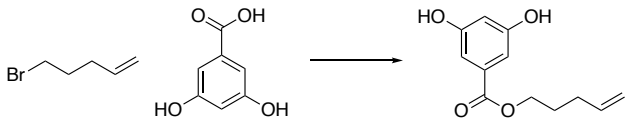

48 **49**

A new compound **49** was prepared using the procedure below.

To a solution of 3,5-dihydroxybenzoic acid (1 g, 6.49 mmol) in water (20 mL), KOH (0.546 g, 9.73 mmol) was added. The resulting mixture was refluxed for 30 min, followed by evaporation under reduced pressure. Then, the resulting salt was dissolved in DMF (20 mL), followed by the addition of 5-bromopent-1-ene (1.450 g, 9.73 mmol). The mixture was allowed to stir at RT over 24 h. Upon completion, DCM was added, and the reaction mixture was washed with brine, and the organic layer was dried over Na_2SO_4. Purification by flash chromatography (3:97 MeOH:DCM) afforded a product as a colorless oil (1.2 g, 83%).

IR: 3350, 1689, 1599; ^{1}H NMR ($CDCl_3$, 500 MHz): 1.79 (quint, 2H, J = 7.35 Hz, 6.75 Hz, CH_2CH_2O), 2.13 (q, J = 14.25 Hz, 7.05 Hz, 2H, CH_2CH_2CH), 4.26 (t, 2H, J = 6.5 Hz, OCH_2), 4.97 (dd, 2H, J = 27.3 Hz, 17.1 Hz, CH_2=), 5.76 – 5.84 (m, 1H, CH_2=CH), 6.60 (s, 1H, CH_{Ar}), 7.05 (s, 2H, 2xCH_{Ar}); ^{13}C NMR ($CDCl_3$, 125 MHz): 27.6 (OCH_2CH_2), 30.0 (O CH_2CH_2CH_2), 65.2 (OCH_2), 107.7 (CH_{Ar}C(OH)), 109.0 (2xC(OH)), 115.4 (CH=CH_2), 131.9 (CC(O)=O), 137.2 (CH=CH_2), 156.9 (C(OH)), 167.4 (OC=O).

Synthesis of (Z)-2,2'-((2,2',3,3'-tetrahydro-[1,1'-biindenylidene]-6,6'-diyl)bis(oxy))bis(ethan-1-ol)

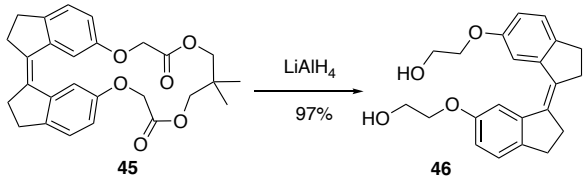

A known compound **46** was prepared using the literature procedure. [23]

To a solution of ester **45** (0.42 g, 0.936 mmol) in anhydrous THF (15 mL), LAH (0.089 g, 2.341 mmol) was added in several portions carefully at 0 °C. Upon completion, the reaction mixture was quenched with MeOH, filtered, concentrated, washed with HCl solution, and extracted with DCM. The concentration of the solution afforded as a colorless oil (0.32 g, 97%).

^{1}H NMR ($CDCl_3$, 500 MHz): 2.81 (t, 4H, 2xCH_2CH_2C=O), 2.91 (t, 4H, 2xCH_2CH_2C=O), 3.92 (t, 4H, 2xCH_2OH), 4.05 (t, 4H, 2xCH_2O), 6.75 (dd, 2H, 2xCH_{Ar}), 7.17 (d, 2H, 2xCH_{Ar}), 7.68 (d, 2H, 2xCH_{Ar}); ^{13}C NMR ($CDCl_3$, 125 MHz): 29.9, 35.2, 61.3, 70.0, 109.6, 114.7, 125.7, 135.4, 141.1, 141.6, 156.9; MS (ESI, [M+Na]): 375.2; MS (ESI, [M+H]): 353.2.

Synthesis of (Z)-6,6'-bis(2-bromoethoxy)-2,2',3,3'-tetrahydro-1,1'-biindenylidene

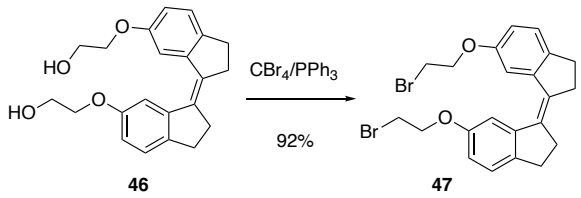

46 47

A known compound **47** was prepared using the literature procedure. [23]

To a solution of (Z)-2,2'-((2,2',3,3'-tetrahydro-[1,1'-biindenylidene]-6,6'-diyl)bis(oxy))diethanol (0.330 g, 0.936 mmol) in 20 mL of DCM containing 4 drops of acetone, carbon tetrabromide (1.242 g, 3.74 mmol) and triphenylphosphine (0.982 g, 3.74 mmol) were added in several portions. The mixture was stirred for 20 min, concentrated and purified without extraction (50:50 PE:DCM). Product **47** was afforded as light-orange liquid (0.41 g) in 92% yield.

^{1}H NMR ($CDCl_3$, 500 MHz): 2.82 (t, 4H, 2xCH_2CH_2C=O), 2.93 (t, 4H, 2xCH_2CH_2C=O), 3.64 (t, 4H, 2xCH_2O), 4.27 (t, 4H, 2xCH_2Br), 6.77 (dd, 2H, 2xCH_{Ar}), 7.20 (d, 2H, 2xCH_{Ar}), 7.63 (d, 2H, 2xCH_{Ar}); ^{13}C NMR ($CDCl_3$, 125 MHz): 29.6, 29.9, 35.3, 68.3, 109.5, 114.7, 125.8, 135.5, 141.5, 141.7, 156.5; HRMS (CI, [M+H]): 477.0043, calcd. 477.0059.

Synthesis of pent-4-en-1-yl 3-hydroxy-5-(2-((3-oxo-2,3-dihydro-1H-inden-5-yl)oxy)ethoxy)benzoate

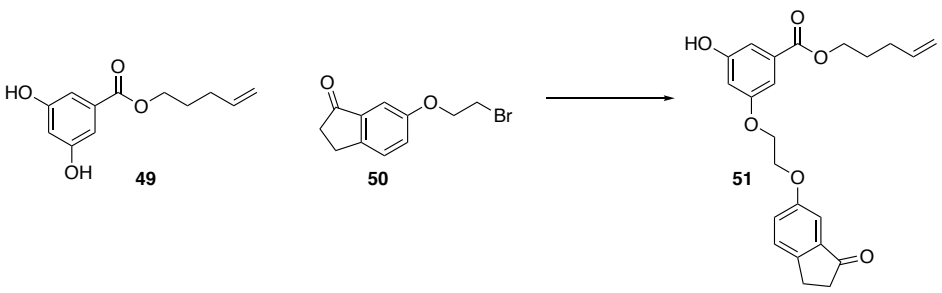

49 50 51

A new compound **51** was prepared using the procedure below.

To a solution of pent-4-en-1-yl 3,5-dihydroxybenzoate (0.481 g, 2.164 mmol) and K_2CO_3 (0.623 g, 4.51 mmol) in acetone (10 mL), 6-(2-bromoethoxy)-2,3-dihydro-1H-inden-1-one (0.46 g, 1.803 mmol) was added at RT. The solution was allowed to stir at 60 °C until completion, followed by work-up with HCl and extraction with DCM. Purification by flash chromatography (1.5:98.5 MeOH:DCM) afforded a colorless oil (0.6 g) in 84% yield.

^{1}H NMR ($CDCl_3$, 500 MHz): 1.85 (quint, 2H, C*H*$_2$CH$_2$O), 2.19 (q, 2H, CH$_2$C*H*$_2$CH), 2.74 (t, 2H, C*H*$_2$C=O), 3.08 (t, 2H, C*H*$_2$CH$_2$C=O), 4.30-4.33 (m, 6H, OC*H*$_2$C*H*$_2$O, OC*H*$_2$), 5.02 (dd, 2H, C*H*$_2$=CH), 5.82 – 5.90 (m, 1H, CH$_2$=C*H*), 5.99 (br s, 1H, OH), 6.68 (t, 1H, C*H*$_{Ar}$), 7.21 – 7.22 (m, 2H, 2xC*H*$_{Ar}$), 7.26 – 7.28 (m, 2H, 2xC*H*$_{Ar}$), 7.39 – 7.41 (m, 1H, C*H*$_{Ar}$); ^{13}C NMR ($CDCl_3$, 125 MHz): 25.2 (OCH$_2$*C*H$_2$), 27.8 (OCH$_2$CH$_2$*C*H$_2$), 30.1 (C*C*H$_2$CH$_2$C=O), 37.0 (CCH$_2$*C*H$_2$C=O), 64.7 (O=C(O)*C*H$_2$), 66.7 (O*C*H$_2$*C*H$_2$O), 105.8 (O=CC*C*H$_{Ar}$C(OH)), 107.2 (OC*C*H$_{Ar}$C(OH)), 107.7 (OC*C*H$_{Ar}$CC(O)=O), 109.7 (CH$_2$C(=O)C*C*H$_{Ar}$), 115.4 (*C*H$_2$=CH), 124.8 (CH$_{Ar}$*C*H$_{Ar}$CO), 127.5 (*C*C(=O)O), 132.2 (*C*H$_{Ar}$CH$_{Ar}$CO), 137.4 (*C*H=CH$_2$), 138.1 (*C*C(=O)CH$_2$), 148.6 (CH$_2$C(=O)*C*CH$_{Ar}$), 156.9 (CH$_2$CH$_2$*C*CH$_{Ar}$), 158.3 (*C*(OH)), 159.7 (CH$_2$C(=O)CCH$_{Ar}$*C*O), 166.2 (*C*(=O)O), 207.4 (CH$_2$C=O); HRMS (CI, [M+H]): 397.1662, calcd. 397.1646

Synthesis of di(pent-4-en-1-yl) 5,5'-((((2,2',3,3'-tetrahydro-[1,1'-biindenylidene]-6,6'-diyl)bis(oxy))bis(ethane-2,1-diyl))bis(oxy))(Z)-bis(3-(2-((3-oxo-2,3-dihydro-1H-inden-5-yl)oxy)ethoxy)benzoate)

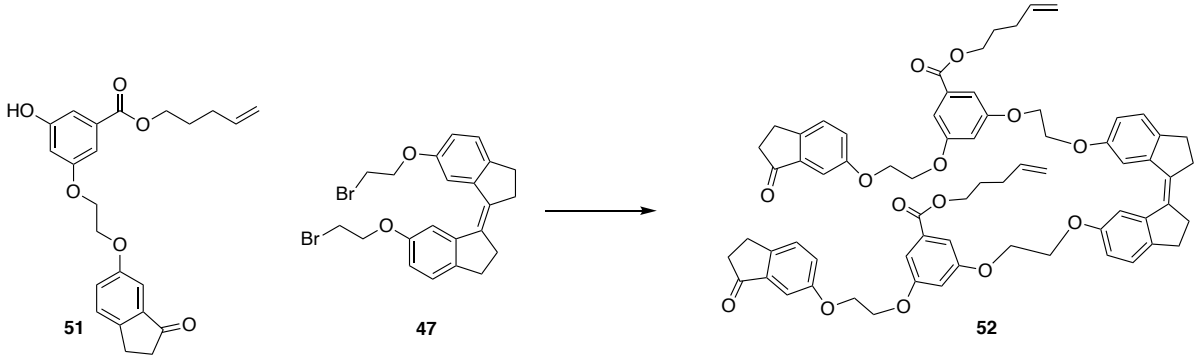

A new compound **52** was prepared using the procedure below.

To a solution of(Z)-6,6'-bis(2-bromoethoxy)-2,2',3,3'-tetrahydro-1,1'-biindenylidene (0.2 g, 0.418 mmol) in 5 mL anhydrous DMF was added pent-4-en-1-yl 3-hydroxy-5-(2-((3-oxo-2,3-dihydro-1H-inden-5-yl)oxy)ethoxy)benzoate (0.414 g, 1.046 mmol) and K_2CO_3 (0.173 g, 1.255 mmol) , then the mixture was stirred at RT for 48 h. Upon completion the mixture was concentrated and purified by flash chromatography (5:95 MeOH: DCM) to afford a product **52** (0.37 g) in 80% yield.

^{1}H NMR: 1.84-1.87 (m, 4H, 2xOCH$_2$C*H$_2$*), 2.17-2.20 (m, 4H, 2xOCH$_2$CH$_2$C*H$_2$*), 2.68-2.70 (m, 8H, 2xC*H$_2$*C=O, 2xC*H$_2$*=C), 3.04-3.06 (m, 8H, 2xC*H$_2$*CH$_2$C=O, 2xC*H$_2$*CH$_2$C=), 4.30-4.35 (m, 20H, 5xOC*H$_2$*), 4.98-5.07 (m, 4H, 2xCH=C*H$_2$*), 5.79-5.86 (m, 2H, 2xC*H*=CH$_2$), 6.75 (d, 2H, 2xOCC*H$_{Ar}$*CH$_{Ar}$CCH$_2$CH$_2$C=C), 7.21 – 7.25 (m, 12H, 12xCH$_{Ar}$), 7.37 (d, 4H, 4xOCC*H$_{Ar}$*CC=C).

Synthesis of compound 53

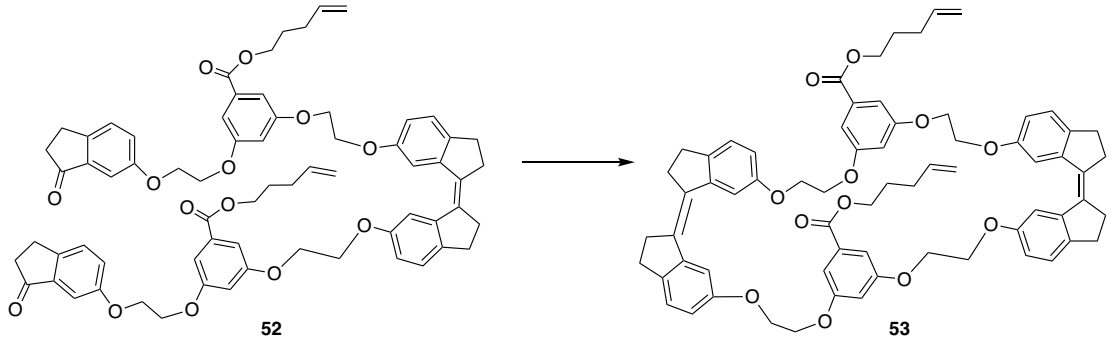

A new compound **53** was prepared using the procedure below.

To a vigorously stirred solution of zinc (0.413 g, 6.31 mmol) in THF (50 mL), titanium tetrachloride (0.348 ml, 3.16 mmol) was slowly added at 0°C. The solution was heated until 70 °C and refluxed for 1.5 h, followed by a slow dropwise addition of compound **52** (0.7 g, 0.631 mmol) over 20 min. The reaction was monitored by TLC. Upon completion, the reaction mixture was cooled down to RT, washed with saturated solution of K_2CO_3, filtered through

Celite, and extracted with DCM. Purification by flash chromatography (40:60 EtOAc: PE) afforded a product as a yellow oil (0.54 g) in 80%.

^{1}H NMR ($CDCl_3$, 500 MHz): 1.82 (quint., J = 7.60 Hz, 6.85 Hz, 4H, 2xOCH_2CH_2), 2.18 (q, J = 7.65 Hz, 6.95 Hz, 4H, 2x$OCH_2CH_2CH_2$)), 2.81-2.86 (m, 8H, 4xCH_2=C), 2.92-2.96 (m, 8H, 4xCH_2CH_2C=), 4.18 - 4.33 (m, 20H, 10xOCH_2), 4.97-5.07 (m, 4H, 2xCH=CH_2), 5.78-5.86 (m, 2H, 2xCH=CH_2), 6.40 (t, J = 2.10 Hz, 2H, 2xCH=CH_2), 6.79 (dd, J = 8.3 Hz, 2.10 Hz, 4H, 4xOCC$H_{Ar}CH_{Ar}CCH_2CH_2C$=C), 7.02 (d, J = 2.25 Hz, 6H, 3xCH_{Ar}), 7.20 (d, J = 8.25 Hz, 4H, 4xOCCH_{Ar}C$H_{Ar}CCH_2CH_2C$=C), 7.75 (d, J = 1.95 Hz, 4H, 4xC=CCCH_{Ar}CO); ^{13}C NMR ($CDCl_3$, 125 MHz): 27.8 (OCH_2CH_2), 29.8 ($OCH_2CH_2CH_2$), 30.1 (CCH_2CH_2C=), 35.3 (CCH_2CH_2C=), 64.5 (C(=O)OCH_2), 66.7 (OCH_2), 66.8 (OCH_2), 105.6 (OCCH_{Ar}CO), 108.0 (CH_{Ar}CC(=O)O)), 108.9 (CC(=O)O), 114.9 (=CCCH_{Ar}CO), 115.3 (CH=CH_2), 125.8 (OC$CH_{Ar}CH_{Ar}$C), 132.0 (OCC$H_{Ar}CH_{Ar}$C)) , 135.5 (C=C), 137.5 (CH=CH_2), 141.1 (OCCH_{Ar}C(=O)O), 141.6 (=CCH_2CH_2C), 156.8 (=$CCCH_{Ar}$)), 159.4 (OCCH_{Ar}CC=), 165.9 (OC=O); HRMS (FTMS+pNSI, [M+Na]): obs. 1099.4612, calcd. 1099.4603.

Synthesis of macrocycle 54

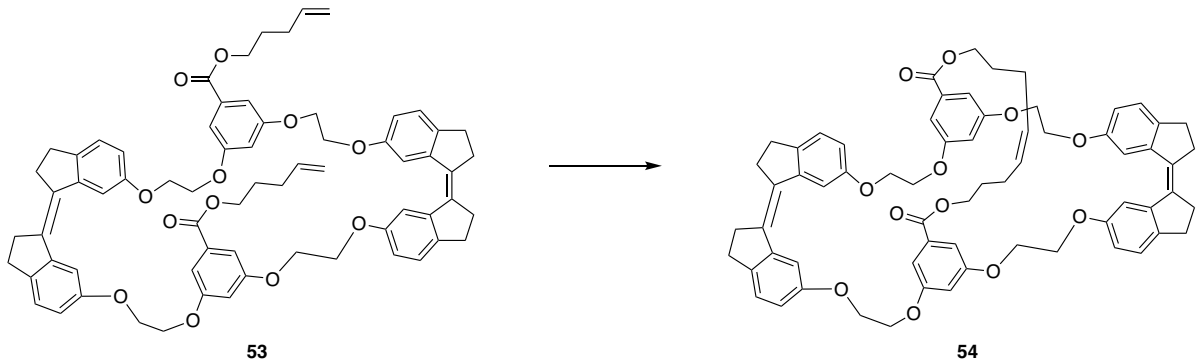

53 **54**

A new compound **54** was prepared using the procedure below.

A solution of starting macrocycle **53** (0.1 g, 0.095 mmol), CsCl (15 mg, 0.09 mmol), and the Grubbs II catalyst (1.91 mg, 0.00225 mmol) in DCM (10 mL) was degassed for 20 min and

allowed to stir at 45 °C for 1 h. The starting material was fully consumed with the formation of one spot on TLC plate. The catalyst was quenched with water; the reaction product was extracted with DCM, followed by concentration to afford a brown solid in a quantitative amount (0.1 g).

^{1}H NMR (500 MHz, $CDCl_3$): 1.76-1.90 (m, 8H, 2xOCH$_2$C*H$_2$*, 2xOCH$_2$CH$_2$C*H$_2$*), 2.07-2.36 (m, 8H, 4xC*H$_2$*C=C), 2.84-2.96 (m, 8H, 4xC*H$_2$*CH$_2$C=), 4.20-4.38 (m, 20H, 10xOC*H$_2$*), 5.45-5.55 (m, 2H, C*H*=C*H*), 6.39-6.41 (dt, 2H, 2.25 Hz, 2xOCC*H$_{Ar}$*CO), 6.82 (dd, 4H, 2 Hz, 6.2 Hz, 4xOCC*H$_{Ar}$*CC(=O)O), 6.93 (dd, 4H, 4.25 Hz, 32.7 Hz, OCC*H$_{Ar}$*CH$_{Ar}$CCH$_2$CH$_2$C=C), 7.15-7.72 (m, 4H, OCCH$_{Ar}$C*H$_{Ar}$*CCH$_2$CH$_2$C=C), 7.77 (s, 4H, 4xC=CCC*H$_{Ar}$*CO), ^{13}C NMR (125 MHz, $CDCl_3$): 29.8 (OCH$_2$*C*H$_2$), 29.9 (OCH$_2$CH$_2$*C*H$_2$), 35.3 (C*C*H$_2$CH$_2$C=), 35.3 (CCH$_2$*C*H$_2$C=), 66.5 (C(=O)O*C*H$_2$), 66.6 (O*C*H$_2$), 66.7 (O*C*H$_2$), 107.8 (OC*C*H$_{Ar}$CO), 108.9 (*C*H$_{Ar}$CC(=O)O)), 114.8 (*C*C(=O)O)), 115.0 (=CC*C*H$_{Ar}$CO), 125.8 (=CCH$_2$CH$_2$C*C*H$_{Ar}$), 130.4 (*C*H=*C*H), 135.5 (*C*=*C*), 141.1 (O*C*CH$_{Ar}$CC(=O)O), 141.6 (=CCH$_2$CH$_2$*C*), 141.6 (=C*C*CH$_{Ar}$), 156.9 (O*C*CH$_{Ar}$C(=O)O)), 159.4 (O*C*CH$_{Ar}$CH$_{Ar}$C), 165.9 (*C*=O), HRMS (FTMS+pNSI, [M+NH_4^+]): 1066.4729, calcd. 1066.4736

CHAPTER 3. FOLDAMERS

3.1. Overview

Despite the significant development of the foldamers field, its major challenge remains the design and synthesis of well-organized strand architectures able to form supramolecular assemblies or functional materials. The most recent definition of foldamer is "any oligomer that folds into a conformationally ordered state in solution, the structures of which are stabilized by a collection of noncovalent interactions between nonadjacent monomer units".[51] Foldamers have a wide spread of applications in molecular recognition,[44, 45, 51, 52, 84-93] catalysis,[94-106] design of smart materials[107, 108] and bioactive molecules.[109-114] The main interest for foldamers research is their ability to mimic biomolecules by folding into specific conformations.

This Chapter focuses on the design and synthesis of the helical foldamer model as a supramolecular mechanophore with the strong stability to form easily synthesizable secondary motifs (double helices) capable of surviving at low concentration and coupling to commercial polymers.

Abiotic aromatic foldamers based on the aryl backbone ensure stability in structure using hydrogen bonding, π-π stacking, and hydrophobic interaction. Backbones include phenylene ethylene, [115] benzoyl urea,[116] aromatic benzyl [117, 118] and heterocyclic[46, 119] amines.[44] Existing π-π stacking, which lacks aliphatic foldamers, ensures the rigidity of the 3D structure. For example, helical foldamers, consisting of pyridine-monomers (AOA) (Figure 15), seem to offer these opportunities of high stability, predictability, ease of synthesis, and tunability. [41, 43, 47, 120] These aromatic oligoamides hybridize into supramolecular double helices. A remarkable

feature of AOAs is the ability of their single helices to extend mimicking springs and reassemble into double helices (Figure 15).[42, 46, 121] Strands of AOAs self-organize into single using NH-N and NH-O hydrogen bonding interactions. However, double helix formation is driven by face-to-face aromatic stacking.[49, 51]

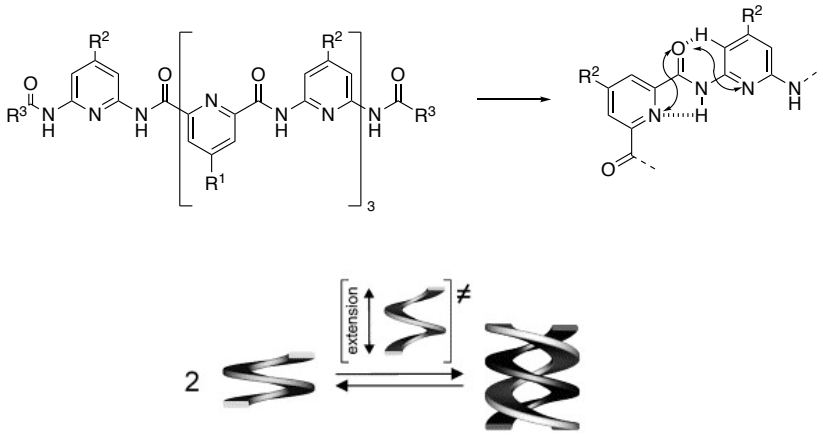

Figure 15. Schematic representation of single and double helical pyridine oligoamides (AOA) folding via intramolecular hydrogen bonds. The double-headed arrows show electrostatic repulsions; hash lines indicate the extension of the structure.[49]

Essential design parameters to consider during the design of double helices include the following:

- intrinsic factors[52] (length of the foldamer and side chains) determine the kinetics and thermodynamics of folding
- external environment (solvent, temperature, concentration)[42, 46] facilitates or destroys the dimerization.

Huc and Lehn report in their studies that, in general, dimerization constants increase with the oligomers' length.[46, 54] However, they also revealed unexpected observation that dimerization increases with oligomer length up to a certain point and then decreases to undetectable levels

for the longest strands.[49] Initial hypothesis based on the increasing number of stabilizing interstrand interactions with longer foldamer length did not match the results. The observed phenomenon was explained by comparing the enthalpic gain and entropic loss of oligomers hybridization into a duplex. When the strand length increases, both the enthalpic gain and entropic loss decreases.

Dimerization is further controlled by side chains, which can increase stacking interactions between strands.[46] Table below compares previous work on the pyridine-based heptamers (Figure 15). The previous research on side chains (Table 2) reports that alkoxy substituents, regardless of their length, favordimerization possibly due to increased interactions between side chains and aromatic rings with electron-donor groups (entries 3, 4, 6 and 8). The highest dimerization constant ($8.2*10^4$ L/mol, entry 6) corresponds to a heptamer-amine with methoxy substituents. The change of alkoxy groups' length did not significantly affect the dimerization constant. Dimerization constants of AOAs with longer dodecyloxy substituents were calculated as $6.9*10^4$ and $6.9*10^4$ L/mol (entries 4 and 3), *tert*-butoxy substituted foldamers' dimerization constant is $3.1*10^4$ L/mol (entry 8). A high degree of dimerization is sensitive to the foldamers' end groups. Dimerization constants above are associate with amine, Boc, and long aliphatic nonanyl end groups. However, the dimerization constant of Cbz protected foldamers drastically drops to 1500 L/mol for dodecyloxy-substituted heptamers and 1000 L/mol for foldamers with methoxy substituents. A pattern of substitution also affects the degree of dimerization. Described cases are based on substituting all pyridine rings, while the alternating pattern of substitution (entry 2 vs entry 3) decreases the dimerization on three orders of magnitude.

Table 2. Dimerization constants of AOAs

#	R^1	R^2	R^3	K_{dim} ($CDCl_3$) at RT
1	H	H	Boc	110-120
2	$OC_{10}H_{21}$	H	C_9H_{19}	25-30
3	$OC_{10}H_{21}$	$OC_{10}H_{21}$	C_9H_{19}	$6.5*10^4$
4	$OC_{10}H_{21}$	$OC_{10}H_{21}$	NH_2	$6.9*10^4$
5	$OC_{10}H_{21}$	$OC_{10}H_{21}$	Cbz	1500
6	OMe	OMe	NH_2	$8.2*10^4$
7	OMe	OMe	Cbz	1000
8	OtBu	OtBu	Boc	$3.1*10^4$

Non-polar solvents (eg. chlorohydrocarbons), high concentrations, and low temperatures favour dimerization, while any presence of moisture[46] destroys the double-helical conformation, presumably by interfering with the formation of H-bonds within the foldamer.

Summarizing the literature cases of preparation aromatic foldamers described above, the general parameter of successful foldamers dimerization is a length. The development of a synthetic protocol of new foldamers minimizing toxicity to the environment but increasing their length is a work strategy.

3.1.1. Previous work on synthesis and characterization of foldamers

The basic units for AOA have been pyridine/quinoline derivatives,[42, 43] which grow by converged synthesis (Scheme 24).[44] The main techniques used to characterize the secondary structures of long aromatic foldamers are X-Ray and ^{1}H NMR spectroscopy.

The synthesis of the single helical oligoamides, developed by Huc, is straightforward, and a representative unsubstituted heptamer **16** can be prepared in three steps starting from the corresponding diaminopyridine **12**, and pyridine dicarboxylic esters. [42]

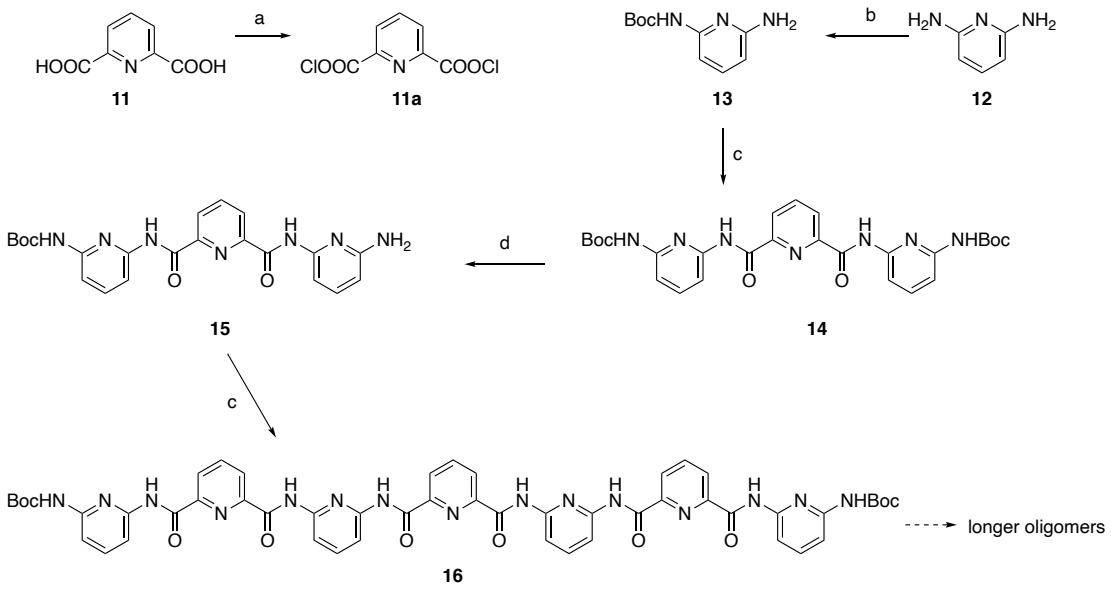

Scheme 24. Synthesis of heptamer **16**.[42] Conditions: a) $SOCl_2$, reflux; b) LiHMDS, Boc_2O, THF, RT; c) **11a**, NEt_3, THF, RT; d) TMSI, chloroform, then MeOH, reflux.

The hybridization of compound **16** was characterized using NMR spectroscopy by monitoring proton shifts. Terminal amide NH signals of the double helix appear upfield in comparison to the spectrum of monomer (Table 3).[52]

Table 3. ^{1}H NMR peaks of trimer's and heptamer's protons[52]

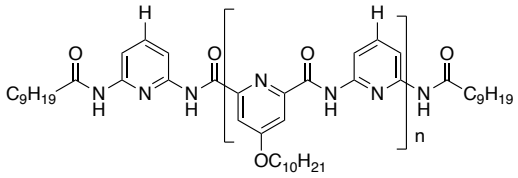

n = 1, trimer **55**
n = 3, heptamer **56**

foldamer	Terminal C<u>H</u>$_2$CON<u>H</u> signals (ppm)	aromatic protons (ß/ß') (ppm)
Trimer **55**	2.39 and 8.42	7.40 and 7.88
Heptamer **56**	1.97 and 7.54	7.92

Dimerization can be facilitated by lowering the temperature of the environment. The change of the spectrum of AOA with temperature is shown in Figure 16. High-temperature experiments caused proton peaks broadening,[46] associated with slow conformational changes within a double helix or equilibration with larger aggregates.[46] At lower temperature (25 °C), sharp peaks with precise splitting were observed. New peaks appeared upon temperature increase, while decreasing temperature led to the original spectra. This experiment shows that the same compound can have various conformations, which may associate with aggregation at higher temperatures. For example, at 25-35 °C strong signals appear and correspond to double helix, upon temperature increase, 45-55 °C monomer species appear, and signals coalesce, at T higher than 55 °C single helix ratio increase, and peaks start to sharpen until double helix completely disappears (Figure 16).

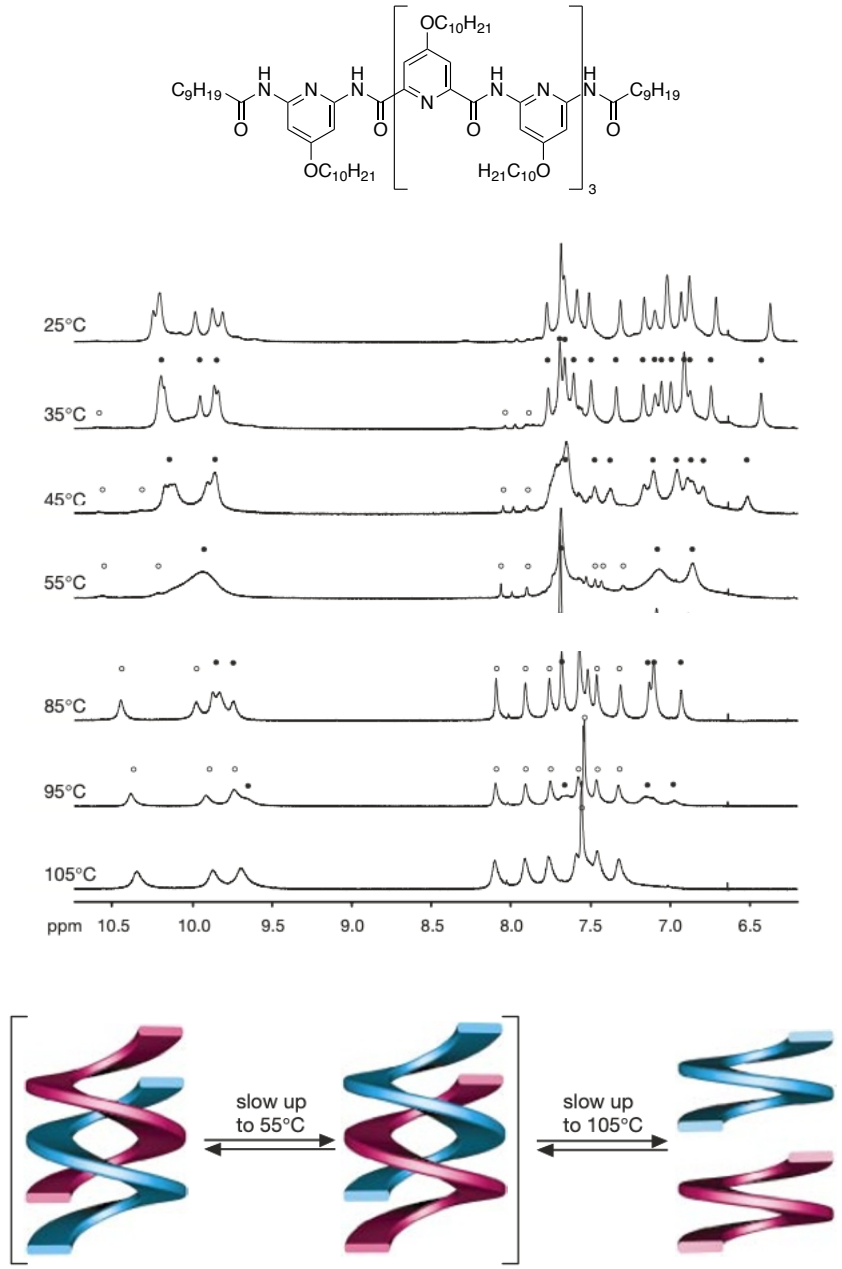

Figure 16. NMR Interconversion between double and single helices upon temperature change.[46] Formation and interconversion of double helices described by 400-MHz ^{1}H spectra (8.2 mM in $C_2D_2Cl_4$ at various temperatures). Filled circles indicate peaks describing double helix, and unfilled circles indicate single helix. The bottom scheme represents the interconversion between two identical double helices by a sliding motion and their dissociation into two single helices

Based on the previous research described above, our synthetic design relied on simplified literature procedure (1) by using commercially available unsubstituted starting amine to avoid using toxic ammonia gas and bromine, but (2) by increasing the length of the foldamer to maximize supramolecular interactions and consequently, dimerization constant (Scheme 25).

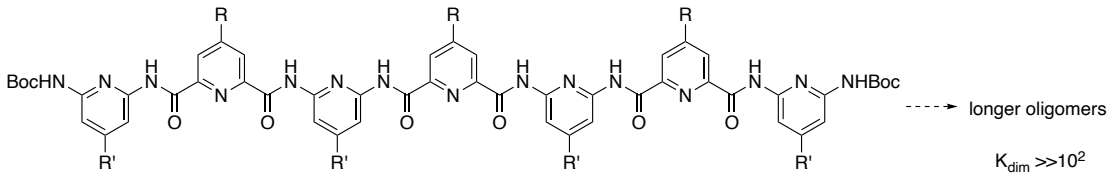

Scheme 25. Model foldamer

As starting materials, we chose chelidamic acid to be transformed into alkoxy pyridine and diaminopyridine (Scheme 26). The research above shows that alternating pattern with alkoxy substituents has a lower degree of dimerization compared to all substitution patterns of aromatic rings, while the later system's dimerization constant reaches a maximum at a certain length. Based on this conclusion, we decided to synthesize longer oligomers with alternating substitution patterns to control better the dimerization related to the length of the foldamer.

The retrosynthesis of the foldamer series is shown below:

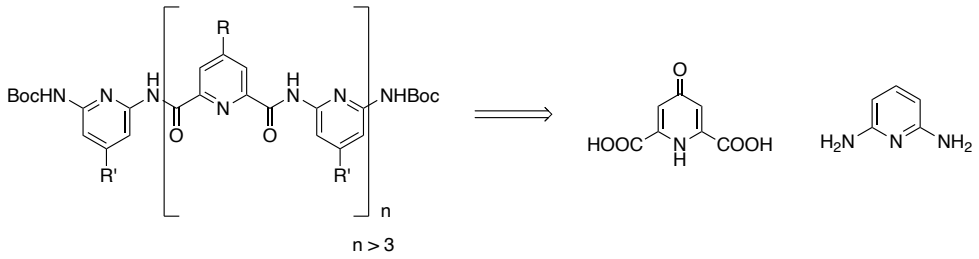

Scheme 26. Retrosynthesis of model foldamer

3.1.2. Previous work on the synthesis of the double helices

Successful syntheses of foldamers rely on a convergent approach. The main challenge in the synthesis of foldamers is their tendency to fold into helices, which reduces yields of coupling due to steric inaccessibility of the terminal amine groups that are sequestered inside the helix and complicates purification. To overcome these problems including possible side reactions such as chlorination and hydroxylation of the backbones, a chromatography-free scalable protocol yielded a quinoline-based octamer.[5] Researchers replaced the use of $SOCl_2$ with oxalyl chloride as $SOCl_2$ caused overchlorination of long aromatic oligomers, and acid-sensitive foldamers found that Ghosez's reagent is the best as well as proposed optimized ratios of reagents for each reaction step towards octamer formation to avoid purification by chromatography.[5]

3.2. Synthesis of foldamers

Synthesis of aromatic foldamers adapted the strategy of doubling the segment using the guidance of chromatography-free synthetic protocol[5] by using chelidamic acid and *tert*-butyl (6-aminopyridin-2-yl)carbamate as starting monomer units (Scheme 27). The route was based on coupling acid chloride with the amine in the presence of DIPEA as a base. Activation of acids was essential due to the poor nucleophilic nature of aromatic amines.

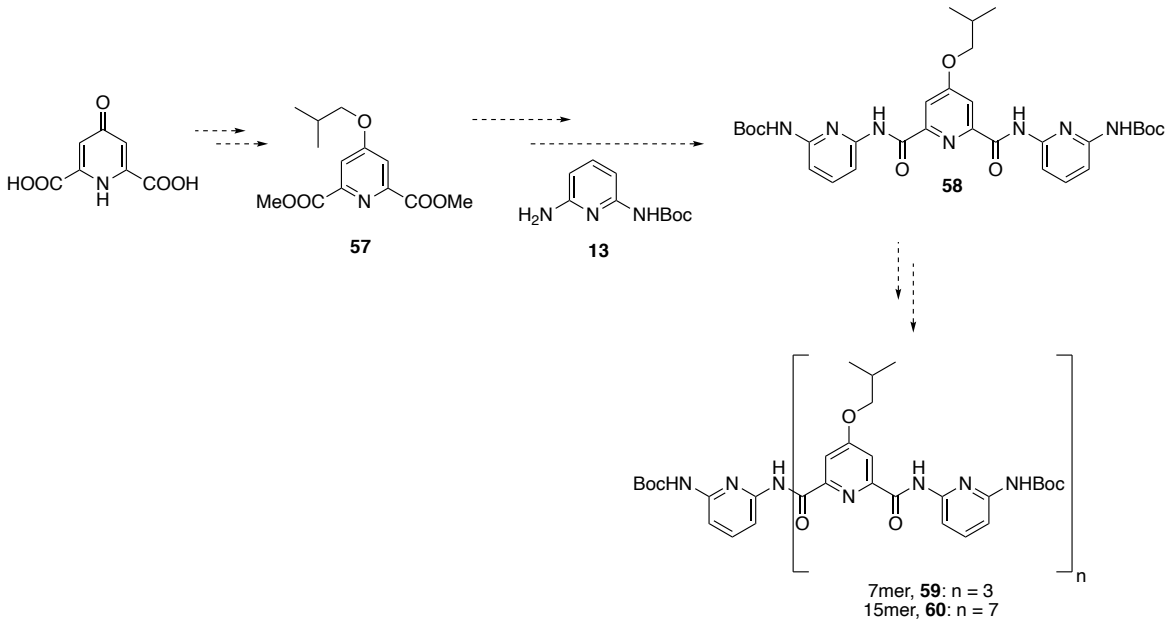

Scheme 27. Proposed synthesis of foldamers

First, chelidamic acid was transformed into diester **61** using a chlorinating agent in a quantitative yield (Scheme 28) to avoid side reactions in the next step.

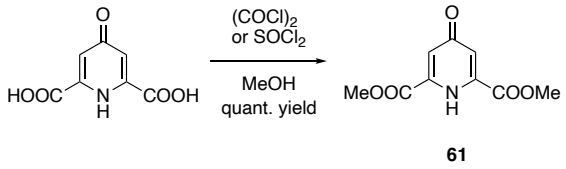

Scheme 28. Synthesis of diester **61**

Next, etherification reaction with *tert*-butyl iodide under basic conditions in DMF provided the desired product **57** in 97% yield (Scheme 29).

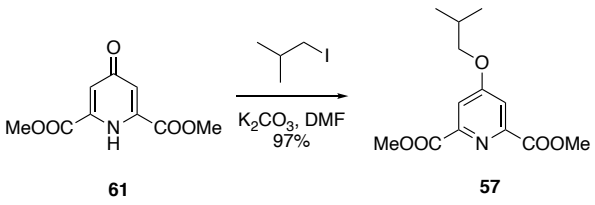

Scheme 29. Preparation of compound **57**

Before the coupling step, compound **57** was converted to monoester **62** using 1 equivalence of NaOH in MeOH/THF mixture or diacid **63** using an excess of base (Scheme 30).

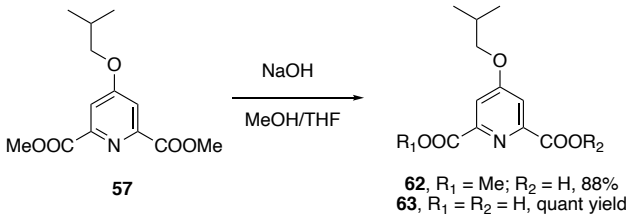

Scheme 30. Deprotection of compound **57**

The second monomer, *tert*-butyl (6-aminopyridin-2-yl)carbamate **13**, was prepared in 75% yield by treating 2,6-diaminopyridine **12** with 1 equivalent of Boc-anhydride (Scheme 31).

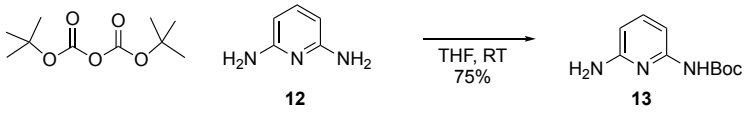

Scheme 31. Formation of monoamine **13**

Using coupling reactions, the corresponding dimer **66**, trimer **58** were obtained in high yields (Scheme 32 and Scheme 33) via chloride intermediate in 67% and 74% yields, respectively.

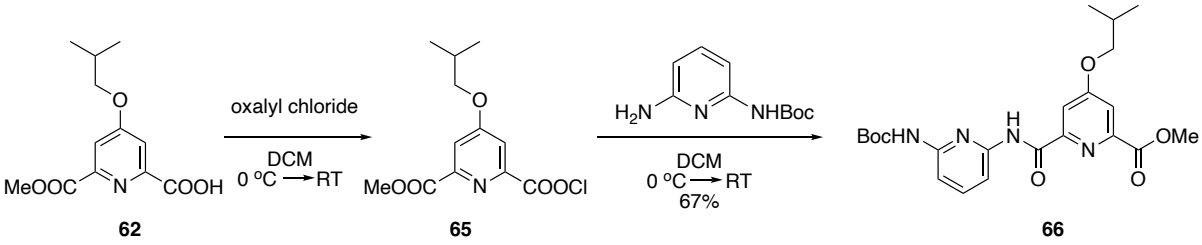

Scheme 32. Synthesis of dimer **66**

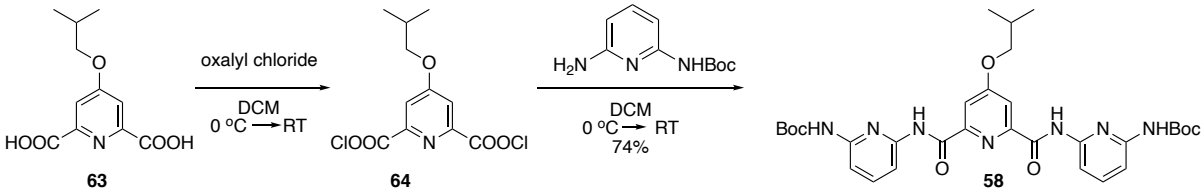

Scheme 33. Synthesis of trimer **58**

The next step was a saponification reaction in MeOH/THF mixture to obtain dimer acid **68** in a quantitative yield (Scheme 34)

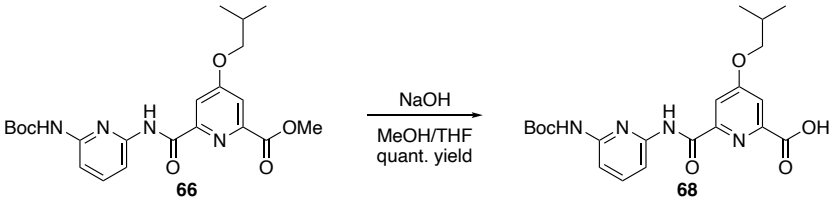

Scheme 34.Saponification of compound **66**

Boc deprotection reaction of trimer **58** in the presence of TFA afforded trimer-diamine **67** in 96% yield (Scheme 35).

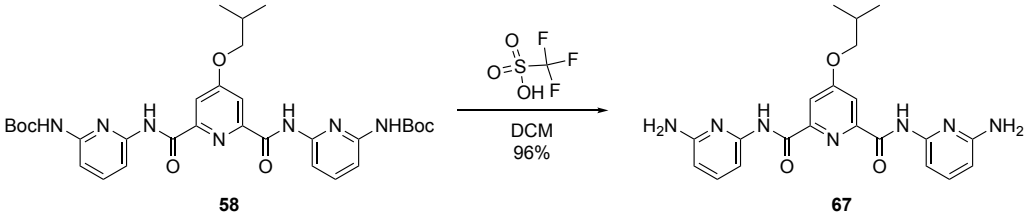

Scheme 35. Synthesis of compound **67**

An alternative approach, coupling monoester **62** and diamine **12** (Scheme 36) using EDC as the coupling reagent was low yielding and difficult to extend to longer oligomers.

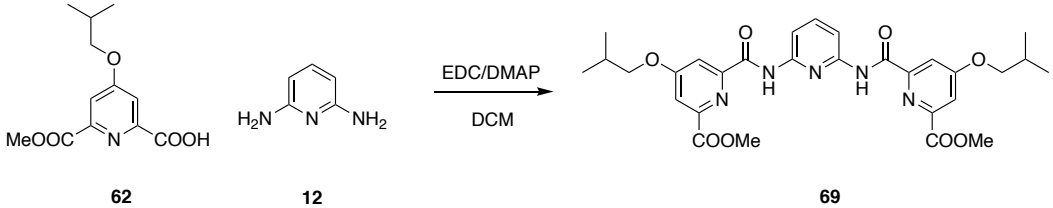

Scheme 36. Low-yielding coupling of monoester and diamine

Treatment of acid **68** with oxalyl chloride to form acyl chloride **71**, followed by the addition to the solution of diamine **67** and DIPEA did not lead to the formation of desired heptamer **59** (Scheme 37). One of the possible reasons could be the sensitivity to acidic conditions as HCl is generated as the by-product.

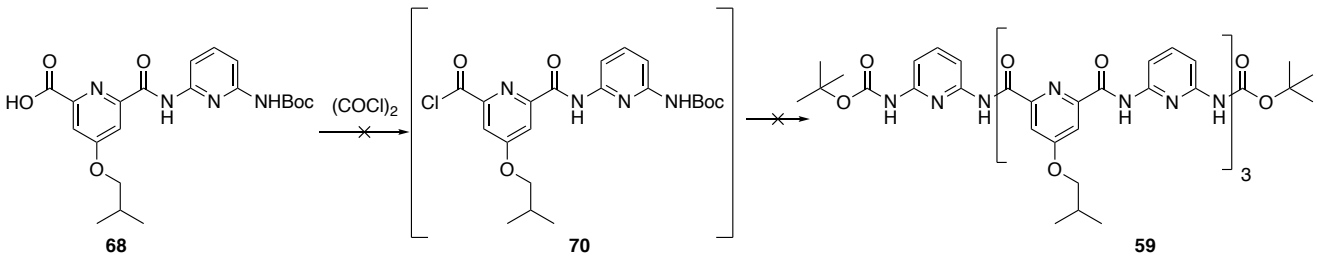

68 **70** **59**

Scheme 37. Failed trial of heptamer formation using oxalyl chloride as the activating reagent

According to the literature, sensitivity to acid increases with the length of foldamers, and oligomers prefer activation by neutral Ghosez's reagent (Scheme 38). Heptamer **59** was formed in a 60% yield over two steps (Scheme 39). ^{1}H NMR spectrum of compound **59** is shown in Figure 19.

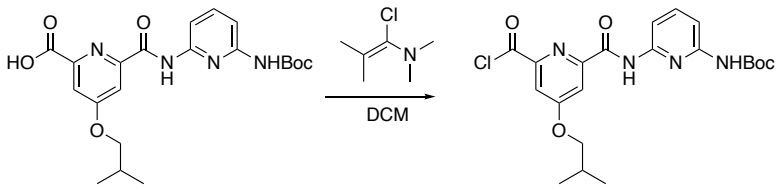

68 **70**

Scheme 38. Chlorination reaction using Ghosez's reagent

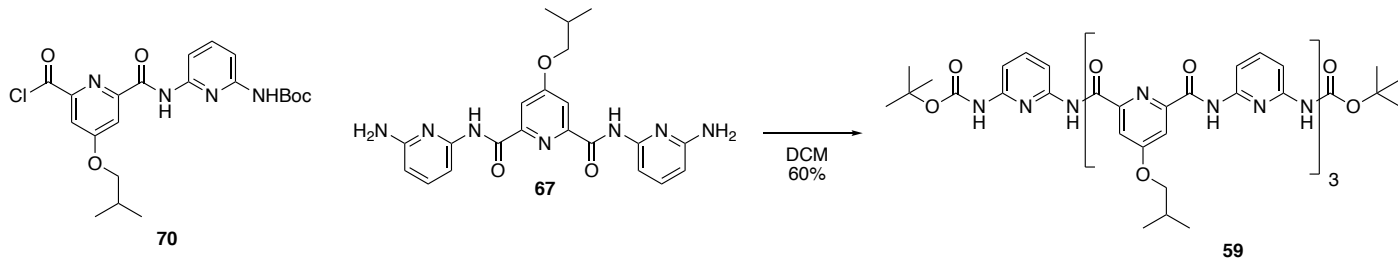

Scheme 39. Synthesis of heptamer. Use of oxalyl chloride was unsuccessful towards heptamer formation and was replaced by neutral Ghosez's reagent to afford **59** in 60% yield over two steps

In the next step, one of the Boc groups of **59** was selectively removed using TMSI, followed by reflux in MeOH to obtain heptamer-monoamine **72**, which was treated with dichloride **64** to afford pentadecamer **60** (Scheme 40).

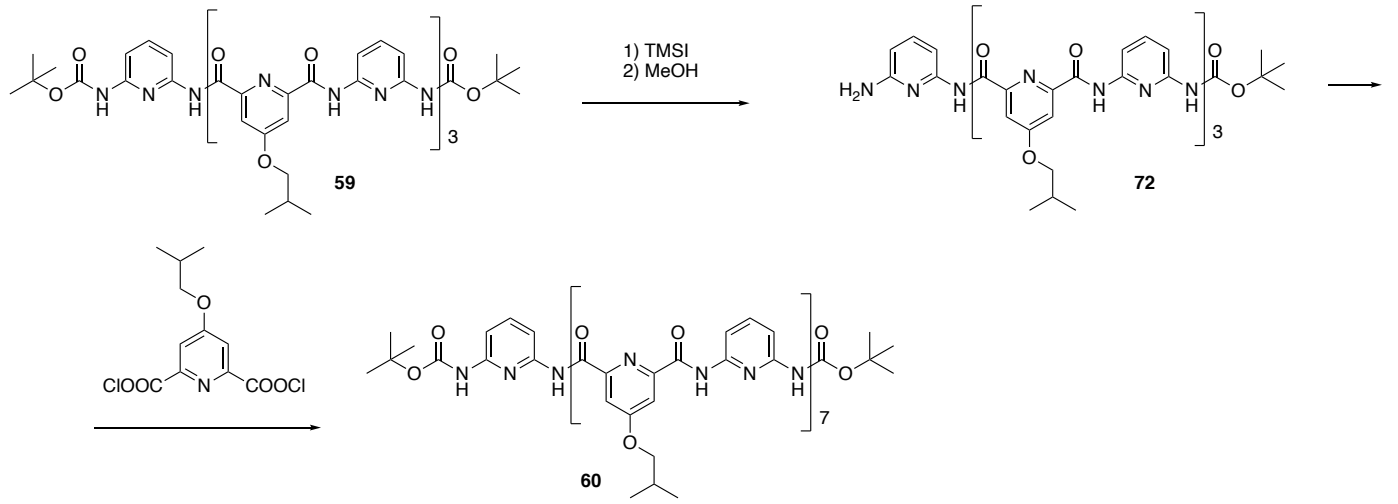

Scheme 40. Synthesis of pentadecamer using selective deprotection procedure.

All intermediates, except for **72** due to the purification difficulties, and final products **59** and **60** were characterized by ^{1}H NMR spectroscopy and confirmed by MS analysis.

The characterization of the helical structure was determined according to the shifts of amide signals. From the previous studies, strong signals of double-helical amide hydrogens (9.2 – 10 ppm) shift upfield compared to single helical hydrogens (10 – 11 ppm) as the length of foldamer increases due to the π-π stacking interactions, which increase ring current effects. Thus, upfield shifts of 15mer indicate the formation of double-helical conformation (Figure 17), and the observed signal at ~ 10 ppm for heptamer indicates that double helix is formed at a concentration higher than 13 mM (Figure 18).

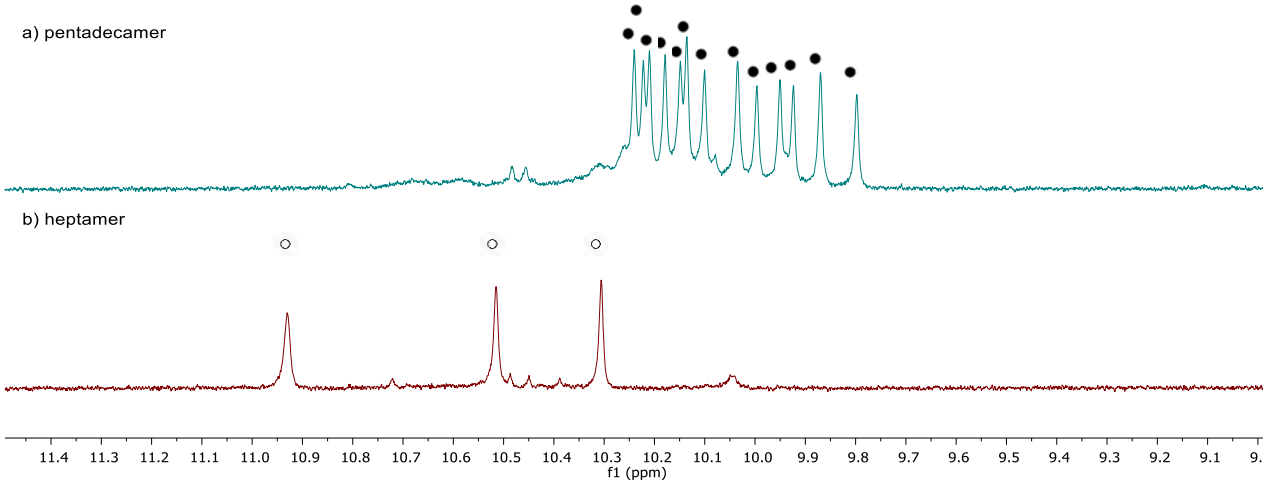

Figure 17. ^{1}H NMR spectra (500 MHz, $CDCl_3$) showing amide NH region of a) pentadecamer **60** (4 mM) and b) heptamer **59** (5.5 mM), peaks of the single helix are indicated by unfilled circles; filled circles indicate peaks of the double helix

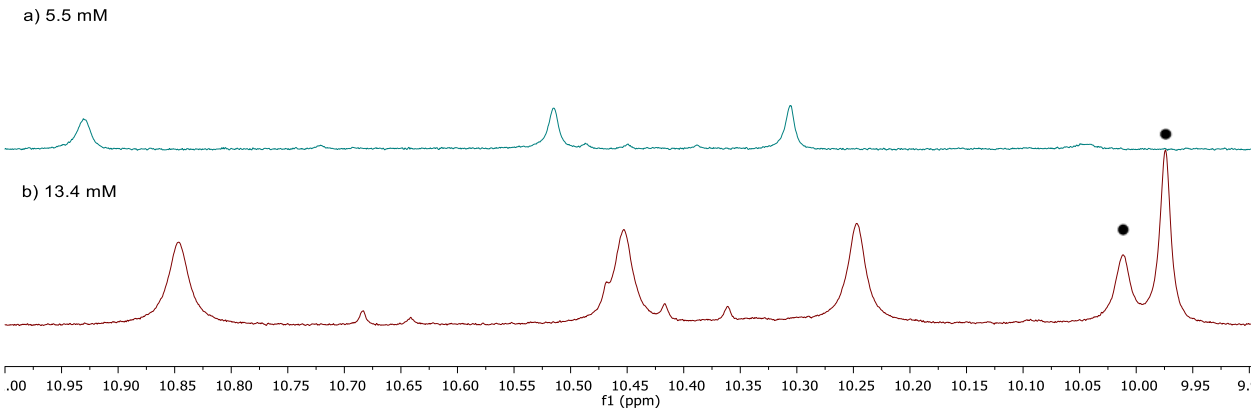

Figure 18. ^{1}H NMR spectra of heptamer at a) 5.5 mM and b) 13.4 mM ($CDCl_3$, RT)

^{1}H NMR measurements of **59** and **60** are shown in Figure 19 and Figure 20, respectively. In the aromatic region (7.00 – 8.50 ppm), peaks of both foldamers lie in the same range, while proton peaks of amides NH are in a different range. Amide protons of heptamer confirm the symmetrical structure of the foldamer, while amide protons of 15mer shifted upfield and non-equivalent. Peaks of the aliphatic chains of both compounds are observed in the same region. The peak at 2 ppm on heptamer's spectrum may arise from impurity. This peak disappears on the 15mer's spectrum. HRMS of compound **60** confirms the purity of the product (Figure 21). Overall, integration values match the expected number of hydrogens which suggest that species exist in single conformation under identified conditions: 5.5 mM ($CDCl_3$) for heptamer, 4 mM ($CDCl_3$) for 15mer.

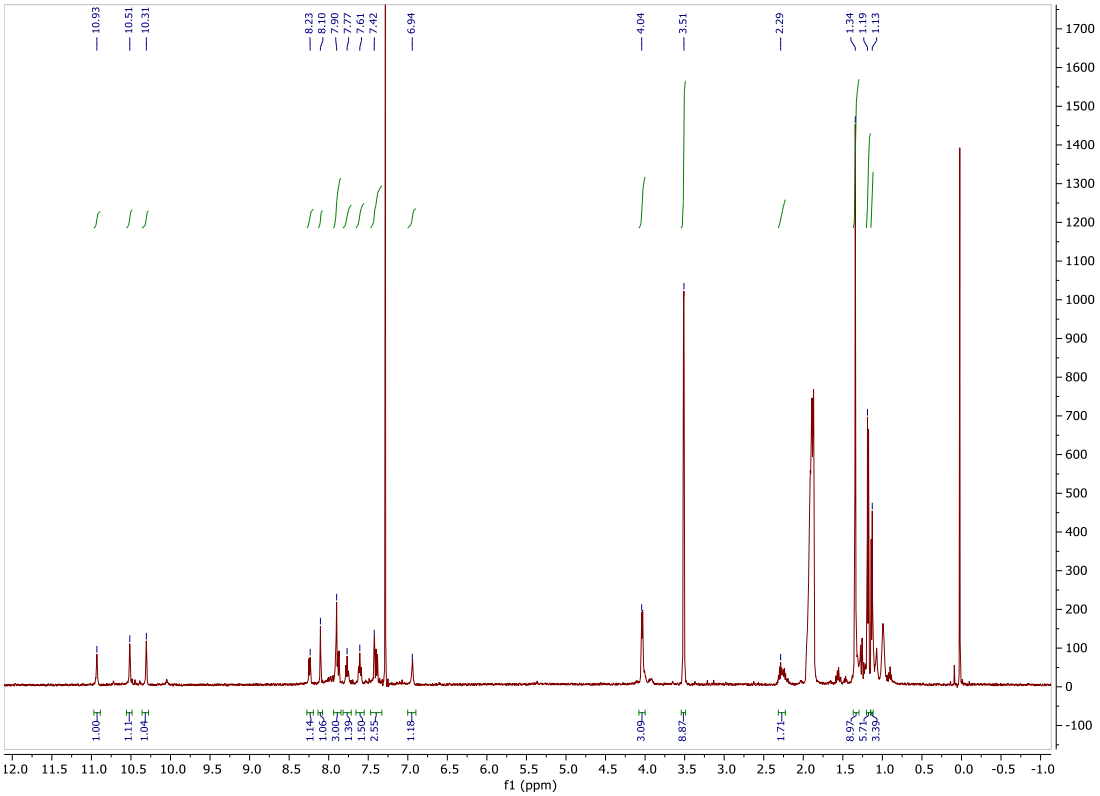

Figure 19. ^{1}H NMR of heptamer **59** (5.5 mM, $CDCl_3$)

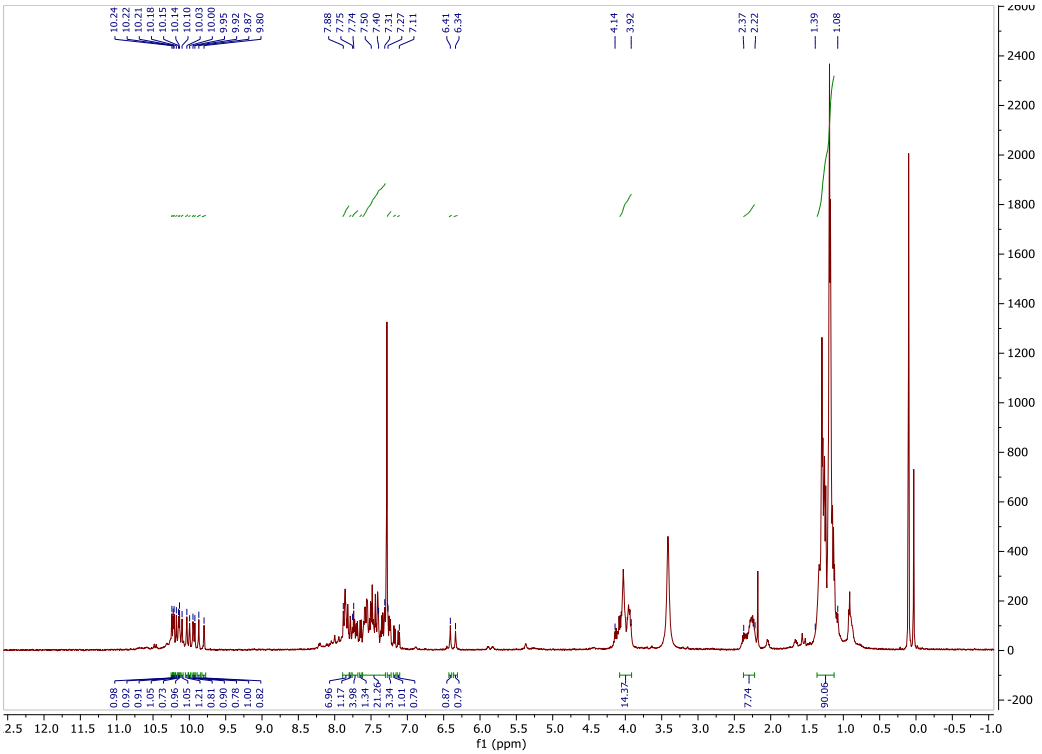

Figure 20. ^{1}H NMR of 15mer **60** (4 mM, $CDCl_3$)

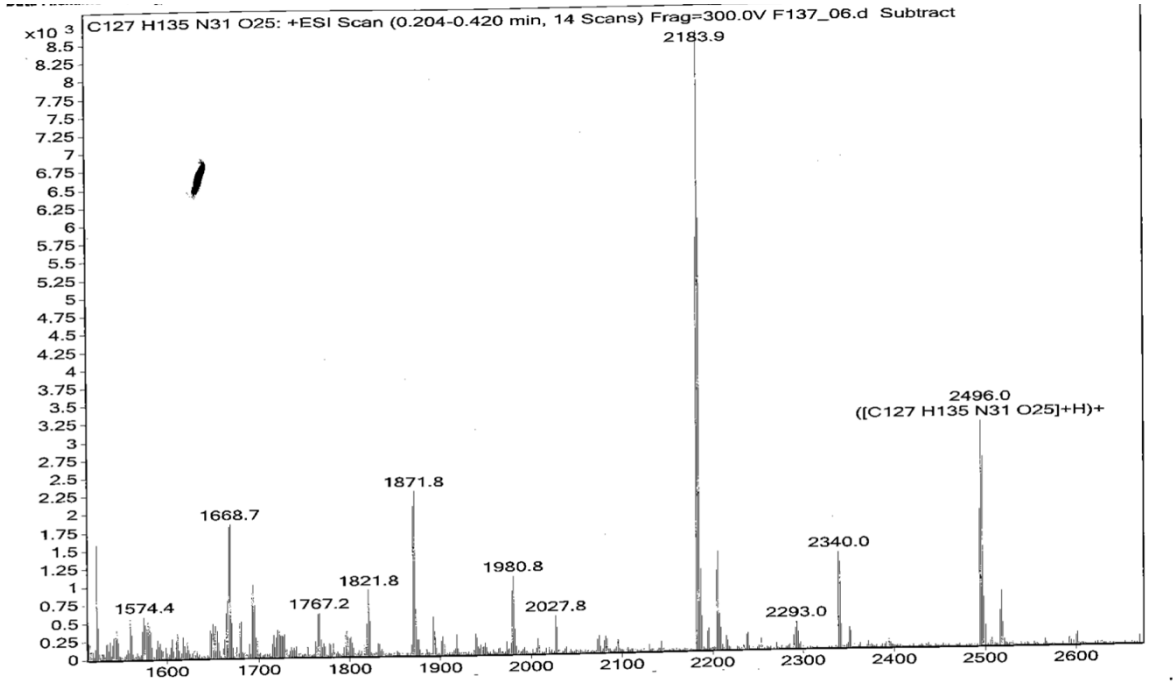

Figure 21. HRMS of **60**

3.3. Analysis of the dimerization

We note an important difference between proton signals of heptamer and 15mer, specifically interstrand amides N**H.** First, the location of peaks of 15mer is shifted upfield compared to heptamer, which is a characteristic of a double helix based on the literature. Looking at Figure 17 and Figure 18 above, it is apparent that heptamer **59** in $CDCl_3$ shows that the foldamer is largely dimerized at concentration >13 mM, but signals of the single helix are still present. However, 15mer **60** is fully hybridized into a double helix at a much lower concentration ~3 mM.

The previous study involving oligoimides of pyridine derivatives showed that dimerization could occur up to a certain length of a foldamer, after which the dimerization constant drastically decreases.[49] In this work, dimerization constants for 7mer and 15mer in $CDCl_3$ were determined as 37 L/mol and $>10^5$ L/mol, respectively, by integrating ^{1}H NMR peaks of single and double helices (Figure 22 and Figure 23) and using the equation below:

$$Kdim = \frac{[double\ helix]}{[single\ helix]^2}$$

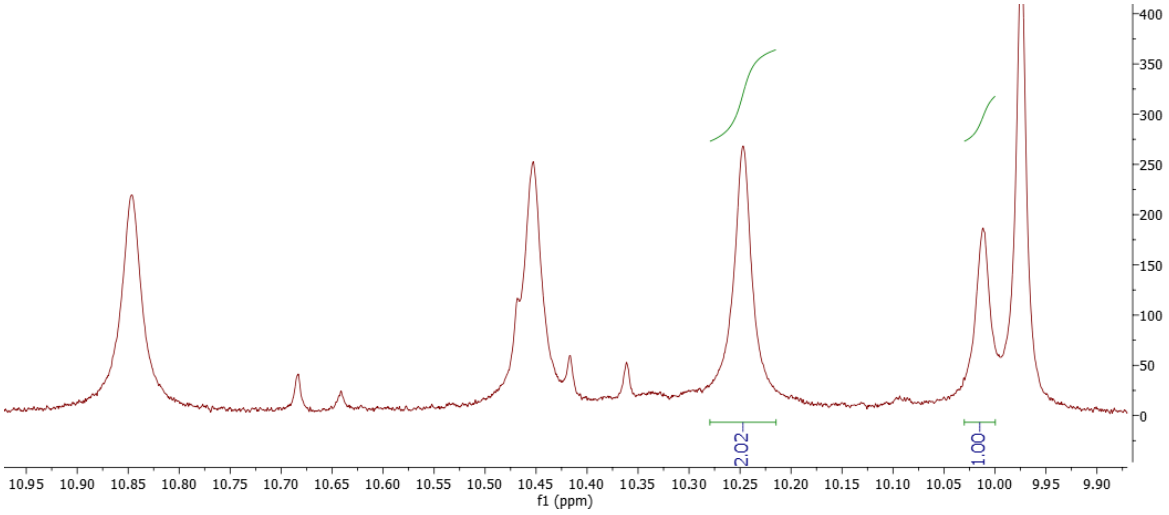

Figure 22. ^{1}H NMR of 7mer in $CDCl_3$, concentration = 13.4 mM. The ratio of protons between the double helix and single helix is 1 to 2.02. K_{dim} = 37 L/mol

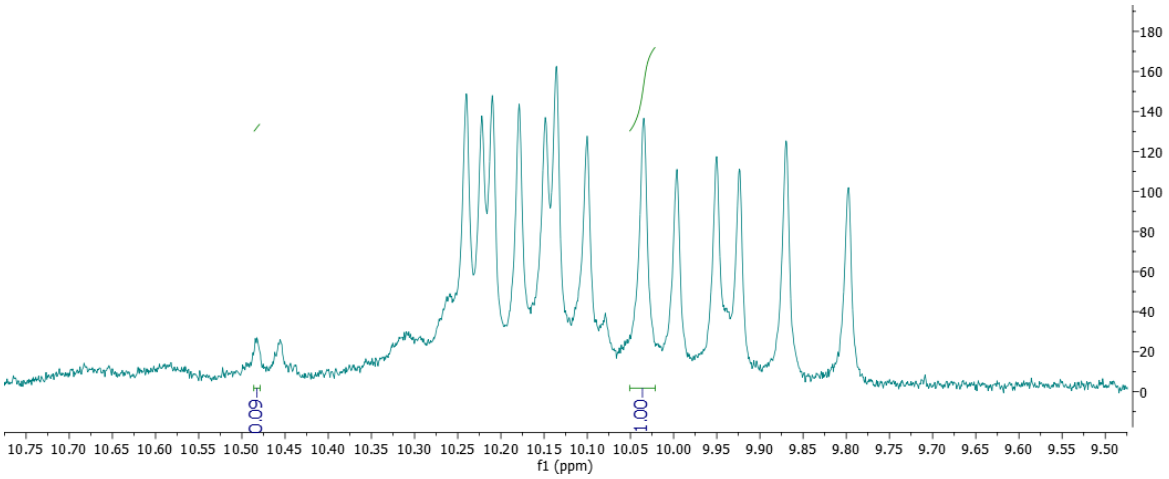

Figure 23. ^{1}H NMR of 15mer in $CDCl_3$, concentration = 4 mM. The ratio of protons between the double helix and single helix is 1 to 0.09. $K_{dim} > 10^5$ L/mol

Another difference is the non-equivalent environment of aromatic rings in the double-helical 15mer **60** in $CDCl_3$. In the hydrogen-bonded amide region (9.75 – 10.30 ppm) 13 sharp peaks are observed instead of 7 peaks, which can be explained by asymmetrical double helical structures with non-equivalent ends of each single strand. When two individual strands slide

along in a spiralling motion without dissociation, the ends of each strain experience different states and environments.[46] Additionally, the temperature variation experiments indicated that the proportions of signals remained the same. Temperature change experiments using foldamer **60** in $CDCl_3$ are summarized in Figure 24. At 25 °C, the overlap of some signals is observed, while at 40 °C, signals were splitted better, while at 50 °C, all peaks were split apart. As peaks did not shift downfield at elevated temperature, variable-temperature NMR experiments confirm the robustness of 15mer as a double helix (Figure 24).

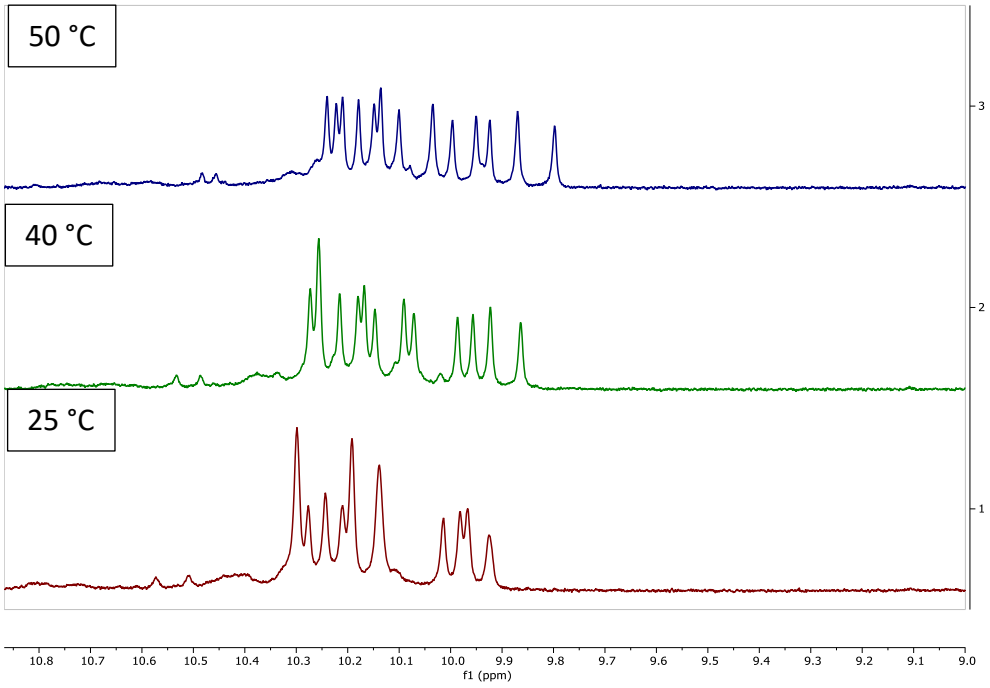

Figure 24. Effect of T on double helix stability. 4 mM, $CDCl_3$, T = 25 – 50 °C

Despite changing the solvent to polar in DMSO, decreasing the concentration up to 4 mM, and increasing temperature up to 50 °C, 15 pyridine units containing $(\mathbf{60})_2$ remain ~75% in a mixture (Figure 25).

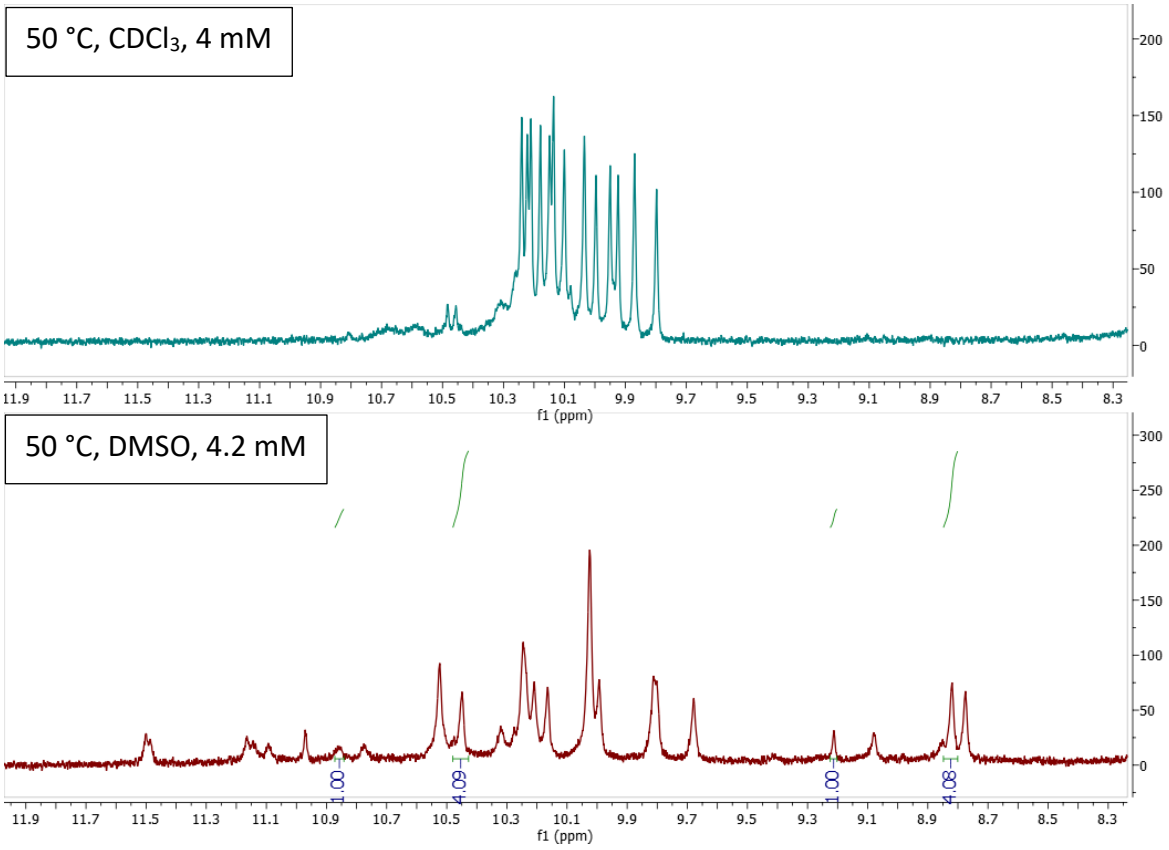

Figure 25. Effect of solvent and concentration on 15mer (**60**)$_2$. In polar DMSO-d6 at low concentration, the major species is a double helix. The integration ratio between amide protons NH of single vs. double helices is 1:4.

In summary, a foldamer-based mechanophore was successfully synthesized as 15 pyridine units containing an amide oligomer. The prepared oligomer consisted of two alternating units, diaminopyridine and *tert*-butoxypyridine. Dimerization constant of heptamer matches previously reported values of foldamers with alternating substitution pattern of alkoxy groups.

Doubling 7mer into 15mer allowed to drastically increase the dimerization constant from 37 L/mol to >10^5 L/mol. 15mer exists as a double helix with non-equivalent ends due to the sliding motion of strands. It has a high potential to be employed as a supramolecular

mechanophore in a polymer due to the robustness of a double helix as it is not sensitive to the solvent environment and variations of temperature and concentration.

Characterization of foldamers was done by NMR analysis. Due to the complex architecture and aggregation, 7mer and 15mer were assigned partially and preliminary. Literature used NMR and X-ray to characterize complex foldamers fully. In this project, crystallization did not work for newly synthesized 7mer and 15mer as they were liquid. The best result was a dendrimer 7mer obtained by slow evaporation of $CDCl_3$ solvent from the NMR tube but unsuitable for X-ray. These results will allow us to accurately determine the 3D structure of foldamers with the exact location of H-bonding and stacking interactions and their distances. This data helps to determine the symmetry and modeling of further steps of coupling foldamers with polymers.

3.4. Experimental

Synthesis of dimethyl 4-oxo-1,4-dihydropyridine-2,6-dicarboxylate

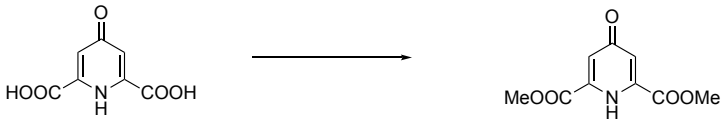

61

A known compound **61** was synthesized using the literature procedure.[122]

To a solution of chelidamic acid monohydrate (2 g, 9.95 mmol) in MeOH (10 mL), thionyl chloride (2 mL) was added at 0 °C. The reaction was left to stir at RT overnight, followed by reflux for additional 2 h. The reaction mixture was concentrated to afford **61** as a white solid (2.10 g, quant yield), which was further used in the next without purification.

IR: 3230, 2420, 1741, 1609, 1259; ^{1}H NMR (500 MHz, MeOD): 3.63 (s, 6H), 7.89 (br s, 2H); ^{13}C NMR (125 MHz, MeOD): 56.3, 118.0, 145.0, 160.8, 174.2.

Synthesis of *tert*-butyl (6-aminopyridin-2-yl)carbamate

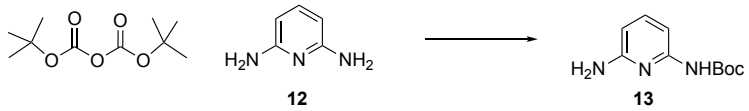

A known compound **13** was synthesized using the literature procedure.[123]

Di-*tert*-butylcarbonate (1.0 g, 4.58 mmol) was added to a solution of 2-6 diaminopyridine (0.5 g, 4.58 mmol) in THF (12 ml). The resulting solution was stirred a 60 °C overnight. After cooling the solvent was removed under vacuum and purified using CombiFlash to afford **13** as a white solid (75% yield).

IR: 3417, 3386, 1697, 1152; ^{1}H NMR (500 MHz, $CDCl_3$): 1.50 (s, 9H), 4.39 (br s, 2H), 6.15 (d, J = 8.0 Hz, 1H), 7.21 (d, J = 8.0 Hz, 1H), 7.40 (t, J = 8.0 Hz, 1H), 7.56 (br s, 1H); ^{13}C NMR (125 MHz, $CDCl_3$): 28.3 (C, 3x*C*H_3), 80.7 (C, *C*CH_3), 101.7 (C, H_2NC=*C*), 102.9 (C, *C*C(NH), 139.9 (C, *C*CC(NH), 150.6 (C, HN*C*=N), 152.4 (C, *C*=O), 157.2 (C, *C*NH_2).

Synthesis of dimethyl 4-isobutoxypyridine-2,6-dicarboxylate

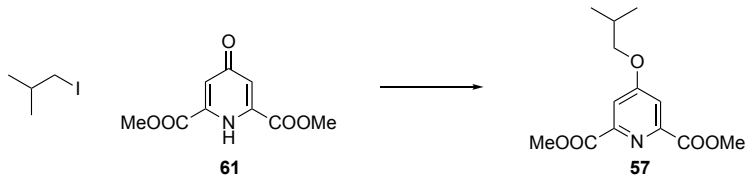

A known compound **57** was synthesized using the literature procedure.[122]

A solution of diester 61 (2 g, 7.48 mmol) and K_2CO_3 (3.27 g, 23.68 mmol) in DMF (12 mL) was refluxed for 2 h, followed by the addition of 1-iodo-2-methylpropane (2.61 g, 14.21 mmol) at

0 °C and the reaction mixture was left to reflux for 12 h; concentrated; purified using flash chromatography. White solid **57** was formed in 97% yield (2 g).

IR: 2963, 1752, 1714, 1104; ^{1}H NMR (500 MHz, $CDCl_3$): 1.05 (d, J = 6.7 Hz, 6H), 2.15 (septet, J = 6.7 Hz, 1H), 3.89 (d, J = 6.5 Hz, 2H), 4.01 (s, 6H), 7.80 (s, 2H); ^{13}C NMR (125 MHz, $CDCl_3$): 19.0, 28.0, 53.2, 75.2, 114.5, 149.7, 165.2, 167.2.

Synthesis of 4-isobutoxypyridine-2,6-dicarboxylic acid

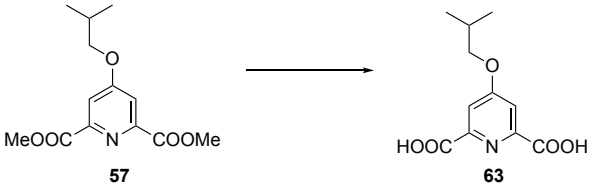

A new compound **63** was synthesized using the procedure below.

To a solution of diester **57** (2 g, 7.48 mmol) in MeOH/THF (1:5), NaOH (0.9 g, 22.45 mmol) was added in 3 portions at RT. The reaction was monitored by TLC until the starting material is fully consumed. The reaction was acidified with 1 M HCl solution, concentrated under reduced pressure, and dried under high vacuum overnight to afford **63** as a white solid in quantitative amount (1.81 g).

IR: 3396, 1702, 1584, 1035; ^{1}H NMR (500 MHz, MeOD): 1.07 (d, J = 6.7 Hz, 6H, 2xCH_3), 2.14 (septet, J = 6.6 Hz, 1H, CH(CH_3)$_2$), 3.98 (d, J = 6.4 Hz, 2H, OCH_2), 7.79 (s, 2H, 2xCH_{Ar}); ^{13}C NMR (125 MHz, MeOD): 19.2 (2xCH$_3$), 29.2 (CHCH$_3$), 77.6 (OCH$_2$), 115.8 (CH$_{Ar}$), 148.3 (2xCC(=O)OH), 164.7 (COCH$_2$), 171.9 (COOH).

Synthesis of di-*tert*-butyl (((4-isobutoxypyridine-2,6-dicarbonyl)bis(azanediyl))bis(pyridine-6,2-diyl))dicarbamate

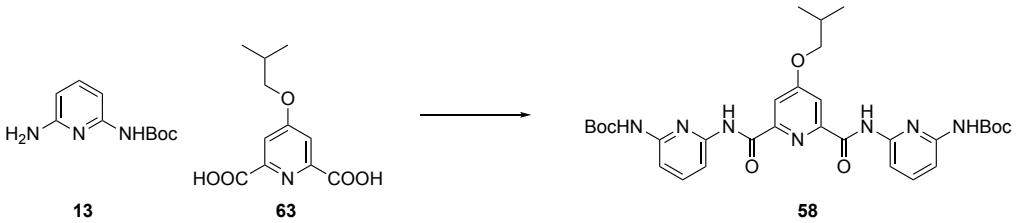

13 63 58

A new compound **58** was synthesized using the procedure below.

To a diacid **63** (434 mg, 1.82 mmol, 0.27 mmol) in DCM, oxalyl chloride (0.2 mL) was added at 0 °C stirred for 12 h at RT. The mixture was concentrated without heating water bath and put under high vac for 5 h.

The residue was dissolved in dry DCM (10 mL) and was added via cannula to a previously prepared solution of *tert*-butyl (6-aminopyridin-2-yl)carbamate (0.082 g, 0.39 mmol) in dry DCM (10 mL) and diisopropylethylamine (1.08 mL, 0.98 mmol) at 0 °C. The reaction mixture was stirred at RT for 24 h. The solvent was removed, and the residue was purified by flash chromatography to yield the white solid **58** (179 mg, 74%).

^{1}H NMR (500 MHz, $CDCl_3$): 1.07 (d, J = 8.4 Hz, 6H, 2xCH_3), 1.53 (s, 18H, 2xC(CH_3)$_3$), 2.17 (septet, J = 8.3 Hz, 1H, CH(CH_3)$_2$), 3.91 (d, J = 8.2 Hz, 2H, OCH_2), 7.65-7.68 (m, 4H, 2xCH_{Ar}CH$_{Ar}$CH_{Ar}), 7.73 (br s, 2H, 2xNHBoc), 7.88 (s, 2H, 2xOCCH_{Ar}), 7.96 (t, 2H, 2xCH$_{Ar}$CH_{Ar}CH$_{Ar}$), 9.96 (s, 2H, 2xNHC(=O)CN); ^{13}C NMR (125 MHz, $CDCl_3$): 19.0 (CH(CH_3)$_2$), 28.0 (CH(CH_3)$_2$), 28.2 (C(CH$_3$)$_3$), 75.3 (OCH$_2$), 81.1 (OC(CH_3)$_3$), 108.6 (CH$_{Ar}$CH$_{Ar}$CH$_{Ar}$), 109.0 (CH$_{Ar}$CH$_{Ar}$$CH_{Ar}$), 112.1 ($CH_{Ar}CCH_{Ar}$), 140.5 (CH$_{Ar}$$CH_{Ar}CH_{Ar}$), 148.9 (N$C$C(=O)NH), 150.6 ($C$(=O)OC($CH_3$)$_3$), 150.7 (N$C$C(=O)NH), 152.3 ($COCH_2$), 161.7 (N$C$NHC(=O)O), 168.2 (HN$C$(=O)CN); HRMS (ESI, [M+Na]): 644.2791, calcd. 644.2809.

Synthesis of trimer-diamine 67

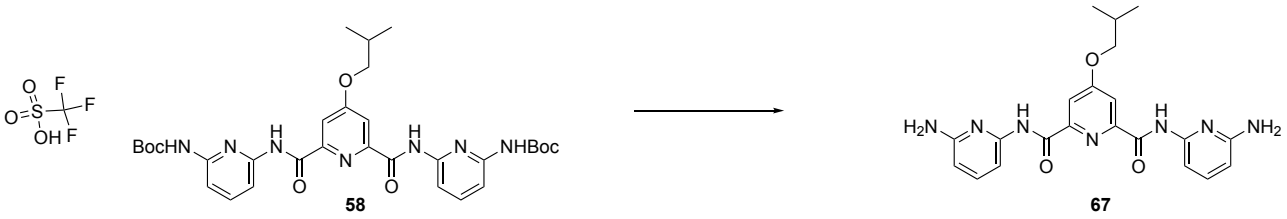

A new compound **67** was synthesized using the procedure below.

To a solution of 3mer **58** (1.5 g, 2.41 mmol) in DCM (2 mL), TFA/DCM mixture 10 mL (1:1) was added at 0 °C, the whole mixture was allowed to stir for 6 h at RT until completion of starting material. The reaction mixture was adjusted to pH about 8-10 using saturated solution of $NaHCO_3$, the product was extracted with DCM and purified using flash chromatography to afford diamine **67** as a white solid in 96% yield (0.98 g).

IR: 3315, 3209, 1726, 1464; ^{1}H NMR (500 MHz, $CDCl_3$): 1.06 (d, J = 6.7 Hz, 6H, 2xCH_3), 2.16 (septet, J = 6.6 Hz, 1H, $CH(CH_3)_2$), 3.96 (d, J = 6.5 Hz, 2H, OCH_2), 4.75 (br s, 4H, 2xNH_2), 6.33 (d, J = 8.0 Hz, 2H, H_2NCCH_{Ar}), 7.52 (t, J = 8.0 Hz, 2H, 2x$CH_{Ar}CH_{Ar}CH_{Ar}$), 7.76 (d, J = 7.9 Hz, 2H, $H_2NCH_{Ar}H_{Ar}CH_{Ar}$), 7.94 (s, 2H, 2x$CH_{Ar}CCH_{Ar}$), 10.12 (br s, 2H, 2xN*H*C=O); ^{13}C NMR (125 MHz, $CDCl_3$): 19.0 ($CH(CH_3)_2$), 28.0 ($CH(CH_3)_2$), 75.3 (OCH_2), 103.7 ($CH_{Ar}CH_{Ar}CH_{Ar}$), 105.0 ($CH_{Ar}CH_{Ar}CH_{Ar}$), 140.3 ($CH_{Ar}CCH_{Ar}$), 140.3 ($CH_{Ar}CCH_{Ar}$), 149.3, 150.5, 157.4, 161.4 (), 168.4 (HNC(=O)CN).

Synthesis of compound 62

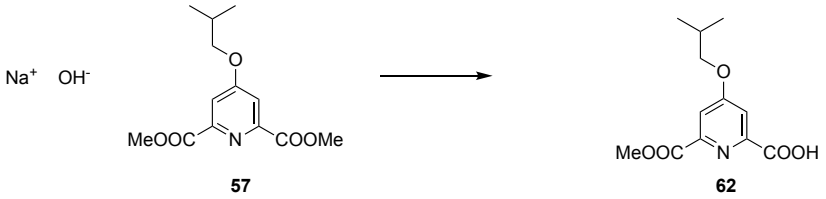

A new compound **62** was synthesized using the procedure below.

To a solution of diester **57** (0.3 g, 1.12 mmol) in MeOH/THF (1:5), NaOH (45 mg, 1.12 mmol) was added in 3 portions at RT. The reaction was monitored by TLC until the starting material is fully consumed. The reaction was acidified with 1 M HCl solution, concentrated under reduced pressure, and dried under high vacuum overnight to afford monoacid **62** as a white solid (0.28 g, 88%).

IR: 3217, 1962, 1720, 1698, 1597, 1030; ^{1}H NMR (500 MHz, $CDCl_3$): 1.05 (d, J = 6.7 Hz, 6H, 2xCH_3), 2.15 (septet, J = 6.7 Hz, 1H, $CH(CH_3)_2$), 3.91 (d, J = 6.5 Hz, 2H, OCH_2), 4.00 (s, 3H, $COOCH_3$), 7.81 (br s, 1H, CH_{Ar}), 7.84 (br s, 1H, COOH); ^{13}C NMR (125 MHz, $CDCl_3$): 19.0 ($CH(CH_3)_2$), 28.0 ($CH(CH_3)_2$), 53.1 ($COOCH_3$), 75.6 (OCH_2), 112.2 ($CH_{Ar}CCOOCH_3$), 115.8 ($CH_{Ar}CCOOH$), 148.0 (NCC=O), 163.7 ($COCH_2$), 164.5 ($COOCH_3$), 168.1 (COOH).

Synthesis of methyl 6-((5-((*tert*-butoxycarbonyl)amino)pyridin-3-yl)carbamoyl)-4-isobutoxypicolinate 66

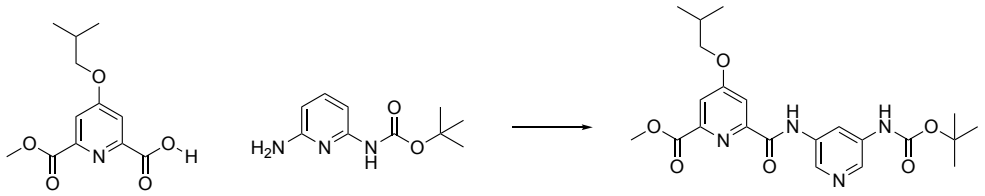

62 **13** **66**

A new compound **66** was synthesized using the procedure below.

To a monoacid **62** (0.2 g, 0.8 mmol) in DCM, oxalyl chloride (0.2 mL) was added at 0 °C stirred for 2 h at RT. The mixture was concentrated without heating water bath and put under high vacuum for 5 h.

The residue was dissolved in dry DCM (10 mL) and was added via cannula to a previously prepared solution of *tert*-butyl (6-aminopyridin-2-yl)carbamate (0.14 g, 0.65 mmol) in dry DCM (10 mL) and diisopropylethylamine (1.5 mL) at 0 °C. The reaction mixture was stirred at

RT for 24 h. The solvent was removed, and the residue was purified by flash chromatography to yield the white solid **66** (0.2 g, 67%)

^{1}H NMR (500 MHz, $CDCl_3$): 1.05 (d, J = 6.8 Hz, 6H, CH(C*H*$_3$)$_2$), 1.53 (s, 9H, C(C*H*$_3$)$_3$), 2.16 (septet, J = 6.7 Hz, 1H, C*H*(CH_3)$_2$), 3.92 (d, J = 6.5 Hz, 2H, OC*H*$_2$), 4.02 (s, 3H, OC*H*$_3$), 7.21 (s, 1H, C*H*$_{Ar}$), 7.69-7.75 (m, 2H, N*H*Boc, C*H*$_{Ar}$), 7.76 (d, J = 2.5 Hz, 1H, C*H*$_{Ar}$), 7.92 (d, J = 2.5 Hz, 1H, C*H*$_{Ar}$), 8.01 (d, J = 7.7 Hz, 1H, C*H*$_{Ar}$), 10.25 (s, 1H, CN*H*C(=O)CN); ^{13}C NMR: 19.0 (C, CH(*C*H_3)$_2$), 28.0 (C, *C*H(CH_3)$_2$), 28.2 (C, 3xCH_3), 53.0 (C, COO*C*H_3), 75.3 (C, O*C*H_2), 81.1 (C, O*C*(CH_3)$_3$), 108.1 (C, HNC*C*H_{Ar}CNH), 108.3 (C, HNC(=O)C*C*H_{Ar}), 111.1 (C, *C*H_{Ar}COCH_2), 114.9 (C, N*C*H_{Ar}CN), 140.5 114.9 (C, N*C*H_{Ar}CN), 148.3 (C, OC(=O)NH*C*CH_{Ar}N), 149.1 (C, OC(=O)NH*C*CH_{Ar}CNH), 150.5 (C, *C*COOCH_3), 151.4 (C, *C*OCH_2), 152.2 (C, N*C*C(=O)NH), 161.7 (C, *C*OOC(CH_3)$_3$), 165.0 (C, HN*C*(=O)CN), 167.7 (C, *C*OOCH_3); HRMS (ESI, [M+Na]): 467.1910, calcd. 467.1907.

Synthesis of 6-((6-((tert-butoxycarbonyl)amino)pyridin-2-yl)carbamoyl)-4-isobutoxypicolinic acid 68

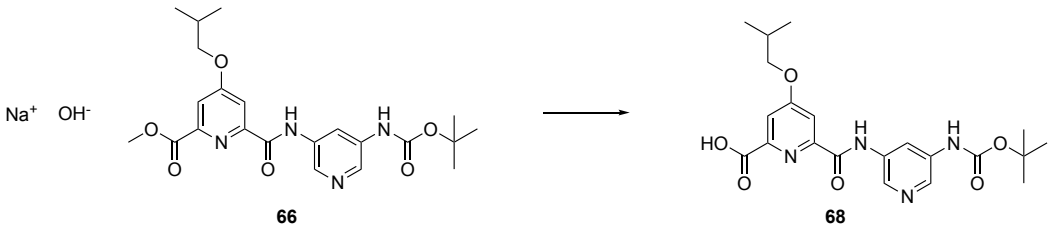

A new compound **68** was synthesized using the procedure below.

Methyl 6-((6-((*tert*-butoxycarbonyl)amino)pyridin-2-yl)carbamoyl)-4-isobutoxypicolinate (0.65 g, 1.462 mmol) in 25 mL dioxane was added sodium hydroxide (0.117 g, 2.92 mmol) in 2 mL water. The resulting mixture was stirred at 40 °C for 3 h. The solution was acidified by (0.5 M) HCl and extracted with DCM to give dimer **68** (0.57 g) in quantitative amount.

^{1}H NMR (500 MHz, $CDCl_3$): 1.06 (d, J = 6.7 Hz, 6H, CH(CH_3)$_2$), 1.55 (s, 9H, CH(CH_3)$_3$), 2.16 (septet, J = 6.6 Hz, 1H, CH(CH_3)$_2$), 3.92 (d, J = 6.4 Hz, 2H, OCH_2), 7.71-7.85 (m, 4H, 4xCH_{Ar}), 7.87 (d, J = 2.1 Hz, 1H, CH_{Ar}), 7.96 (d, J = 2.1 Hz, 1H, CH_{Ar}), 8.07 (d, J = 7.7 Hz, 1H, CH_{Ar}), 10.8 (br s, 1H, C(=O)N*H*C); ^{13}C NMR (500 MHz, $CDCl_3$): 19.0 (CH(CH_3)$_2$), 28.0 (CH(CH_3)$_2$), 28.2 (C(CH_3)$_2$), 75.3 (OCH_2), 81.4 (OC(CH_3)$_3$), 108.6 (HNCCH_{Ar}CNH), 108.9 (C, OCCH_{Ar}CC(=O)), 112.4 (C, OCCH_{Ar}CC(=O)NH), 114.3 (C, 2xNCH_{Ar}), 141.4 (*C*NHC(=O)O), 148.1 (HN*C*CH_{Ar}CNHC(=O)O), 148.9 (C, HOOC*C*), 150.8 (C, *C*C(=O)NH), 152.1 (*C*OCH_2), 161.9 (*C*OOC(CH_3)$_3$), 166.2 (NC*C*(=O)NH), 168.1 (*C*OOH).

Synthesis of heptamer 59

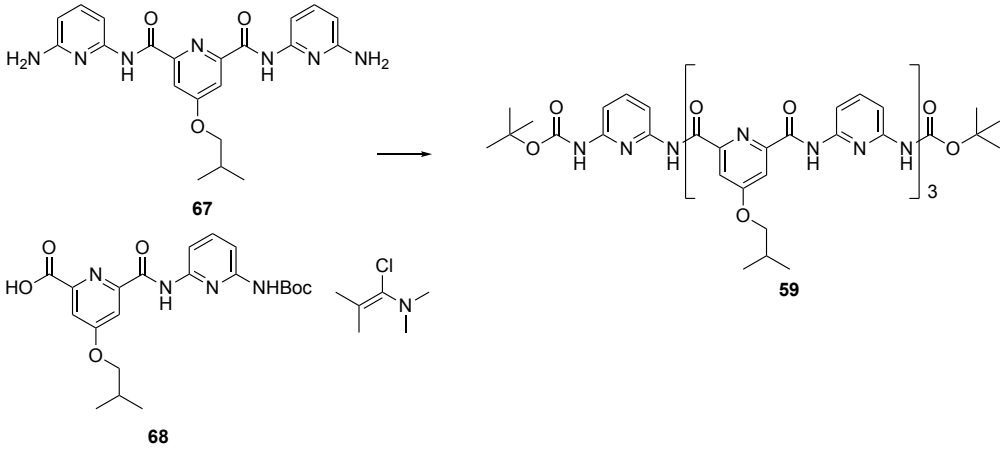

A new compound **59** was synthesized using the procedure below.

1-Chloro-*N,N*,2-trimethylpropenylamine (5.6 mmol, 0.74 g) was added to dimer acid **68** (1 g, 2.32 mmol) dissolved in dry CH_2Cl_2 (5 mL) under a nitrogen atmosphere. The mixture was stirred for 12 h at 25 °C. Excess chloroenamine was removed under reduced pressure. The residue obtained was dissolved in dry CH_2Cl_2 (2 mL) and added dropwise to a previously prepared solution of monomer di-amine **67** (0.39 g, 0.93 mmol) in dry CH_2Cl_2 (5 mL) and diisopropylethylamine (0.72 g, 5.6 mmol) at 25 °C. The mixture was stirred at ambient

temperature for 12 h. The solvent was removed, and the residue was purified by flash chromatography to yield the product **59** in 60.4%.

NMR peaks at aromatic region were assigned partially and preliminary due to the complexity of 3D structure and overlapping of signals of single and double helices.

^{1}H NMR (500 MHz, $CDCl_3$): 1.13 (d, J = 6.7 Hz, 6H, 2xCH(CH_3)$_2$), 1.19 (d, J = 6.7 Hz, 12H, 4xCH(CH_3)$_2$), 1.34 (s, 18H, 2xC(CH_3)$_3$), 2.19-2.30 (m, 3H, 3xCH(CH_3)$_2$), 4.04 (d, J = 6.1 Hz, 6H, 3xOCH_2), 6.94 (s, 2H, 2xN$H_{terminal}$), 7.37 – 7.42 (m, 4H + impurity), 7.61 (t, J = 8.0 Hz, 2H+impurity), 7.77 (t, J = 7.6 Hz, 2H), 7.85-7.90 (m, 6H), 8.10 (s, 2H), 8.23 (d, J = 7.6 Hz, 2H), 10.31 (br s, 2H, NCNHC(=O)C), 10.51 (br s, 2H, NCNHC(=O)C), 10.93 (br s, 2H, NCNHC(=O)C); ^{13}C NMR (125 MHz, $CDCl_3$): 19.1 (CH(*C*H_3)$_2$), 27.7 (C(*C*H_3)$_3$), 27.9 (*C*H(CH_3)$_2$), 75.4 (O*C*H_2), 81.1 (O*C*(CH_3)$_3$), 108.0, 108.1, 110.1, 110.2, 111.6, 112.1, 112.2, 140.9, 141.2, 148.4, 149.0, 149.1, 149.2, 149.8, 150.1, 151.4 (*C*OCH_2), 160.4, 161.1 (NC*C*(=O)NH), 161.3 (*C*OOC(CH_3)$_3$), 168.1 (N*C*(=O)OC(CH_3)$_3$); HRMS (FTMS+pNSI, [M+Na]): 1268.5266, calcd. 1268.5248.

Synthesis of heptamer-monoamine 72

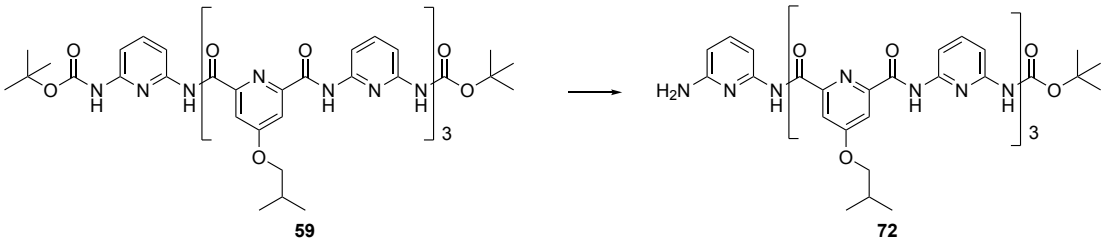

A new compound **72** was synthesized using the procedure below.

To the solution of 7mer **59** (162 mg, 0.13 mmol) in DCM (12 mL), 0.9 mL of 0.2 M TMSI solution in DCM (stock solution: 1 mL of TMSI in 5 mL DCM) added at 0 °C and the reaction mixture was stirred at RT for 2 h. Then, DCM was evaporated, and the concentrated mixture was redissolved in 12 mL of MeOH and refluxed for 4 h, followed by evaporation and

purification by column chromatography. In the next step, the reaction mixture was concentrated and purified using CombiFlash to afford a colorless oil in 64% yield.

NMR peaks at aromatic region were assigned preliminary due to the complexity of 3D structure and overlapping of signals of single and double helices.

^{1}H NMR (500 MHz, $CDCl_3$): 0.84 – 2.35 (m, 36 aliphatic Hs + impurities), 3.99 (m, (OC*H*$_2$)x3), 5.38 (br s, 1H, N*H*H), 5.85 (br s, 1 H, NH*H*), 6.96 (br s, 1H, N*H*), 7.39 – 8.27 (m, 18H, H_{Ar}), 10.23 (br s, 1H, N*H*), 10.37 (br s, 1H, N*H*), 10.56 – 10.58 (m, 2H, 2xN*H*), 10.91 (br s, 1H, N*H*), 10.98 (br s, 1H, N*H*); HRMS (ESI, [M+H]): 1146.4862, calcd. 1146.4904; IR: 3348, 3350, 2921, 1692, 1455.

Synthesis of pentadecamer 60

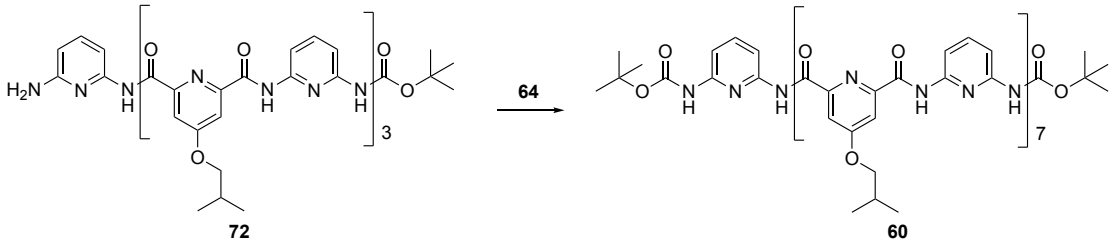

A new compound **60** was synthesized using the procedure below.

Diacid **21** (104 mg, 0.44 mmol) in oxalyl chloride (0.1 mL) was stirred at RT for 1 h. Concentrated, extra oxalyl chloride was removed under high vacuum. The crude product **22** was dissolved in DCM (10 mL) and added to a solution of monoamine **29** (0.5 g, 0.44 mmol) in DCM (5 mL) and DIPEA (1 mL) at RT. The mixture was stirred at RT overnight. Concentrated and purified using column chromatography to afford white solid (520 mg) in 48% yield.

NMR peaks at aromatic region were assigned preliminary due to the complexity of 3D structure and overlapping of signals of single and double helices.

^{1}H NMR (500 MHz, $CDCl_3$): 1.09-1.30 (m, 60 aliphatic H + impurities), 2.15-2.33 (m, 7H, 7xC*H*$(CH_3)_2$), 3.92-4.14 (m, 14H, 7xOCH_2), 6.34 (s, 1H, N*H*), 6.41 (s, 1H, N*H*), 7.11-7.88 (m, 39 H, 38x CH_{Ar}, N*H*), 9.80 (s, 1H, N*H*), 9.87 (s, 1H, N*H*), 9.92(s, 1H, N*H*), 9.95 (s, 1H, N*H*), 10.00 (s, 1H, N*H*), 10.03 (s, 1H, N*H*), 10.10 (s, 1H, N*H*), 10.14 (s, 1H, N*H*), 10.15 (s, 1H, N*H*), 10.18 (s, 1H, N*H*), 10.21 (s, 1H, N*H*), 10.22 (s, 1H, N*H*), 10.24 (s, 1H, N*H*); HRMS (ESI, [M+H]): 2496.0277, calcd. 2496.0318.

CHAPTER 4. Synthesis of polymers

4.1. Overview

The multiscale nature of polymer mechanochemistry makes it challenging and an attractive area to create mechanically functional materials, which requires a synthetic effort to embed desired force-responsive functional moieties within a bulk material. Four mechanophores and mechanochromic force probes mainly dominate the polymer mechanochemistry: dicyclohalopropane,[16, 124] stiff-stilbene,[13, 124] azobenzene[12, 124] and spiropyran.[10, 11, 18, 124] Mechanochemically active polymers can be synthesized either by coupling a mechanophore to a pair of polymer chains (Scheme 41a) or by polymerizing a mechanophore containing monomer (Scheme 41b). The former yields chains containing a single mechanophore per chain, while the latter creates multi-mechanophore polymers. [2, 125]

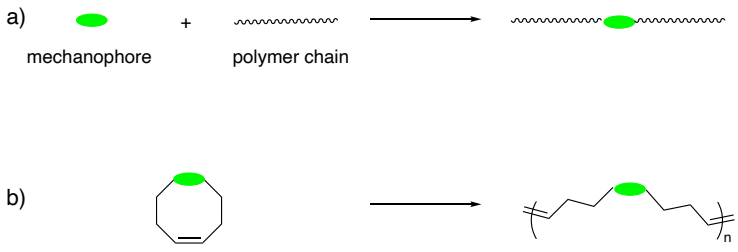

Scheme 41. General overview of mechanophore incorporation into a polymer chain

(a – chain-centred mechanophore polymer; b – mechanophore rich polymer)

The development of new mechanically active polymers yields smart materials[2] such as self-strengthening and self-healing through bond formation mechanisms such as cross-linking as a response to the applied force.

Previous chapters of this thesis provided information about the architecture and synthesis of potential mechanophores with allosteric and supramolecular properties. This Chapter reports the polymerization of **54** (Scheme 42), whose synthesis and properties are described in **Chapter 2** and end-derivatization of polystyrene with foldamers, whose structure, synthesis, and properties are reported in **Chapter 3** (Scheme 43).

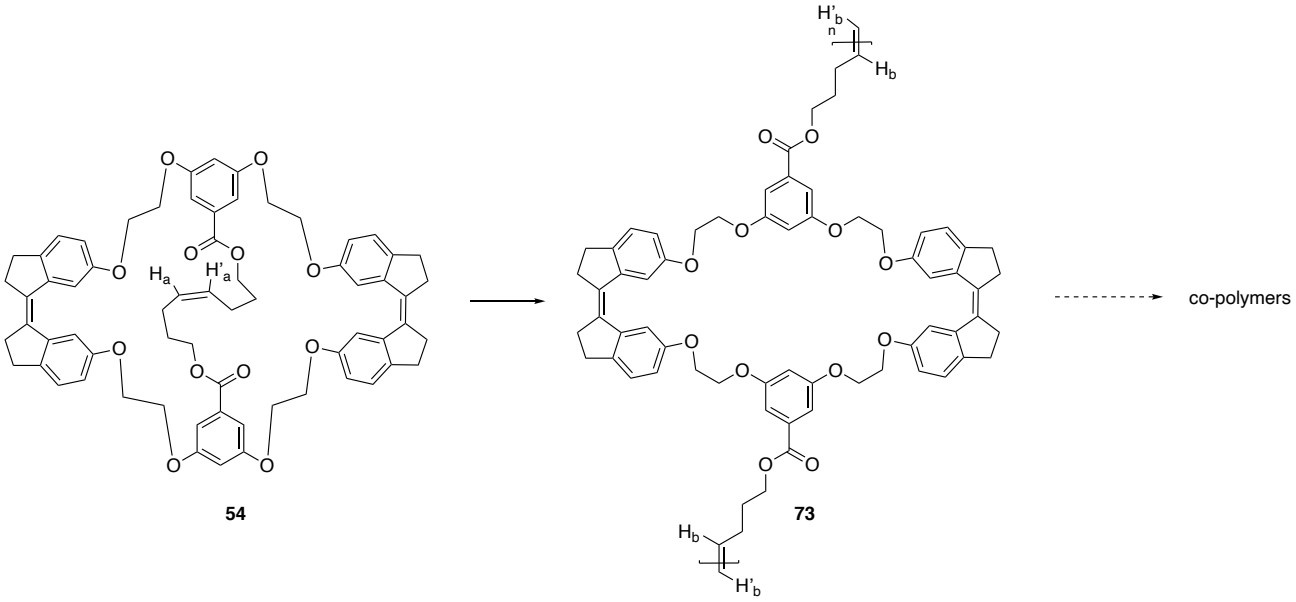

Scheme 42. ROMP of the stiff-stilbene macrocycle

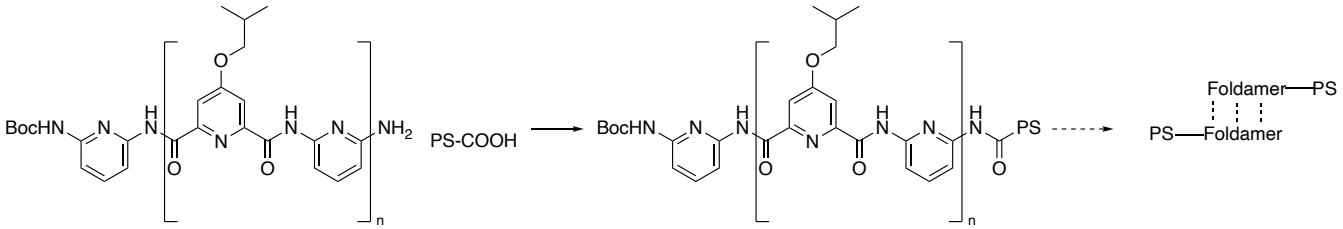

Scheme 43. End-derivatization of polystyrene with foldamers

4.2. Ring-Opening Metathesis Polymerization

Ring-opening metathesis polymerization is a powerful technique to polymerize strained olefinic monomers,[64, 126-128] usually small cycles from three to eight atoms. The driving force for these monomers' polymerization is either the ring or angular strain.[126-128] Common ROMP catalysts are Grubbs II and III (Figure 26), where Grubbs III manifests greater functional group tolerance, air-stability, and fast initiation and propagation rates.[129, 130]

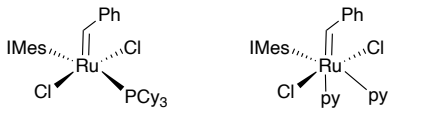

Grubbs II gen catalyst Grubbs III gen catalyst

Figure 26. Structures of the Grubbs II and Grubbs III generation catalysts

Even though this methodology is limited as macrocycles (ring size >14) usually have a little or no strain,[131] successful entropy-driven ROMP has been achieved by effective design of olefinic macrocycles, catalyst choice, and reaction conditions.[127] For example, Shimizu and co-workers[132] reported successful ROMP of 30-membered stilbene-containing macrocycle in a 1 M solution with Grubbs II generation catalyst, and catalyst loading 1 mol% at T = 60 °C to achieve Mn = 45 kDa (Scheme 44a). UV-Vis analysis of the product provided the unexpected result of isomerization of starting cis-stilbene into trans isomer. Other examples of

entropically-driven ROMP of macrocycles include preparation of spiropyran and gem-dichlorocyclopropane (gDCC) polymers (Scheme 44b)[18] Co-polymerization with 9-oxabicyclo[6.1.0]non-4-ene of 0.3 M toluene solutions used 10 mol% Grubbs II catalyst. A final noteworthy example is the preparation of poly-catenated polymers by ROMP (Scheme 44c)[133] of a macrocyclic catenane and gem-dicyclopropane derivative under Grubbs III catalysis (1.5 mol%) in DCM to afford 211 kDa polymer.

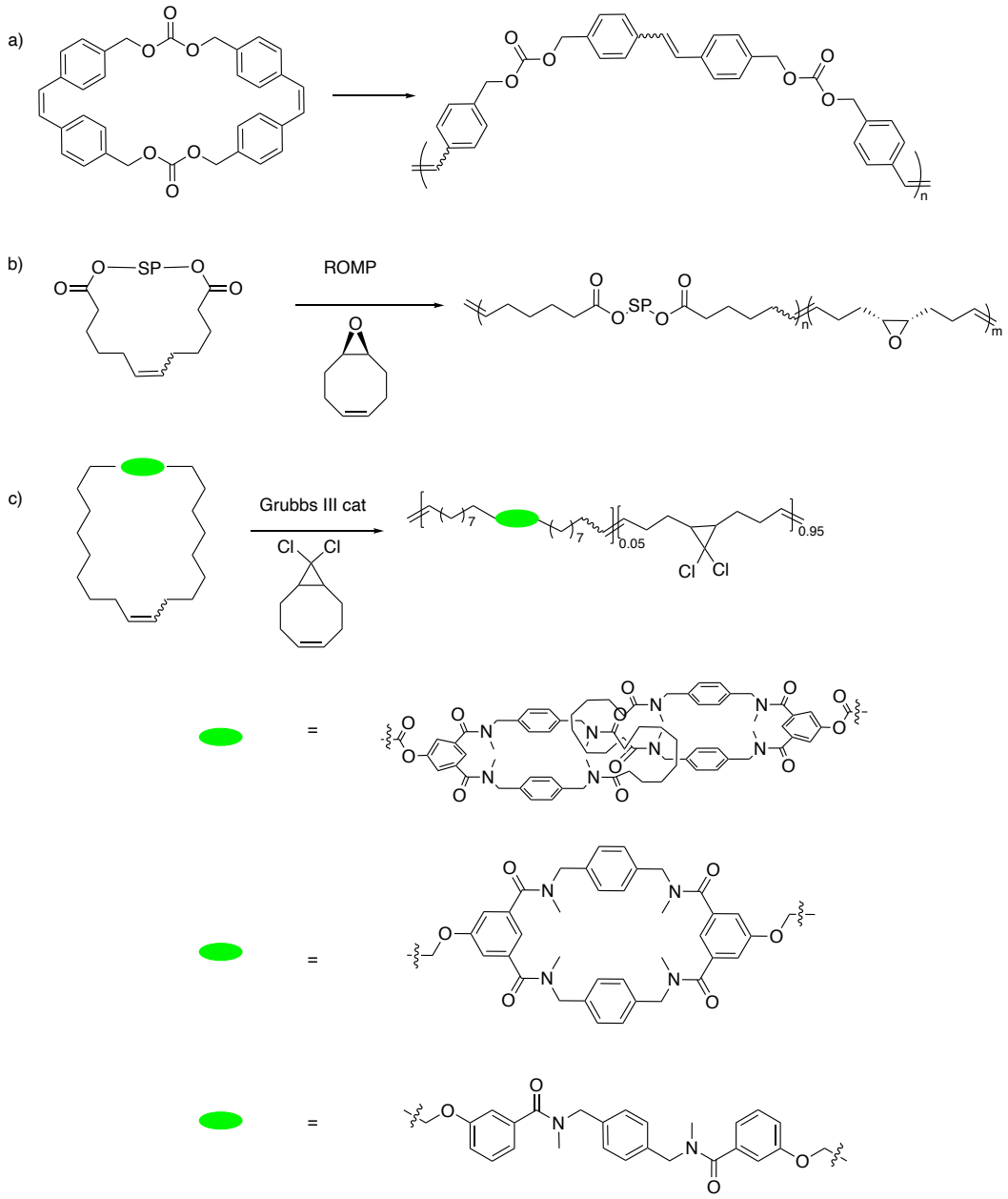

Scheme 44. Examples of ROMP of macrocycles (SP – spiropyran)

These examples encouraged us to search for conditions to enable ROMP of macrocycle **54** (Scheme 42) by screening the two Grubbs catalysts, two solvents and a range of concentrations of the monomer (0.3 – 1 M), the catalyst loading (1-10 mol%), and temperature (RT - 60 °C).

4.2.1. Synthesis of the allosteric stiff-stilbene polymer

Twelve ROMP experiments were performed under standards conditions (DCM, RT, N_2 atmosphere) by varying catalyst, catalyst loading, and monomer's concentration (Table 4). The crude products were analyzed by analytical SEC, and the chromatogram is shown in Figure 28.

Table 4. ROMP trials and results

#	catalyst	Conditions/catalyst loading	Results (kDa)
1	Grubbs II	DCM, RT, 1 M, N_2/1 mol%	3-25
2	Grubbs II	DCM, 50 °C, 1 M, N_2/1 mol%	3-25
3	Grubbs II	DCM, RT, 0.1 M, N_2/1 mol%	No polymer was formed
4	Grubbs II	DCM, RT, 0.1 M, N_2/2 mol%	3-25
5	Grubbs II	DCM, RT, 5 M, N_2/1 mol%	3-25
6	Grubbs II	DCM, RT, 5 M, N_2/10 mol%	2 (dimer)
7	Grubbs II	DCM, RT, 5 M, N_2/0.1 mol%	No polymer was formed
8	Grubbs II	DCM, RT, 1 M, N_2/0.1 mol%	No polymer was formed
9	Grubbs III	DCM, RT, 1 M, N_2/0.5 mol%	No polymer was formed
10	Grubbs III	DCM, RT, 5 M, N_2/0.5 mol%	No polymer was formed
11	Grubbs III	DCM, RT, 5 M, N_2/1.5 mol%	No polymer was formed
12	Grubbs III	DCM, RT, 5 M, N_2/2.5 mol%	No polymer was formed

The polymerization of monomer **54** was investigated using Grubbs II and III generation catalysts (0.1 – 10 mol%) in CH_2Cl_2 (Scheme 42). Grubbs II catalyst yielded polymer **73** with

nominal MW ranging from 2 to 25 kDa (nominal Mp = 6 kDa) (Figure 29) as determined by SEC (Figure 28) calibrated against polystyrene mass standards.

ROMP using Grubbs III catalyst did not result in any polymer formation. This result was unexpected as Grubbs III, due to the faster initiation activity than Grubbs II should at least provide narrow dispersity ROMP product between 3 – 25 kDa. Change of concentration and catalyst loading did not result in any improvement, suggesting that the initiation rate does not affect the ED ROMP of the macrocycle. Roles of Grubbs II and Grubbs III can differ in properties in ED-ROMP reactions compared to ROMP of strained systems.[134] This result needs to be further investigated.

The general ^{1}H NMR of the ROMP mixture is shown below. The purification of the ROMP product was done by recrystallization using DCM/MeOH mixture. Upon MeOH addition (1 drop), polymer precipitated, filtered, and dried. ^{1}H NMR spectrum of product mixture (Figure 27) shows the disappearance of monomer's alkene peaks at 5 ppm forming new signals around 5.5 and 5.8 ppm.

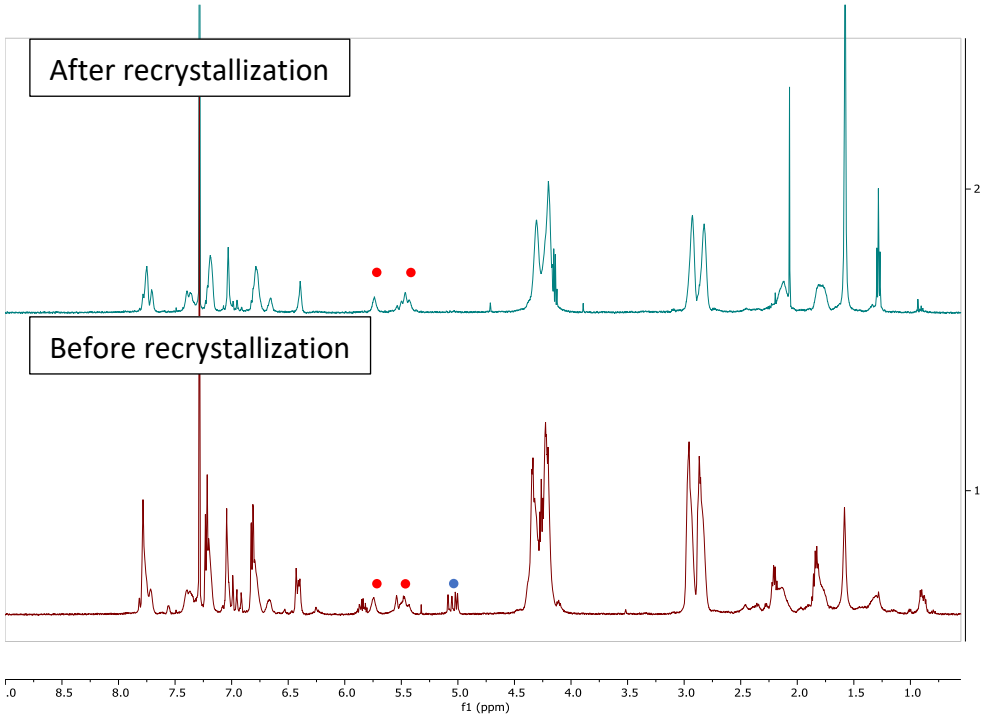

Figure 27. Comparison of ^{1}H NMR spectra of ROMP products (blue dot – starting monomer's peaks, red dot – product's peaks) before and after purification by crystallization.

Compounds **53** and **54** have high solubility in DCM, but polar solvents like MeOH start to precipitate, which causes difficulties during MS characterization. A mixture of DCM and NH_4OAc allowed running HRMS on the monomer **54**. However, it did not work for polymer **73**. Polymer **73** was characterized using SEC calibrated against PS standards.

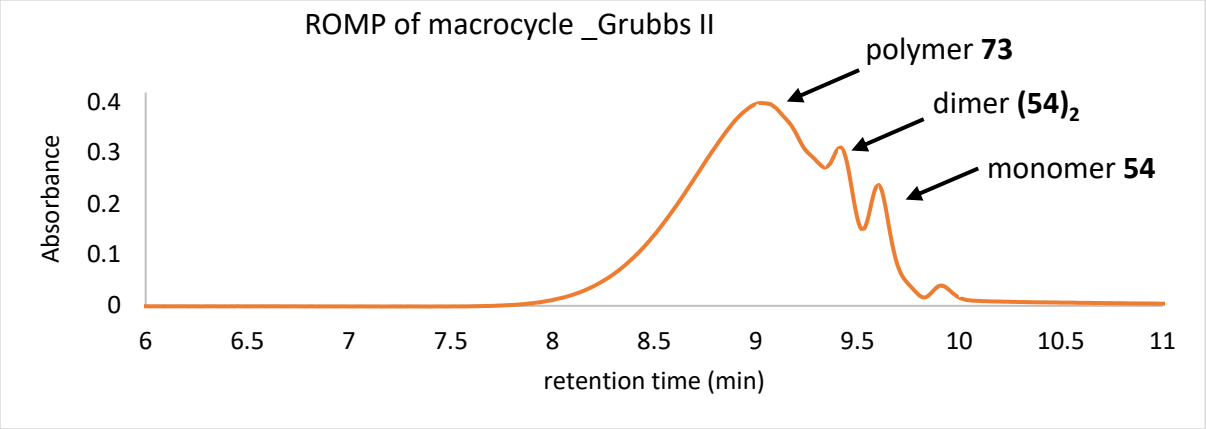

Figure 28. SEC of ROMP of stiff-stilbene macrocycle **54.** Calibration against PS standards.

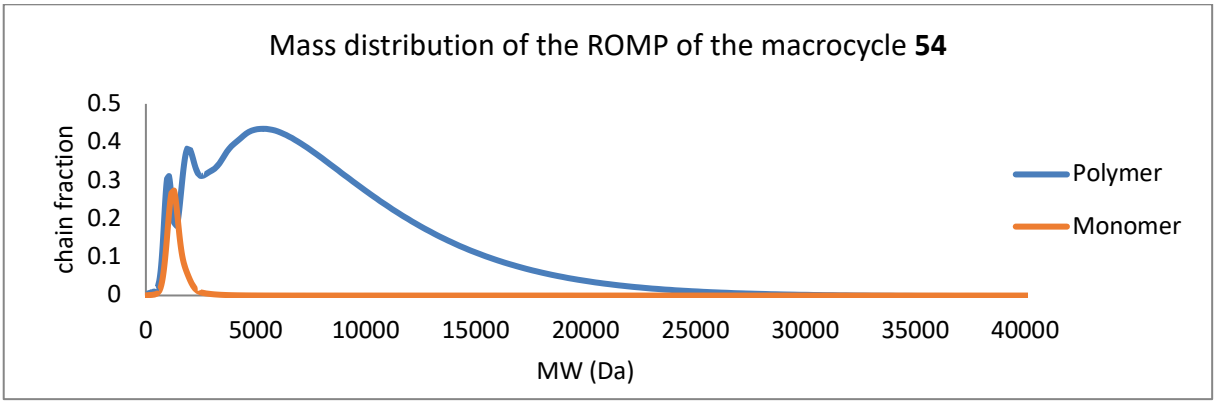

Figure 29. Mass distribution of the stiff-stilbene polymer

UV-Vis analysis of product mixture shows the presence of cis-stiff-stilbene as the major isomer with characteristic absorbance at 358 nm (Figure 30).

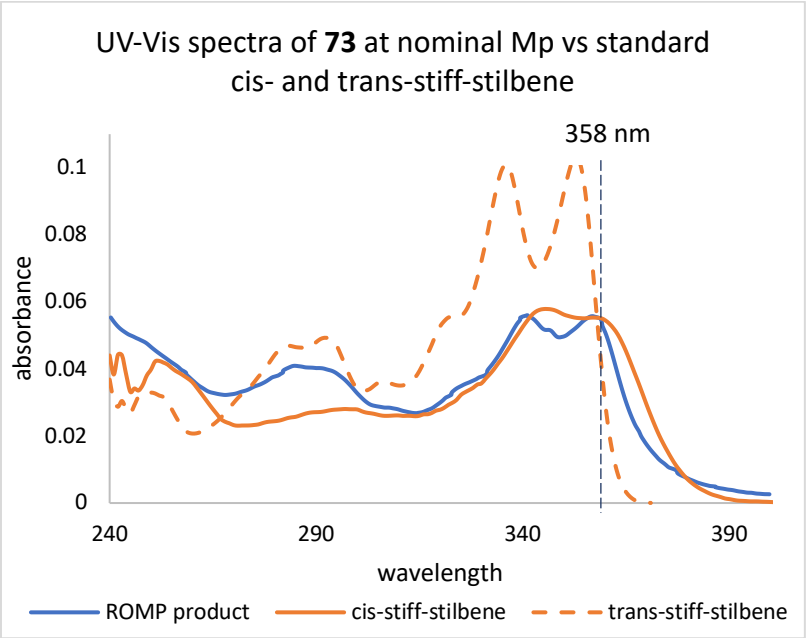

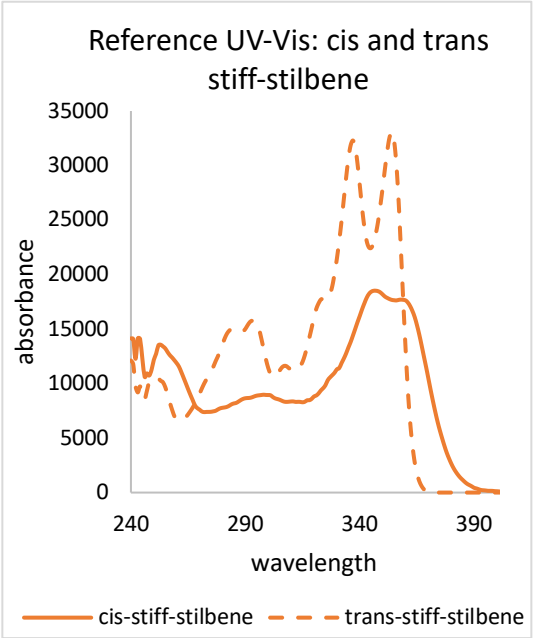

Figure 30. Left: UV-Vis spectra extracted from SEC data (PDA detector) of compound **73** at nominal Mp = 6 kDa vs standard cis- and trans-stiff-stilbene. Right: Reference UV-Vis spectra of stiff-stilbene isomers

ROMP of model compound **41** (Scheme 5) resulted in Mp <1 kDa, which correspond to 5 monomer units only (Figure 31). SEC and extracted UV-Vis data are shown below (Figure 31). SEC spectra of both model and macrocyclic compounds show several peaks, corresponding for monomer (reagent) and polymer (product). The product peak is very broad, which means a wide distribution of polymer molecular weight.

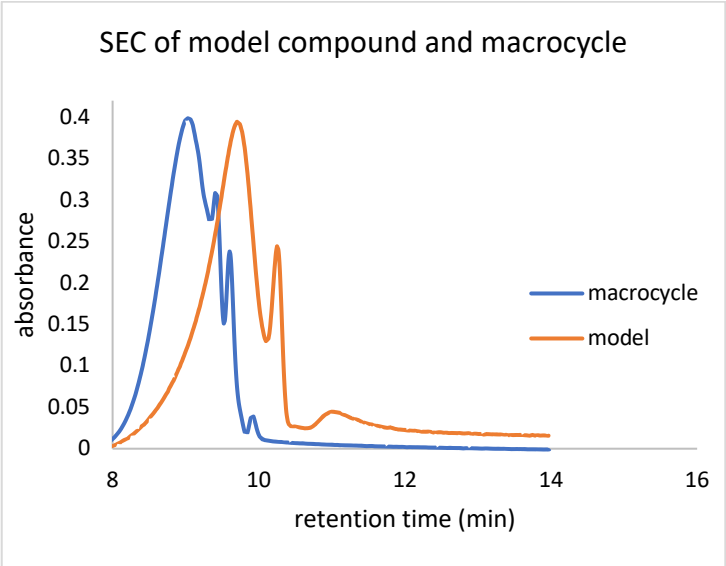

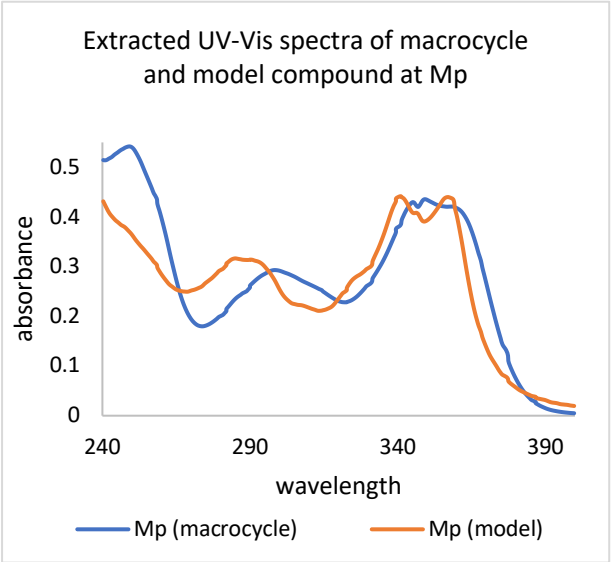

Figure 31. Left: SEC spectra of ROMP of the model compound and macrocycle. Right: UV-Vis spectra of model compound and macrocycle at Mp

4.2.2. Discussion

Polymerization of macrocycle yielded the product with Mp = 5 kDa, confirming that the macrocyclic monomer can be opened with ED-ROMP approach.

The main approaches in the literature to increasing ED-ROMP efficiency including identifying a better catalyst, such as Grubbs III, increasing the monomer concentration, increasing the temperature, and optimizing catalyst loadings. The reaction of ROMP using standard conditions (Grubbs II, DCM) allowed to achieve Mp = 5 kDa. However, when the catalyst was changed from Grubbs II to Grubbs III, the reaction failed despite superior polymerization properties of Grubbs III, which is unexpected as Grubbs III catalyst showcase better efficiency in other ED-ROMP cases than Grubbs II due to the faster initiation properties. A possibility that Grubbs III has degraded is excluded as it worked for control polymerization reactions using cyclooctene. A potential explanation can be the different coordination sites of two polymers. As Grubbs II was effective for the opening reaction, it possibly was coordinated by

oxygen functional groups, while Grubbs III may have a higher stacking with stiff-stilbenes that resulted in no reaction. The short, stiff linker in the monomer can be an additional constraint for ineffective Grubbs-III catalyzed ED-ROMP.[128] Changing the linker to a more flexible alternative may provide insight if the reactivity of polymerization increases using Grubbs III.

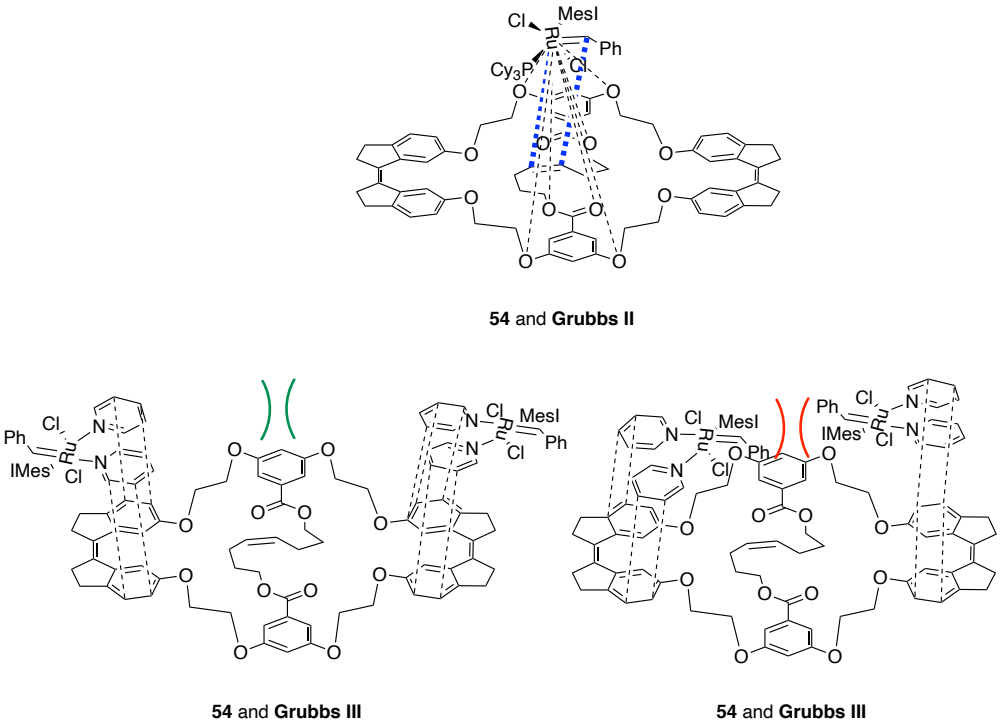

Figure 32. Potential coordination complexes between macrocycle **54** and Grubbs catalysts. Top: Grubbs II is coordinated by oxygens over the double bond. Bottom: Grubbs III has two pyridine rings that can stack over stiff-stilbene but are directed away from the double bond due to bulky Mesityl group.

The above results suggest that changes in the concentration of the monomer and the reaction temperature did not affect the resulting product **73**, while the catalyst loading was an essential factor in obtaining polydisperse polymer or resulting in no or short-chain products. It is necessary to run the reaction (Scheme 42) in the interval of catalyst loading from 0.5 – 1 mol% under the same ROMP conditions since it was unsuccessful below 0.5 mol% and catalyst

loading above 1 mol% did not lead to better polymerization results (Table 4). Perhaps a specific loading will allow shifting Mp to the higher MW.

NMR analysis of the produced polymer suggests the formation of linear chain oligomer over a macrocyclic stiff-stilbene analog due to the shift of alkene peaks from 5 ppm (Scheme 42, Ha) to 5.5 and 5.8 ppm (Scheme 42, Hb) region, which implies structural changes associated with the macrocycle's opening into a chain. This result is a good indication of desired linear polymer chain formation but not a side product.

Experimental data on polymerization of macrocycle into allosteric polymer allowed to achieve a product with Mp = 5 kDa confirming the possibility of opening monomers with a macrocycle-like design using the ED-ROMP approach.

The literature suggests various tools to increase ED-ROMP efficiency with a superior catalyst, such as Grubbs III, higher monomer concentration, elevated temperature, and various catalyst loadings. The reaction of ROMP using standard conditions (Grubbs II, DCM) allowed to achieve Mp = 5 kDa. However, when the catalyst was changed from Grubbs II to Grubbs III, the reaction did not produce superior polymerization properties, which is unexpected as Grubbs III catalyst showcase better efficiency in other ED-ROMP cases than Grubbs II due to the faster initiation properties. A possibility that Grubbs III has degraded is excluded as it worked for other polymerization reactions in the group. A potential explanation can be the different coordination sites of two polymers. As Grubbs II afforded the opening reaction, it was coordinated by oxygen functional groups, while Grubbs III may have a higher stacking with stiff-stilbenes that resulted in no reaction. The robust linker in the monomer can be an

additional constraint, explaining ineffective Grubbs-III catalyzed ED-ROMP.[128] Changing the linker to a more flexible alternative may provide insight if the reactivity of polymerization increases using Grubbs III.

The above data suggest that changes in the solution's concentration and the temperature did not affect the resulting product, while the catalyst loading was an essential factor in obtaining polydisperse polymer or resulting in no or short-chain products. It is necessary to put the reaction in the interval under the same ROMP conditions since it was unsuccessful below 0.5 mol% and catalyst loading above 1 mol% did not lead to better polymerization results. Perhaps a specific loading will allow shifting Mp to the higher MW, which is possible due to the broad polymer molecular weight distribution.

NMR analysis of the produced polymer suggests the formation of linear chain oligomer over a macrocyclic analog due to the shift of alkene peaks from 5 ppm (Scheme 42, Ha) to 5.5 and 5.8 ppm (Scheme 42, Hb) region, which implies structural changes associated with the macrocycle's opening into a chain. This result is a good indication of desired linear polymer chain formation but not a side product.

4.3. ATTEMPTED SYNTHESIS OF FOLDAMERS – POLYSTYRENE SYSTEMS

The second part of this chapter is devoted to incorporating supramolecular bonds into polymer chain via amine-carboxylic acid coupling synthesis to study the strength of weak supramolecular bonds vs strong covalent bonds under force conditions. Coupling amine and carboxylic acid to form an amide linkage is one of the most popular synthetic reactions[135] with applications in drug discovery, peptide synthesis and polymer synthesis.

This work will focus on four coupling methods between amine- and carboxylic acid terminated reagents (Scheme 45) and discuss their advantages and disadvantages towards foldamer-polystyrene systems formation.

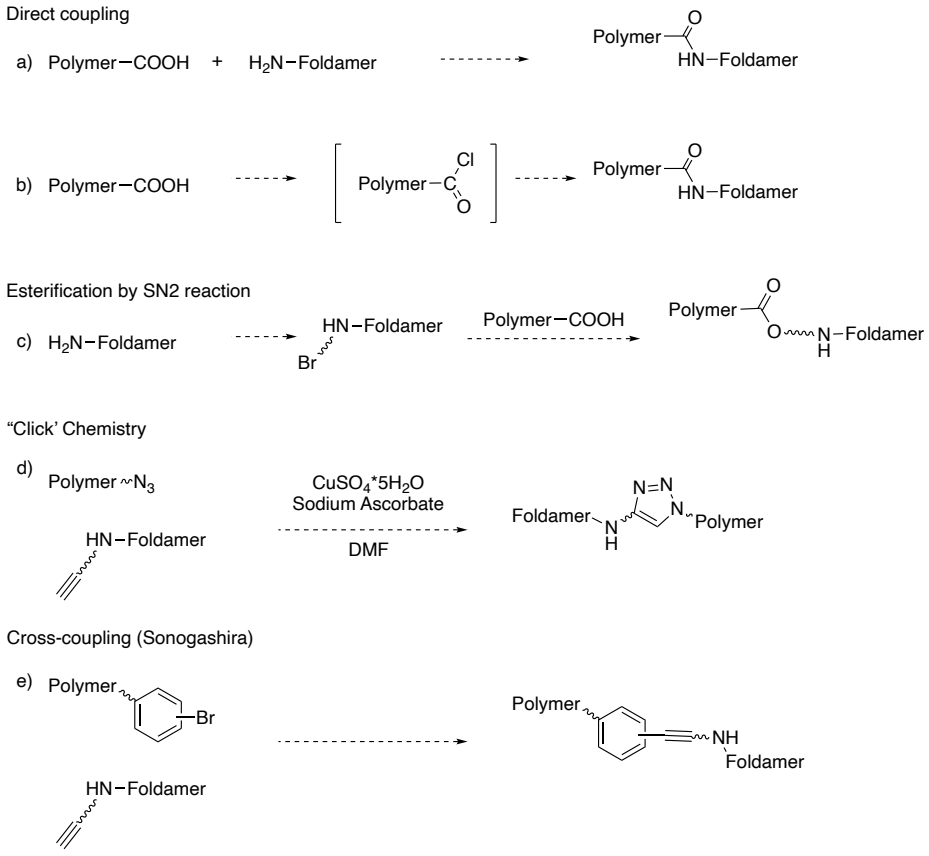

Scheme 45. The general strategy of connecting polymer and foldamer (wiggly line represents a spacer with a specific functional group)

The first approach is the direct amidation, which can be achieved with peptide coupling reagents such as PyBOP,[136, 23] DCC,[137] EDC,[138] etc., where DCC and EDC in apolar solvents (DCM), and PyBOP requires an organic base in a polar aprotic organic solvent (DMF). These reactions produce ureas as by-products (Scheme 46).

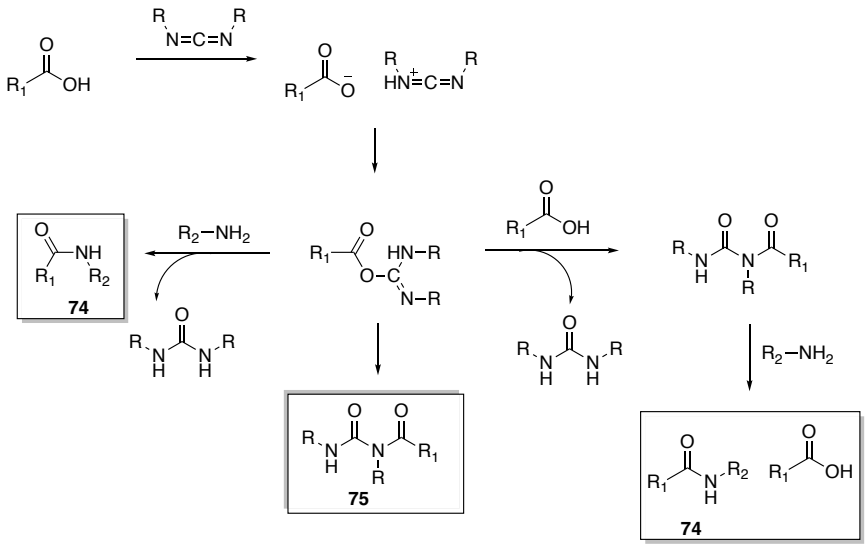

Scheme 46. Mechanism of the amine and carboxylic acid coupling under DCC conditions

The literature provides a successful example of such coupling[136] between a single helical foldamer and a commercial polyethylene glycol in the presence of PyBOP and DIPEA. The reaction was performed overnight to produce a polymer **78** in 40% (Scheme 47).

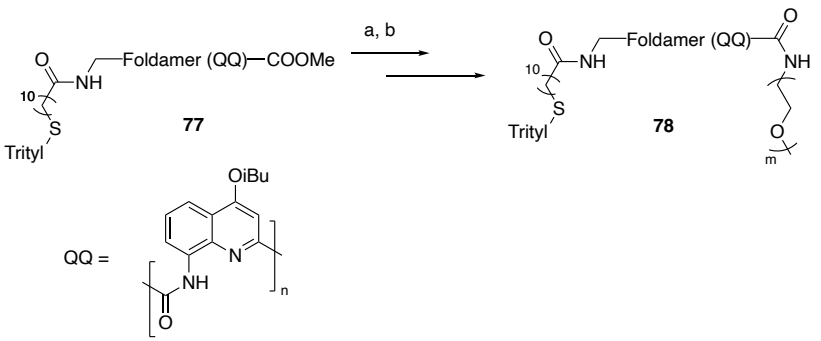

Scheme 47. Amide formation using PyBOP. Conditions: a) NaOH, THF/MeOH, r.t., 0.5 h to overnight; b) PEG-NH_2, PyBOP, DIPEA, $CHCl_3$, RT, overnight

The second method is the esterification of carboxylic acid by S_N2 reaction. It is a direct approach of coupling amine bromide and carboxylic acid to afford a corresponding ester via the S_N2 mechanism. Wang and co-workers[139] reported a successful synthesis of low-molecular

weight gelators in the form of hybrid amide-esters (Scheme 48). First, starting amine was converted into bromo amide using bromo-acetyl chloride or bromide, followed by carboxylic acid with various side chains.

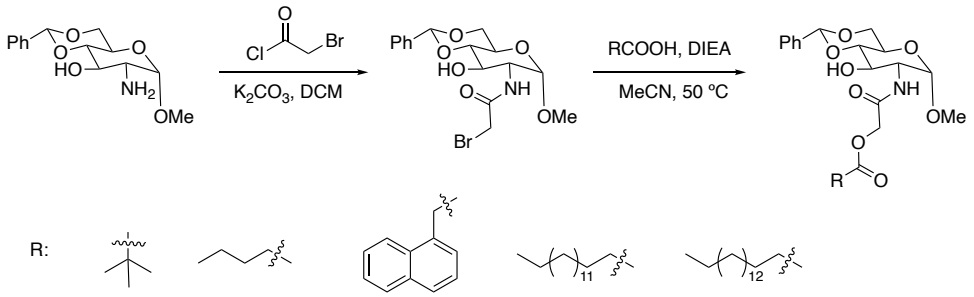

Scheme 48. Synthesis of hybrid amide and ester derivatives

The third method is coupling a small molecule and polymer using "click"-like reactions, i.e. azide-alkyne cycloaddition under organometallic catalyst.[138, 140] The Cu^{I}-catalyzed azide/alkyne cycloaddition (CuAAC) reaction proved its efficiency in polymer systems by forming a triazole ring as a product with polymers (Scheme 49).[23] However, this method has the main disadvantage as the reaction requires an aqueous environment, unfavorable for foldamer dimerization.

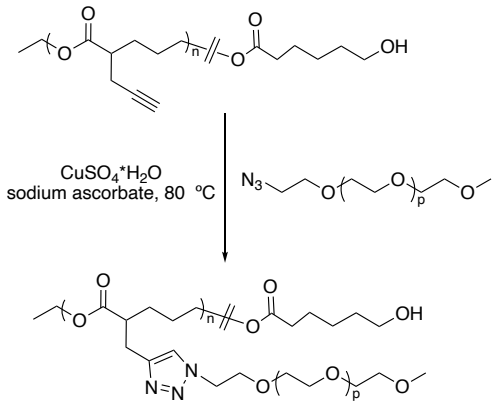

Scheme 49. Example of CuAAC reaction

The fourth alternative approach can be a robust Sonogashira cross-coupling. Both foldamer and polystyrene have to be transformed in its alkyne and halide derivatives to perform this reaction.

4.3.1. Synthesis of foldamer-terminated polystyrenes

The scheme below shows a general research design of coupling double helical foldamer with commercial polystyrene (Scheme 50). Coupling should provide a system of Foldamer-PS **80**, which can be characterized using SEC or GPC with the appearance of a new peak corresponding to a molecular mass twice larger than the starting PS. To confirm the supramolecular nature of the coupling product, the dilution experiment should break supramolecular bonds of the double helix with the self-healing ability upon concentration. Still, the addition of water to the system should completely break non-covalent interactions (Scheme 50).

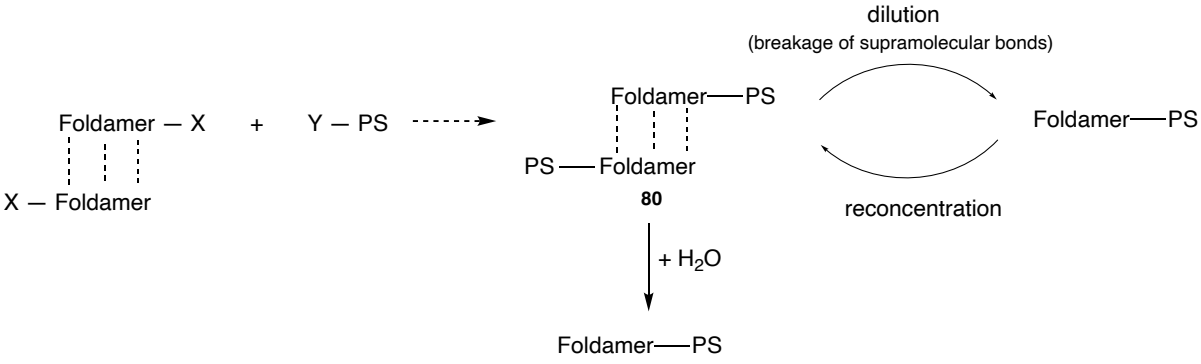

Scheme 50. A general research design of coupling double-helical foldamer with PS, where X and Y are end groups. Using dilution/reconcentration and water addition experiments should confirm the proposed product **80**. Dilution experiment should result in partial or complete decomposition **80** into single helix Foldamer-PS with self-healing ability into double helix upon reconcentration. At the same time, water addition should completely break supramolecular bonds.

Before we attempted the synthesis of dihelical foldamer **60** and polystyrene, we tested our coupling hypothesis on the model foldamer. For the model study, we chose a simple foldamer containing 3 pyridine units, 3mer (Figure 33), to perform the proposed end-derivatization of polystyrene experiments shown on Scheme 51.

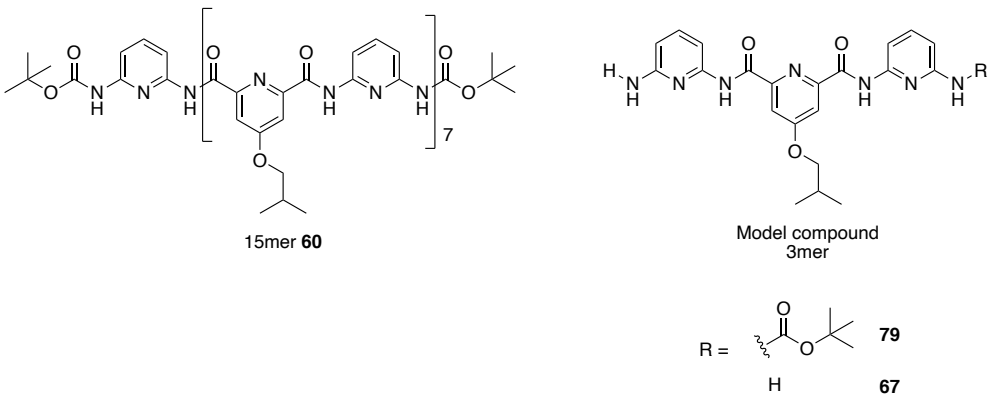

Figure 33. Structures of double-helical foldamer **60** and model compounds **67** and **79**.

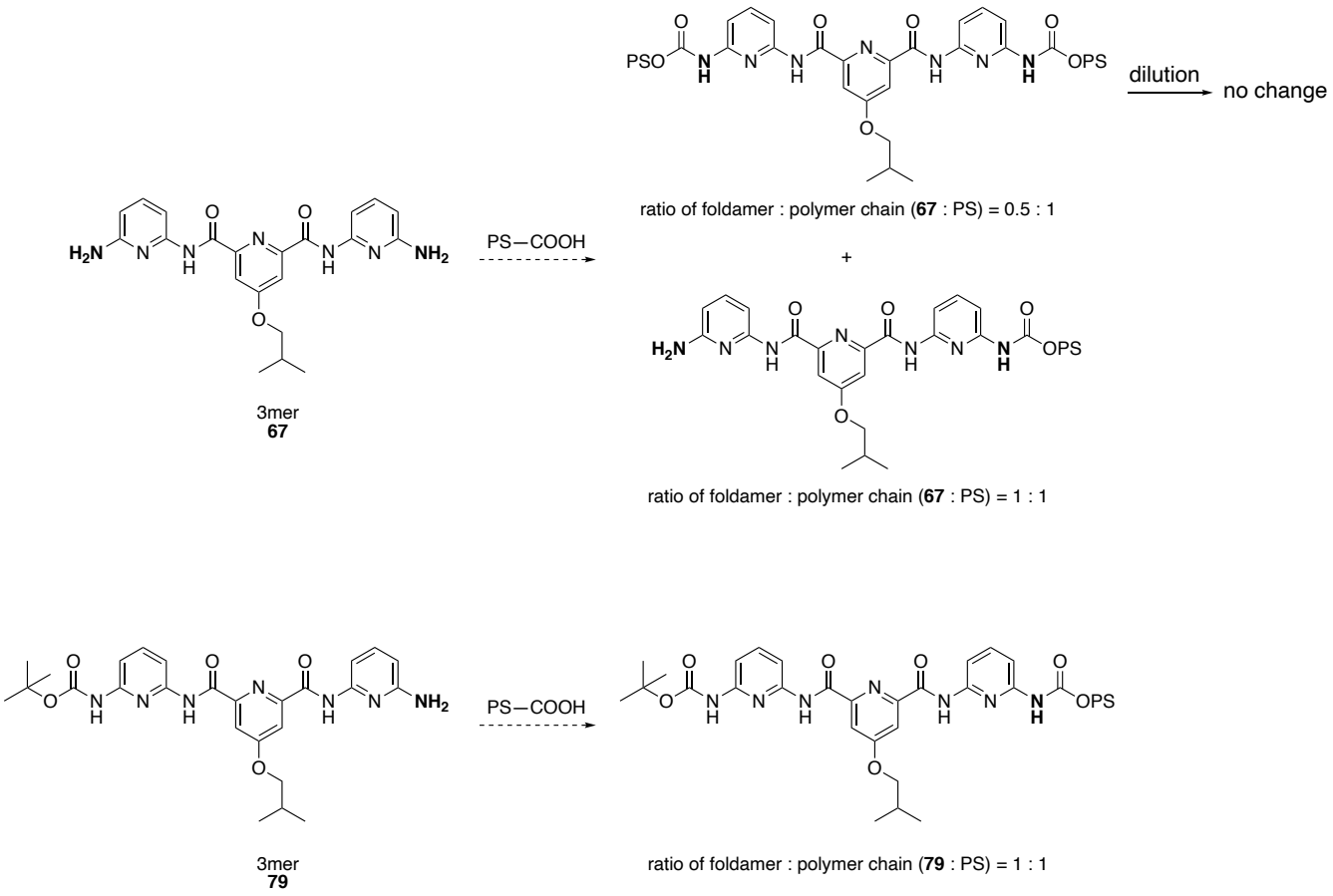

Scheme 51. Proposed coupling of model systems with monocarboxylic acid terminated polystyrene (PS-COOH). Products can be differentiated using UV-Vis analysis of SEC peaks by calculating the ratio of foldamer to a polymer chain.

To characterize the foldamer-polystyrene systems (Scheme 51), the following formula was used (Figure 34 bottom). The calculation of all extracted SEC peaks foldamer per polymer chain ratio was performed by automated MatLab function, which extracted absorbance values at 303 nm for a foldamer and 260 nm for PS (Figure 34 top).

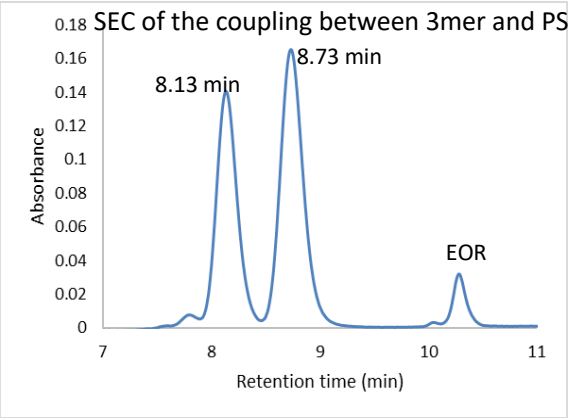

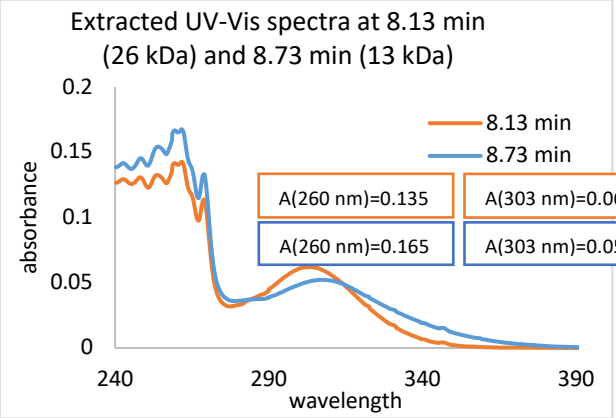

$$\text{ratio of foldamer per polymer chain} = \frac{\frac{A_{303\ nm}}{\epsilon_{Foldamer,\ 303\ nm}}}{\frac{A_{260\ nm}}{MW\ (PS) * \epsilon_{PS,\ 260\ nm}}}$$

A - absorbance
ϵ - extinction coefficient

Figure 34. Left top: SEC spectra of the coupling reaction between 3mer and PS. Right top: extracted UV-Vis spectra of each peak. 8.12 min corresponds to 26 kDa and 8.72 min corresponds to 13 kDa. Bottom: formula used to calculate ratio of foldamer per polystyrene chain. Absorbance at 260 nm is characteristic for PS and absorbance at 303 nm corresponds to foldamer.

The first direct coupling trials between polystyrene with a mass of 13 kDa and foldamer **67** was achieved using DCC as a coupling agent in D<F and afforded polymeric products of 26 kDa and 13 kDa in 12 h at RT (Figure 37). 26 kDa peak was a major product with a foldamer to polymer chain ratio 2:1, but 13 kDa peak also contained a foldamer with a ratio of 1:1 (foldamer:PS). This unexpected result of 26 kDa implies that supramolecular forces bound two systems of foldamer-PS, or a covalent PS-Foldamer-PS system is connected to the second foldamer by non-covalent interactions (Figure 35).

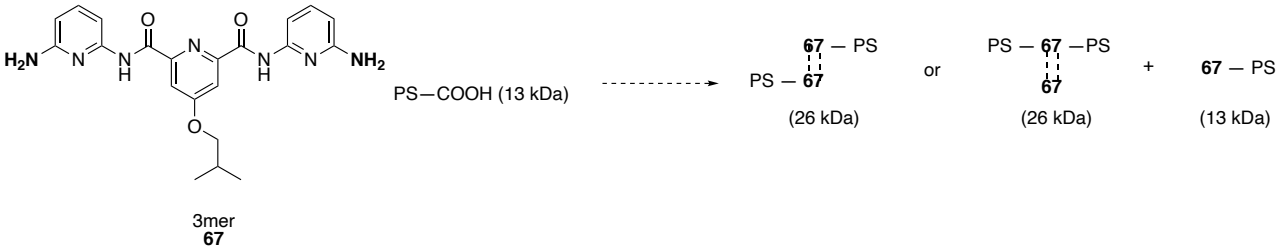

Figure 35. Coupling reaction between **67** and PS-COOH. Products with molecular weights of 26 and 13 kDa were produced. Hash lines represent supramolecular interactions.

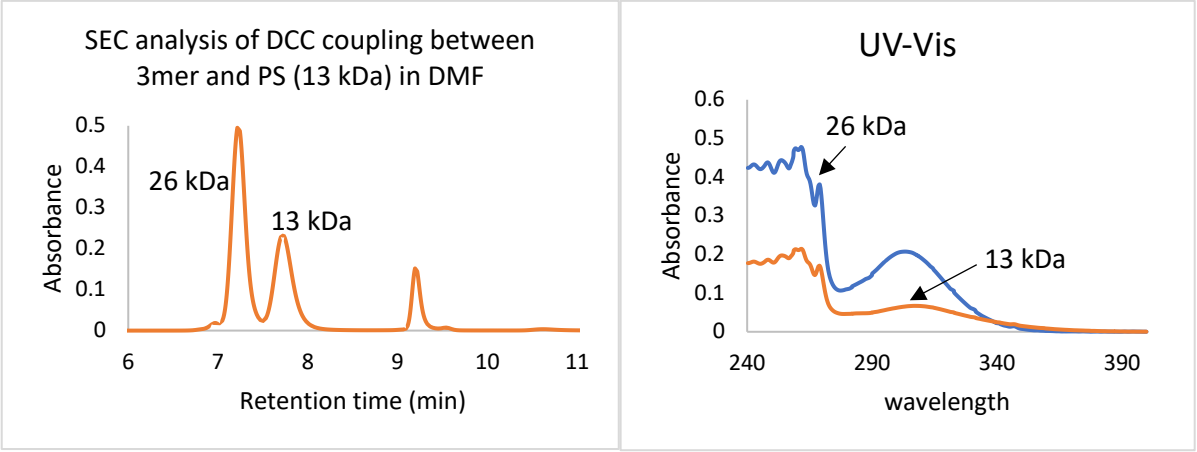

Figure 36. Left: SEC data of coupling between 3mer-diamine **67** (orange) in DMF. Right: UV-Vis spectra of peak 1 (26 kDa, 7.25 min, blue) and peak 2 (13 kDa, 7.75 min, orange, standardized to match absorbance values of peak 1).

Changing solvent from DMF to DCM did not result in the mechanophore-active polymer (Table 5, entry 5). Other trials using carboxylic acid activating chlorinating agents, PyBOP, EDC (Table 5, entries 1,2, 3) did not afford desired products.

Table 5. Coupling trials of foldamer and PS and results

entry	reagents	Reaction conditions	Results
1	NH_2-3mer-NH_2 **67** PS-COCl (13 kDa)	DCM, DIPEA 0 to RT, 24 h	No reaction
2	NH_2-3mer-NH_2 **67** PS-COOH (13 kDa)	DCM, PyBOP, DIPEA, RT, 24 h	No reaction
3	NH_2-3mer-NH_2 **67**	DCM, EDC, RT, 24 h	No reaction

	PS-COOH (13 kDa)		
4	NH_2-3mer-NH_2 **67** PS-COOH (13 kDa)	DMF, DCC, DMAP, RT, 12 h	• Dimer 26 kDa (major, foldamer/chain = 2) • Monomer 13 kDa (minor, foldamer/chain = 1)
5	NH_2-3mer-NH_2 **67** PS-COOH 13 kDa	DCM, DCC, DMAP RT, 36 h	• Dimer 26 kDa (minor, foldamer/chain = 0) • Monomer 13 kDa (major, foldamer/chain = 0)
6	Control: PS-COOH 13 kDa	DMF, DCC, DMAP, 24 h	No reaction
7	Control: PS-COOH 13 kDa	DCM, DCC, DMAP, 24 h	No reaction

To confirm that DCC is essential, a control reaction was performed by mixing **67**, and PS did not result in any reaction. The optimized direct coupling conditions were based on mixing **67** (2 equivalence), PS (1 equivalence), DCC (2 equivalence), DMAP (0.1 equivalence) and 1 mL of DMF per 1 g of PS in the DryBox.

Coupling of 3mer-monoamine **79** with a 13 kDa polystyrene (Scheme 52) was performed under optimized conditions described above using DCC and DMAP to afford 26 kDa and 13 kDa products with a foldamer to polystyrene ratios of 1.6:1 and 0.9:1, respectively. Coupling of foldamer-monoamine system with PS excludes forming a PS – Foldamer – PS system due to the Boc protection of one terminal amine.

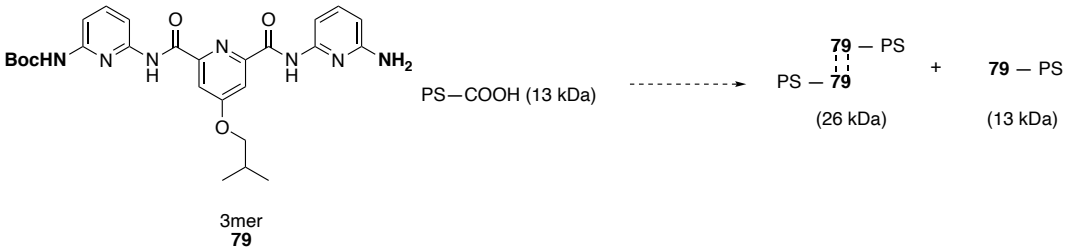

Scheme 52. Coupling of **79** and PS-COOH (13 kDa).

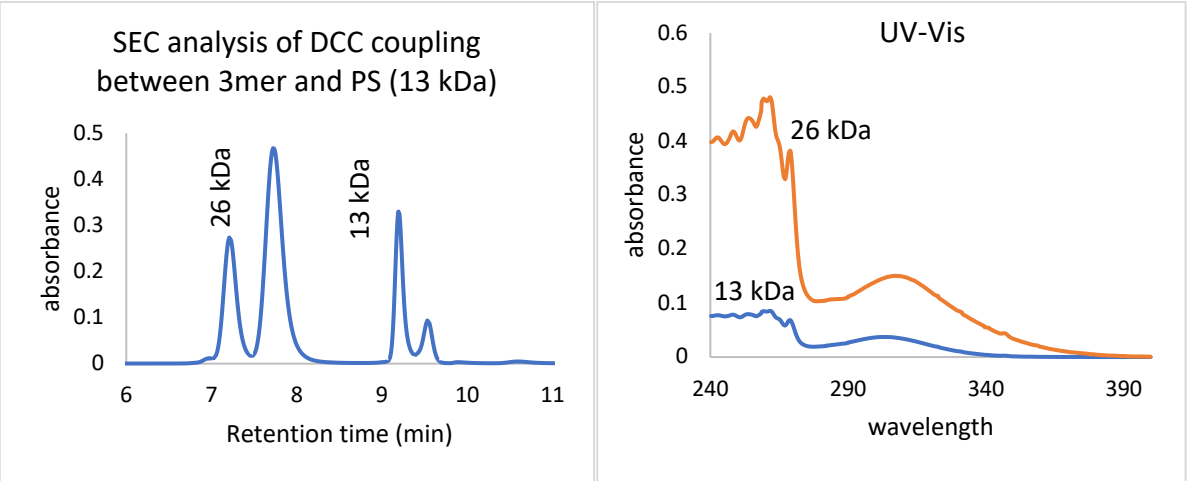

Figure 37. Left: SEC data of couplings between 3mer-diamine **67** (orange) and 3mer-monoamine **79** and PS (13 kDa) coupling (blue). Right: UV-Vis spectra of peak 1 (26 kDa, 7.25 min, orange) and peak 2 (13 kDa, 7.75 min, blue).

The reaction between heptamer and PS required a longer reaction time to afford a 26 kDa product. The formed product had a 0.7 ratio of foldamer to PS chain, suggesting that the polymer chain quenches the absorbance value and requires a longer time to observe the chromophore. The repeated analysis confirmed the hypothesis after 30 days. The ratio of foldamer to PS was increased up to almost 2.

Unfortunately, no reaction was observed by mixing 15mer **60** with PS in the presence of DCC and DMAP in 7 days, even at elevated temperature.

Table 6. Summary of coupling reactions between foldamers with one amine group and PS-COOH

entry	reagents	Products	Foldamer/PS ratio
1	Boc-3mer-NH_2 **79**	• 26 kDa product (minor)	• 1.6

	PS-COOH 13 kDa	• 13 kDa product (major)	• 0.9
2	Boc-7mer-NH_2 **72** PS-COOH 13 kDa	3 days: • 26 kDa product (minor) • 13 kDa product (major) 3 days: • 26 kDa product (minor) • 13 kDa product (major)	3 days: • 0.7 • 0.2 30 days: • 1.8 • 0.9
3	Boc-15mer-NH_2 PS-COOH 13 kDa (7 days, RT to 50)	No reaction	No reaction

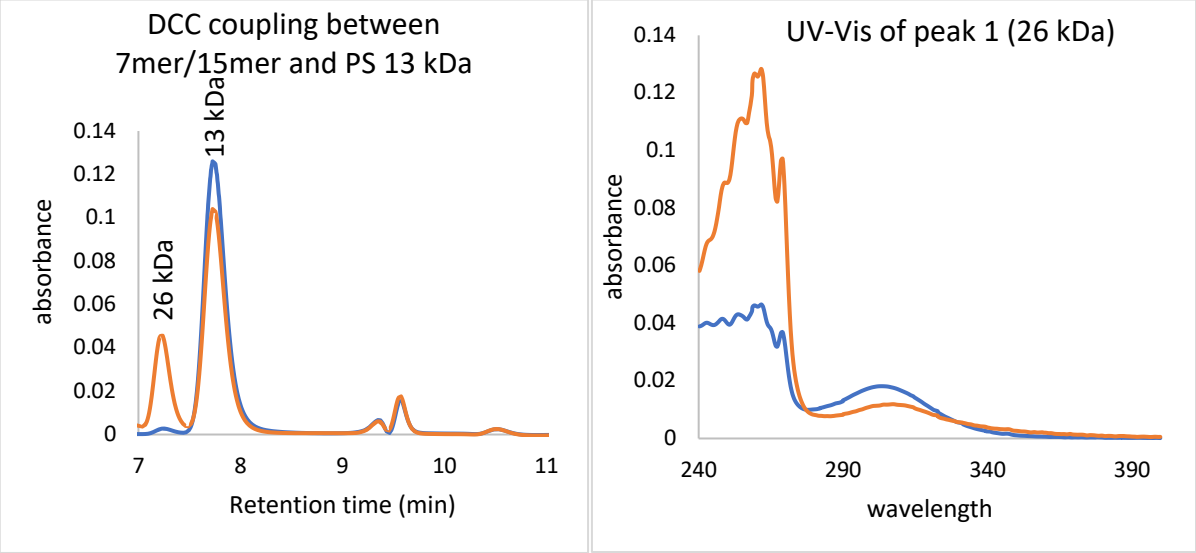

Figure 38. Left: SEC analysis of the DCC coupling between 7mer and PS 13 kDa (blue – reaction time = 3 days, orange – reaction time = 30 days). Right: UV-Vis of 30 days reaction time of peak 1 (26 kDa, 7.25 min)

The change of polymer's mass from 13 to 50 kDa, resulted in unexpected products. The SEC analysis provided the spectra of the dimer (100 kDa) and monomer (50 kDa); upon storage, these peaks shifted to hexamer (300 kDa) and trimer (150 kDa), while the foldamer's peak's intensity decreased (9.25 min) (Figure 39).

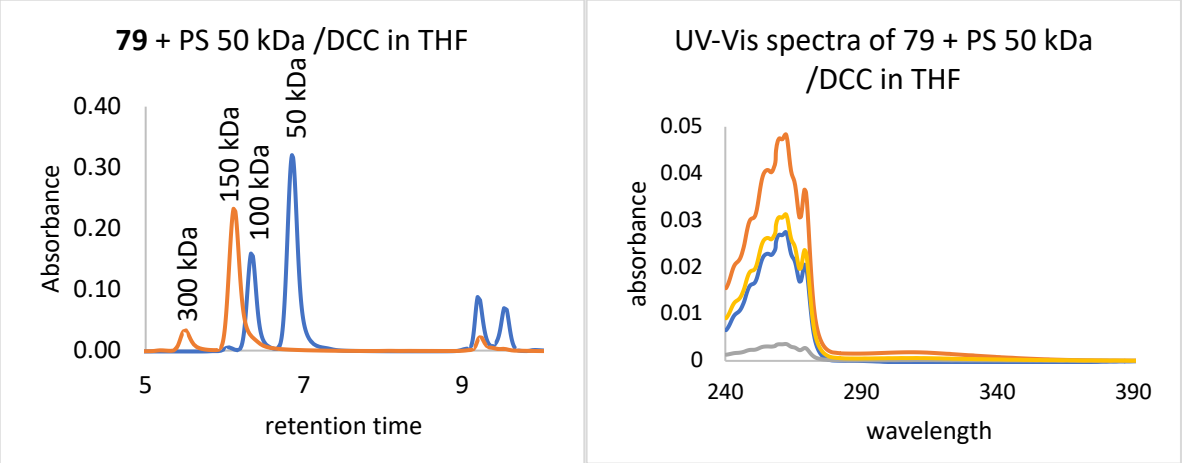

Figure 39. Left: SEC analysis of the coupling between 3mer-monoamine **79** and PS 50 kDa (orange 50 kDa 6.87 min, yellow 6.14 min, blue 6.35, green 5.56). Right: extracted UV-Vis of SEC spectra at peaks 1-4 (300, 150, 100, 50 kDa, respectively).

The second synthetic approach relied on S_N2 reaction. First, bromoacetyl bromide was added to 3mer to form the corresponding 3mer **81**, which was further added to a PS-COOH solution in the presence of a base. An inorganic base K_2CO_3 led to the decomposition of **81**, while an organic DIPEA base afforded the mixture of polymer (26 and 13 kDa) (Scheme 48).

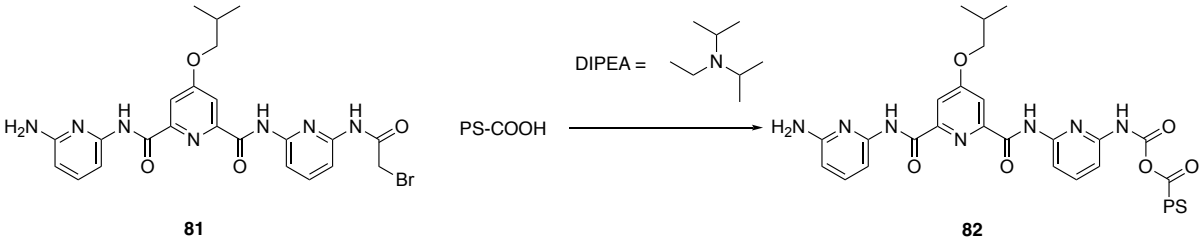

Scheme 53. Coupling of trimer halide and PS in the presence of DIPEA

When the reaction's solvent was DMF, the foldamer to polymer chain ratio was calculated around 2.5 for the dimer, while the foldamer to polymer chain ratio in DCM was 0 (Figure 40). This reaction could not be performed on longer foldamers as the synthesis of 7mer and bromoacetyl bromide was unsuccessful due to heptamer's sensitivity to acidic medium.

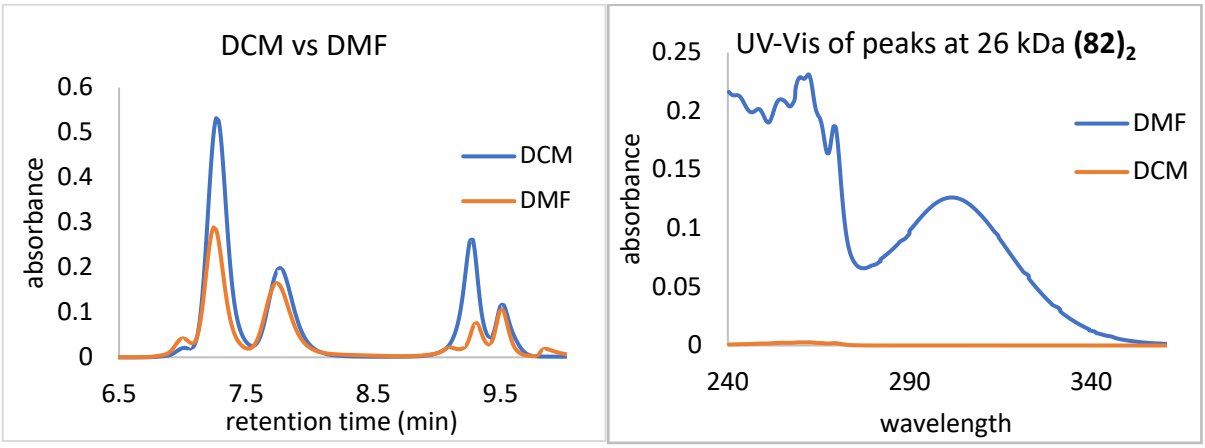

Figure 40. Left: SEC data of the coupling between **81** and PS 13 kDa in DCM and DMF. Right: extracted UV-Vis spectra of dimer peak at 7.29 min, 26 kDa (blue – reaction solvent DCM, orange – reaction solvent DMF)

To synthesize foldamer-terminated polystyrene by a cross-coupling reaction, I performed two model reactions. The first trial of coupling bromophenyl-terminated polystyrene **83** and alkyne **84** was successful (Scheme 54).

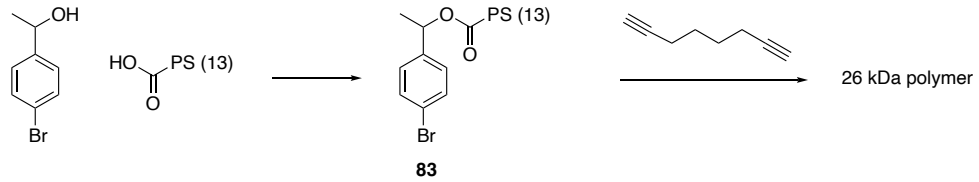

Scheme 54. Cross-coupling using 1,7-octadiyne

The second model was synthesized from diacid **63** to afford dialkyne **84** in 82% yield using EDC as the coupling reagent.

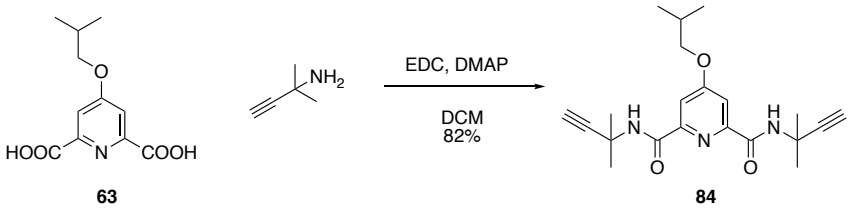

Scheme 55. Preparation of dialkyne **84**

Cross-coupling between dialkyne **84** and the bromophenyl terminated polystyrene failed, so further experiments did not proceed (Scheme 56).

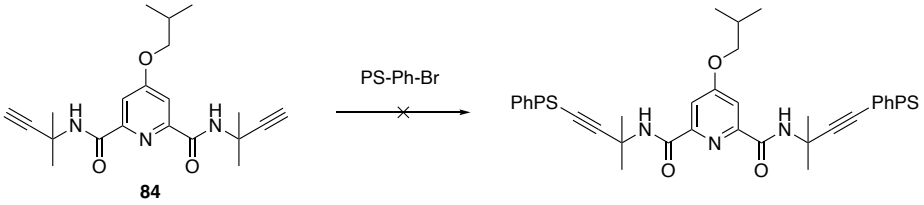

Scheme 56. Cross-coupling trial between **84** and PS-Ph-Br

4.3.2. Effects of moisture and concentration

The following experiments of dilution/reconcentration and water addition were performed to study the presence of supramolecular interactions within foldamer-PS systems.

The coupling of 3mer-diamine **67** + PS (Figure 35) afforded an unexpected peak at 26 kDa, which can be formed either by supramolecular bonding of two foldamer-PS systems or by covalent bonding of 2 PS to foldamer with two amine groups (PS-foldamer-PS). By diluting the original solution (1 mL of solvent/1 g of polymer) hundred times (100 mL of solvent/1 g of

polymer), we observed that peak 1 (26 kDa) decreased in its intensity. In contrast, the intensities of peak 1 (13 kDa) and foldamer's peak at 9.16 min increased. Upon storage for several days no changes were observed, which implies that product is PS-**67**-PS + **67** likely to be formed as the major product due to the observed intensity of the foldamer's peak, but minor product in the form of (PS-**67**)$_2$ is also present due to the partial dissociation into peak 2 (13 kDa) (Figure 42, orange). The addition of water did not change the diluted system, which also confirms the covalent bond formation between 2 PS and **67**.

The reconcentration step did not result in the original spectra (Figure 42, blue), which can explain that foldamers are highly sensitive to air and moisture and need highly inert conditions to afford dynamic behavior.

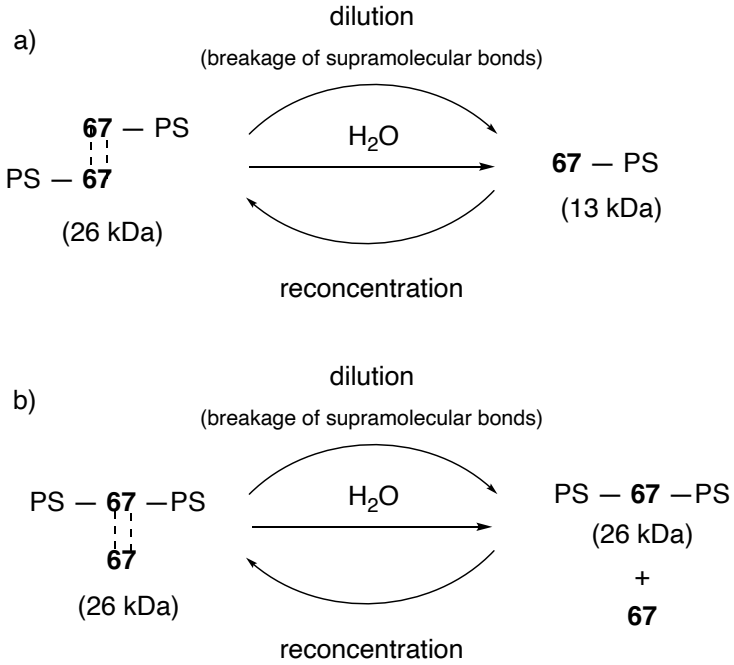

Figure 41. Experimental outline to study the supramolecular behavior of Foldamer-PS systems. A) (PS-3mer)$_2$ of 26 kDa upon dilution should dissociate into 13 kDa PS-3mer system and reform into original 26 kDa system, while water addition should break

completely supramolecular bonds. B) PS-3mer-PS + 3mer of 26 kDa should break non-covalent bond without changes of 26 kDa peak

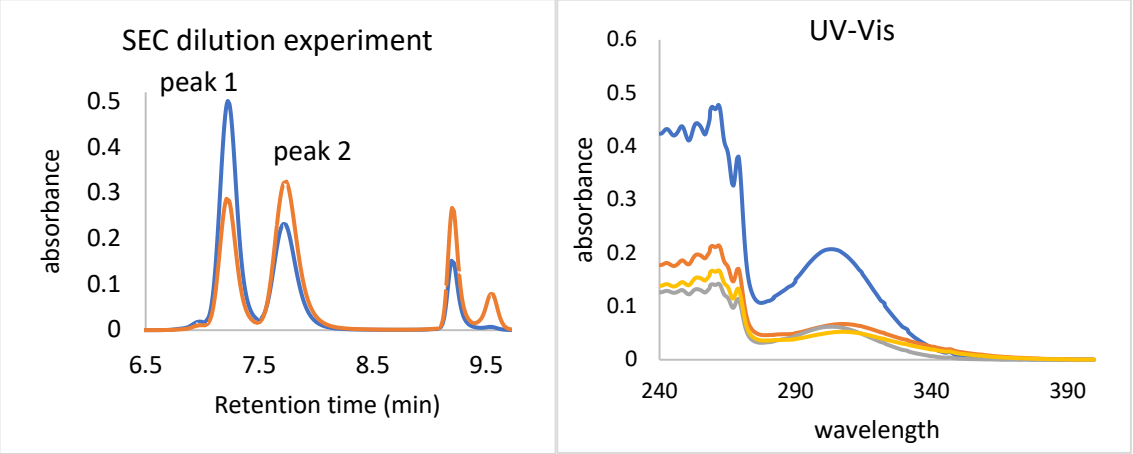

Figure 42. Left: SEC of the dilution effect on the products mixture of 3mer **79** and PS 13 kDa coupling (blue – original mixture, orange – diluted mixture). Right: UV-Vis data: blue – original peak 1, orange – original peak 2, grey – diluted peak 1, yellow – diluted peak 2.

Using the methodology described above, systems of monoamine 3mer **79** and 7mer **72** and bromo derivative of 3mer **81** attached to PS were analyzed using dilution/reconcentration and water addition experiments.

Table 7. Results of the dilution and water addition experiments

entry	mixture	Effect of dilution/reconcentration	Effect of moisture
1	**67** + PS 13	Partial 26 kDa peak dissociation associated with the increase in the intensities of the 13 kDa peak and foldamer's peak.	
2	**79** + PS 13	Partial 26 kDa peak dissociation associated with the increase in the intensities of the 13 kDa peak and foldamer's peak.	
3	**79** + PS 50	No change	
4	**72** + PS	Complete 26 kDa peak dissociation associated with the increase in the intensity of the 13 kDa peak.	

5	**81** + PS/DMF	Appearance of new EOR peak	Appearance of 6.5 kDa peak, 0.5 monomer

Dilution experiments showed partial or complete dissociation of 26 kDa peak, but no reversibility upon concentration was observed. End of run peaks spectra changed, which may confirm the hypothesis of the amine sensitivity to air and moisture that does not allow the self-healing process to occur.

Interestingly, the product mixture of the **81** and PS 13 kDa reaction upon addition of 1 drop of water to 1 mL solution produced a new peak with MW of half of the starting monomer in 3 days (Figure 43). This new product peak is only possible if the polymer chain breaks precisely in the middle (ratio of foldamer per polymer chain = 0.5). During the water addition experiment, the end-of-run (EOR) peak at 9.5 min increased in intensity, and new EOR peaks appeared. As new EOR peaks do not exhibit characteristics for foldamer UV-Vis spectra, their appearance can be associated with the decomposition of one or several of the reaction species.

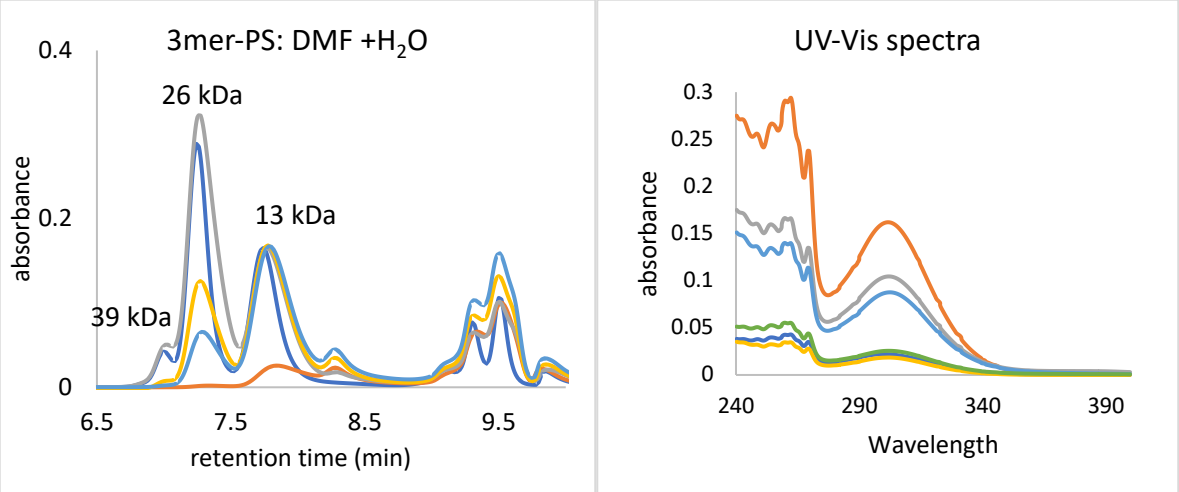

Figure 43**.** Left: SEC analysis of the effect of water on polymer-foldamer (**81**) mixture. Dark blue – control, no water; orange – solution with water; grey – after 12 h; yellow – after 36 h; light blue – after 3 days. Right: UV-Vis dark blue – 39 kDa control no water; orange – 26 kDa no water; grey – 13 kDa no water; yellow – 26 kDa 3 days; light blue – 13 kDa 3 days; yellow – 6.5 kDa 3 days

To highlight, no change was observed in the mixture of 50 kDa PS and 3mer, which suggests that the formation of higher assemblies (150 and 300 kDa moieties) is based on covalent bonds.

4.3.3. Discussion

Among the four methods for coupling of a foldamer to a polystyrene tested, only two yielded detectable products. Both direct couplings using DCC and S_N2 esterification reaction in DMF produced dimers with the expected foldamer to polystyrene ratio of 2. This ratio was calculated by comparing absorbance values at 260 nm and 303 nm (Figure 34).

When conducting experiments in various solvents, it was noticed that mechanophore is UV-Vis active at 303 nm in DMF but not in DCM. Foldamers within a structure of dimer (Figure 35) formed as a reaction product in polar DMF, absorbed at ~303 nm. Coupling reactions in DCM afforded dimers, which did not show any additional absorption compared to pure polystyrene. This behavior may correlate with the sensitivity of foldamers to the polarity of solvents. Compared to the inert DCM, DMF may facilitate the reaction of a foldamer and polystyrene with a potential intermediate foldamer-DMF complex using H-bonding, which can catalyze the reaction. At the same time, DMF may decompose to $NH(CH_3)_2$ and CO during the foldamer-DMF-PS-COOH reaction, resulting in the increased intensity of end-of-run peaks as was observed in the experiment.

To check if the formed dimer is supramolecular or covalent, dilution tests were performed. Upon dilution, the product mixture changed as the major component was a single helical product with associate increase in monomer's peak intensity in SEC (Figure 42), but upon concentration, no change in chromatograms was observed, which can suggest that either foldamers are highly sensitive to air as the SEC experiment introduces air into the system or that couplings occurred via covalent bonds rather than supramolecular due to the potential epimerization, base-catalyzed over-coupling or intramolecular rearrangements.[141] To check the hypothesis of air-sensitivity, two samples should be subjected to the dilution/concentration cycle: one in air and the other under N_2.

Unexpected peak in a SEC at Mp ~6.5 KDa was observed upon the addition of water to the solution (Figure 43). UV-Vis analysis of newly formed peak of 6.5 kDa showed the presence of both foldamer and polystyrene with a ratio of 1:1, which can imply the breakage of covalent

bond in the middle of polystyrene chain to form the third peak of 6.5 kDa molecular weight in the form of Foldamer-PS (6.5 kDa) + PS (6.5 kDa).

However, it is highly doubtful that the covalent bond in the hydrocarbon polymer chain breaks upon the water addition. There could be several explanations for such behavior. The first may associate with a reagent bottle containing 13 kDa PS-COOH. It is possible if during a polymer preparation using template synthesis, which includes the usage of an organometallic catalyst,[142, 143] the polymer product of 13 kDa contains intermediate with a part of scissile organometallic catalyst in the middle that may easily dissociate upon the addition of water. A simple experiment should be done to approve this hypothesis. A sample from the reagent bottle should be dissolved in DMF, analyzed by SEC, followed by the addition of water to the sample, and again analyzed by SEC. If a peak of 6.5 kDa is observed, then the reagent bottle contains impurities. If no peak with 6.5 kDa is observed, a foldamer can be a reason for forcing a polymer chain in a strained configuration by weakening it precisely in the middle. If the scenario with a damaged jar is not confirmed, then an exciting question arises from a scientific point of view on the rupture of strong covalent chains by adding supramolecular structures that have the functions of coordinating inert polymer chains with the weakening of a specific point in the chain.

Experimental

Synthesis of polymer 73

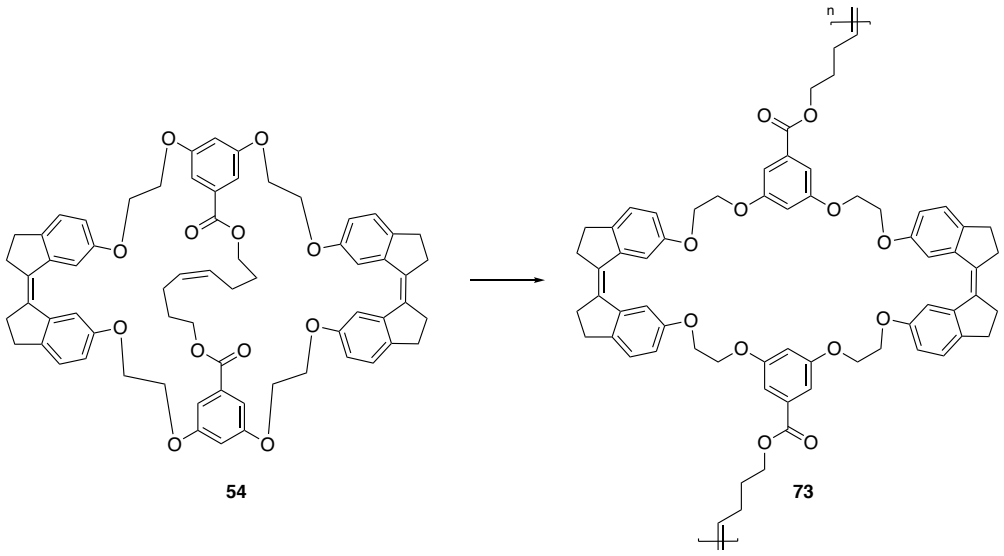

A new compound **73** was prepared using the procedure below.[141]

0.1 M solution of the macrocycle **54** (100 mg, 0.01 mmol) in dry, degassed $CDCl_3$ were prepared under an atmosphere of N_2, followed by the addition of Grubbs II (0.08 mg, 1 mol%) under inert conditions. Reaction was left for stirring until completion, followed by quenching with water and extraction with DCM. The polymer was cha

^{1}H NMR ($CDCl_3$): 1.73 – 1.84 (C*H*$_2$CH$_2$CH$_2$O), 2.11 – 2.19 (CH$_2$C*H*$_2$CH$_2$O), 2.78 – 2.98 (C*H*$_2$C*H*$_2$C=C), 4.12 – 4.37 (OC*H*$_2$), 5.39 – 5.54 (br m, C*H*=C*H*), 6.34 – 6.44, 6.72 – 6.85, 6.99 – 7.04 (br s, C*H*$_{Ar}$), 7.14 – 7.21 (br m, C*H*$_{Ar}$), 7.34 – 7.42 (br m, C*H*$_{Ar}$), 7.70 – 7.81 (br m, C*H*$_{Ar}$).

Synthesis of compound 84

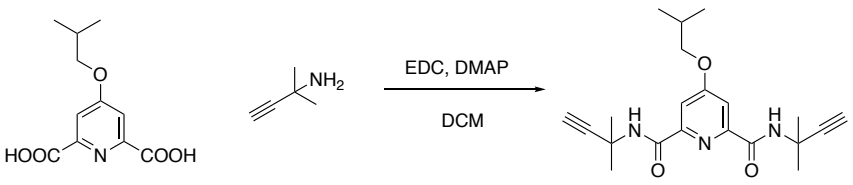

A new compound **84** was prepared using the procedure below.

A mixture of 2-methylbut-3-yn-2-amine (70 mg, 0.84 mmol), 4-isobutoxypyridine-2,6-dicarboxylic acid (100 mg, 0.42 mmol), DMAP (5 mg, 0.042 mmol) and EDC (160 mg, 0.84 mmol) were mixed in DCM (5 mL) under N_2 atmosphere and stirred at RT for 18 h. Upon completion, the reaction mixture was filtered, concentrated and purified using column chromatography to give a yellow solid in 82%.

^{1}H NMR ($CDCl_3$): 1.04 (d, 6H, CH(C*H*$_3$)$_2$), 1.81 (s, 12H, 2xC(C*H*$_3$)$_2$), 2.14 (m, 1H, OCH_2C*H*) 2.42 (s, 2H, 2xCCH), 3.91 (d, 2H, OCH_2), 7.83 (s, 2H, 2xCH_{Ar}), 7.86 (br s, 2H, 2xNH).

Synthesis of trimer-monoamine 79

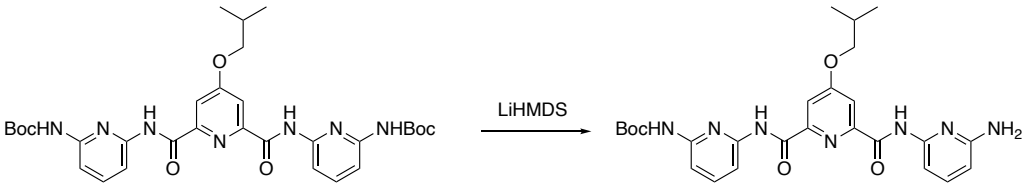

A new compound **79** was prepared using the procedure below.

To a solution of 3mer (0.35 g, 0.56 mmol) in THF (5 mL), LiHMDS (0.2 g. 1.13 mmol) was added dropwise over 10 min at 0 ^{o}C under N_2 atm. The solution was stirred at RT for additional 15 min, followed by the addition of $(Boc)_2O$ (0.11 g, 0.51 mmol) in 3 mL THF at 0 ^{o}C under N_2 atm. The reaction mixture was monitored by TLC. Upon completion, the reaction mixture was quenched by water and extracted with EtOAc three times, followed by the purification using Flash Chromatography. The product was formed in 75% yield as a white solid.

^{1}H NMR ($CDCl_3$): 1.10 (d, J = 6.75 Hz, 6H, CH(C*H*$_3$)$_2$), 1.55 (s, 9H, OC(C*H*$_3$)$_3$), 2.20 (m, 1H, C*H*$(CH_3)_2$), 3.97 (d, J = 6.5 J, 2H, OC*H*$_2$), 6.28 (d, J = 8Hz, 1H, CH_{Ar}C*H*$_{Ar}$$CH_{Ar}$), 6.48 (d, J = 6Hz, 1 H, CH_{Ar}C*H*$_{Ar}$$CH_{Ar}$), 7.21 – 8.02 (m, 10H, 10xC*H*$_{Ar}$), 10.43 (s, 1H, N*H*C(=O)C), 10.69 (s, 1 H, N*H*C(=O)C); ^{13}C NMR ($CDCl_3$): 19.1 (C, 2x*C*H_3), 23.9 (C, *C*HCH_3), 28.3 (C, 3x*C*H_3), 40.9 (C,

C(CH_3)$_3$), 75.4 (C, O*C*H_2), 101.0 (C, *C*H_{Ar}), 103.3 (C, *C*H_{Ar}), 105.6 (C, *C*H_{Ar}), 108.4 (C, *C*H_{Ar}), 108.8 (C, *C*H_{Ar}), 112.1 (C, *C*H_{Ar}), 140.5 (C, *C*H_{Ar}), 141.9 (C, *C*H_{Ar}), 149.2 (C, *C*$_{Ar}$), 150.1 (C, *C*$_{Ar}$), 150.4 (C, *C*$_{Ar}$), 150.6 (C, *C*$_{Ar}$), 152.3 (C, *C*$_{Ar}$), 155.5 (C, *C*$_{Ar}$), 156.1 (C, *C*$_{Ar}$), 161.7 (C, *C*$_{Ar}$), 168.3 (C, *C*$_{Ar}$).

Synthesis of compound 77

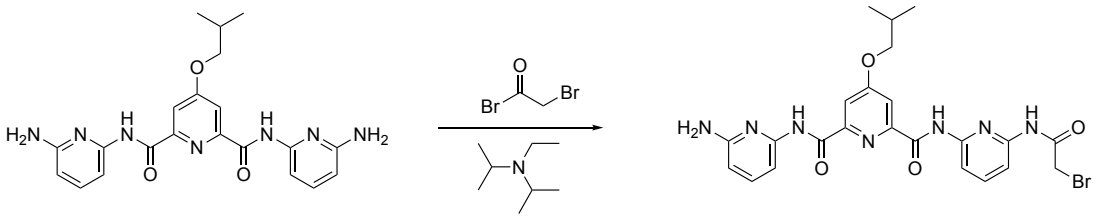

To a solution of N2, N6-bis(6-aminopyridin-2-yl)-4-isobutoxypyridine-2,6-dicarboxamide (82 mg, 0.2 mmol) in DCM (5 mL), DIPEA (40.8 uL, 0.23 mmol) and bromoacetyl bromide (13.54 uL, 0.16 mmol) were added at 0 °C under N_2 atmosphere. The solution was stirred for 6 h at RT. Then, the reaction was washed with water and extracted with DCM. Purification by flash chromatography afforded a yellow oil in 85% yield.

^{1}H NMR ($CDCl_3$): 1.08 (d, J = 6.7 Hz, 6H, CH(C*H*$_3$)$_2$), 2.14 – 2.22 (m, 1H, C*H*(CH_3)$_2$), 3.96-4.08 (m, 4H, OC*H*$_2$, C*H*$_2$Br), 6.25 (d, J = 8Hz, 1H), 6.45 (d, J = 6Hz, 1 H), 7.29 – 7.99 (m, 10H, C*H*$_{Ar}$, 2xN*H*), 10.40 (s, 1H, N*H*C(=O)N), 10.66 (s, 1 H, N*H*C(=O)N).

UV-Vis spectra of extinction coefficients (260-360 nm)

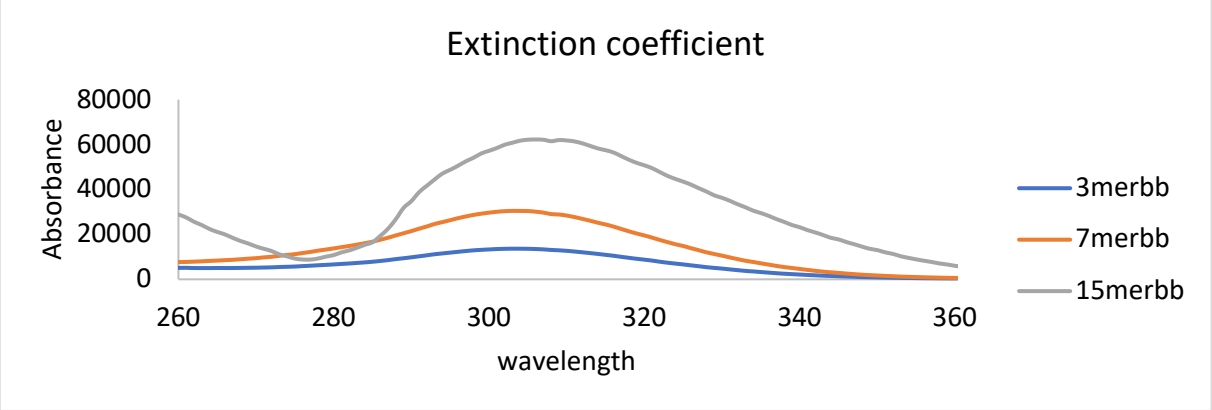

compound	Extn coefficient at 303 nm
58 (blue)	13640
59 (orange)	30472
60 (grey)	60818

UV-Vis of polystyrene (240 – 300 nm)

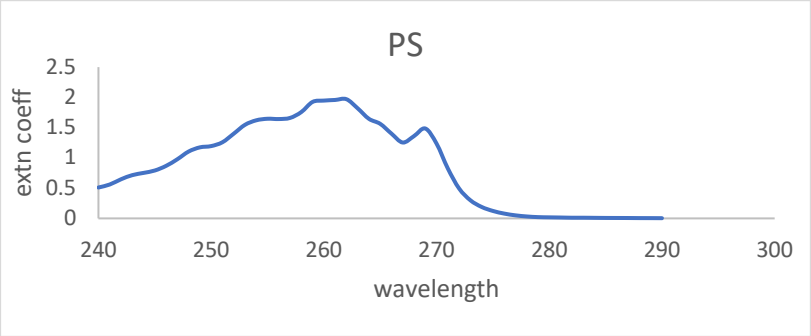

Chapter 5. Conclusion and outlook

In summary, this work answered two key questions to develop further a framework of polymer mechanochemistry: first – if the macrocycle **54** is polymerizable into allosteric polymers; second – if a synthesis of robust double-helical supramolecular structures as potential mechanophores is possible.

Based on previous knowledge, this project focused on synthesizing allosteric and supramolecular polymers. At the current stage, this work developed general synthetic pathways for two mechanophores with allosteric and self-healing properties to attempt polymerization reactions using ROMP or direct coupling with commercial PS. The design of the first mechanophore was inspired by the allostery to develop a stiff-stilbene-containing macrocycle, switching from Z (R state) to E (T) state conformations. The second

supramolecular mechanophore was designed as a double helix using abiotic aromatic foldamers due to their robust properties, predictability, and ease of synthesis.

In chapter 2, the synthesis of the bis-stiff-stilbene macrocycle was described. The starting material of the synthetic route was the indanone ring, followed by two McMurry coupling reactions to couple two indanone rings and RCM as a precursor for ROMP polymerizations. The second McMurry provided a macrocycle as a mixture of E: Z stiff-stilbenes in 1:4 ratio and RCM reaction afforded a closed ring as cis isomer exclusively. The synthetic route consisted of 10 steps with an overall yield of 37%. The main challenge of the synthesis was the RCM step as standard conditions (Grubbs II, DCM) did not work even at high-temperature conditions. Based on performed experiments, CsCl was the essential additive to coordinate oxygens in the macrocycle and afford the desired compound as a mixture of isomers. As the outlook, it is recommended to optimize the RCM step to control the formation of isomers, specifically cis and trans. Producing a single isomer exclusively will allow quantifying the isomerization response in the next ROMP step. Additionally, it is recommended to build several models of macrocycles with various linkers to compare the effect of the linker (size, flexibility, functional groups, etc.) towards metathesis reactions.

The synthesis of foldamers, in chapter 3, involved a doubling segment strategy involving chelidamic acid and diaminopyridine as starting materials. A series of 3mer, 7mer, and 15mer foldamers were prepared, but only 15mer with $K_{dim} > 10^5$ showed the robustness of a double helix despite dilution (4 mM), changes of solvent ($CHCl_3$, DMSO), and elevated temperature (50 °C). The challenge was the purity of obtained foldamers and their characterization. The analysis of double versus single helices was relied on the 1H NMR to quantify the fractions of

the monomeric versus dimeric helices because the two have distinct chemical shifts of the NH protons. Further work can be done by crystallizing 7mer and 15mer to obtain a single crystal X-Ray data, which will be helpful to see the exact 3D structure of foldamers and model reactions with different polymers in various solvents.

Chapter 4, described my attempt to polymerize the macrocyclic bis-stiff stilbene monomer or attach the foldamer to a terminus of commercial polystyrene. Polymerization of the macrocycle yielded the product with a nominal MW ranging from 2 to 25 kDa (Mp of 5 kDa), according to the SEC calibration against PS standards, under ROMP with Grubbs II catalysis. Modifying the monomer linker may increase the achievable degree of polymerization. The positive aspect is that the UV analysis confirmed that polymerization conditions did not cause distinct conformations changes from Z to E form.

The end-derivatization of polystyrene experiments using model foldamer resulted in forming dimer systems with expected ratios of foldamer to a polymer chain. However, dilution and reconcentration experiments did not provide the expected dissociation and reassociation mechanism potentially due to humidity coming from the air. Further control experiments need to be continued to understand the effect of external environmental factors. An alternative to studying this system is to synthesize a double-helical foldamer in aqueous media to perform a “click” chemistry with PEG.

Appendix
NMR SPECTRA

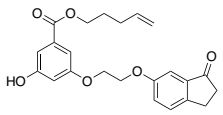

51

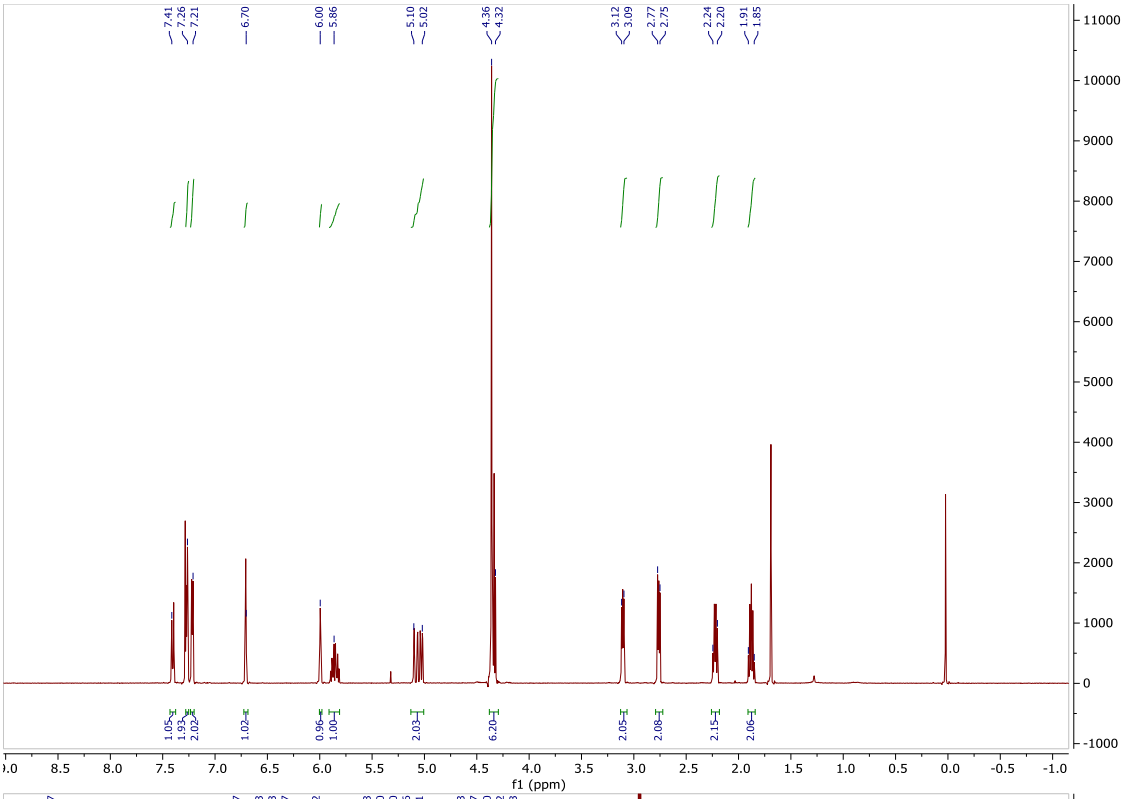
7.41
7.26
7.21
6.70
6.00
5.86
5.10
5.02
4.36
4.32
3.12
3.09
2.77
2.75
2.24
2.20
1.91
1.85
1.05
1.93
2.02
1.02
0.96
1.00
2.03
6.20
2.05
2.08
2.15
2.06
f1 (ppm)

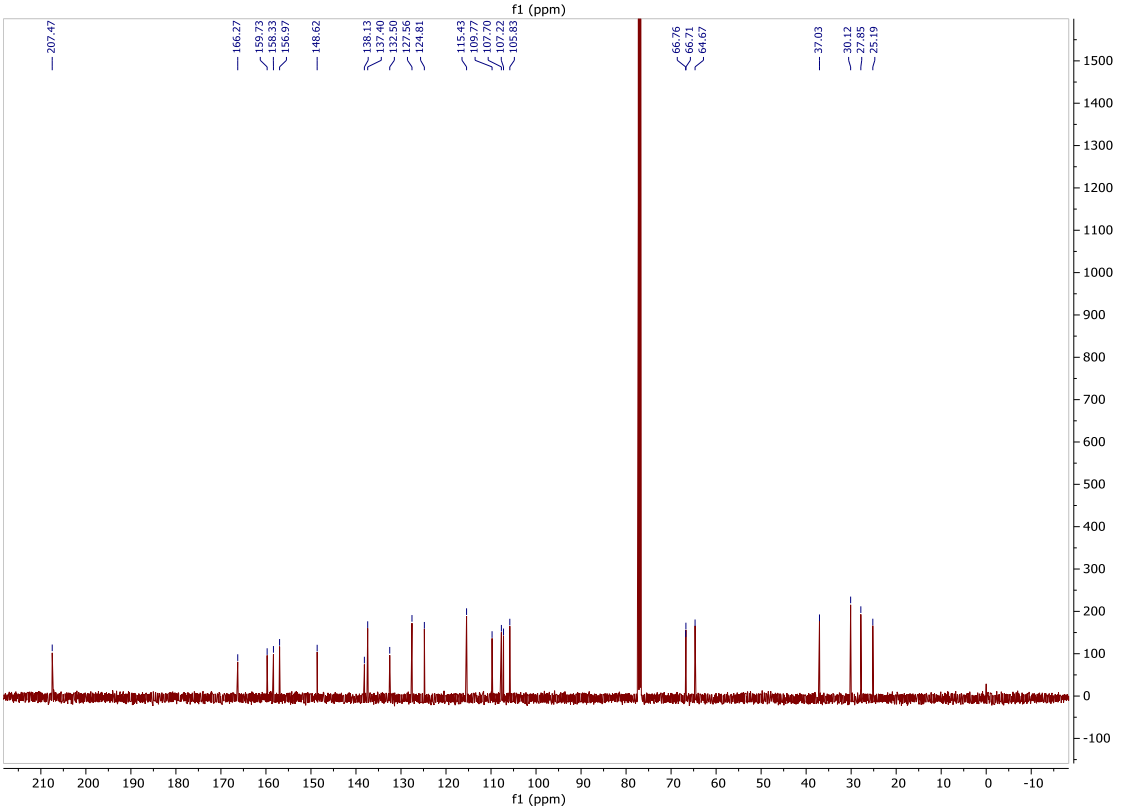
207.47
166.27
159.73
158.33
156.97
148.62
138.13
137.40
132.50
127.56
124.81
115.43
109.77
107.70
107.22
105.83
66.76
66.71
64.67
37.03
30.12
27.85
25.19
f1 (ppm)

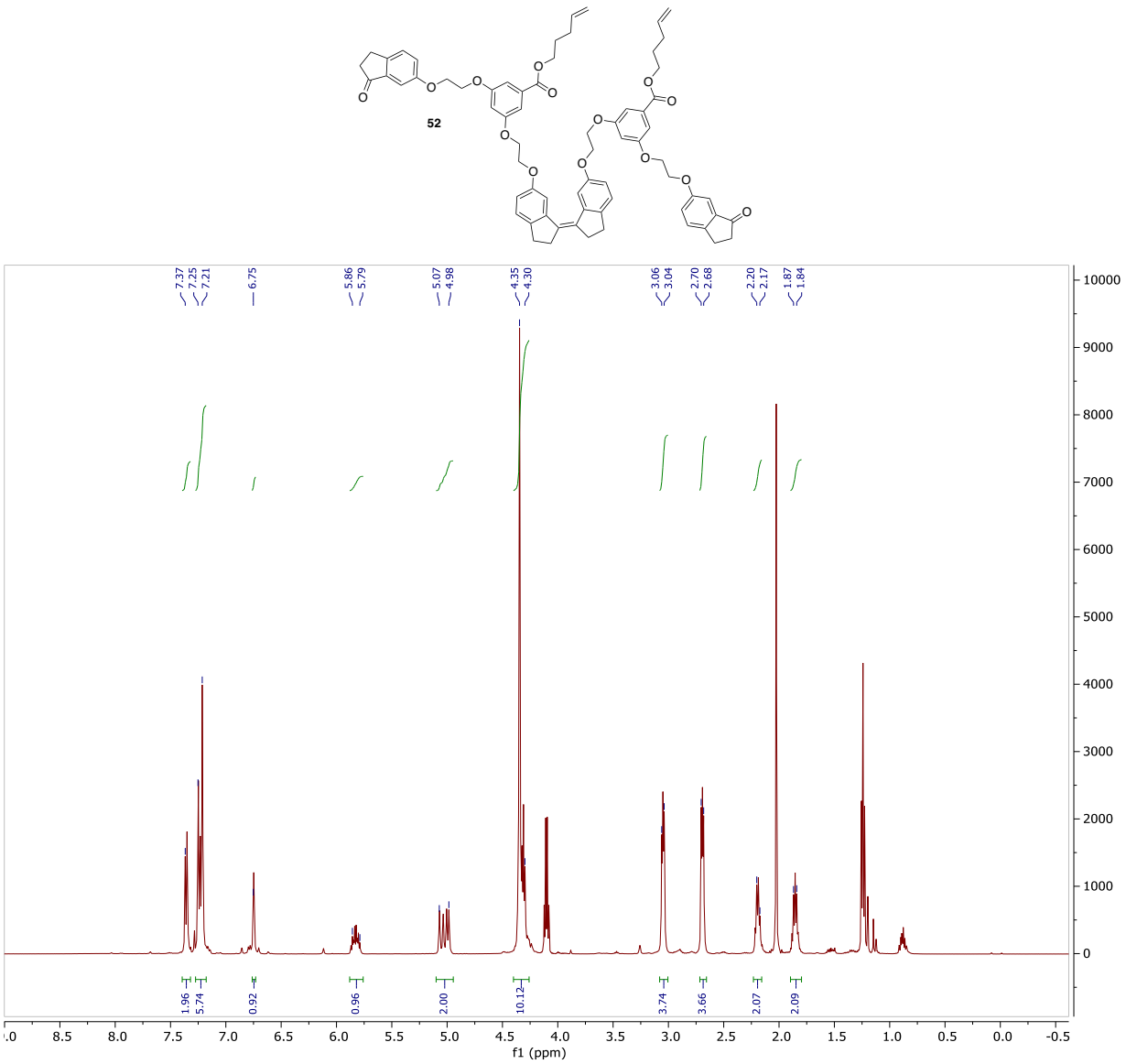
52
7.37
7.25
7.21
6.75
5.86
5.79
5.07
4.98
4.35
4.30
3.06
3.04
2.70
2.68
2.20
2.17
1.87
1.84
1.96
5.74
0.92
0.96
2.00
10.12
3.74
3.66
2.07
2.09
f1 (ppm)

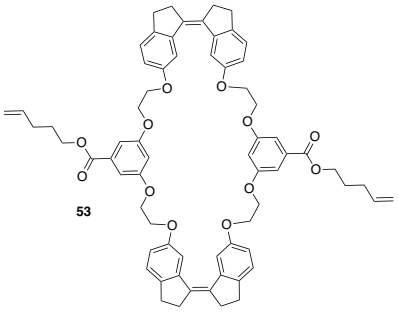
53

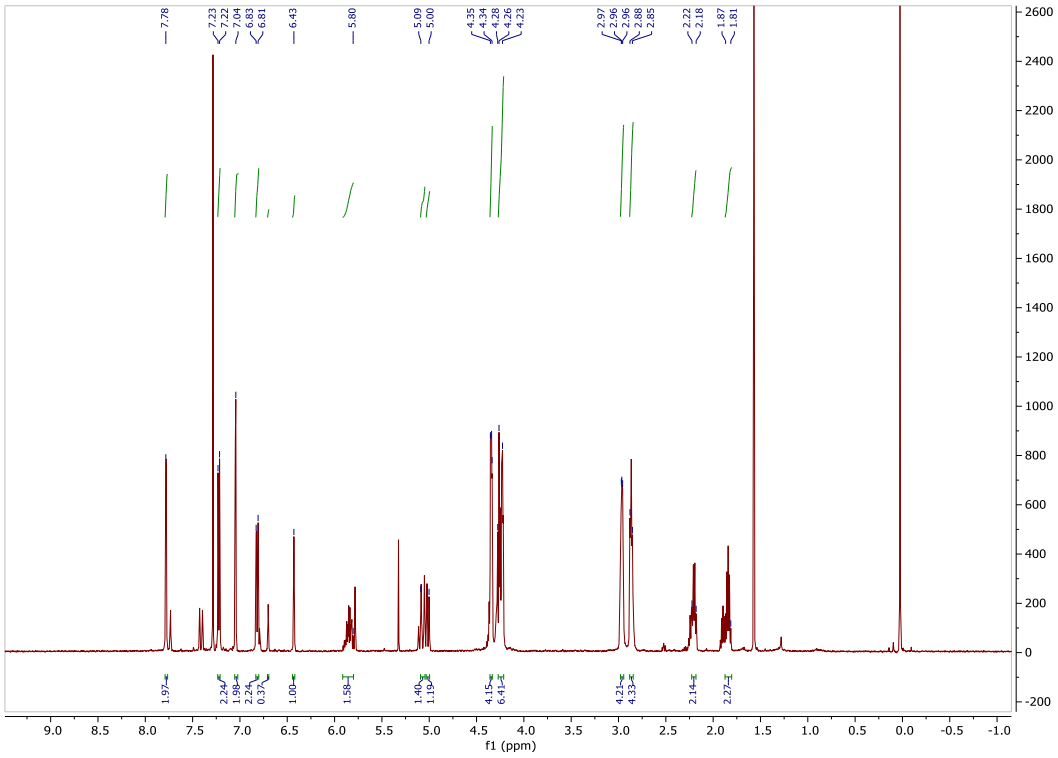
7.78
7.23
7.22
7.04
6.83
6.81
6.43
5.80
5.09
5.00
4.35
4.34
4.28
4.26
4.23
3.97
2.96
2.96
2.88
2.85
2.22
2.18
1.87
1.81
1.97
2.24
1.98
2.24
0.37
1.00
1.58
1.40
1.19
4.15
6.41
4.21
4.33
2.14
2.27
f1 (ppm)

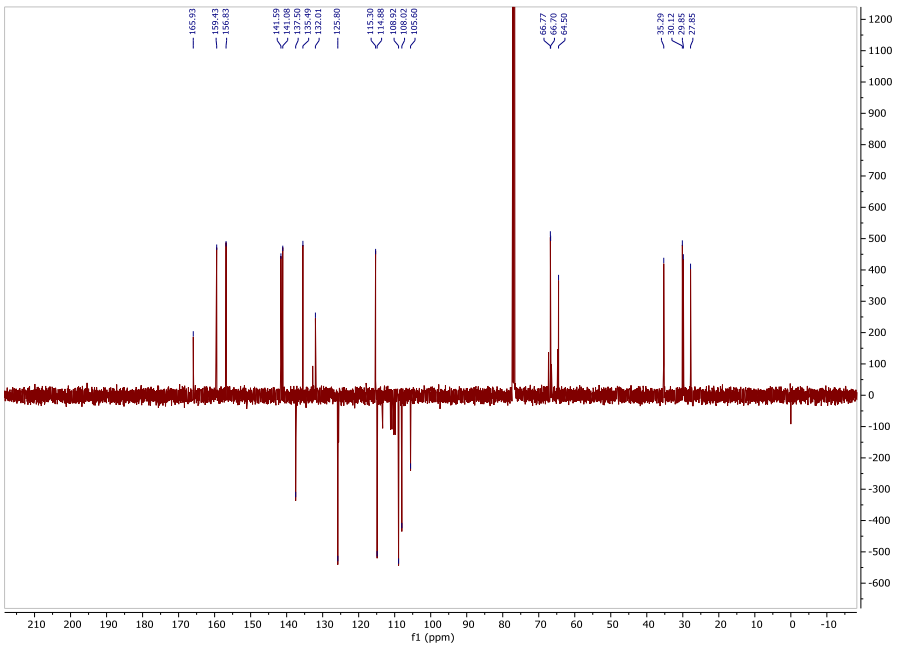
165.93
159.43
156.83
141.59
141.08
137.50
135.49
132.01
125.80
115.30
114.88
108.07
108.02
105.60
66.77
66.70
64.50
35.29
31.22
29.85
27.85
f1 (ppm)

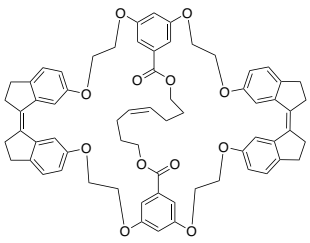

54

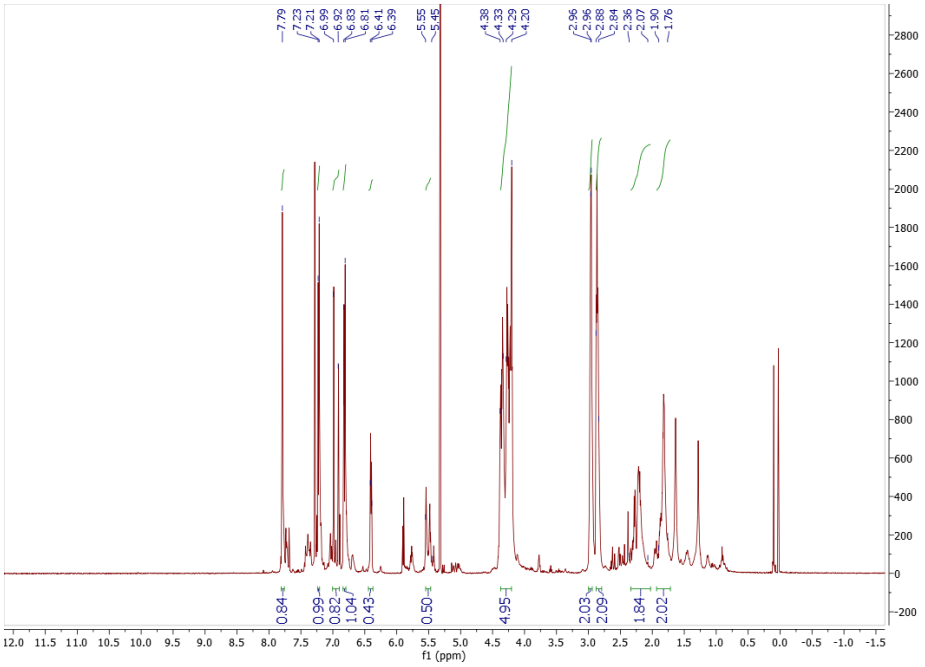
7.79
7.23
7.21
6.99
6.82
6.83
6.81
6.41
6.39
5.55
5.45
4.38
4.33
4.29
4.20
2.96
2.96
2.88
2.84
2.36
2.07
1.90
1.76
0.84
0.99
0.82
1.04
0.43
0.50
4.95
2.03
2.09
1.84
2.02
f1 (ppm)

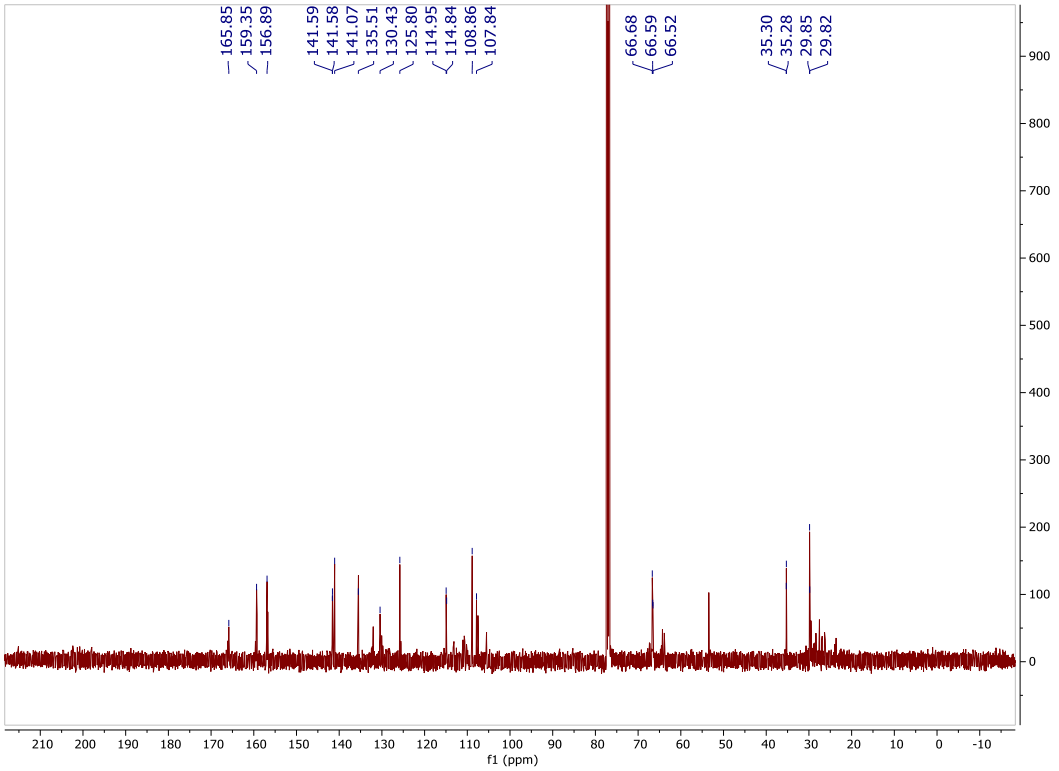
165.85
159.35
156.89
141.59
141.58
141.07
135.51
130.43
125.80
114.95
114.84
108.86
107.84
66.68
66.59
66.52
35.30
35.28
29.85
29.82
f1 (ppm)

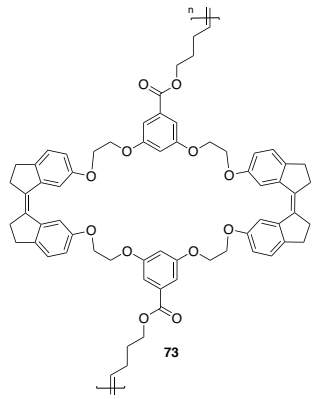

73

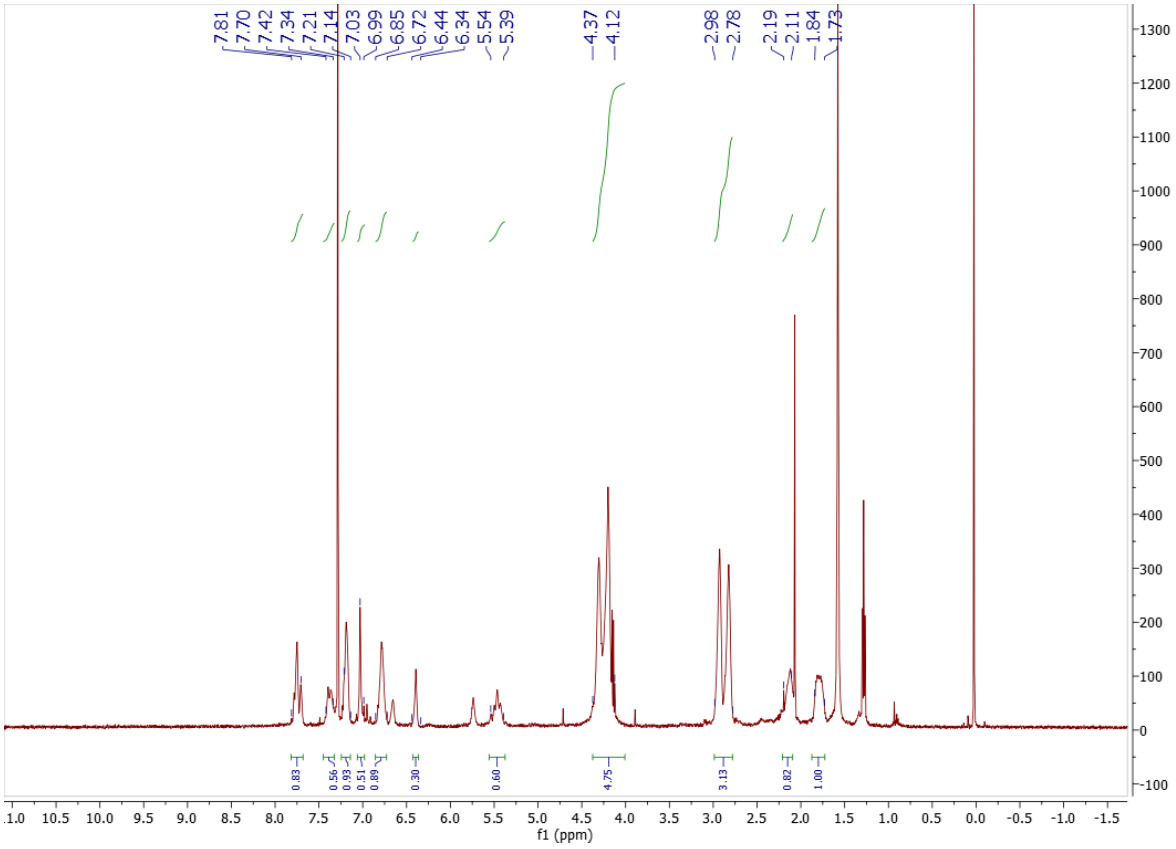
7.81
7.70
7.42
7.34
7.21
7.14
7.03
6.99
6.85
6.72
6.44
6.34
5.54
5.39
4.37
4.12
2.98
2.78
2.19
2.11
1.84
1.73
0.83
0.56
0.93
0.51
0.89
0.30
0.60
4.75
3.13
0.82
1.00
f1 (ppm)

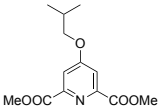
MeOOC
N
COOMe
O

57

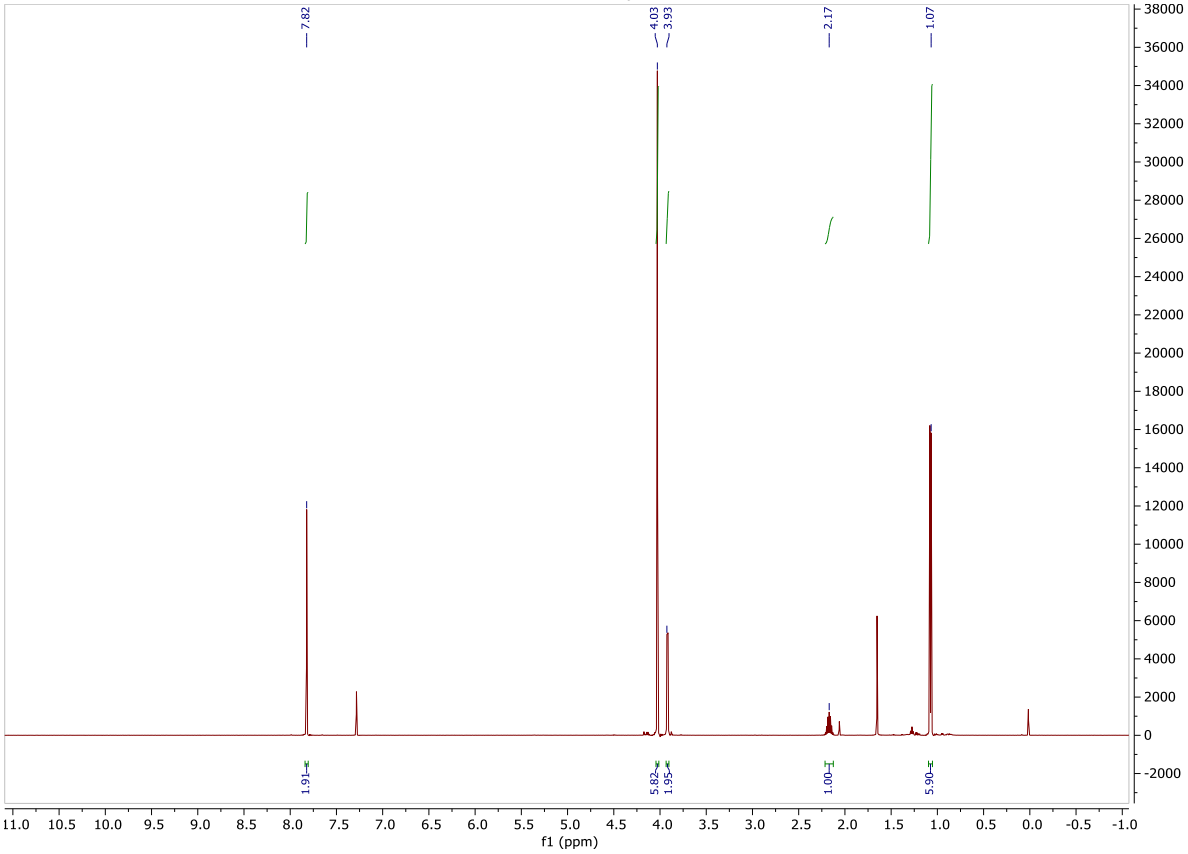
7.82
4.03
3.93
2.17
1.07
1.91
5.82
1.95
1.00
5.90
f1 (ppm)

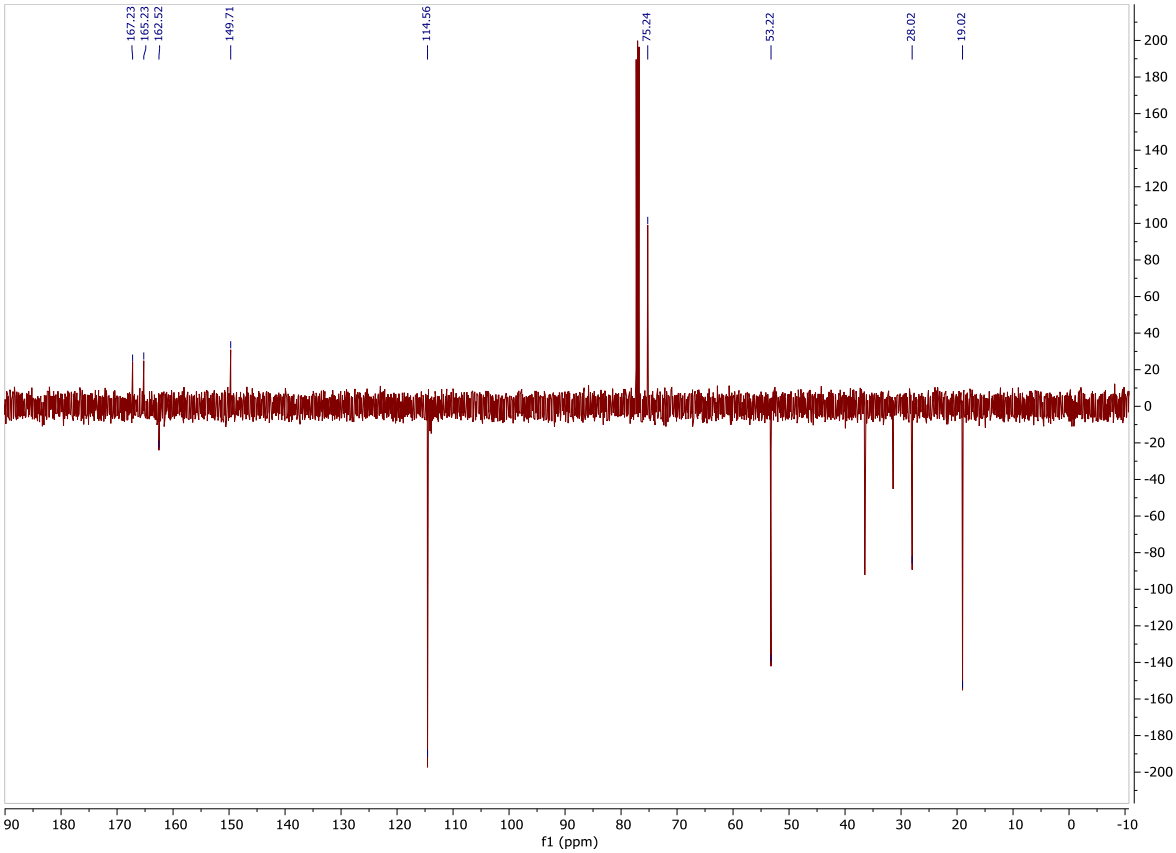
167.23
165.23
162.52
149.71
114.56
75.24
53.22
28.02
19.02
f1 (ppm)

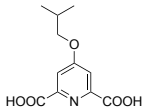
HOOC
N
COOH

63

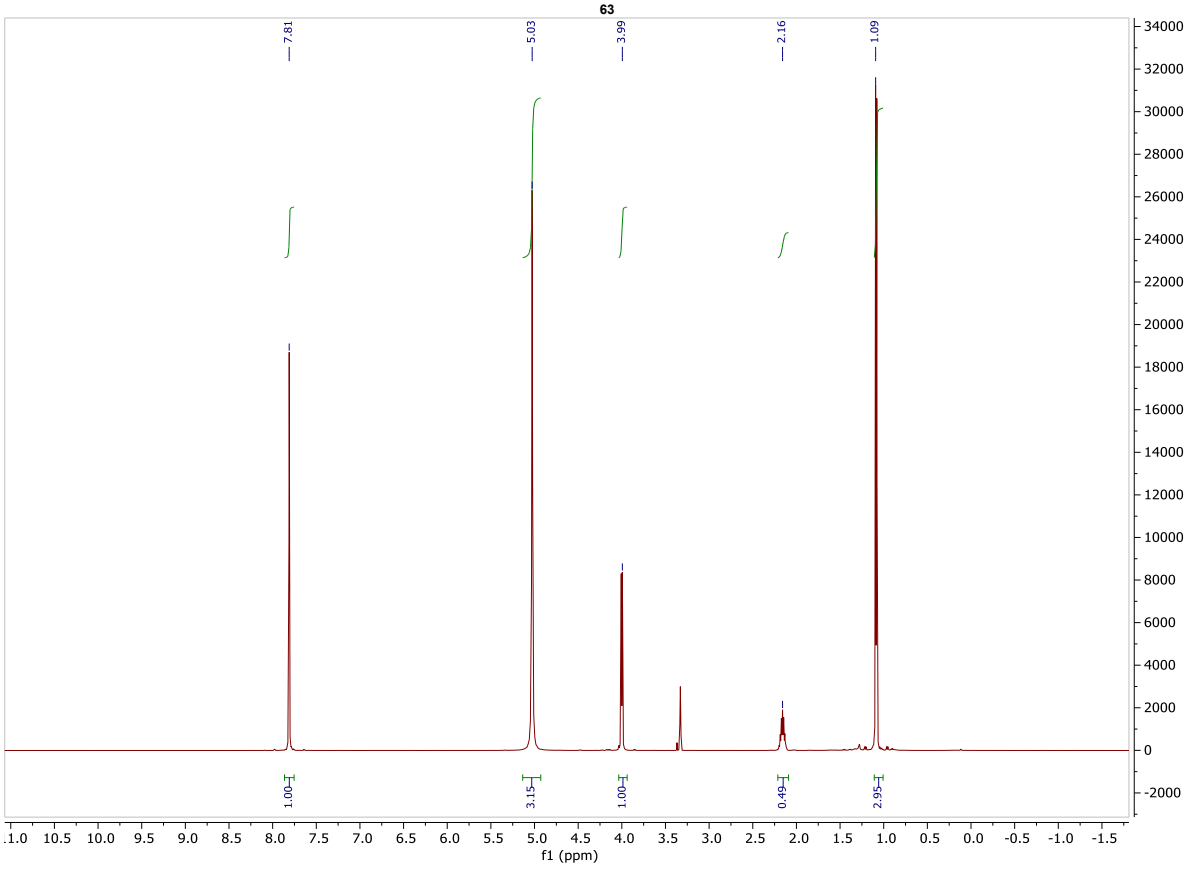
7.81
5.03
3.99
2.16
1.09
1.00
3.15
1.00
0.49
2.95
f1 (ppm)

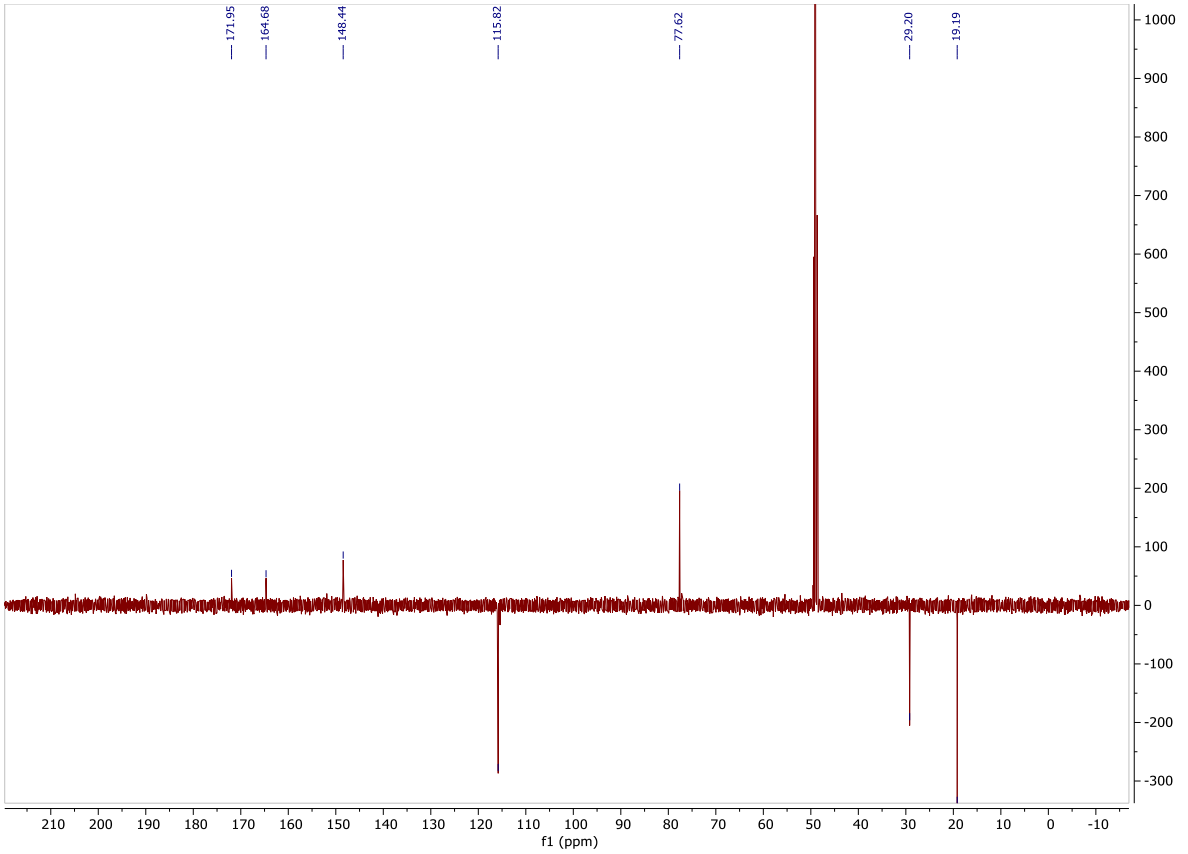
171.95
164.68
148.44
115.82
77.62
29.20
19.19
f1 (ppm)

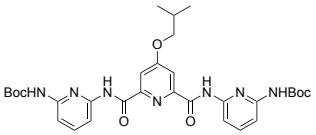
BocHN
NHBoc
O
H
N
O

58

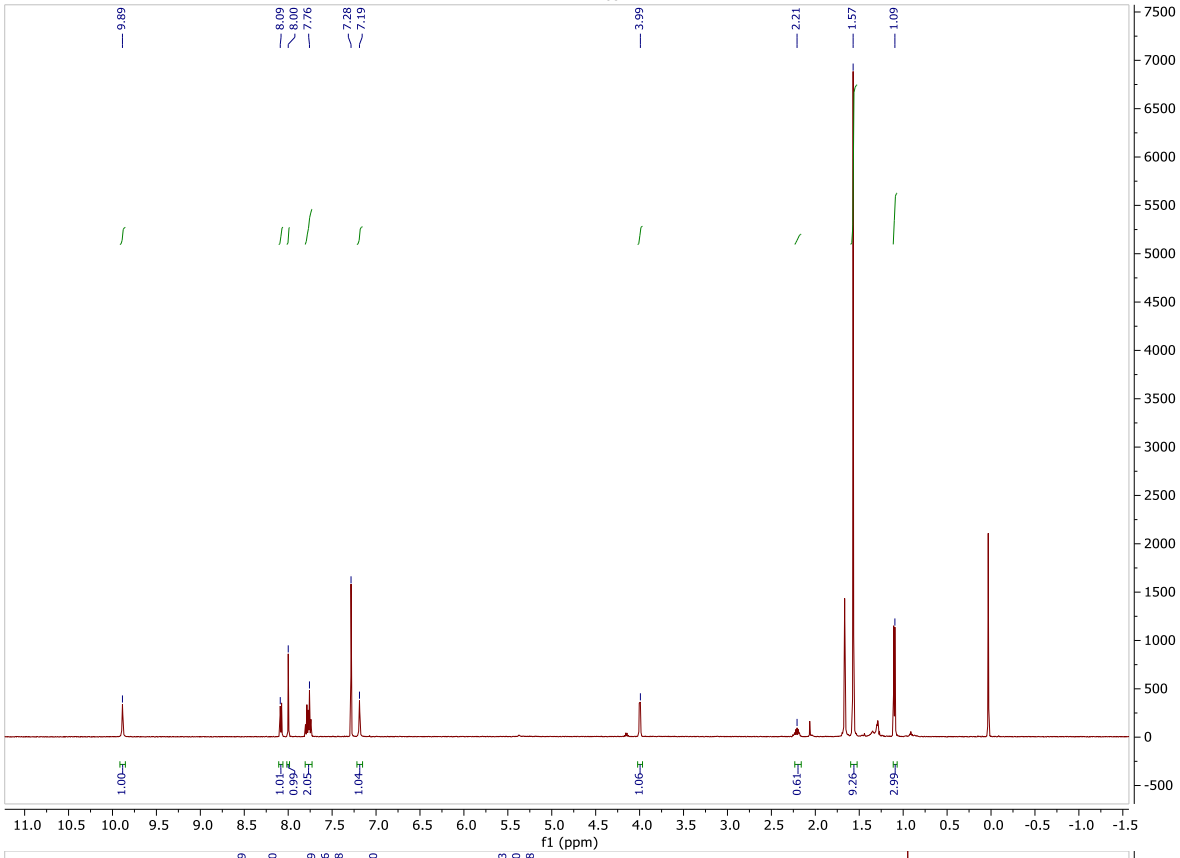
9.89
8.09
8.00
7.76
7.28
7.19
3.99
2.21
1.57
1.09
1.00
1.01
0.99
2.05
1.04
1.06
0.61
9.26
2.99
f1 (ppm)

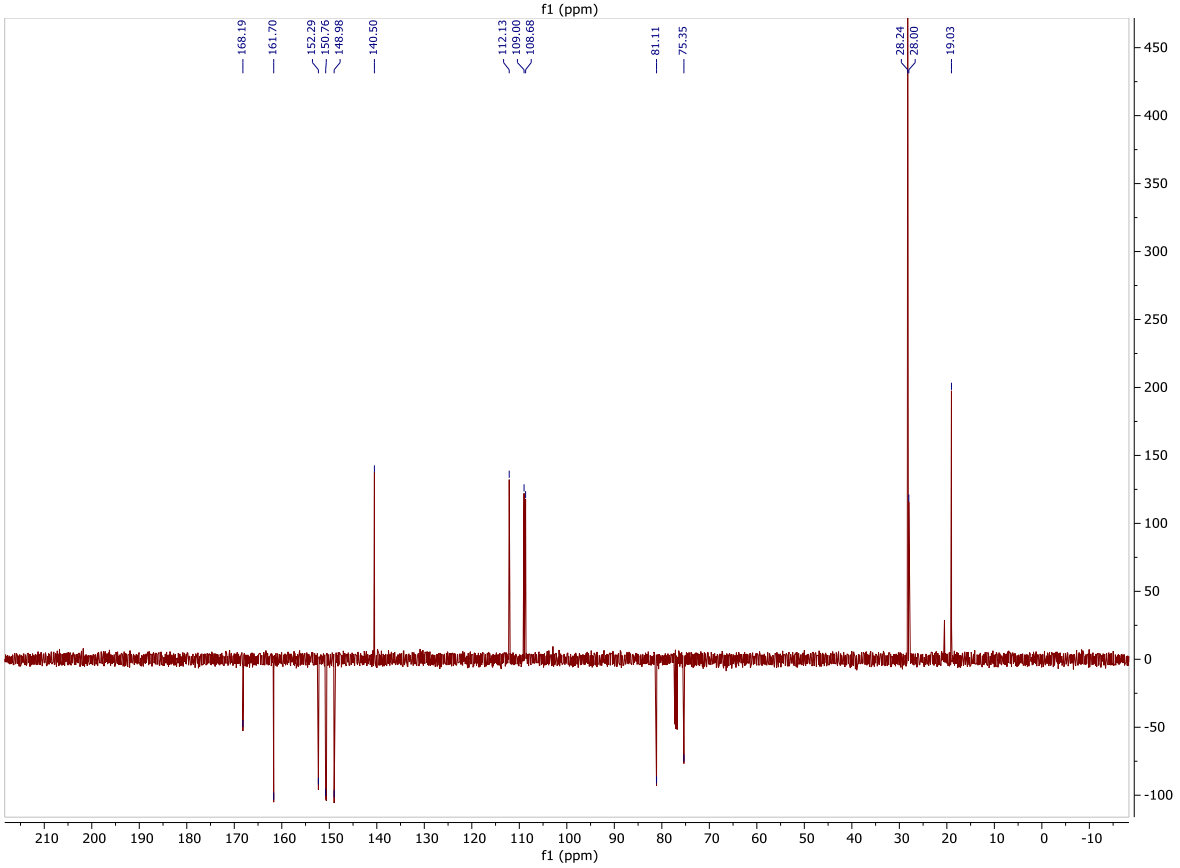
168.19
161.70
152.29
150.76
148.98
140.50
112.13
109.00
108.68
81.11
75.35
28.24
28.00
19.03
f1 (ppm)

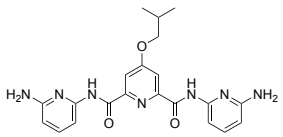

67

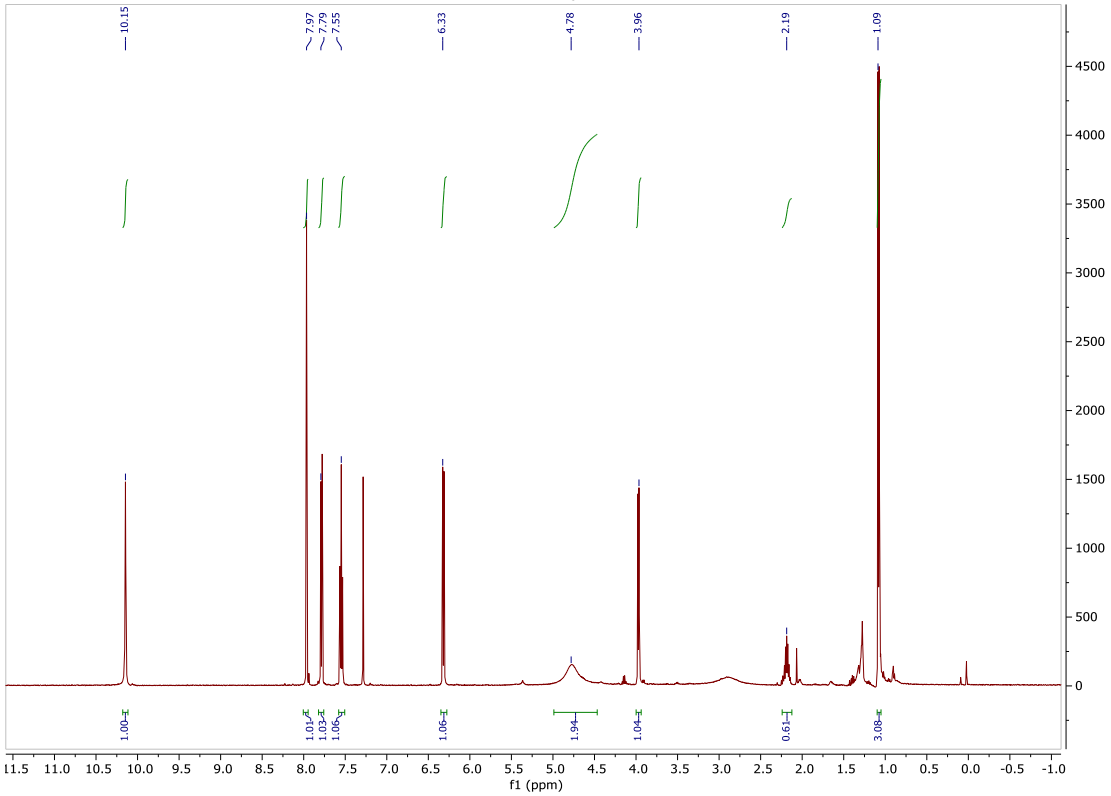
10.15
7.97
7.79
7.55
6.33
4.78
3.96
2.19
1.09
1.00
1.01
1.03
1.06
1.06
1.94
1.04
0.61
3.08
f1 (ppm)

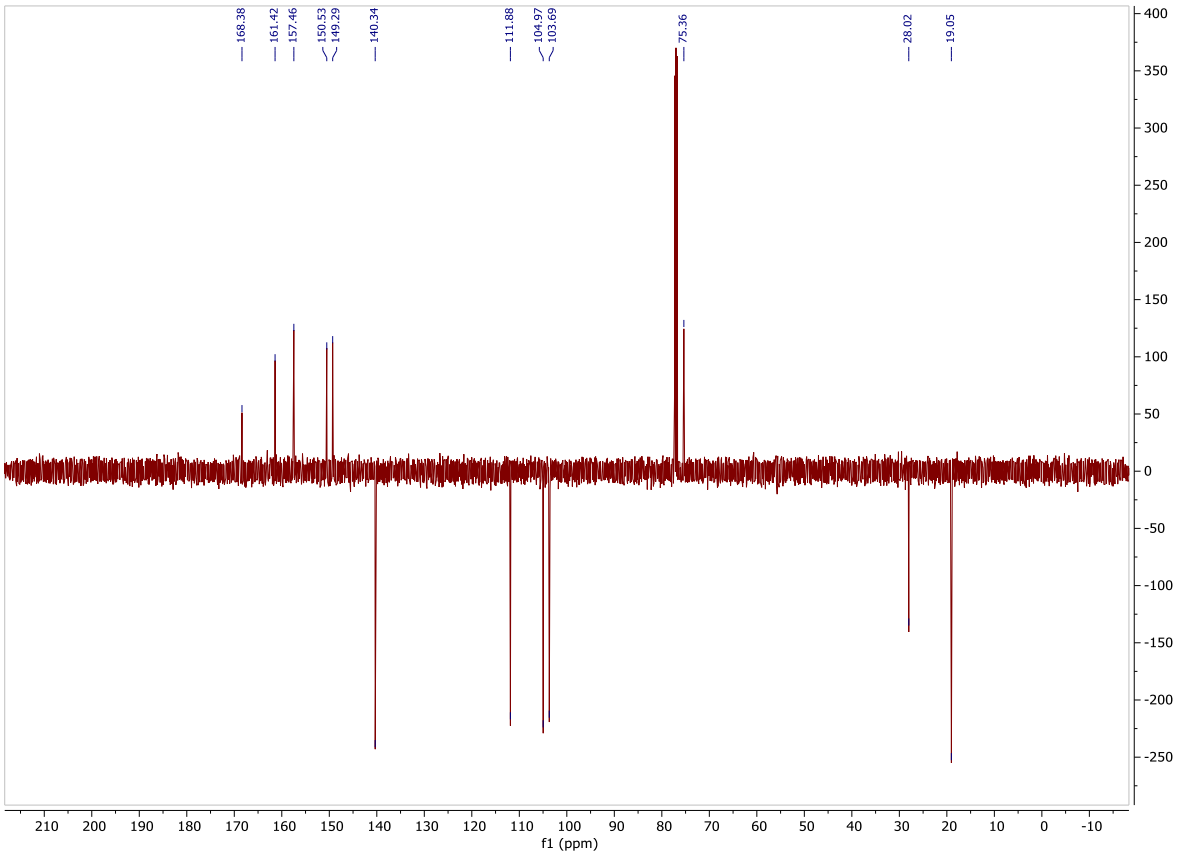
168.38
161.42
157.46
150.53
149.29
140.34
111.88
104.97
103.69
75.36
28.02
19.05
f1 (ppm)

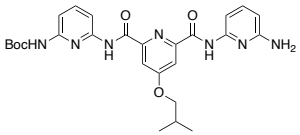
BocHN
N
H
O
N
O
N
H
N
NH2
O

79

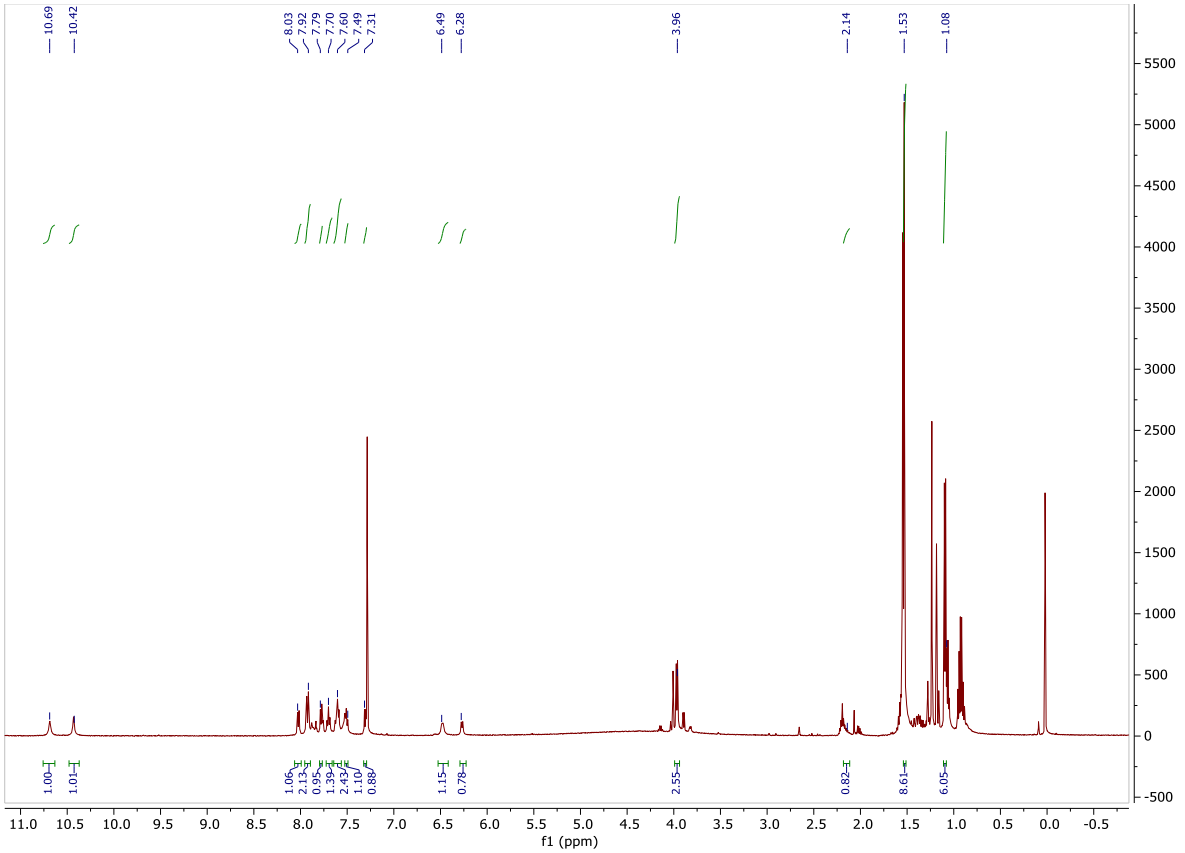
10.69
10.42
8.03
7.92
7.79
7.70
7.60
7.49
7.31
6.49
6.28
3.96
2.14
1.53
1.08
1.00
1.01
1.06
2.13
0.95
1.39
2.43
1.10
0.88
1.15
0.78
2.55
0.82
8.61
6.05
f1 (ppm)

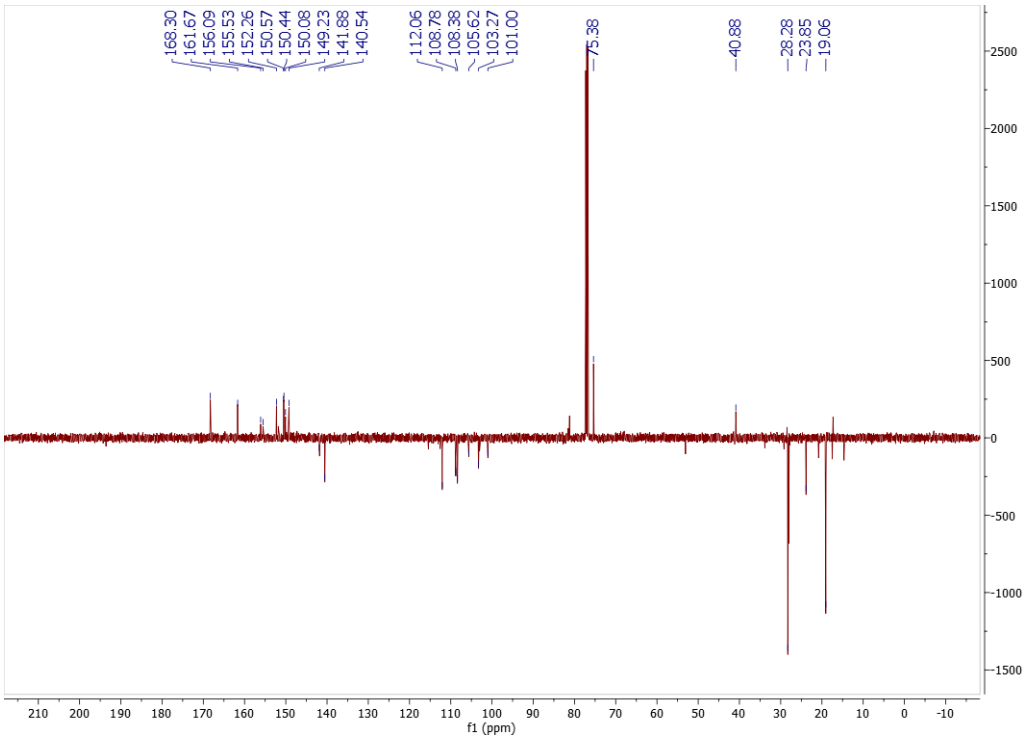
168.30
161.67
156.09
155.53
152.26
150.57
150.44
150.08
149.23
141.88
140.54
112.06
108.78
108.38
105.62
103.27
101.00
75.38
40.88
28.28
23.85
19.06
f1 (ppm)

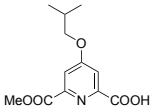
O
MeOOC
N
COOH

62

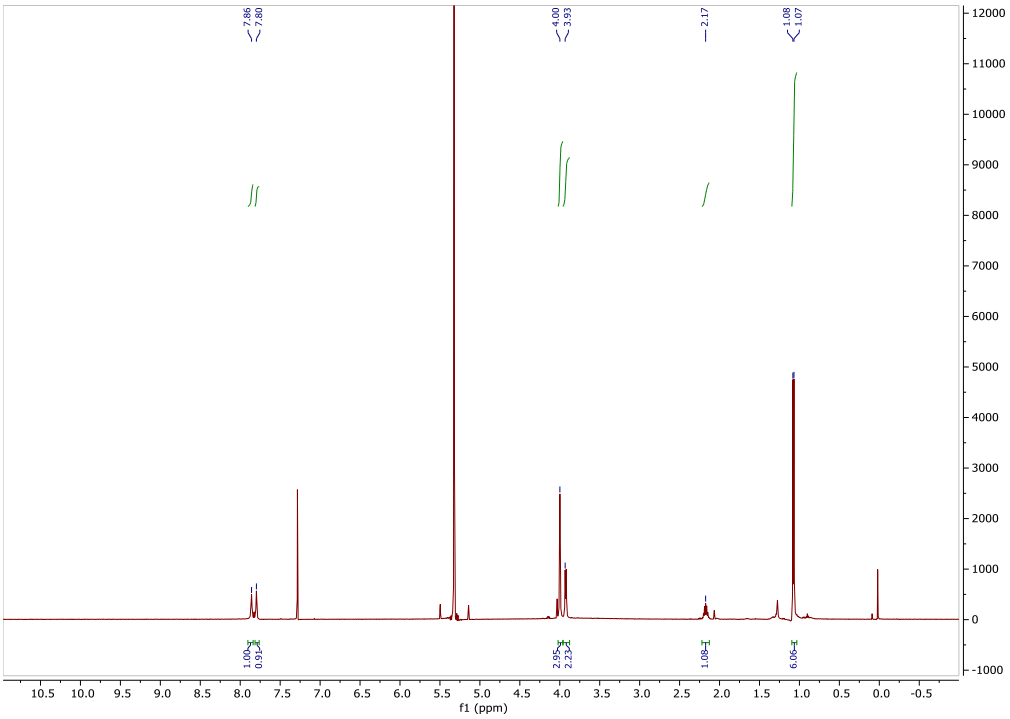
7.86
7.80
4.00
3.93
2.17
1.08
1.07
1.00
0.91
2.95
2.23
1.08
6.06
f1 (ppm)

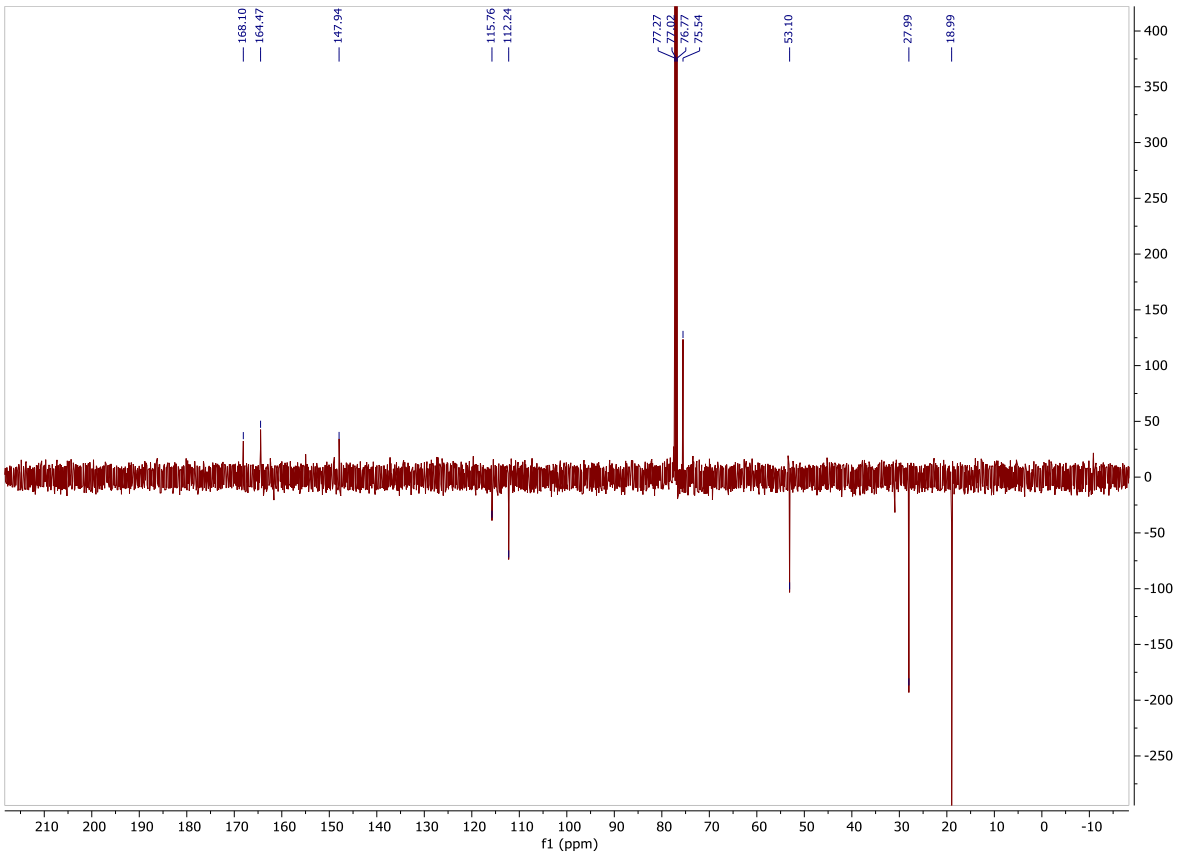
168.10
164.47
147.94
115.76
112.24
77.27
77.02
76.77
75.54
53.10
27.99
18.99
f1 (ppm)

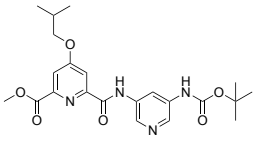

66

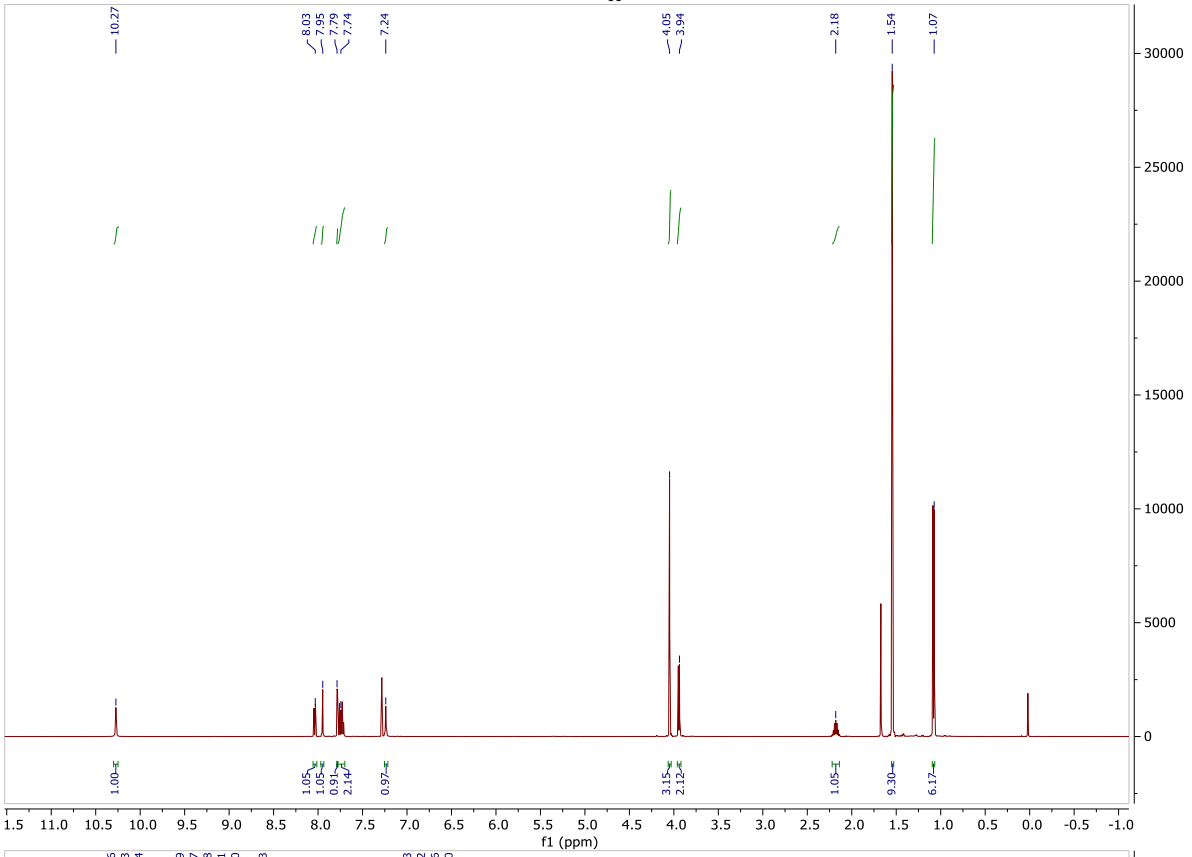
10.27
8.03
7.95
7.79
7.74
7.24
4.05
3.94
2.18
1.54
1.07
1.00
1.05
1.05
0.91
2.14
0.97
3.15
2.12
1.05
9.30
6.17
f1 (ppm)

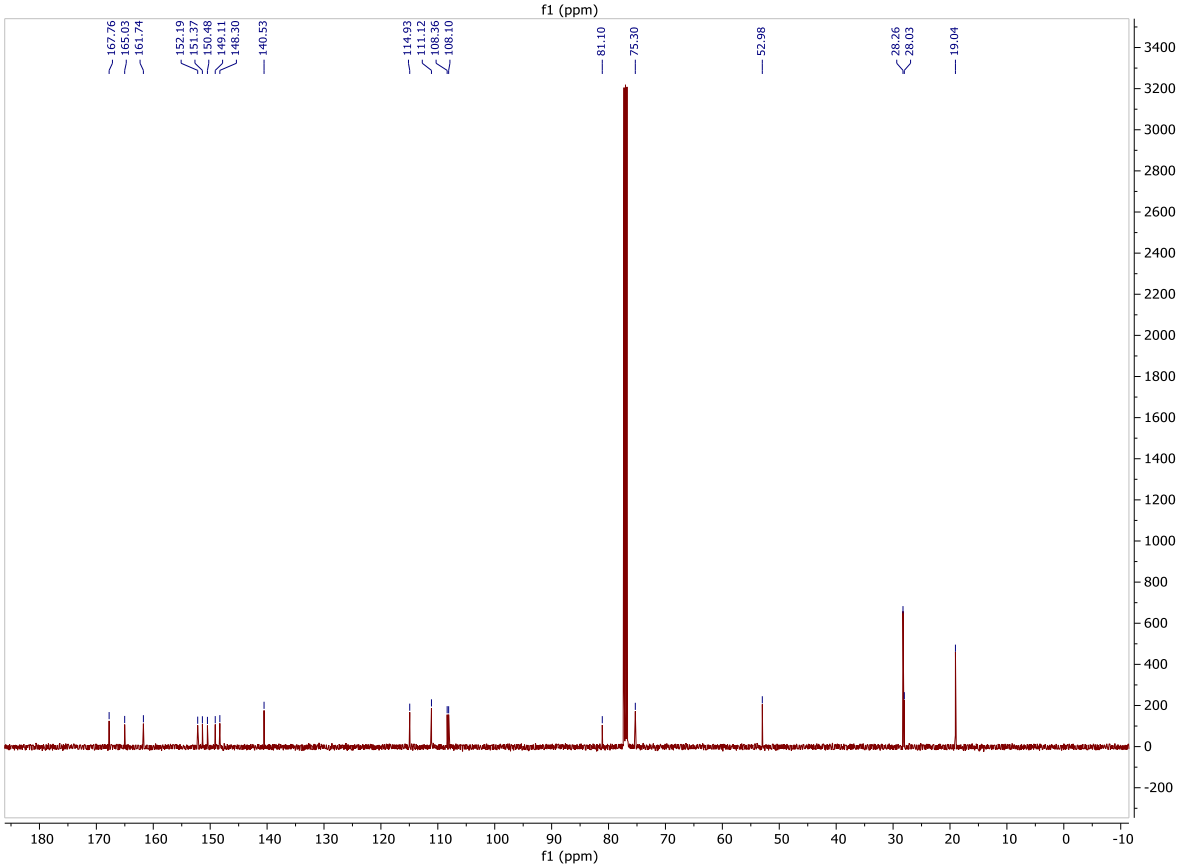
167.76
165.03
161.74
152.19
151.37
150.48
149.11
148.30
140.53
114.93
111.12
108.36
108.10
81.10
75.30
52.98
28.26
28.03
19.04
f1 (ppm)

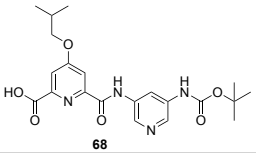

68

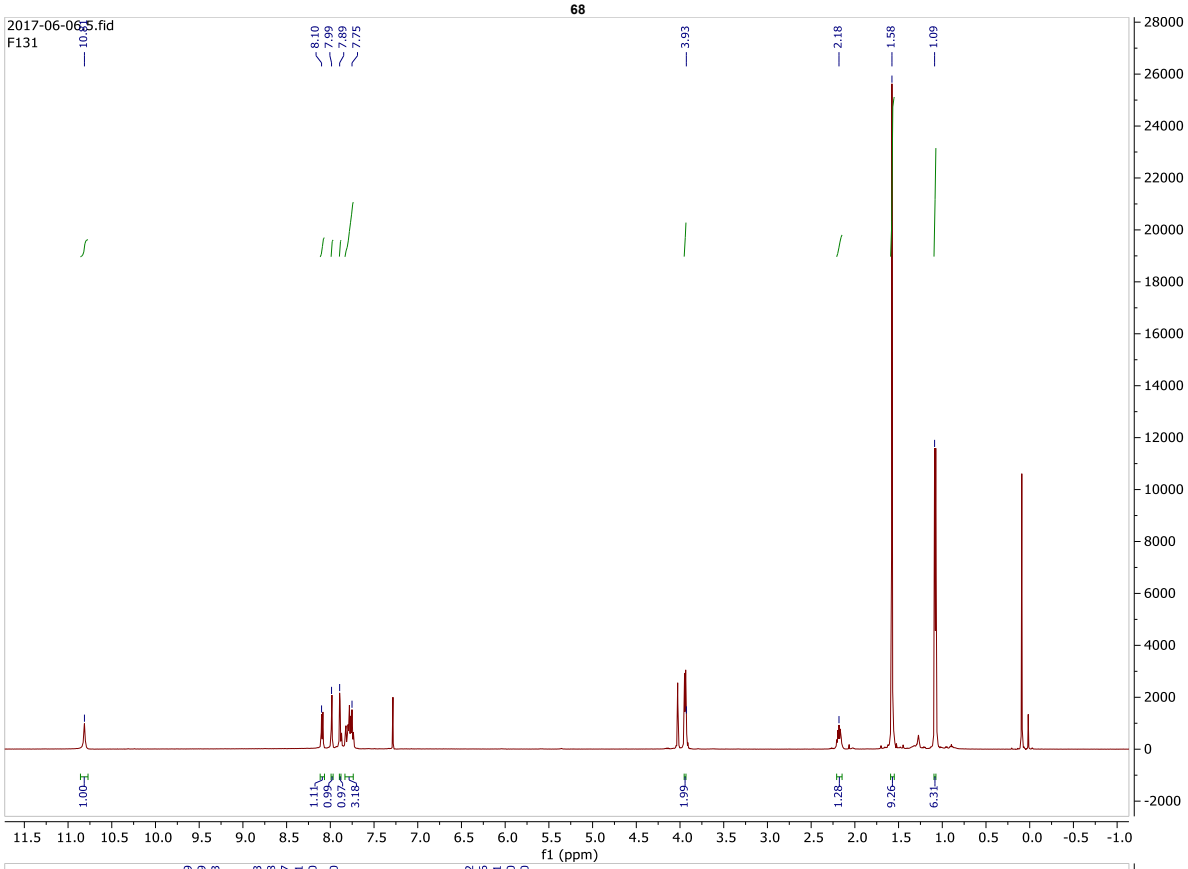
2017-06-065.fid
F131
10.62
8.10
7.99
7.89
7.75
3.93
2.18
1.58
1.09
1.00
1.11
0.99
0.97
3.18
1.99
1.28
9.26
6.31
f1 (ppm)

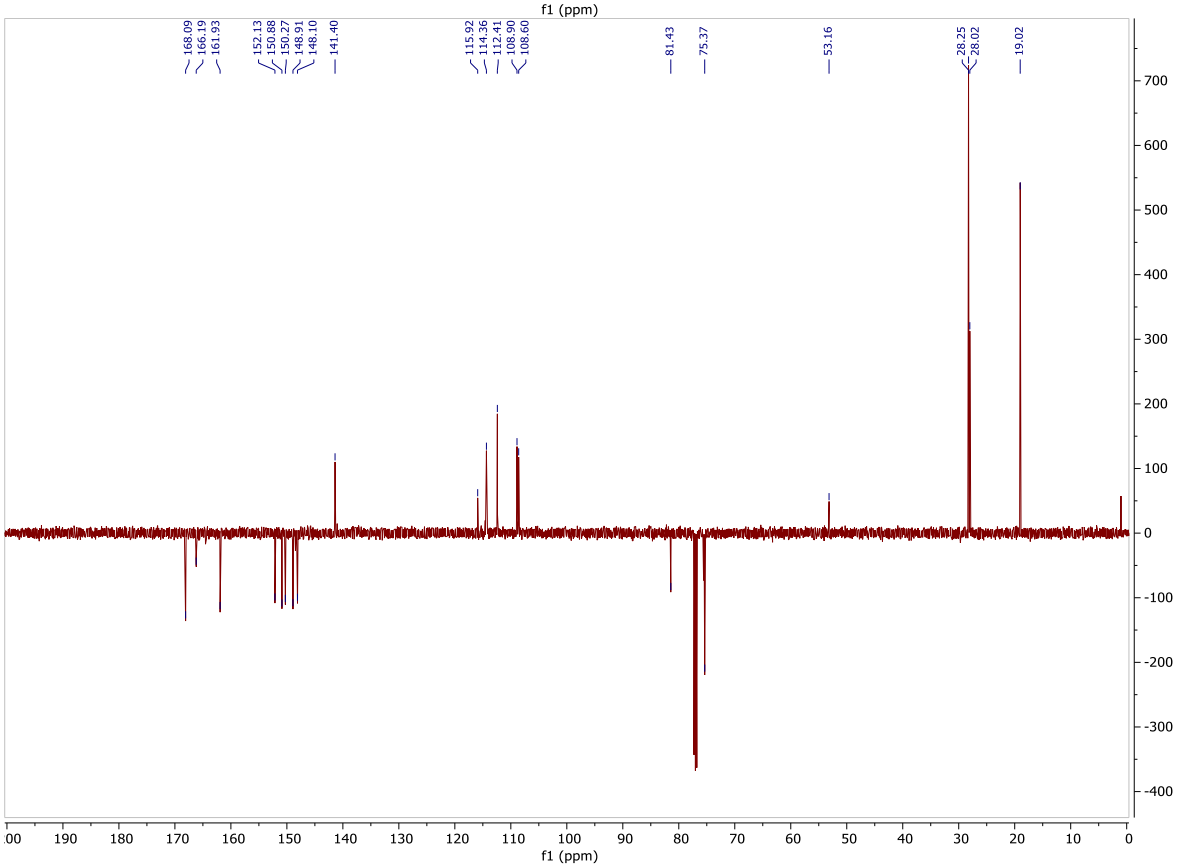
168.09
166.19
161.93
152.13
150.88
150.27
148.91
148.10
141.40
115.92
114.36
112.41
108.90
108.60
81.43
75.37
53.16
28.25
28.02
19.02
f1 (ppm)

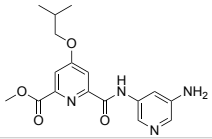

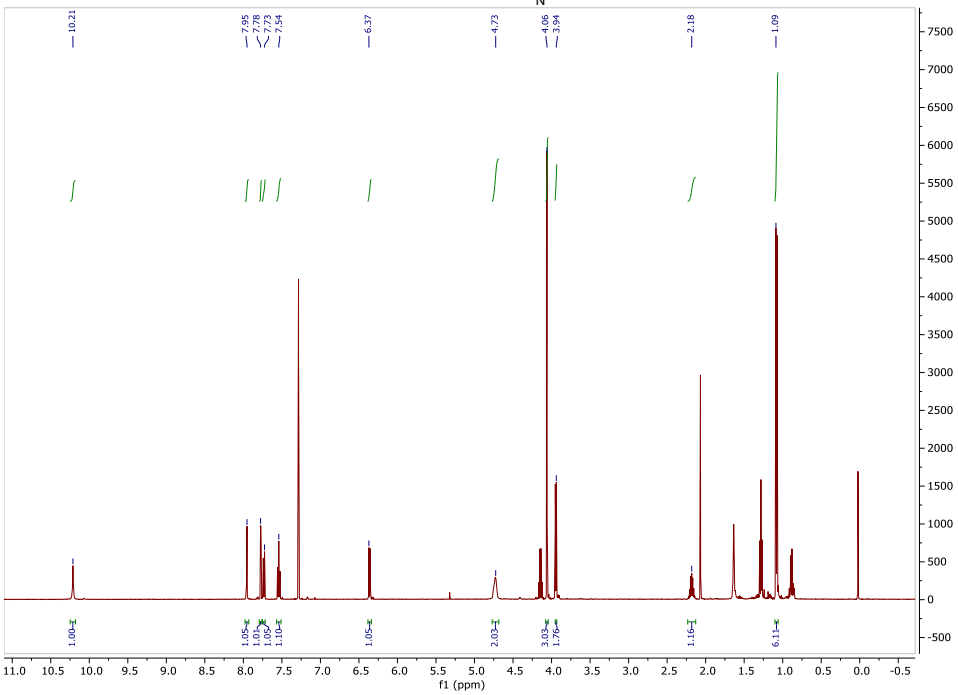
10.21
7.95
7.78
7.73
7.54
6.37
4.73
4.06
3.94
2.18
1.09
f1 (ppm)

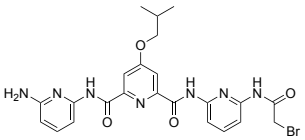

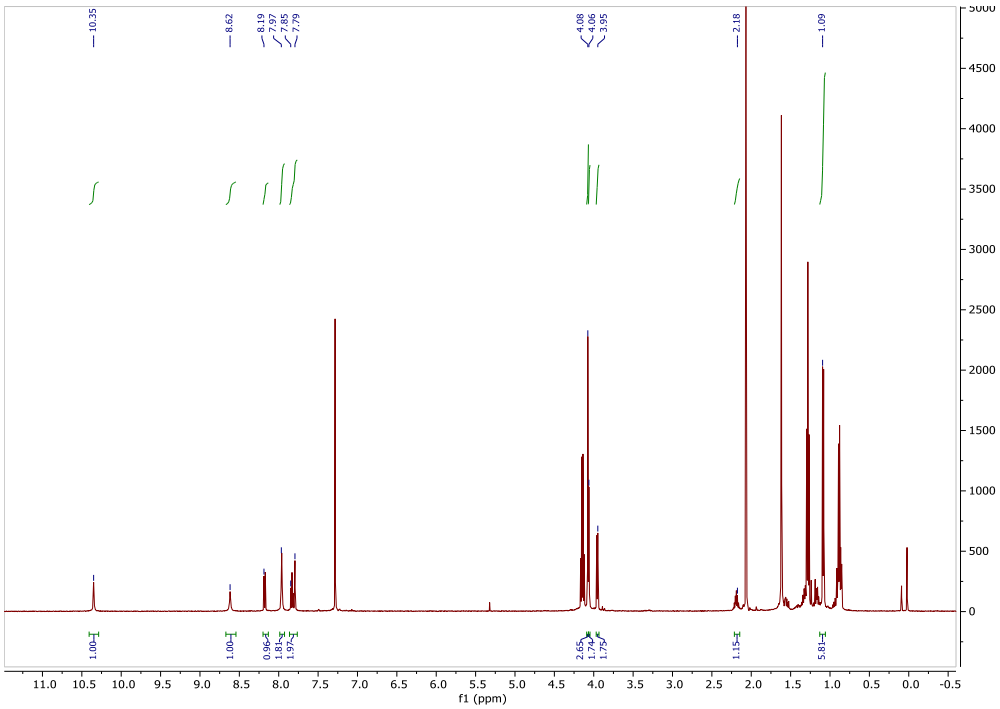
10.35
8.62
8.19
7.97
7.85
7.79
4.08
4.06
3.95
2.18
1.09
f1 (ppm)

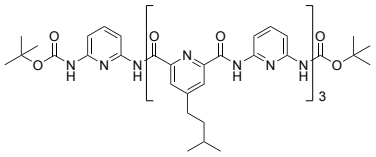

59

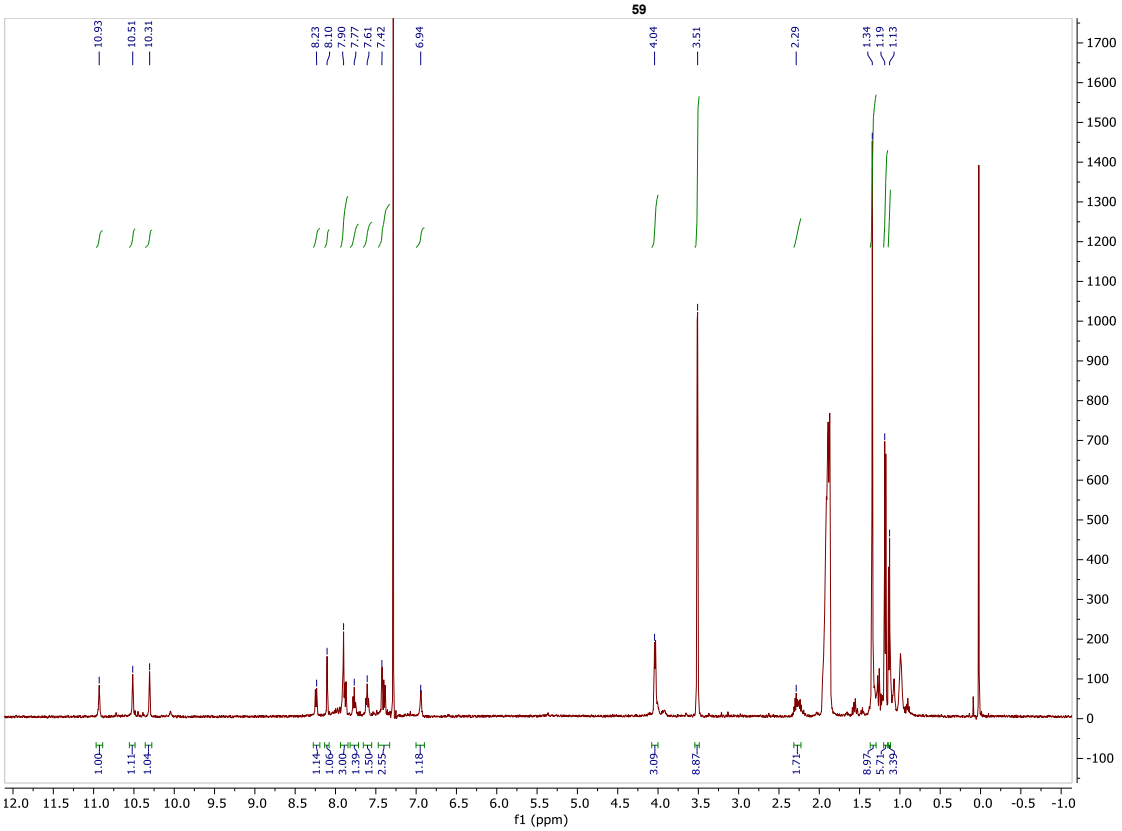
10.93
10.51
10.31
8.23
8.10
7.90
7.77
7.61
7.42
6.94
4.04
3.51
2.29
1.34
1.19
1.13
1.00
1.11
1.04
1.14
1.06
3.00
1.39
1.50
2.55
1.18
3.09
8.87
1.71
8.97
5.71
3.39
f1 (ppm)

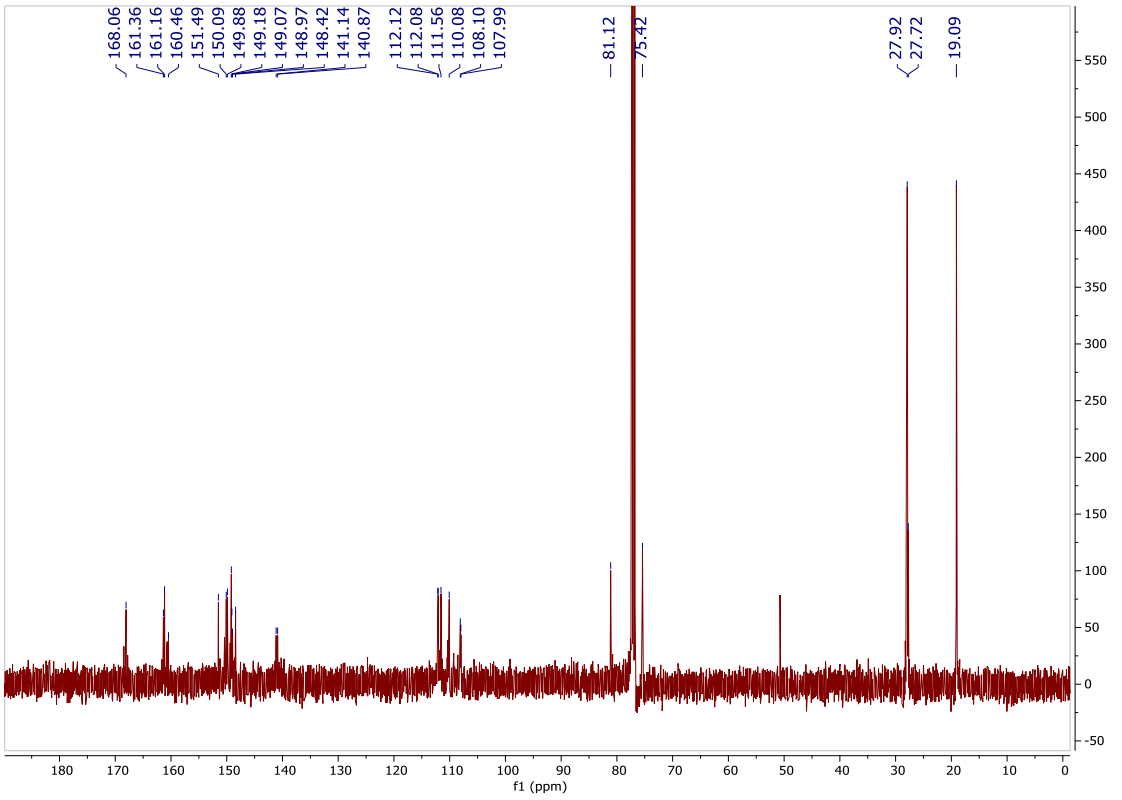
168.06
161.36
161.16
160.46
151.49
150.09
149.88
149.18
149.07
148.97
148.42
141.14
140.87
112.12
112.08
111.56
110.08
108.10
107.99
81.12
75.42
27.92
27.72
19.09
f1 (ppm)

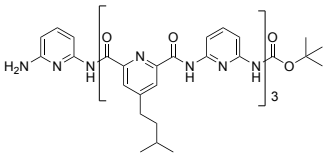

72

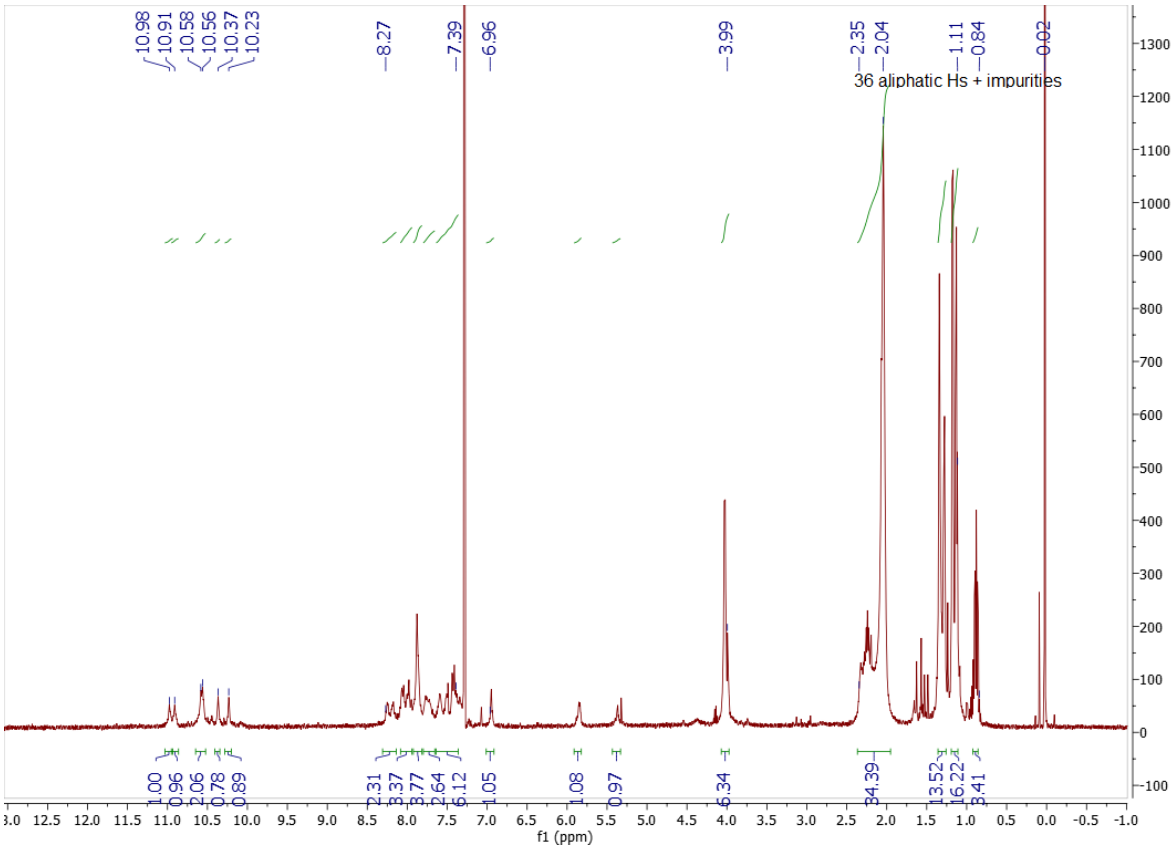
10.98
10.91
10.58
10.56
10.37
10.23
8.27
7.39
6.96
3.99
2.35
2.04
1.11
0.84
0.02
36 aliphatic Hs + impurities
1.00
0.96
2.06
0.78
0.89
2.31
3.37
3.77
2.64
6.12
1.05
1.08
0.97
6.34
34.39
13.52
16.22
3.41
f1 (ppm)

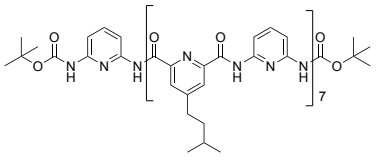

60

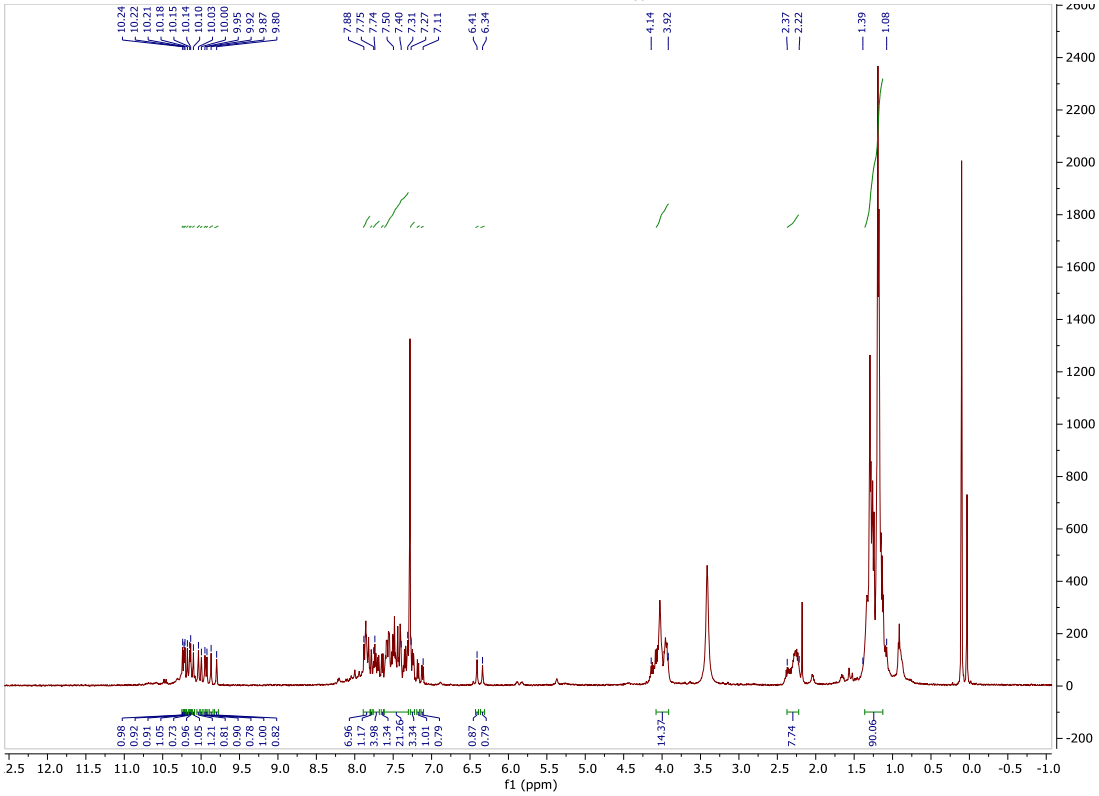
10.24
10.22
10.21
10.18
10.15
10.14
10.10
10.03
10.00
9.95
9.92
9.87
9.80
7.88
7.75
7.74
7.50
7.40
7.31
7.27
7.11
6.41
6.34
4.14
3.92
2.37
2.22
1.39
1.08
0.98
0.92
0.91
1.05
0.73
0.96
1.05
1.21
0.81
0.90
0.78
1.00
0.82
6.96
1.17
3.98
1.34
21.26
3.34
1.01
0.79
0.87
0.79
14.37
7.74
90.06
f1 (ppm)

REFERENCES

1. Staudinger, H.; Heuer, W., Über hochpolymere Verbindungen, 93. Mitteil.: Über das Zerreißen der Faden-Moleküle des Poly-styrols. *Berichte der deutschen chemischen Gesellschaft (A and B Series)* **1934,** *67* (7), 1159-1164.
2. Boulatov, R., *Polymer Mechanochemistry*. Springer: 2015; Vol. 369.
3. Boulatov, R., Demonstrated leverage. *Nature chemistry* **2013,** *5* (2), 84-86.
4. Beyer, M. K.; Clausen-Schaumann, H., Mechanochemistry: the mechanical activation of covalent bonds. *Chemical Reviews* **2005,** *105* (8), 2921-2948.
5. Watson, W., Mechanico-chemical reactions of polymers. *Die Makromolekulare Chemie: Macromolecular Chemistry and Physics* **1959,** *34* (1), 240-252.
6. TJ, K.; R, B.; Knopf, G. K.; Otani, Y., *Optical nano and micro actuator technology*. CRC Press: 2012.
7. White, T. J., Light to work transduction and shape memory in glassy, photoresponsive macromolecular systems: trends and opportunities. *Journal of Polymer Science Part B: Polymer Physics* **2012,** *50* (13), 877-880.
8. Lenhardt, J. M.; Black, A. L.; Craig, S. L., gem-Dichlorocyclopropanes as abundant and efficient mechanophores in polybutadiene copolymers under mechanical stress. *Journal of the American Chemical Society* **2009,** *131* (31), 10818-10819.
9. Davis, D. A.; Hamilton, A.; Yang, J.; Cremar, L. D.; Van Gough, D.; Potisek, S. L.; Ong, M. T.; Braun, P. V.; Martínez, T. J.; White, S. R., Force-induced activation of covalent bonds in mechanoresponsive polymeric materials. *Nature* **2009,** *459* (7243), 68-72.
10. Beiermann, B. A.; Davis, D. A.; Kramer, S. L.; Moore, J. S.; Sottos, N. R.; White, S. R., Environmental effects on mechanochemical activation of spiropyran in linear PMMA. *Journal of Materials Chemistry* **2011,** *21* (23), 8443-8447.
11. Lee, C. K.; Beiermann, B. A.; Silberstein, M. N.; Wang, J.; Moore, J. S.; Sottos, N. R.; Braun, P. V., Exploiting force sensitive spiropyrans as molecular level probes. *Macromolecules* **2013,** *46* (10), 3746-3752.
12. Hugel, T.; Holland, N. B.; Cattani, A.; Moroder, L.; Seitz, M.; Gaub, H. E., Single-molecule optomechanical cycle. *Science* **2002,** *296* (5570), 1103-1106.
13. Yang, Q.-Z.; Huang, Z.; Kucharski, T. J.; Khvostichenko, D.; Chen, J.; Boulatov, R., A molecular force probe. *Nature Nanotechnology* **2009,** *4* (5), 302-306.
14. Waldeck, D. H., Photoisomerization dynamics of stilbenes. *Chemical Reviews* **1991,** *91* (3), 415-436.
15. Brantley, J. N.; Wiggins, K. M.; Bielawski, C. W., Polymer mechanochemistry: the design and study of mechanophores. *Polymer International* **2013,** *62* (1), 2-12.
16. Klukovich, H. M.; Kouznetsova, T. B.; Kean, Z. S.; Lenhardt, J. M.; Craig, S. L., A backbone lever-arm effect enhances polymer mechanochemistry. *Nature chemistry* **2013,** *5* (2), 110-114.
17. Piermattei, A.; Karthikeyan, S.; Sijbesma, R. P., Activating catalysts with mechanical force. *Nature chemistry* **2009,** *1* (2), 133-137.
18. Gossweiler, G. R.; Kouznetsova, T. B.; Craig, S. L., Force-rate characterization of two spiropyran-based molecular force probes. *Journal of the American Chemical Society* **2015,** *137* (19), 6148-6151.
19. Groote, R.; Jakobs, R. T.; Sijbesma, R. P., Mechanocatalysis: forcing latent catalysts into action. *Polymer Chemistry* **2013,** *4* (18), 4846-4859.
20. Ferguson, J. R., Impact shock absorbing material. Google Patents: 2012.

21. Venkatraman, P.; Tyler, D., Impact-Resistant Materials and Their Potential. *Materials and Technology for Sportswear and Performance Apparel* **2015**, 205-230.
22. Keizer, H. M.; van Kessel, R.; Sijbesma, R. P.; Meijer, E., Scale-up of the synthesis of ureidopyrimidinone functionalized telechelic poly (ethylenebutylene). *Polymer* **2003,** *44* (19), 5505-5511.
23. Xu, J. F.; Chen, Y. Z.; Wu, D.; Wu, L. Z.; Tung, C. H.; Yang, Q. Z., Photoresponsive hydrogen-bonded supramolecular polymers based on a stiff stilbene unit. *Angewandte Chemie* **2013,** *125* (37), 9920-9924.
24. Brantley, J. N.; Bailey, C. B.; Wiggins, K. M.; Keatinge-Clay, A. T.; Bielawski, C. W., Mechanobiochemistry: harnessing biomacromolecules for force-responsive materials. *Polymer Chemistry* **2013,** *4* (14), 3916-3928.
25. Motlagh, H. N.; Wrabl, J. O.; Li, J.; Hilser, V. J., The ensemble nature of allostery. *Nature* **2014,** *508* (7496), 331-339.
26. Osada, Y., Conversion of chemical into mechanical energy by synthetic polymers (chemomechanical systems). In *Polymer Physics*, Springer: 1987; pp 1-46.
27. Rodríguez-Padrón, D.; Puente-Santiago, A. R.; Caballero, A.; Benítez, A.; Balu, A. M.; Romero, A. A.; Luque, R., Mechanochemical design of hemoglobin-functionalised magnetic nanomaterials for energy storage devices. *Journal of Materials Chemistry A* **2017,** *5* (31), 16404-16411.
28. Li, Y.; Wang, Y.; Huang, G.; Gao, J., Cooperativity principles in self-assembled nanomedicine. *Chemical reviews* **2018,** *118* (11), 5359-5391.
29. Pelley, J. W., *Elsevier's Integrated Review Biochemistry E-Book: with STUDENT CONSULT Online Access*. Elsevier Health Sciences: 2011.
30. Feldman, K. E.; Kade, M. J.; de Greef, T. F.; Meijer, E.; Kramer, E. J.; Hawker, C. J., Polymers with multiple hydrogen-bonded end groups and their blends. *Macromolecules* **2008,** *41* (13), 4694-4700.
31. Akbulatov, S.; Tian, Y.; Huang, Z.; Kucharski, T. J.; Yang, Q.-Z.; Boulatov, R., Experimentally realized mechanochemistry distinct from force-accelerated scission of loaded bonds. *Science* **2017,** *357* (6348), 299-303.
32. Boulatov, R., The liberating force of ultrasound. *Nature chemistry* **2021,** *13* (2), 112-114.
33. Akbulatov, S.; Tian, Y.; Boulatov, R., Force–reactivity property of a single monomer is sufficient to predict the micromechanical behavior of its polymer. *Journal of the American Chemical Society* **2012,** *134* (18), 7620-7623.
34. Wu, D.; Lenhardt, J. M.; Black, A. L.; Akhremitchev, B. B.; Craig, S. L., Molecular stress relief through a force-induced irreversible extension in polymer contour length. *Journal of the American Chemical Society* **2010,** *132* (45), 15936-15938.
35. Boulatov, R., Reaction dynamics in the formidable gap. *Pure and Applied Chemistry* **2010,** *83* (1), 25-41.
36. Anderson, L.; Boulatov, R., Polymer mechanochemistry: a new frontier for physical organic chemistry. *Advances in Physical Organic Chemistry* **2018,** *52*, 87-143.
37. Lehn, J.-M., Supramolecular chemistry: Where from? Where to? *Chemical Society Reviews* **2017,** *46* (9), 2378-2379.
38. Boulatov, R., Mechanochemistry: Demonstrated leverage. *Nature chemistry* **2013,** *5* (2), 84.

39. Sluysmans, D.; Devaux, F.; Bruns, C. J.; Stoddart, J. F.; Duwez, A.-S., Dynamic force spectroscopy of synthetic oligorotaxane foldamers. *Proceedings of the National Academy of Sciences* **2017**, 201712790.
40. Wojtecki, R. J.; Meador, M. A.; Rowan, S. J., Using the dynamic bond to access macroscopically responsive structurally dynamic polymers. *Nature materials* **2011,** *10* (1), 14.
41. Guichard, G.; Huc, I., Synthetic foldamers. *Chemical Communications* **2011,** *47* (21), 5933-5941.
42. Berl, V.; Huc, I.; Khoury, R. G.; Lehn, J. M., Helical Molecular Programming: Folding of Oligopyridine-dicarboxamides into Molecular Single Helices. *Chemistry-A European Journal* **2001,** *7* (13), 2798-2809.
43. Qi, T.; Deschrijver, T.; Huc, I., Large-scale and chromatography-free synthesis of an octameric quinoline-based aromatic amide helical foldamer. *Nature protocols* **2013,** *8* (4), 693.
44. Zhang, D.-W.; Zhao, X.; Hou, J.-L.; Li, Z.-T., Aromatic amide foldamers: structures, properties, and functions. *Chemical reviews* **2012,** *112* (10), 5271-5316.
45. Gellman, S. H., Foldamers: a manifesto. *Accounts of Chemical Research* **1998,** *31* (4), 173-180.
46. Berl, V.; Huc, I.; Khoury, R. G.; Krische, M. J.; Lehn, J.-M., Interconversion of single and double helices formed from synthetic molecular strands. *Nature* **2000,** *407* (6805), 720.
47. Huc, I., Aromatic oligoamide foldamers. *European Journal of Organic Chemistry* **2004,** *2004* (1), 17-29.
48. Haldar, D.; Jiang, H.; LÚger, J.-M.; Huc, I., Double versus single helical structures of oligopyridine-dicarboxamide strands. Part 2: The role of side chains. *Tetrahedron* **2007,** *63* (27), 6322-6330.
49. Jiang, H.; Maurizot, V.; Huc, I., Double versus single helical structures of oligopyridine-dicarboxamide strands. Part 1: Effect of oligomer length. *Tetrahedron* **2004,** *60* (44), 10029-10038.
50. Baptiste, B.; Zhu, J.; Haldar, D.; Kauffmann, B.; Léger, J. M.; Huc, I., Hybridization of Long Pyridine-Dicarboxamide Oligomers into Multi-Turn Double Helices: Slow Strand Association and Dissociation, Solvent Dependence, and Solid State Structures. *Chemistry–An Asian Journal* **2010,** *5* (6), 1364-1375.
51. Hill, D. J.; Mio, M. J.; Prince, R. B.; Hughes, T. S.; Moore, J. S., A field guide to foldamers. *Chemical Reviews* **2001,** *101* (12), 3893-4012.
52. Gan, Q.; Wang, Y.; Jiang, H., Aromatic oligoamide foldamers: A paradigm for structure-property relationship. *Current Organic Chemistry* **2011,** *15* (9), 1293-1301.
53. Dolain, C.; Grélard, A.; Laguerre, M.; Jiang, H.; Maurizot, V.; Huc, I., Solution structure of quinoline-and pyridine-derived oligoamide foldamers. *Chemistry-a European Journal* **2005,** *11* (21), 6135-6144.
54. Berl, V.; Huc, I.; Khoury, R. G.; Lehn, J. M., Helical Molecular Programming: Supramolecular Double Helices by Dimerization of Helical Oligopyridine-dicarboxamide Strands. *Chemistry-A European Journal* **2001,** *7* (13), 2810-2820.
55. Mukaiyama, T.; Sato, T.; Hanna, J., Reductive coupling of carbonyl compounds to pinacols and olefins by using TiCl4 and Zn. *Chemistry Letters* **1973,** *2* (10), 1041-1044.
56. Tyrlik, S.; Wolochowicz, I., APPLICATION OF TRANSITION-METAL COMPLEXES IN LOW OXIDATION STATES TO ORGANIC SYNTHESIS. 1. NEW SYNTHESIS OF OLEFINS STARTING

FROM A CARBONYL COMPOUND. *BULLETIN DE LA SOCIETE CHIMIQUE DE FRANCE PARTIE II-CHIMIE MOLECULAIRE ORGANIQUE ET BIOLOGIQUE* **1973,** (6), 2147-2148.
57. McMurry, J. E.; Fleming, M. P., New method for the reductive coupling of carbonyls to olefins. Synthesis of. beta.-carotene. *Journal of the American Chemical Society* **1974,** *96* (14), 4708-4709.
58. Ephritikhine, M., A new look at the McMurry reaction. *Chemical Communications* **1998,** (23), 2549-2554.
59. McMurry, J. E., Carbonyl-coupling reactions using low-valent titanium. *Chemical Reviews* **1989,** *89* (7), 1513-1524.
60. Takeda, T.; Tsubouchi, A., The McMurry Coupling and Related Reactions. *Organic Reactions* **2004,** *82*, 1-470.
61. Villemin, D., Synthese de macrolides par methathese. *Tetrahedron Letters* **1980,** *21* (18), 1715-1718.
62. Tsuji, J.; Hashiguchi, S., Application of olefin metathesis to organic synthesis. Syntheses of civetone and macrolides. *Tetrahedron Letters* **1980,** *21* (31), 2955-2958.
63. Schrock, R. R., Multiple metal–carbon bonds for catalytic metathesis reactions (Nobel lecture). *Angewandte Chemie International Edition* **2006,** *45* (23), 3748-3759.
64. Grubbs, R. H., Olefin-metathesis catalysts for the preparation of molecules and materials (Nobel lecture). *Angewandte Chemie International Edition* **2006,** *45* (23), 3760-3765.
65. Monfette, S.; Fogg, D. E., Equilibrium ring-closing metathesis. *Chemical reviews* **2009,** *109* (8), 3783-3816.
66. Jean-Louis Hérisson, P.; Chauvin, Y., Catalyse de transformation des oléfines par les complexes du tungstène. II. Télomérisation des oléfines cycliques en présence d'oléfines acycliques. *Die Makromolekulare Chemie: Macromolecular Chemistry and Physics* **1971,** *141* (1), 161-176.
67. Ivin, K. J.; Mol, J. C., *Olefin metathesis and metathesis polymerization*. Elsevier: 1997.
68. Xu, Z.; Johannes, C. W.; Houri, A. F.; La, D. S.; Cogan, D. A.; Hofilena, G. E.; Hoveyda, A. H., Applications of Zr-catalyzed carbomagnesation and Mo-catalyzed macrocyclic ring closing metathesis in asymmetric synthesis. Enantioselective total synthesis of Sch 38516 (Fluvirucin B1). *Journal of the American Chemical Society* **1997,** *119* (43), 10302-10316.
69. Michrowska, A.; Wawrzyniak, P.; Grela, K., Synthesis of Macrocyclic Carbonates with Musk Odor by Ring-Closing Olefin Metathesis. *European Journal of Organic Chemistry* **2004,** *2004* (9), 2053-2056.
70. Arakawa, K.; Eguchi, T.; Kakinuma, K., An olefin metathesis approach to 36-and 72-membered archaeal macrocyclic membrane lipids. *The Journal of Organic Chemistry* **1998,** *63* (14), 4741-4745.
71. Mitchell, L.; Parkinson, J. A.; Percy, J. M.; Singh, K., Selected substituent effects on the rate and efficiency of formation of an eight-membered ring by RCM. *The Journal of organic chemistry* **2008,** *73* (6), 2389-2395.
72. Creighton, C. J.; Leo, G. C.; Du, Y.; Reitz, A. B., Design, synthesis, and conformational analysis of eight-membered cyclic peptidomimetics prepared using ring closing metathesis. *Bioorganic & medicinal chemistry* **2004,** *12* (16), 4375-4385.
73. Kotha, S.; Lahiri, K., Synthesis of diverse polycyclic compounds via catalytic metathesis. *Synlett* **2007,** *2007* (18), 2767-2784.

74. Kotha, S.; Khedkar, P.; Ghosh, A. K., Synthesis of Symmetrical Sulfones from Rongalite: Expansion to Cyclic Sulfones by Ring-Closing Metathesis. *European journal of organic chemistry* **2005,** *2005* (16), 3581-3585.
75. Fürstner, A.; Thiel, O. R.; Ackermann, L., Exploiting the Reversibility of Olefin Metathesis. Syntheses of Macrocyclic Trisubstituted Alkenes and (R, R)-(−)-Pyrenophorin. *Organic letters* **2001,** *3* (3), 449-451.
76. Arisawa, M.; Kato, C.; Kaneko, H.; Nishida, A.; Nakagawa, M., Concise synthesis of azacycloundecenes using ring-closing metathesis (RCM). *Journal of the Chemical Society, Perkin Transactions 1* **2000,** (12), 1873-1876.
77. Tae, J.; Yang, Y.-K., Efficient synthesis of macrocyclic paracyclophanes by ring-closing metathesis dimerization and trimerization reactions. *Organic letters* **2003,** *5* (5), 741-744.
78. Albrecht, M., Template-Directed Synthesis of Symmetric as well as Unsymmetric Macrocycles from Rigid or Flexible Building Blocks. *Synthesis* **2008,** *2008* (15), 2451-2461.
79. Kucharski, T. J.; Huang, Z.; Yang, Q. Z.; Tian, Y.; Rubin, N. C.; Concepcion, C. D.; Boulatov, R., Kinetics of thiol/disulfide exchange correlate weakly with the restoring force in the disulfide moiety. *Angewandte Chemie International Edition* **2009,** *48* (38), 7040-7043.
80. Muthusamy, S.; Gnanaprakasam, B.; Suresh, E., New approach to the synthesis of macrocyclic tetralactones via ring-closing metathesis using Grubbs' first-generation catalyst. *The Journal of organic chemistry* **2007,** *72* (4), 1495-1498.
81. Torborg, C.; Szczepaniak, G.; Zieliński, A.; Malińska, M.; Woźniak, K.; Grela, K., Stable ruthenium indenylidene complexes with a sterically reduced NHC ligand. *Chemical Communications* **2013,** *49* (31), 3188-3190.
82. De Frëmont, P.; Clavier, H.; Montembault, V.; Fontaine, L.; Nolan, S. P., Ruthenium–indenylidene complexes in ring opening metathesis polymerization (ROMP) reactions. *Journal of Molecular Catalysis A: Chemical* **2008,** *283* (1), 108-113.
83. P'Poo, S. J.; Schanz, H.-J., Reversible inhibition/activation of olefin metathesis: A kinetic investigation of ROMP and RCM reactions with Grubbs' catalyst. *Journal of the American Chemical Society* **2007,** *129* (46), 14200-14212.
84. Horne, W. S.; Gellman, S. H., Foldamers with heterogeneous backbones. *Accounts of chemical research* **2008,** *41* (10), 1399-1408.
85. Nowick, J. S., Exploring β-sheet structure and interactions with chemical model systems. *Accounts of chemical research* **2008,** *41* (10), 1319-1330.
86. Stone, M. T.; Heemstra, J. M.; Moore, J. S., The chain-length dependence test. *Accounts of chemical research* **2006,** *39* (1), 11-20.
87. Saraogi, I.; Hamilton, A. D., Recent advances in the development of aryl-based foldamers. *Chemical Society Reviews* **2009,** *38* (6), 1726-1743.
88. Juwarker, H.; Suk, J.-m.; Jeong, K.-S., Foldamers with helical cavities for binding complementary guests. *Chemical Society Reviews* **2009,** *38* (12), 3316-3325.
89. Gan, Q.; Ferrand, Y.; Bao, C.; Kauffmann, B.; Grélard, A.; Jiang, H.; Huc, I., Helix-rod host-guest complexes with shuttling rates much faster than disassembly. *Science* **2011,** *331* (6021), 1172-1175.
90. Bao, C.; Gan, Q.; Kauffmann, B.; Jiang, H.; Huc, I., A self-assembled foldamer capsule: combining single and double helical segments in one aromatic amide sequence. *Chemistry–A European Journal* **2009,** *15* (43), 11530-11536.
91. Roy, A.; Prabhakaran, P.; Baruah, P. K.; Sanjayan, G. J., Diversifying the structural architecture of synthetic oligomers: the hetero foldamer approach. *Chemical Communications* **2011,** *47* (42), 11593-11611.

92. Li, Z.; Hou, J.; Li, C.; Yi, H., Chem. dAsian J. 2006, 1, 766–778;(b) Li, Z.-T.; Hou, J.-L.; Li, C. *Acc. Chem. Res* **2008,** *41*, 1343-1353.
93. Zhao, X.; Li, Z.-T., Hydrogen bonded aryl amide and hydrazide oligomers: a new generation of preorganized soft frameworks. *Chemical Communications* **2010,** *46* (10), 1601-1616.
94. Dolain, C.; Zhan, C.; Léger, J.-M.; Daniels, L.; Huc, I., Folding Directed N-Oxidation of Oligopyridine− Dicarboxamide Strands and Hybridization of Oxidized Oligomers. *Journal of the American Chemical Society* **2005,** *127* (8), 2400-2401.
95. Yi, H.-P.; Wu, J.; Ding, K.-L.; Jiang, X.-K.; Li, Z.-T., Hydrogen bonding-induced aromatic oligoamide foldamers as spherand analogues to accelerate the hydrolysis of nitro-substituted anisole in aqueous media. *The Journal of organic chemistry* **2007,** *72* (3), 870-877.
96. Smaldone, R. A.; Moore, J. S., Reactive sieving with foldamers: inspiration from nature and directions for the future. *Chemistry–A European Journal* **2008,** *14* (9), 2650-2657.
97. Srinivas, K.; Kauffmann, B.; Dolain, C.; Léger, J.-M.; Ghosez, L.; Huc, I., Remote substituent effects and regioselective enhancement of electrophilic substitutions in helical aromatic oligoamides. *Journal of the American Chemical Society* **2008,** *130* (40), 13210-13211.
98. Muller, M. M.; Windsor, M. A.; Pomerantz, W. C.; Gellman, S. H.; Hilvert, D., A Rationally Designed Aldolase Foldamer This work was supported by the Schweizerischer Nationalfonds, NIH grant GM056414 (to SHG), and the Nanoscale Science and Engineering Center at UW-Madison (NSF DMR-042588). We thank Dr. Dennis Gillingham for help with substrate preparation. *Angewandte Chemie-German Edition* **2009,** *121* (5), 940.
99. Müller, M. M.; Windsor, M. A.; Pomerantz, W. C.; Gellman, S. H.; Hilvert, D., A rationally designed aldolase foldamer. *Angewandte Chemie International Edition* **2009,** *48* (5), 922-925.
100. Ren, C.; Maurizot, V.; Zhao, H.; Shen, J.; Zhou, F.; Ong, W. Q.; Du, Z.; Zhang, K.; Su, H.; Zeng, H., Five-fold-symmetric macrocyclic aromatic pentamers: high-affinity cation recognition, ion-pair-induced columnar stacking, and nanofibrillation. *Journal of the American Chemical Society* **2011,** *133* (35), 13930-13933.
101. Qin, B.; Chen, X.; Fang, X.; Shu, Y.; Yip, Y. K.; Yan, Y.; Pan, S.; Ong, W. Q.; Ren, C.; Su, H., Crystallographic evidence of an unusual, pentagon-shaped folding pattern in a circular aromatic pentamer. *Organic letters* **2008,** *10* (22), 5127-5130.
102. Zhao, H.; Ong, W. Q.; Zhou, F.; Fang, X.; Chen, X.; Li, S. F.; Su, H.; Cho, N.-J.; Zeng, H., Chiral crystallization of aromatic helical foldamers via complementarities in shape and end functionalities. *Chemical Science* **2012,** *3* (6), 2042-2046.
103. Zhu, J.; Wang, X.-Z.; Chen, Y.-Q.; Jiang, X.-K.; Chen, X.-Z.; Li, Z.-T., Hydrogen-bonding-induced planar, rigid, and Zigzag oligoanthranilamides. synthesis, characterization, and self-assembly of a metallocyclophane. *The Journal of organic chemistry* **2004,** *69* (19), 6221-6227.
104. Jiang, H.; Léger, J.-M.; Guionneau, P.; Huc, I., Strained aromatic oligoamide macrocycles as new molecular clips. *Organic letters* **2004,** *6* (17), 2985-2988.
105. Yuan, L.; Feng, W.; Yamato, K.; Sanford, A. R.; Xu, D.; Guo, H.; Gong, B., Highly efficient, one-step macrocyclizations assisted by the folding and preorganization of precursor oligomers. *Journal of the American Chemical Society* **2004,** *126* (36), 11120-11121.
106. Araghi, R. R.; Koksch, B., A helix-forming αβγ-chimeric peptide with catalytic activity: a hybrid peptide ligase. *Chemical Communications* **2011,** *47* (12), 3544-3546.

107. Shi, Z.-M.; Huang, J.; Ma, Z.; Zhao, X.; Guan, Z.; Li, Z.-T., Foldamers as cross-links for tuning the dynamic mechanical property of methacrylate copolymers. *Macromolecules* **2010,** *43* (14), 6185-6192.
108. Zhang, K. D.; Zhao, X.; Wang, G. T.; Liu, Y.; Zhang, Y.; Lu, H. J.; Jiang, X. K.; Li, Z. T., Foldamer-Tuned Switching Kinetics and Metastability of [2] Rotaxanes. *Angewandte Chemie International Edition* **2011,** *50* (42), 9866-9870.
109. Yin, H.; Hamilton, A. D., Strategies for targeting protein–protein interactions with synthetic agents. *Angewandte Chemie International Edition* **2005,** *44* (27), 4130-4163.
110. Cummings, C. G.; Hamilton, A. D., Disrupting protein–protein interactions with non-peptidic, small molecule α-helix mimetics. *Current opinion in chemical biology* **2010,** *14* (3), 341-346.
111. Adler, M. J.; Hamilton, A. D., Oligophenylenaminones as scaffolds for α-helix mimicry. *The Journal of organic chemistry* **2011,** *76* (17), 7040-7047.
112. Azzarito, V.; Long, K.; Murphy, N. S.; Wilson, A. J., Inhibition of α-helix-mediated protein–protein interactions using designed molecules. *Nature chemistry* **2013,** *5* (3), 161.
113. Sadowsky, J. D.; Schmitt, M. A.; Lee, H.-S.; Umezawa, N.; Wang, S.; Tomita, Y.; Gellman, S. H., Chimeric (α/β+ α)-peptide ligands for the BH3-recognition cleft of Bcl-XL: critical role of the molecular scaffold in protein surface recognition. *Journal of the American Chemical Society* **2005,** *127* (34), 11966-11968.
114. Delaurière, L.; Dong, Z.; Laxmi-Reddy, K.; Godde, F.; Toulmé, J. J.; Huc, I., Deciphering aromatic oligoamide foldamer–DNA interactions. *Angewandte Chemie International Edition* **2012,** *51* (2), 473-477.
115. Nelson, J. C.; Saven, J. G.; Moore, J. S.; Wolynes, P. G., Solvophobically driven folding of nonbiological oligomers. *Science* **1997,** *277* (5333), 1793-1796.
116. Rodriguez, J. M.; Hamilton, A. D., Benzoylurea oligomers: synthetic foldamers that mimic extended α helices. *Angewandte Chemie* **2007,** *119* (45), 8768-8771.
117. Hamuro, Y.; Geib, S. J.; Hamilton, A. D., Oligoanthranilamides. Non-peptide subunits that show formation of specific secondary structure. *Journal of the American Chemical Society* **1996,** *118* (32), 7529-7541.
118. Zhu, J.; Parra, R. D.; Zeng, H.; Skrzypczak-Jankun, E.; Zeng, X. C.; Gong, B., A new class of folding oligomers: crescent oligoamides. *Journal of the American Chemical Society* **2000,** *122* (17), 4219-4220.
119. Jiang, H.; Léger, J.-M.; Huc, I., Aromatic δ-peptides. *Journal of the American Chemical Society* **2003,** *125* (12), 3448-3449.
120. Berl, V.; Huc, I.; Khoury, R. G.; Krische, M. J.; Lehn, J.-M., Interconversion of single and double helices formed from synthetic molecular strands. *Nature* **2000,** *407* (6805), 720-723.
121. Acocella, A.; Venturini, A.; Zerbetto, F., Pyridinedicarboxamide strands form double helices via an activated slippage mechanism. *Journal of the American Chemical Society* **2004,** *126* (8), 2362-2367.
122. Rasheed, O.; McDouall, J.; Muryn, C.; Raftery, J.; Vitorica-Yrezabal, I.; Quayle, P., The assembly of “S 3 N”-ligands decorated with an azo-dye as potential sensors for heavy metal ions. *Dalton Transactions* **2017,** *46* (16), 5229-5239.
123. McGrath, J. M.; Pluth, M. D., Understanding the Effects of Preorganization, Rigidity, and Steric Interactions in Synthetic Barbiturate Receptors. *The Journal of organic chemistry* **2014,** *79* (2), 711-719.

124. Akbulatov, S.; Boulatov, R., Experimental polymer mechanochemistry and its interpretational frameworks. *ChemPhysChem* **2017,** *18* (11), 1422-1450.
125. Bowser, B. H.; Craig, S. L., Empowering mechanochemistry with multi-mechanophore polymer architectures. *Polymer Chemistry* **2018,** *9* (26), 3583-3593.
126. Dubois, P.; Coulembier, O.; Raquez, J.-M., *Handbook of ring-opening polymerization*. John Wiley & Sons: 2009.
127. Pearce, A. K.; Foster, J. C.; O'Reilly, R. K., Recent developments in entropy-driven ring-opening metathesis polymerization: Mechanistic considerations, unique functionality, and sequence control. *Journal of Polymer Science Part A: Polymer Chemistry* **2019,** *57* (15), 1621-1634.
128. Xue, Z.; Mayer, M. F., Entropy-driven ring-opening olefin metathesis polymerizations of macrocycles. *Soft Matter* **2009,** *5* (23), 4600-4611.
129. Camm, K. D.; Martinez Castro, N.; Liu, Y.; Czechura, P.; Snelgrove, J. L.; Fogg, D. E., Tandem ROMP− hydrogenation with a third-generation grubbs catalyst. *Journal of the American Chemical Society* **2007,** *129* (14), 4168-4169.
130. Yasir, M.; Liu, P.; Tennie, I. K.; Kilbinger, A. F., Catalytic living ring-opening metathesis polymerization with Grubbs' second-and third-generation catalysts. *Nature chemistry* **2019,** *11* (5), 488-494.
131. Hodge, P., Entropically driven ring-opening polymerization of strainless organic macrocycles. *Chemical Reviews* **2014,** *114* (4), 2278-2312.
132. Xu, Y.; Xu, W. L.; Smith, M. D.; Shimizu, L. S., Self-assembly and ring-opening metathesis polymerization of a bifunctional carbonate–stilbene macrocycle. *RSC Advances* **2014,** *4* (4), 1675-1682.
133. Lee, B.; Niu, Z.; Craig, S. L., The mechanical strength of a mechanical bond: sonochemical polymer mechanochemistry of poly (catenane) copolymers. *Angewandte Chemie* **2016,** *128* (42), 13280-13283.
134. Peng, Y.; Decatur, J.; Meier, M. A.; Gross, R. A., Ring-opening metathesis polymerization of a naturally derived macrocyclic glycolipid. *Macromolecules* **2013,** *46* (9), 3293-3300.
135. Mahjour, B.; Shen, Y.; Liu, W.; Cernak, T., A map of the amine–carboxylic acid coupling system. *Nature* **2020,** *580* (7801), 71-75.
136. Li, X. Synthesis and physical properties of helical nanosized quinoline-based foldamers: structure, dynamics and photoinduced electron transport. 2016.
137. Makida, H.; Abe, H.; Inouye, M., Highly efficient stabilisation of meta-ethynylpyridine polymers with amide side chains in water by coordination of rare-earth metals. *Organic & biomolecular chemistry* **2015,** *13* (6), 1700-1707.
138. Misawa, T.; Kanda, Y.; Demizu, Y., Rational Design and Synthesis of Post-Functionalizable Peptide Foldamers as Helical Templates. *Bioconjugate chemistry* **2017,** *28* (12), 3029-3035.
139. Morris, J.; Kozlowski, P.; Wang, G., Synthesis and Characterization of Hybrid Glycolipids as Functional Organogelators and Hydrogelators. *Langmuir* **2019,** *35* (45), 14639-14650.
140. Parrish, B.; Breitenkamp, R. B.; Emrick, T., PEG-and peptide-grafted aliphatic polyesters by click chemistry. *Journal of the American Chemical Society* **2005,** *127* (20), 7404-7410.
141. Elling, B. R.; Su, J. K.; Xia, Y., Ring-opening metathesis polymerization of 1, 2-disubstituted cyclopropenes. *Chemical Communications* **2016,** *52* (58), 9097-9100.

142. Kim, D. H.; Park, S. S.; Park, S. H.; Jeon, J. Y.; Kim, H. B.; Lee, B. Y., Preparation of polystyrene–polyolefin multiblock copolymers by sequential coordination and anionic polymerization. *RSC advances* **2017,** *7* (10), 5948-5956.
143. Zhou, Q.; Liang, H.; Wei, W.; Meng, C.; Long, Y.; Zhu, F., Synthesis of amphiphilic diblock copolymers of isotactic polystyrene-block-isotactic poly (p-hydroxystyrene) using a titanium complex with an [OSSO]-type bis (phenolate) ligand and sequential monomer addition. *RSC advances* **2017,** *7* (32), 19885-19893.